Jørgen Apeland

Application of FE-analysis in Design and Verification of Bolted Joints According to VDI 2230 at CERN

MSc Thesis

Genève, February 2018

Supervisor: Torgeir Welo, NTNU
Antonio Lafuente Mazuecos, CERN
Luca Dassa, CERN

CERN-THESIS-2018-006
17/02/2018

Norwegian University of Science and Technology
Faculty of Engineering
Department of Mechanical and Industrial Engineering

NTNU
Norwegian University of
Science and Technology

Preface

This master thesis was written the Fall of 2017 and early 2018, and concludes my degree in Mechanical Engineering at the Norwegian University of Science and Technology. The master project has been carried out while being a technical student in the engineering department at CERN, the European Organisation for Nuclear Research.

The thesis is about how computer simulation tools can be combined with VDI 2230, a calculation guideline for bolted joints, to achieve quality and productivity rewards in design and verification of bolted joints. The scope was also to lower the threshold and making it easier to perform such assessments.

It takes basis in a specific engineering case, which demonstrates the need for improved knowledge and an analysis strategy. A complete framework with a simplified workflow and support material is presented and demonstrated. In the end, specific recommendations for the initial engineering case are given.

The reader is expected to have basic knowledge in mechanics, springs, bolted joints and finite element analysis. *ANSYS Workbench V17.2* has been used for FE-analysis, and *Mathcad Prime V4.0* for engineering calculations.

Genève, 2018

Jørgen Apeland

Acknowledgements

I would like to thank my CERN supervisors Luca Dassa and Antonio Lafuente for their guidance, discussions, and thorough feedback during my research. They have been essential for the initiation and development of the project.

I would also like to thank my supervisor at NTNU, Torgeir Welo, for his contributions and reviews, and for making this project possible.

The design and analysis office in EN-MME has provided a friendly and international working environment, and they have provided useful input on user experiences and needs related to analysis of bolted joints.

Finally, I would like to thank CERN and the Technical Student Programme for establishing a framework where students can come and take part in cutting edge technology development, and get practical and valuable experiences in a high competence environment.

Abstract

This thesis investigates how finite element analysis (FEA) can be used to simplify and improve analysis of bolted joints according to the guideline VDI 2230. Some aspects of how FEA can be applied to aid design and verification of bolted joints are given in the guideline, but not in a streamlined way that makes it simple and efficient to apply.

The scope of this thesis is to clarify how FEA and VDI 2230 can be combined in analysis of bolted joints, and to present a streamlined workflow. The goal is to lower the threshold for carrying out such combined analysis. The resulting benefits are improved analysis validity and quality, and improved analysis efficiency.

A case from the engineering department at CERN, where FEA has been used in analysis of bolted joints is used as basis to identify challenges in combining FEA and VDI 2230. This illustrates the need for a streamlined analysis strategy and well described workflow.

The case in question is the Helium vessel (pressure vessel) for the DQW Crab Cavities, which is an important part of the High Luminosity upgrade of LHC (HL-LHC).

Investigations are performed into prying, a relevant source of non-linear bolt loads and unpredictable load development, to understand the phenomenon and influence of preload. A complete analysis framework is then presented, which consist of a streamlined basic workflow, associated calculation template, details of more advanced verifications, a detailed guide with best practices and references, examples where the analysis framework has been applied, and a seminar to educate relevant personnel.

In the end, suggestions and recommendations are provided for a potential revision of the Helium vessel analysis.

The hope is that this thesis can be used as a resource in analysis of bolted joints using VDI 2230 and FEA, and that it will benefit the engineering department at CERN and other relevant users.

Sammendrag

Denne oppgaven tar for seg hvordan datasimuleringer (FEA) kan benyttes til å forenkle og forbedre analyse av boltede forbindelser i henhold til retningslinjene i VDI 2230. Enkelte aspekter av hvordan FEA kan benyttes for å assistere design og verifikasjon av boltede forbindelser er omtalt i retningslinjene, men ikke på en strømlinjeformet måte som gjør det enkelt og effektivt å benytte.

Målet med oppgaven er å redegjøre for hvordan FEA og VDI 2230 kan kombineres, og å presentere en strømlinjeformet arbeidsflyt. Håpet er dermed å senke terskelen for å utføre slike kombinerte analyser. Fordelene er forbedret validitet og kvalitet i analysen, samt forbedret effektivitet i prosessen.

Det er tatt utgangspunkt i en analyse fra ingeniøravdelingen ved CERN, hvor FEA har blitt benyttet i verifikasjon av boltede forbindelser. Denne er brukt som basis for å identifisere utfordringer med å kombinere FEA og VDI 2230, og illustrerer behovet for en strømlinjeformet analyse strategi og detaljert beskrivelse av arbeidsflyten.

Analysen det er tatt utgangspunkt i er en Helium beholder (trykkbeholder) for *DQW Crab Cavities*, som er en viktig del av en kommende oppgradering av LHC kalt *High Luminosity LHC* (HL-LHC).

En aktuell kilde for ikke-lineære bolt laster og uforutsigbar last utvikling kalt *prying* er undersøkt for å forstå fenomenet bedre, samt innvirkningen av forspenning. Et komplett analyse rammeverk er presentert, som består av en strømlinjeformet arbeidsflyt, tilhørende beregnings mal, detaljer om mer avanserte beregninger og verifikasjoner, en detaljert guide med «beste praksis» og relevante referanser, eksempler hvor den foreslåtte arbeidsflyten er benyttet, samt et seminar for å undervise relevant personell.

Til slutt er spesifikke forslag og anbefalinger for en potensiell revisjon av Helium beholder analysen gitt.

Håpet er at denne oppgaven kan bli benyttet som en ressurs innen design og verifikasjon av boltede forbindelser ved bruk av VDI 2230 og FEA, og at den vil være til nytte for ingeniøravdelingen ved CERN og andre relevante brukere.

Table of Contents

1 INTRODUCTION 1

1.1 BACKGROUND 1
1.2 PROBLEM DESCRIPTION 1
1.3 PROJECT SCOPE 1
1.4 STRUCTURE OF REPORT 2
1.5 LITERATURE 2

2 THEORY 3

2.1 TERMS 3
2.2 BASICS OF BOLTED JOINTS 3
2.3 ANALYTIC VDI 2230 PROCEDURE 11
2.4 FEA MODEL CLASSES 13

3 DQW CRAB CAVITIES HELIUM VESSEL ANALYSIS 19

3.1 INTRODUCTION TO THE CRAB CAVITIES 19
3.2 HELIUM VESSEL FOR DQW CRAB CAVITIES 23
3.3 HELIUM VESSEL BOLT ANALYSIS 25
3.4 RQ1: CHALLENGES IN ANALYSIS OF BOLTED JOINTS 30
3.5 RQ2: HOW CAN THE CHALLENGES BE MET? 31

4 INVESTIGATIONS INTO PRYING 33

4.1 WHAT IS PRYING? 33
4.2 WHY AND WHEN IS IT RELEVANT? 36
4.3 HOW SHOULD IT BE ENCOUNTERED? 36
4.4 FEA-STUDY OF PRELOAD INFLUENCE ON PRYING 37
4.5 DISCUSSION 40
4.6 SUMMARY 42

5 FEA AIDED ASSESSMENT OF BOLTED JOINTS 43

5.1 ANALYSIS APPROACH 43
5.2 BASIC FEA WORKFLOW 45
5.3 NON-CRITICAL JOINTS 49
5.4 GUIDE FOR BASIC FEA WORKFLOW 51
5.5 FURTHER ASSESSMENTS 64
5.6 CASE EXAMPLES 66
5.7 SEMINAR ABOUT FEA & VDI 2230 67

6 REVISED CRAB CAVITY HE-VESSEL ANALYSIS 69

6.1 SUGGESTIONS AND RECOMMENDATIONS 69
6.2 REVISED CALCULATIONS 72

7 DISCUSSION 73

7.1 GOAL ACHIEVEMENT 73
7.2 RESEARCH ACTIVITIES 73
7.3 PRODUCTIVITY PARADOX AND SIMULATION DRIVEN DESIGN 74
7.4 FUTURE RESEARCH 75

8 SUMMARY 77

APPENDIX A: Basic FEA Workflow Calculation Template

APPENDIX B: Tightening Torque Template for Non-Critical Bolts

APPENDIX C: Blind Flange Analysis Example

C-1a Blind Flange Case Report

C-1b Calculations for Blind Flange Case

C-2a Blind Flange with Analytic VDI 2230 Procedure

C-2b Calculations for Blind Flange with Analytic VDI 2230 Procedure

APPENDIX D: Bolted Tuner Analysis Example

D-1 HG Cavity Bolted Tuner Analysis

D-2 Analytic Calculations for Tuner Analysis

APPENDIX E: VDI 2230 and FEA Seminar Presentation

APPENDIX F: Revised Calculations for HE-Vessel Joints

List of Figures

FIGURE 1: TTJ & TBJ 4
FIGURE 2: DIMENSIONS ASSOCIATED WITH A BOLT AND TAPPED THREADS 5
FIGURE 3: MECHANICAL SPRING MODEL OF A CLAMPED BJ 5
FIGURE 4: DISTORTION TRIANGLE 6
FIGURE 5: DISTORTION TRIANGLE FOR N<1 7
FIGURE 6: JOINT DIAGRAM WITH ASSOCIATED QUANTITIES 8
FIGURE 7: DEFORMATION CONES FOR A TBJ AND A TTJ 9
FIGURE 8: DEFORMATION CONE AND SLEEVE (LEFT) AND LIMIT CRITERIA G (RIGHT) 10
FIGURE 9: CLAMPING SOLID INTERACTION IN MBJS 10
FIGURE 10: JOINT DIAGRAM WITH ANALYTIC VDI 2230 QUANTITIES 12
FIGURE 11: INTERSECTION FORCES CLASS I 14
FIGURE 12: EFFECT OF RIGID MPCS ON MESH STIFFNESS AND THE RESULTING PRESSURE DISTRIBUTION WITH CLASS II MODEL 15
FIGURE 13: THE CERN ACCELERATOR COMPLEX 19
FIGURE 14: LOCATION OF DETECTORS AROUND LHC 20
FIGURE 15: CRYOMODULE WITH TWO DQW CRAB CAVITIES 21
FIGURE 16: DQW CRAB CAVITY, BARE (LEFT) AND IN HE-VESSEL (RIGHT) 21
FIGURE 17: VISUALISATION OF HOW CRAB CAVITIES ROTATE BUNCHES BEFORE AND AFTER COLLISION POINT 22
FIGURE 18: TWO HELIUM VESSELS FOR DQW CRAB CAVITIES DURING ASSEMBLY IN 2017 22
FIGURE 19: HELIUM VESSEL AND BOLTED JOINTS 23
FIGURE 20: THE THREE JOINT CONCEPTS ON THE HE-VESSEL, WITH FILLET WELDS FOR LEAK-TIGHTNESS 24
FIGURE 21: BCS OF HE-VESSEL FE-MODEL 25
FIGURE 22: BOLT REPRESENTATION IN THE FE-MODEL ACCORDING TO VDI 2230 CLASS II 26
FIGURE 23: AXIAL BOLT LOAD DISTRIBUTION IN ROW 1 27
FIGURE 24: RESULTING PRESSURE DISTRIBUTION IN BOLT ROW 1 (TOP) AND ROW 10 (LOWER) 28
FIGURE 25: DEVELOPMENT IN TOTAL BOLT LOAD WITH INCREASING PRELOADS 30
FIGURE 26: PRYING ACTION IN A FLEXIBLE AND A RIGID JOINT 33
FIGURE 27: PRESSURE DISTRIBUTION IN THE CLAMPING INTERFACE 34
FIGURE 28: ADDITIONAL BOLT LOAD DEVELOPMENT FOR AN OPENING JOINT 34
FIGURE 29: BOLT LOAD BEFORE AND AFTER JOINT OPENING FOR FIVE LEVELS OF PRELOAD 35
FIGURE 30: IMPORTANT PARAMETERS FOR JOINT STIFFNESS [16] 36
FIGURE 31: GEOMETRY USED IN PRYING ANALYSIS 37
FIGURE 32: MAXIMUM BOLT LOADS FOR VARIOUS PRELOAD LEVELS 38
FIGURE 33: ADDITIONAL BOLT LOAD FOR VARIOUS PRELOAD LEVELS 38
FIGURE 34: JOINT OPENING FOR VARIOUS PRELOAD LEVELS 39
FIGURE 35: STRATEGY TO ASSESS PRELOAD LEVEL AND PRESENCE OF PRYING 41
FIGURE 36: COMPARISON OF ANALYTIC AND SEMI ANALYTIC FEA WORKFLOWS 44
FIGURE 37: JOINT DIAGRAM WITH THE ANALYSIS CONCEPT OF THE BASIC WORKFLOW ANALYSIS 48
FIGURE 38: EXTRACT OF STEP S2 FROM THE BASIC WORKFLOW CALCULATION TEMPLATE IN *APPENDIX A* 49
FIGURE 39: TWO EXAMPLES OF PROGRAMMING IN BOLT ASSESSMENT CALCULATIONS 49
FIGURE 40: TABLE WITH TIGHTENING TORQUES AND ASSOCIATED PRELOADS FOR M3-M12 BOLTS 50
FIGURE 41: TYPICAL STRESS-STRAIN CURVES FOR VARIOUS MATERIAL STRENGTHS 54
FIGURE 42: CLASS II AND CLASS III BOLT REPRESENTATION 57
FIGURE 43: CLASS III REPRESENTATION OF BOLT 57
FIGURE 44: EXTRACTION OF SBJ FROM A MBJ 57
FIGURE 45: SIMULATION SETUP IN ANSYS WITH MAX AND MIN PRELOAD 58

FIGURE 46: PRESSURE DISTRIBUTION IN THE INTERFACE, AND JOINT OPENING. 61
FIGURE 47: PLOT OF RELATIVE DEFORMATION FOR TWO EDGES ON THE CLAMPING INTERFACE 61
FIGURE 48: ASSESSMENT OF JOINT OPENING WITH "STATUS" AND SURFACE PRESSURE PLOTS..... 61
FIGURE 49: ANSYS PLOTS FOR ASSESSMENT OF SLIPPING 62
FIGURE 50: BOLT LOAD DEVELOPMENT FOR A JOINT WITH PRYING..... 63
FIGURE 51: GUIDE FOR RECOMMENDED LENGTHS OF TAPPED THREAD ENGAGEMENT..... 66
FIGURE 52: BLIND FLANGE ANALYSIS EXAMPLE 66
FIGURE 53: BOLTED HG CAVITY TUNER SUBJECTED TO MBJ SLIPPING ANALYSIS..... 67
FIGURE 54: DETAIL DRAWINGS OF JOINT TYPE B AND C..... 70
FIGURE 55: SBJ EXTRACTED FROM HE-VESSEL 70
FIGURE 56: GROUP DRIVE..... 74

List of Tables

TABLE 1: OUTLINE OF BJS 4
TABLE 2: OUTLINE OF THE ANALYTIC VDI 2230 PROCEDURE 11
TABLE 3: FACTORS CONSIDERED IN THE CALCULATION PROCEDURE 13
TABLE 4: OVERVIEW OF THE MODEL CLASSES 13
TABLE 5: COMPARISON OF FE-MODEL CLASSES 16
TABLE 6: BOUNDARY AND LOAD CONDITIONS 25
TABLE 7: BEAM PROPERTIES FOR M6 BOLT 26
TABLE 8: LOADS EXTRACTED FROM FEA AND CALCULATED BOLT STRESS, ADAPTED FROM [14] 27
TABLE 9: TWO APPROACHES FOR COMBINING FEA AND VDI 2230 43
TABLE 10: BASIC FEA WORKFLOW FOR ANALYSIS OF BOLDED JOINTS ACCORDING TO VDI 2230 45
TABLE 11: STRATEGIES FOR DETERMINATION OF BOLT WORKLOADS 51
TABLE 12: TYPICAL TIGHTENING FACTOR RANGES FOR TYPICAL TIGHTENING METHODS 55
TABLE 13: BOLT PROPERTIES ACCORDING FOR STEEL AND STAINLESS-STEEL BOLTS 56
TABLE 14: VALUES TO BE EXTRACTED FROM THE SIMULATIONS 59
TABLE 15 : SAFETY FACTOR STRATEGIES FOR FE-ANALYSIS OF BOLTED JOINTS 60

Abbreviations

BJ	Bolted joint, general
FE	Finite element
FEA	Finite element analysis
FEM	Finite element method
TBJ	Through-bolt joint
TTJ	Tapped thread joint
SBJ	Single-bolt joint
MBJ	Multi-bolted joint
MPC	Multiple point constraint
Pt. 1	VDI2230:2014 Part 1
Pt. 2	VDI2230:2014 Part 2

Cross Referencing

[#]	Literature reference
(#)	Equation / calculation
(RX/Y)	Formula from VDI 2230 verification procedure X = calculation step Y = formula number
[X-Y]	Reference to VDI 2230:2014 X= Pt. 1 or Pt. 2 Y= section / figure / table

Nomenclature

Symbol	Designation
A_S	Stress cross section of the bolt thread according to DIN 13-28
D_A	Substitutional outside diameter of the basic solid at the interface
d	Bolt diameter. Outside diameter of the bolt thread. Nominal diameter.
d_h	Bolt clearance hole, hole diameter of the clamped parts [ISO 273]
d_S	Diameter at stress cross section A_S
d_W	Outside diameter of the bolt head bearing surface
d_0	Diameter of the relevant smallest cross section of the bolt
d_2	Pitch diameter of the bolt thread
d_3	Minor diameter of the bolt thread
E	Young`s modulus
E_P	Young`s modulus of the clamped parts
E_S	Young`s modulus of the bolt material
e	Distance of the bolt axis from the edge of the interface on the side at risk of opening
F	Force, general
F_A	Axial load component in the bolt axis direction of the general working load F_B
F_{Aab}	Axial load at the opening limit during eccentric loading
F_B	Working load in any direction
F_K	Clamp load
F_{Kab}	Clamp load at the opening limit
F_{KA}	Minimum clamp load at the opening limit
F_{Kerf}	Clamp load required for sealing functions, friction grip and prevention of one-sided opening at the interface

F_{KP}	Minimum clamp load ensuring a sealing function
F_{KQ}	Minimum clamp load for transmitting a transverse load by friction grip
F_{KR}	Residual clamp load at the interface
F_M	Assembly preload
ΔF_M	Difference between the assembly preload F_M and the minimum preload $F_{M\,\min}$
$F_{M\,\max}$	Maximum assembly preload
$F_{M\,\min}$	Minimum assembly preload which can occur at $F_{M\,\max}$ with preload losses and lack of precision in the tightening method and maximum friction.
F_{Mzul}	Permissible assembly preload
$F_{M\,0,2}$	Assembly preload at 0,2% proof stress of the bolt
F_{PA}	Additional plate load, proportion of the axial load which changes the loading of the clamped parts
F_Q	Transverse load, general; acting perpendicularly to the bolt axis
$F_{Qzul\,\mu}$	Limiting slip force
F_S	Bolt load
F_{SA}	Axial additional bolt load
F_V	Preload, general
ΔF_{Vth}	Additional thermal load, change in the preload as a result of a temperature different from room temperature.
F_Z	Loss of preload as a result of embedding during operation
$F_{0,2}$	Bolt load at the minimum yield point of 0,2% proof stress (no torsional stress)
f	Elastic linear deformation due to the force F
f_{PA}	Elastic linear deformation of the clamped parts due to F_{PA}
f_{SA}	Elongation of the bolt due to F_{SA}
f_Z	Plastic deformation as a result of embedding
G	Limiting value for the dimensions at the interface area in bolted joints

G'	Limiting value for the dimensions at the interface area in tapped thread joints
h	Height, general
$h_{\min}$	The smaller plate thickness of two clamped plates
I	Areal moment of inertia, general
l	Length, general
l_{Gew}	Length of the free loaded thread
l_K	Clamping length
M_A	Tightening torque during assembly for preloading the bolt to F_M
M_B	Working moment (bending moment) acting on the bolting point
M_b	Additional bending moment at the bolting point from the eccentrically applied axial load F_A or the moment M_B
M_G	Proportion of the tightening torque acting in the thread
M_{Sbo}	Maximum additional bending moment, acting on the bolt
M_Y	Torque about the bolt axis
m_{eff}	Effective length of thread engagement or nut height. Effective thread contact length
m_{ges}	Total length of thread engagement or nut height.
n	Load introduction factor
n_S	Number of bolts
P	Pitch of the thread
p	Surface pressure
p_K	Surface pressure under the bolt head
R_m	Tensile strength of the bolt according to DIN EN ISO 898-1
$R_{p0,2}$	0,2% proof stress of the bolt according to DIN EN ISO 898-1
$R_{p0,2P}$	0,2% proof stress of the plate
S_A	Safety margin against shearing off

S_D	Safety margin against fatigue failure
S_F	Safety margin against exceeding the yield point
S_G	Safety margin against slipping
S_P	Safety margin against surface pressure
s_{sym}	Distance of the bolt axis from the axis of the imaginary laterally symmetrical deformation body
T	Temperature
ΔT	Temperature difference
U	Location at which opening starts at the interface
W_P	Polar moment of resistance of a bolt cross section
W_S	Moment of resistance of the stress cross section of the bolt thread
w	Joint coefficient for the type of bolted joint
α_A	Tightening factor
α_P	Coefficient of linear thermal expansion of the plate
α_S	Coefficient of linear thermal expansion of the bolt
β	Elastic bending resilience, general
γ	Skewness or angle of inclination of clamped parts as a result of eccentric loading; bending angle
γ_S	Bending angle of the bolt
δ	Elastic resilience, general
δ_P	Elastic resilience of the clamped parts
δ_S	Elastic resilience of the bolt
μ_G	Coefficient of friction in the thread
μ_K	Coefficient of friction in the head bearing area
μ_T	Coefficient of friction in the interface
ν	Utilisation factor of the bolt proof stress for allowed assembly preload $F_{M.zul}$

σ_a	Continuous alternating stress acting on the bolt
σ_b	Bending stress
$\sigma_{red,B}$	Comparative stress in the working state
$\sigma_{red,M}$	Comparative stress in the assembled state
σ_z	Tensile stress in the bolt in the working state
τ	Torsional stress in the thread as a result of M_G
Φ	Load factor, relative resilience factor
Φ^*_{en}	Load factor with eccentric clamping and eccentric force application via the clamped parts

The nomenclature is based on VDI 2230. Since it is a German guideline, some subscripts are German. Two of the most frequently used subscripts are:

zul - from “zulassige last”, meaning “allowed loading”

erf – from “erforderlich”, meaning “required”

1 INTRODUCTION

1.1 BACKGROUND

CERN is located on the Swiss-French boarder, close to Geneva. At CERN, the European Organization for Nuclear Research, physicists and engineers are probing the fundamental structures of the universe. The instruments used are purpose-built particle accelerators and detectors. Best known is the 27-kilometre *Large Hadron Collider* (LHC), world's largest particle accelerator [1]. Even though particle physics, investigating antimatter and elementary particles are the main activity, a large amount of technical expertise is required to keep it all running. There are ten times more engineers and technicians employed at CERN than research physicists. The technology present are state of the art and includes the world's largest cryogenic system, cooling the magnets close to absolute zero, ensuring superconducting performance.

In the Engineering Department at CERN (EN-MME), accelerator components with bolted joints are frequently developed. As use of FEA-assisted design is becoming more widespread, questions have been raised about how to best apply FEA in design and verification of bolted joints. During development of past projects, there has been uncertainties regarding central aspects in determination of preload for eccentric load conditions, proper bolt representation in FE-models, and combining simulations and analytic calculations. This sparked an initiative to develop knowledge about how to combine the guideline VDI 2230 with FE-analysis, which lead to this MSc project.

By utilizing the strengths of FEA and the analytic approach in VDI 2230, benefits are expected to be improved quality and validity of the assessment, increased efficiency, and lowered threshold for applying FEA in assessments of bolted joints. Thus, making it easier and quicker to perform high quality design and verification of bolted joints.

The author has been a technical student at CERN during the master project, and worked on various projects. Half of the projects involved activities concerning assessment of bolted joints, and the most relevant research and experiences has contributed to this MSc thesis.

1.2 PROBLEM DESCRIPTION

The guideline VDI 2230 Pt.2 contains some descriptions of how FEA can be applied to aid design and verification of bolted joints, but not in a streamlined way that makes it simple and efficient to apply. Thus, the goal of this thesis is to improve the VDI 2230 guideline in terms of applicability, and possibilities in modern FEA tools.

1.3 PROJECT SCOPE

1.3.1 Objectives

By taking basis in a specific engineering challenge in EN-MME, the objective is to investigate various aspects to improve relevant knowledge, to suggest how FEA and VDI 2230 can be combined in a single workflow, and to present the information in a format it can benefit the engineering department at CERN. The MSc thesis along with appendices should provide

sufficient guidance to perform FEA assisted design and verification of bolted joints according to VDI 2230.

1.3.2 Research Questions

The research questions are:

RQ 1: For a specific case, what were the challenges of combining VDI 2230 and FE-analysis?

RQ 2: How can the identified challenges be met, and avoided in the future?

1.4 Structure of Report

First, some general and basic theory about bolted joints and use of FEA in analysis of bolted joints are presented. Then, the specific case of a Helium vessel bolt assessment for the Crab Cavities is described, illustrating challenges and uncertainties in combining FEA and VDI 2230.

Chapter 4 investigates prying by describing what it is, when it is relevant, and how it can be encountered. Then a study is performed to investigate the influence of preload on prying, before the chapter is concluded by a discussion and a summary.

Chapter 5 propose a basic workflow for combining VDI 2230 and FEA, and include a guide, aspects of more advanced assessments, case examples, calculation support material, and a seminar prepared to educate about assessment of bolted joints.

In Chapter 6, suggestions and recommendations for a potential revision of the Helium vessel analysis is presented.

The discussion in Chapter 7 target the MSc project, some larger perspectives of the project, and possible future research. The thesis is concluded by a summary in Chapter 8.

1.5 Literature

The main literature for this thesis is the VDI 2230:2014 guideline in two parts [2, 3], for *Systematic calculation of highly stressed bolted joints*. Part 1 present a 13-step analytic calculation procedure for design and verification of single bolted joints (SBJ). Part 2 detail how SBJs can be extracted from multi bolted joints through *Rigid Body Mechanics* and *Elastomechanic* methods. Aspects of how FEA can be used to aid the analysis are also included.

The book *Introduction to the Design and Behaviour of Bolted Joints* by J. H. Bickford [4] has served as a useful source of supplementary details to VDI 2230, as it presents and discuss many relevant aspects of bolted joints. However, the nomenclature is different from VDI 2230, and Imperial units is often used.

This thesis is based on investigations and studies presented in two reports [5, 6]. One report was written as a pre-project, and the second report was written as the research activities progressed and is in the format of a chronologic research log.

Throughout the thesis, other references are included where relevant.

2 THEORY

This chapter introduce basic concepts and fundamental theory about bolted joints and FEA representation. First, some central terms are defined. The basics of bolted joints and joint diagrams are then introduced, along with the analytic VDI 2230 calculation guideline. Last, FEA model classes and aspects of bolt representation in MBJs are presented.

2.1 TERMS

SBJ (Single bolted joint)	Bolted joint with one bolt.
MBJ (Multi bolted joint)	Bolted joint with multiple bolts. More than one bolt are involved in transmitting a load or in fulfilling the joints function. The individual bolts may be subjected to markedly different loads.
Load	Quantity of the effect of forces and moments on the structure
Global workload	The global load on the structure/component in operation / working state. Can include pressure, forces, self-weight, …
Bolt workload	The part of the global workload applied to a single bolt
Preload	A certain tensional force created in the bolt from tightening and associated elongation of the bolt in assembled state
Clamped plate / plates	Component / components clamped between the bolt head and nut / tapped threads
Clamping / deformation solid	Volume in the clamped part / parts exposed to elastic strain from bolt preload. Can consist of deformation cone and a sleeve
Contact area	Geometrically defined area through which loads are transmitted from one component to the other by means of the bolted joint / joints
Clamping interface	The contact surface between the components that are bolted together and is involved in force transmission. Area of clamping solid in the contact area.

2.2 BASICS OF BOLTED JOINTS

Bolted Joints (BJs) have the function of clamping separate components together, often transferring forces, moments or sealing against pressurized fluids. To transfer those loads and for the joint to behave as a continuous part of the structure while doing it, BJs must have a certain clamping pressure. To ensure this, bolts are tightened into tension, restricted by their maximum load capacity. To be able to make a knowledge based design considering all requirements, a calculation model can be made and used to aid the assessment.

This section provides a brief introduction to some of the most central elements of bolted joint calculations. VDI 2230 contains comprehensive details on the calculation of BJs, and is

introduced in next section. The theory below assumes a concentrically clamped bolt, with concentric and axial loading in tension.

2.2.1 Classification and Characteristics of BJs

Bolted joints can have a variety of designs, resulting in different load characteristics in distribution and type of loading. Table 1 list different types of SBJs and MBJs, with concentric, eccentric, symmetric, and asymmetric geometries and loading. Simplified calculation-models with relevant loads are included, as well as relevant calculation approaches. FEM applies to all joint types. VDI 2230 apply to 1 and 2, and with limited treatment: 3, 4, 6, 7 and 8. The flange with sealing gasket, 5, are covered by *DIN EN 1591*.

Table 1: Outline of BJs [Pt.1 - Table 1]

Single-bolted joints		Multi-bolted joints						Bolted joints
concentric or eccentric		in a plane	axial symmetry			symmetrical	asymmetrical	bolt axes
cylinder or prismatic body	beam	beam	circular plate	flange with sealing gasket	flange with plane bearing face	rectangular multi-bolted joint	multi-bolted joint	joint geometry
①	②	③	④	⑤	⑥	⑦	⑧	
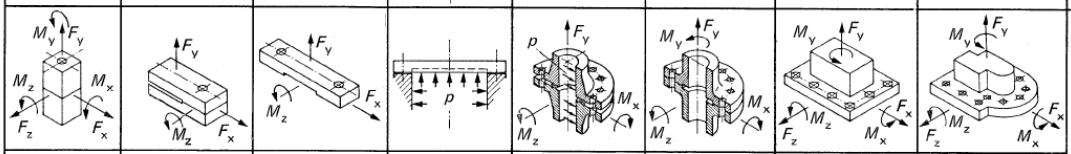								relevant loads
axial force F_A transverse force F_Q working moment M_B	axial force F_A transverse force F_Q moment in the plane of the beam M_Z	axial force F_A transverse force F_Q moment in the plane of the beam M_Z	internal ressure p	axial force F_A (pipe force) working moment M_B internal pressure p	axial force F_A torsional moment M_T working moment M_B	axial force F_A transverse force F_Q torsional moment M_T working moment M_B	axial force F_A transverse force F_Q torsional moment M_T working moment M_B	forces and moments
VDI 2230		limited treatment by VDI 2230		DIN EN 1591 AD 2000 Note B7	limited treatment by VDI 2230			calculation procedure
bending beam theory with additional conditions			plate theory		limited treatment using simplified models			
finite element method (FEM)								

Two main types of bolted joints are shown in Figure 1. In the tapped thread joint (TTJ), the bolt runs through a clearance hole in the first plate, and enters tapped threads in the second plate. The through bolted joint (TBJ) has clearance hole in both plates, and is fastened by a nut. The two types of joints are often referred to in the standard, and both entail special considerations.

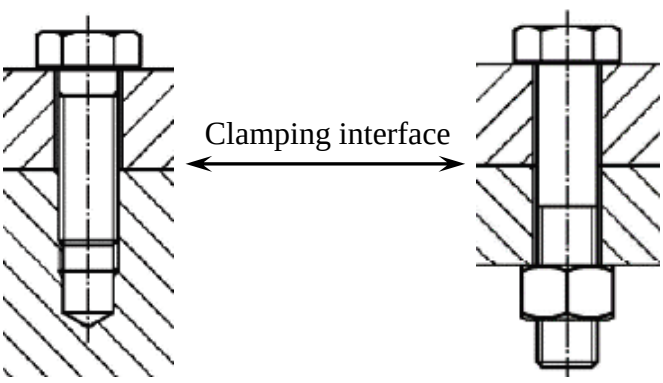

Figure 1: TTJ & TBJ [Pt.2 - Figure 45 & 48]

The most central bolt parameters are illustrated in Figure 2. The bolt is often referred to by its nominal bolt diameter (d). The clamping length (l_K) is the part of the bolt that runs through the clearance hole in the plate / plates. The total thread length or nut height is m_{ges}, and the effective thread length of engagement is referred to as m_{eff}. The part of the bolt shaft without threads are referred to as *shank*. In the Figure 2, the bolt has a section with reduced shank diameter.

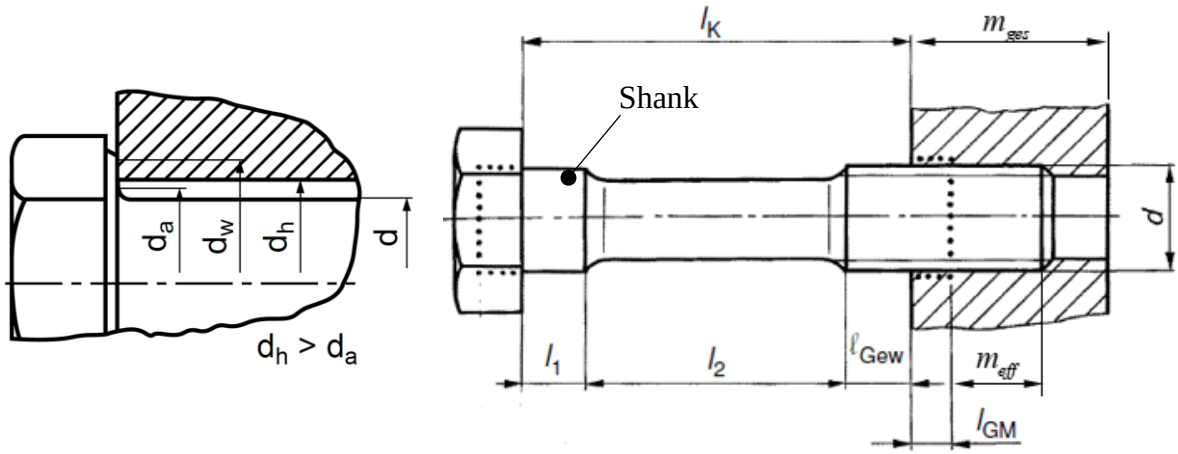

Figure 2: Dimensions associated with a bolt and tapped threads

2.2.2 Spring Model

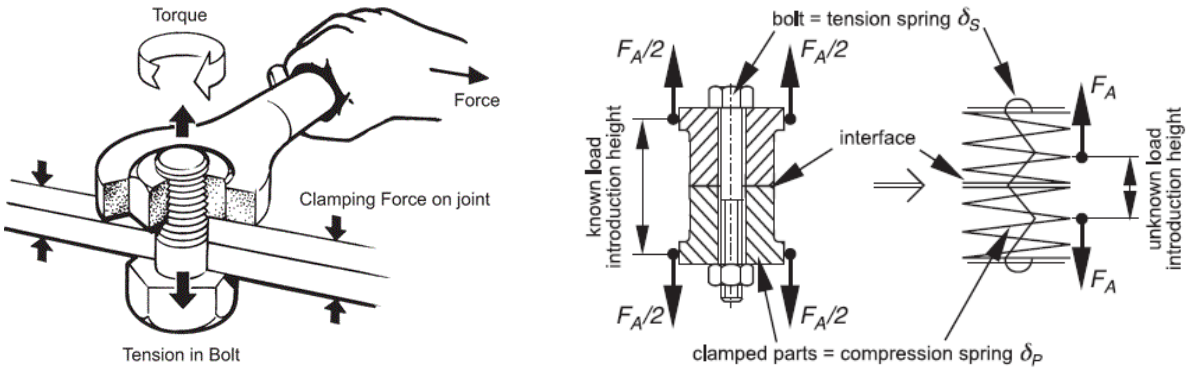

Figure 3: Mechanical Spring Model of a Clamped BJ [Pt.1 - Figure 1]

For a single bolt joint (SBJ), as the bolt is tightened, a force stretches the bolt and clamps the plates together (Figure 3). The bolt and clamped plates behave in an elastic manner. The bolt is elongated, and the clamped parts are compressed. A mechanical spring model, Eq. (1), can be used to describe the relation between forces F and deformations f.

$$F = k \cdot f \tag{1}$$

The stiffness k for a cylindrical body is:

$$k\ [\text{N/mm}] = \frac{E\ [MPa] \cdot A\ [mm^2]}{l\ [mm]} \tag{2}$$

When a bolt consists of multiple cross-sections, the combined stiffness is calculated according to Eq. (3).

$$\frac{1}{k_{tot}} = \frac{1}{k_1} + \frac{1}{k_2} + \frac{1}{k_i} \tag{3}$$

In VDI 2230 however, the term resilience is used, calculated according to Eq. (4). This quantity is the inverse of stiffness and describes the compliance.

$$\delta \text{ [mm/N]} = \frac{l \text{ [mm]}}{E \text{ [MPa]} \cdot A \text{ [mm}^2\text{]}} \tag{4}$$

Using the resilience, summation of multiple cross-sections in series are simple, as Eq. (5) show.

$$\delta_{tot} = \delta_1 + \delta_2 + \delta_i \tag{5}$$

With the quantity resilience, the general force expression of forces is given in Eq. (6).

$$F = \frac{f}{\delta} \tag{6}$$

2.2.3 Joint Diagram

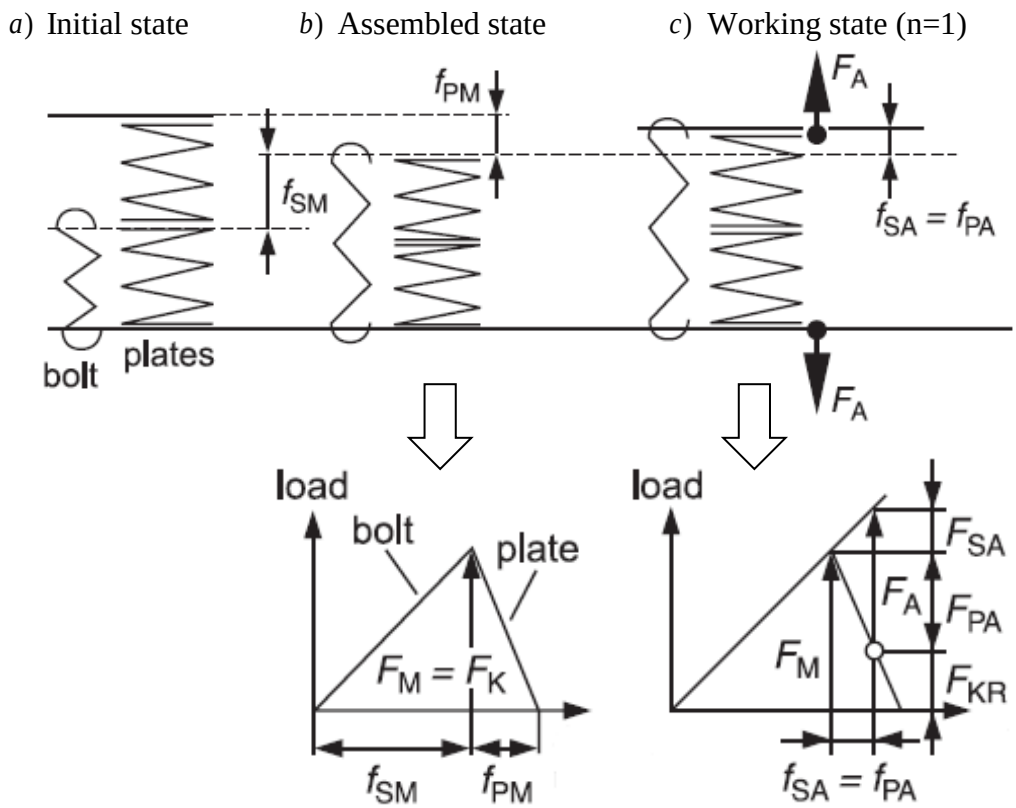

Figure 4: Distortion triangle [Pt.1 - Figure 2]

A joint diagram is a graphic representation of the forces and displacements of the bolt and the clamped parts in a bolted joint. Figure 4 show a BJ in a) initial state, in b) assembled state, and in c) working state. In assembled state, only internal forces apply. When the bolt is tightened, the assembly preload F_M is generated. This give the clamp force F_K at the interface, as seen in

Figure 3. The corresponding displacement of the bolt f_{SM} and of the plates f_{PM} are displayed. The relation between displacements and forces are linear, as Eq. (1) show. The stiffer the component is, the more steep the line becomes.

In working state, an external force is applied. Depending on where the force is applied, this force will increase the load on some parts, and relief others. In Figure 4c, the workload (F_A) is applied to the bolt in the bolt head area (n=1). Depending on the stiffness ratio, or load factor (Φ) between the bolt and the clamped parts, the workload is distributed between stretching the bolt, designated as additional bolt load (F_{SA}), and relieving the clamped parts, designated as additional plate load (F_{PA}). The displacement due to the workload is the same for the bolt and clamped parts ($f_{SA} = f_{PA}$).

The effect of workload is that the bolt load become higher than in assembled state. This gives the load the bolt must be designed to withstand, checking against the maximum capacity of the bolt. The relief of the clamped parts reduces the clamping force in the interface, giving the residual clamp load F_{KR}. This has to be checked against the defined clamping requirements for the bolted joint.

Note that in the working state above, the load introduction factor is: $n = 1$. For most cases the load is introduced somewhere between the clamping interface and the surface ($n < 1$), like in Figure 5. That results in a section of the parts also having to be compressed by the workload, in addition to stretching the bolt. This reduces their combined stiffness. The remaining clamped part get a higher stiffness, increasing the effect of the work load on the residual clamping force. Thus, where the load is introduced in the joint is of great importance. Using analytic methods, this load introduction factor has to be estimated.

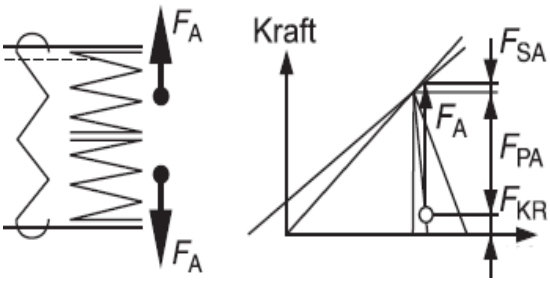

Figure 5: Distortion triangle for n<1

[Pt.1-Figure 2]

2.2.4 Calculation of Forces

The relation between the elastic resilience of the bolt (δ_S) and the clamped parts (δ_P) gives the load factor (Φ), as Eq. (7) show. The load introduction factor n has a value between 0 and 1.

$$\Phi = n \cdot \frac{\delta_P}{\delta_P + \delta_S} \tag{7}$$

The load factor gives the proportion of the applied workload (F_A) that makes up the additional bolt load (F_{SA}) as seen in Eq. (8), and the relief in the clamped parts (additional plate load F_{PA}) as stated in Eq.(9). The sum of the "additional" loads equals the workload, as Eq. (10) show.

$$F_{SA} = \Phi \cdot F_A \tag{8}$$

$$F_{PA} = (1 - \Phi) F_A \tag{9}$$

$$F_A = F_{PA} + F_{SA} \tag{10}$$

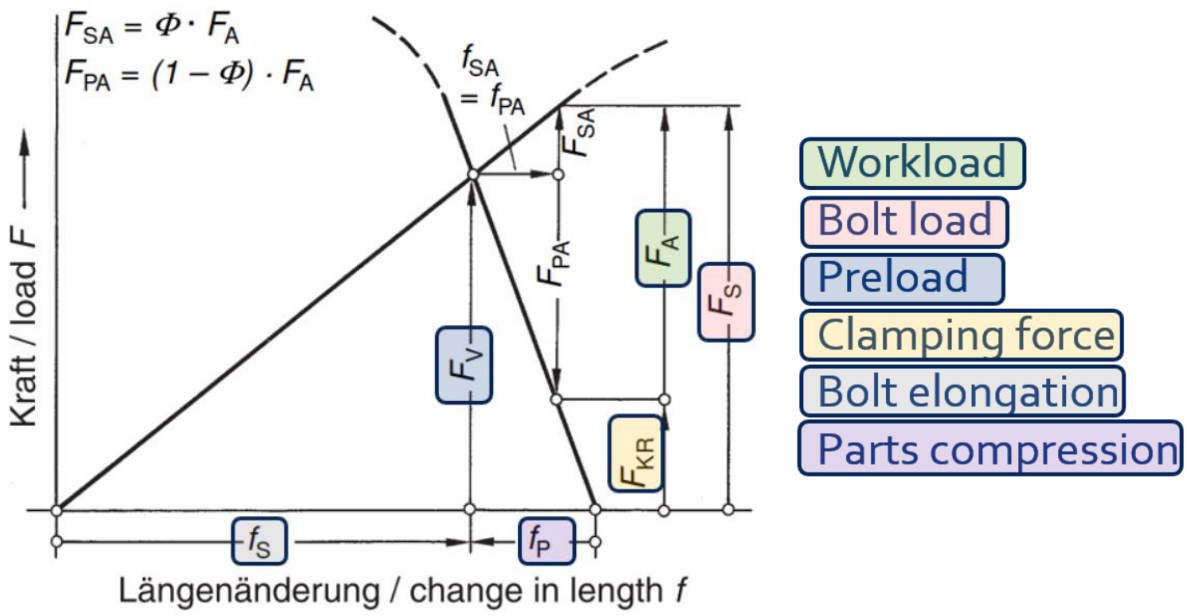

Figure 6: Joint diagram with associated quantities [Pt.1 - Figure 22]

The "additional" loads are a result of the workload, and the total load in the bolt and in the clamping interface depends on the preload. Taking the general preload (F_V) into consideration, the residual clamp load (F_{KR}) , and the bolt load (F_S) can be calculated according to Eq. (11) and Eq. (12). The associated quantities can be identified in Figure 6.

$$F_{KR} = F_V - F_{PA} \tag{11}$$

$$F_S = F_V + F_{SA} \tag{12}$$

The bolt stress can be calculated for both assembly and working states, and are calculated for the bolt stress area (A_S). The assembly stress ($\sigma_{red.M}$) depend on the required tightening torque (M_A) to achieve the permitted assembly preload ($F_{M.zul}$). The working stress ($\sigma_{red.B}$) are based on the maximum bolt load ($F_{S.max}$). These equations are presented later in the thesis.

2.2.5 Additional Factors to Consider

As section 2.2.4 show, the principles of calculating quantities in BJs are not that complicated, and most of VDI 2230 are based on that simple theory. However, the above equations are only valid for concentric joints, both in terms of clamping and loading. In practice, there are many factors that complicate the calculations, which VDI 2230 presents techniques and strategies to handle, making VDI 2230 a comprehensive standard.

Just identifying the bolt workload can be a complex task. There may be transverse loads, moments, and a complex geometry. Both loading and clamping can be eccentric, leading to bending effects and uneven distribution of pressure in the interface that may result in partial joint opening. The preload itself may also change due to numerous reasons: tightening of other bolts in the area, embedding of contact or thread surfaces, self-loosening by rotation, relaxation of the materials, temperature change, or by overloading the BJ.

There is also uncertainty involved in tightening of the bolts, depending on the accuracy of the tightening method. This results in a spread between the maximum and minimum probable

preload. The strategy is then to define a tightening torque to achieve the maximum preload, making sure that the minimum preload is achieved. Verifications then has to be performed for the preload extremes. The maximum bolt load occur with the maximum preload, and the minimum clamp load occur with the minimum preload.

From the above, it is clear that a structured approach is required to perform a safe assessment of bolted joints, taking all the relevant factors into consideration. This is what VDI 2230 provides with defined calculation steps, verification strategies, and assessment criteria. The analytic procedure is described in further detail in section 2.3.

2.2.6 Deformation Cones and MBJ aspects

As described, when the bolt is elongated, the clamped parts are compressed. The volume in the clamped parts that is compressed is assumed to form a prismatic solid, and is referred to as *clamping* or *deformation solid*. The shape of the clamping solid depends on if it is a TBJ or TTJ, as Figure 7 show. The pressure distribution in the clamping interface is different for the two clamping solids, because the clamping interface cut the clamping solids at different locations. If the clamping interface is smaller than the diameter of the clamping solid in the interface cross section, the deformation solid will consist of a cone and a sleeve, as seen in Figure 8. The clamping pressure is then distributed across the whole interface.

The resilience of the clamped parts depends on the volume of the clamping solid, and can be estimated by analytic methods.

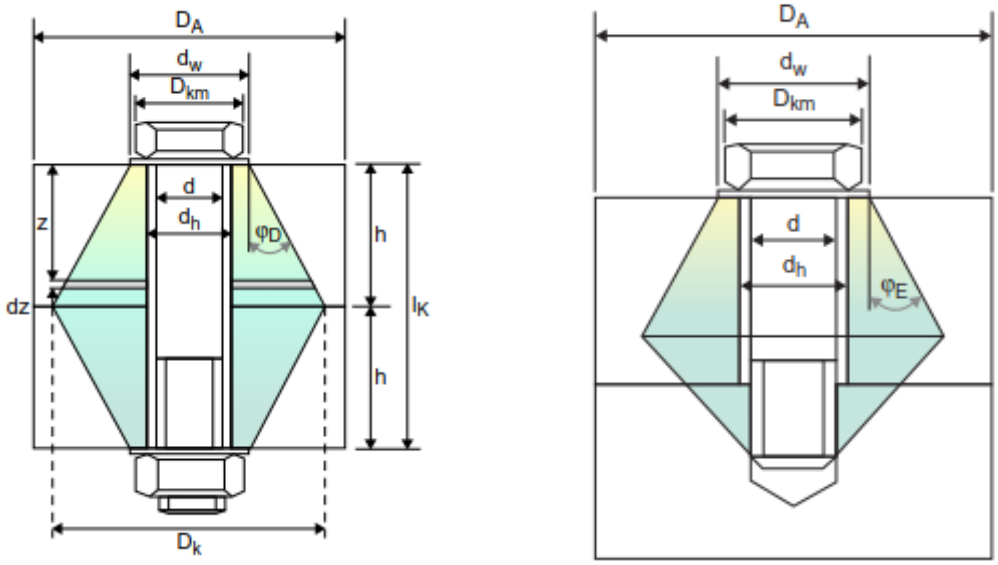

Figure 7: Deformation cones for a TBJ and a TTJ [7]

VDI 2230 defines a limiting diameter G in [Pt.1–5.1.2.2], which is calculated according to (13) . This value defines the diameter where the compressive stresses in the clamping interface is significant. For the analytic VDI 2230 approach to be valid, the clamping interface must be smaller than the limiting diameter G. This is controlled in the step R0.

(R0/1) & **(R0/2)**

$$\begin{aligned} &\text{TBJ:} \quad G = h_{\min} + d_W \\ &\text{TTJ:} \quad G' \approx (1{,}5...2) \cdot d_W \end{aligned} \tag{13}$$

When the limit criteria is fulfilled, there is sufficient pressure at the edges of the clamping interface so that no opening occur, and the analytic equations are valid. If the interface width exceeds the values in (14), joint opening can occur just by preloading the bolt.

$$\begin{aligned} &\text{if } D_A > G \\ &\text{TBJ:} \quad \mathrm{D}_A \approx (1{,}4...1{,}6) h_{\min} + d_W \\ &\text{TTJ:} \quad \mathrm{D}_A \approx 4{,}2 \cdot d_W \end{aligned} \tag{14}$$

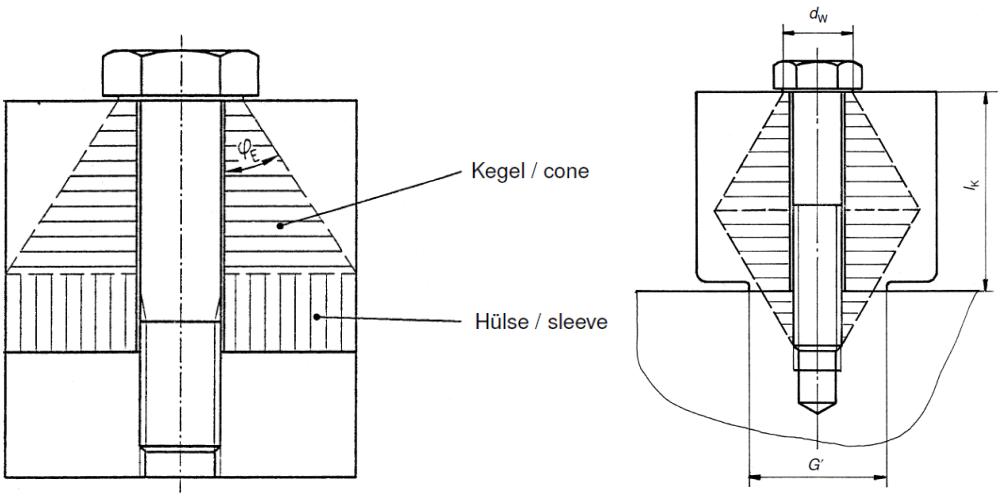

Figure 8: Deformation cone and sleeve (left) and limit criteria G (right)

For MBJs, the same principle of interface-width applies to bolt spacing. The clamping solids must interact to provide a sufficient and continuous pressure in the clamping interface (Figure 9). Put simple, the clamping cone has to be cut on all sides to provide proper clamping pressure in the interface. Conventional bolt spacing e_1 is: $3d_h \leq e_1 \leq 5d_h$.

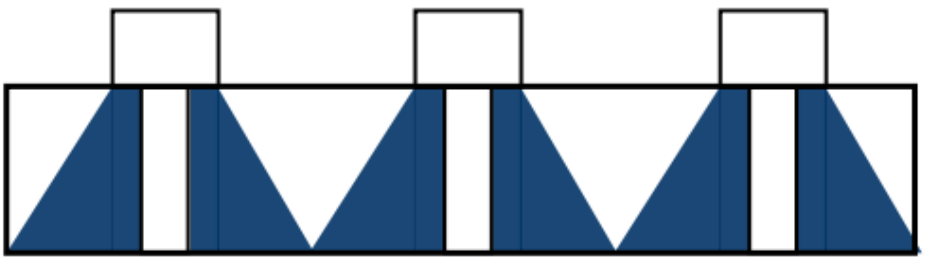

Figure 9: Clamping solid interaction in MBJs

2.3 ANALYTIC VDI 2230 PROCEDURE

The calculation procedure defined in VDI 2230 consist of 13 steps, and is outlined in Table 2. First, input parameters are decided, and the validity is controlled. Then values of the joint diagram are calculated and the clamping requirement is defined. The last steps include stress calculations and strength verifications, before the tightening torque is determined. The factors controlled and accounted for by the procedure are listed in Table 3.

The complete analytic verification procedure is presented in [Pt.1–Ch.4], also containing relevant cross-references.

Table 2: Outline of the analytic VDI 2230 procedure [Pt.1 – 4.1]

Inputs		
R0	Nominal diameter and limiting measurement	d, G
R1	Tightening factor	α_A
R2	Minimum clamp load	F_{Kerf}
Joint Diagram		
R3	Dividing the workload / load factor	F_{SA}, F_{PA}, Φ
R4	Preload changes	$F_Z, \Delta F'_{Vth}$
R5	Minimum assembly preload	$F_{M\,\min}$
R6	Maximum assembly preload	$F_{M\,\max}$
Stress Cases and Strength Verifications		
R7	Assembly stress	$\sigma_{red.M}, F_{Mzul}$
R8	Working stress	$\sigma_{red.B}, S_F$
R9	Alternating stress	$\sigma_a, \sigma_{ab}, S_D$
R10	Surface pressure	$p_{\max}, S_p$
R11	Minimum length of engagement	$m_{eff\,\min}$
R12	Slipping, shearing	$S_G, \tau_{Q\max}$
R13	Tightening torque	M_A

Figure 10 displays a joint diagram containing the most relevant quantities used in the analytic VDI 2230 design and verification procedure. It can be seen from the steps in Table 2 that the required clamp load (F_{Kerf}) is calculated early. Then, preload loss due to embedding (F_Z) and additional thermal load (ΔF_{Vth}) are calculated. Together they give the minimum required assembly preload (F_{Mmin}). Taking the tightening uncertainty (α_A) into account, the required maximum assembly preload (F_{Mmax}) is calculated according to Eq. (15).

$$\begin{aligned} F_{M\,\min} &= F_{Kerf} + (1-\Phi)F_A + F_Z + \Delta F_{Vth} \\ F_{M\,\max} &= \alpha_A \cdot F_{M\,\min} \end{aligned} \tag{15}$$

The permitted assembly preload (F_{Mzul}) is then calculated, and has to be larger than the required maximum assembly preload (F_{Mmax}). If not, the bolt diameter or strength class has to be modified to achieve a higher allowed assembly preload. If it is larger, the permitted assembly preload is used to define the tightening torque. The spread between required and allowed assembly preload provides a safety factor against the clamping requirements.

$$F_{S\,\max} = F_{Mzul} + \Phi F_A - \Delta F_{Vth} \tag{16}$$

Eq. (16) give the max bolt load in working state ($F_{S\,max}$), and is used to calculate the work stress.

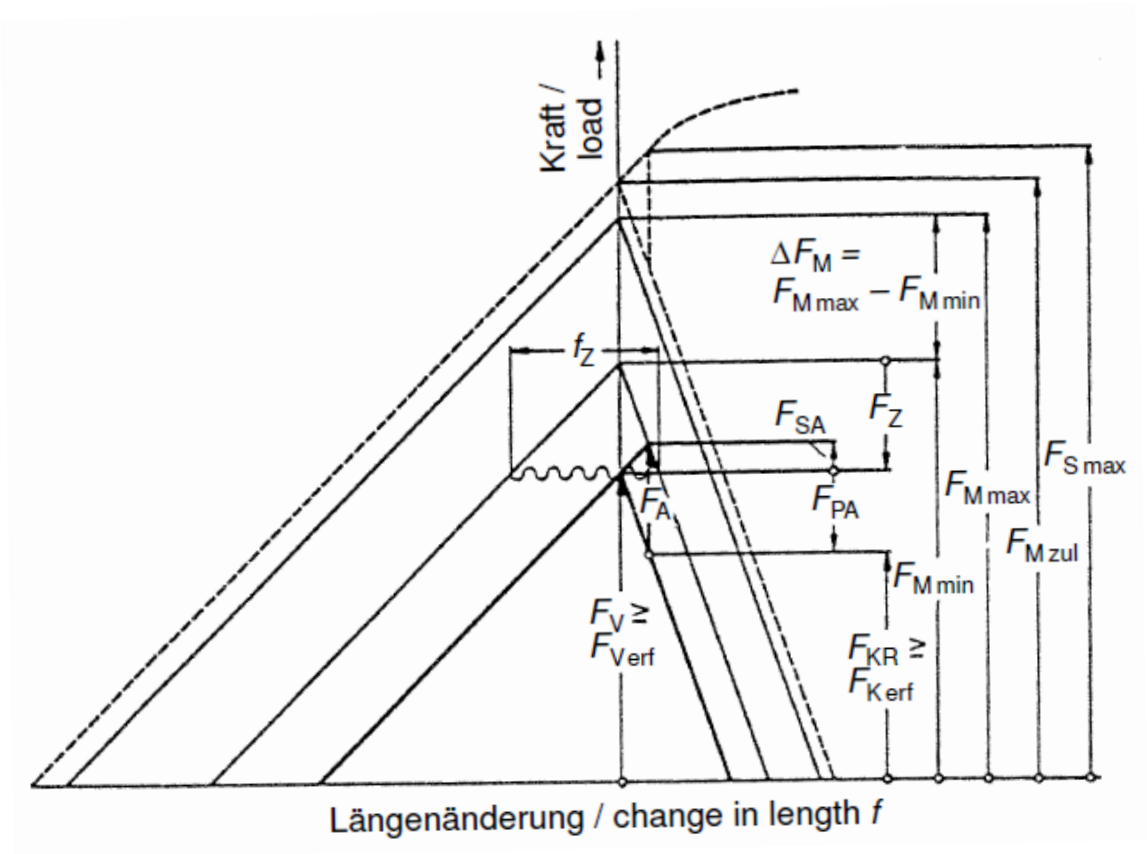

Figure 10: Joint diagram with analytic VDI 2230 quantities [Pt.1 - Figure 5]

The validity of the analytic calculations relies on the following assumptions:

- Liner-elastic material behaviour
- Very small deformations, cross-sections remain flat
- Compliance with the limit distance G or G` (Step R0)

Table 3: Factors considered in the calculation procedure

Factors controlled	Factors accounted for

• Minimum clamping pressure, resisting:
  ○ Transverse slip
  ○ Internal pressure
  ○ Opening of the joint interface
• Assembly stress in bolt
• Working stress during operation
• Fatigue due to alternating stress
• Surface pressure at bolt head bearing area
• Thread engagement length
	• How applied work load divides between increasing bolt load and relieving the clamped parts
	• Uncertainty in preload from tightening
	• Embedding and thermal changes of preload
	• Friction at interface and in the threads
	• Residual tightening torque in bolt

2.4 FEA Model Classes

VDI 2230 Part 2 divides FE-modelling of BJs into four basic model classes, as shown in Table 4. These classes have different level of details, required modelling efforts, and different practical considerations related to applicability in FE-analysis. It is the scope of the analysis that defines which model class most appropriate to use. There are advantages and disadvantages with all classes.

All the classes and how they can be used to derive analytic calculation quantities, and important aspects to achieve as realistic representation as possible are described in [Pt.2–Ch. 7].

Table 4: Overview of the model classes [Pt.2–Table 1]

	Class I	Class II	Class III	Class IV
	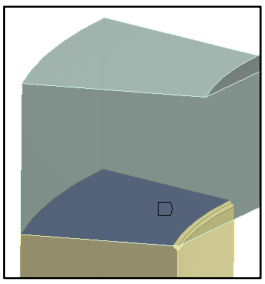	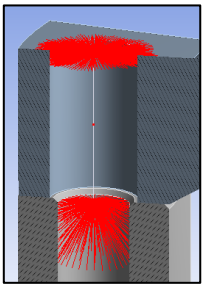	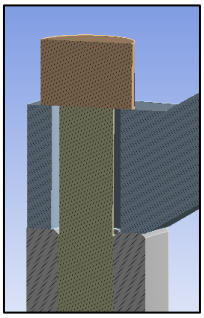	
Characteristic	Bolt and interface are not taken into consideration. Preload is not included in representation	Bolt is represented by a beam. Preload and interface contact can be included	Bolt is represented by a volume body. Preload and interface contact can be included	Bolt is fully modelled and include threads, preload, and contact on all surfaces

Objective of calculation	Internal forces in the clamping interface as determination of workload, or determination of analytic calculation quantities	Internal forces in the bolt	Internal forces in the bolt	Internal forces in the bolt, local stress in bolt threads and clamping area

2.4.1 Class I

The components are modelled as a continuous solid, without any bolt. This allows for extraction of internal loads in the relevant cross-section, when exposed to working loads. The cross-section forces and moment then serve as input parameters for the calculation procedure, giving the bolt workload that the bolt has to withstand. The arm "a" to the application point of eccentric loading can be determined according to Figure 11 and Eq. (17).

If the components are modelled as two bodies, they can be connected using a “bonded” contact formulation. This approach simplifies extraction of the loads in the relevant cross-section. For MBJs, the solids may be connected by spot welds where the bolts are located, for simple extraction of the bolt workload.

The exact influence of the bolt resilience and preload is not considered, and it is not possible to assess the clamping conditions. Therefore, this class has some limitations, and is primarily used for determination of workload (F_A).

$$a = \frac{M_K}{F_K} \tag{17}$$

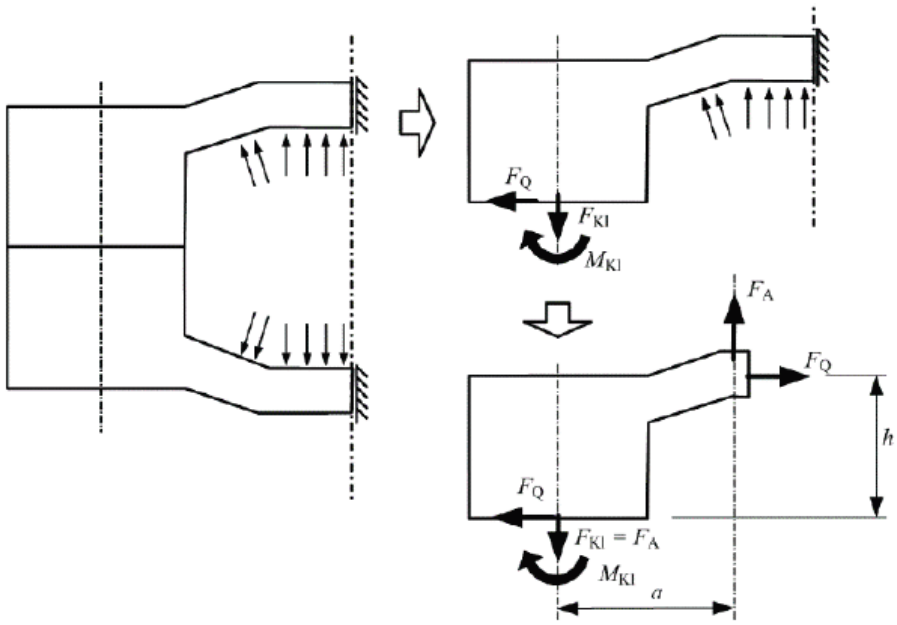

Figure 11: Intersection forces Class I [Pt.2 - Figure 60]

2.4.2 Class II

The bolt is represented by a line-element with the same properties as the bolt in question. The line-element may be a tension-member, beam element or a spring. This element is connected to the components via multiple point constraints (MPC), or kinematic joint definitions. The connections should be applied in the actual bolt head bearing area and tapped tread length only, to have a more realistic compliance. However, using MPC joints to attach the line-element, artificial stiffness is often introduced. If the bolt properties are defined from the analytic axial and bending resilience, this can be partially avoided. Also note the effect of MPC connection for TTJs on the pressure distribution in the clamping interface, demonstrated in Figure 12. It can be seen that artificial high pressures are present close to where the MPCs are connected.

Preload can be applied and clamping pressure in the interface and joint opening can be assessed. Internal bolt forces is easily be extracted, and can serve as input parameter for analytical calculations. Joint slip due to low clamping pressure is challenging to identify, as both ends of the beam are fixed to the components. Some techniques to assess slipping include monitoring of shear force and bending moment in the beam. Sudden changes, or high values, can indicate that slipping would happen. Analytic verification calculations can be used to assess the safety factor against slipping.

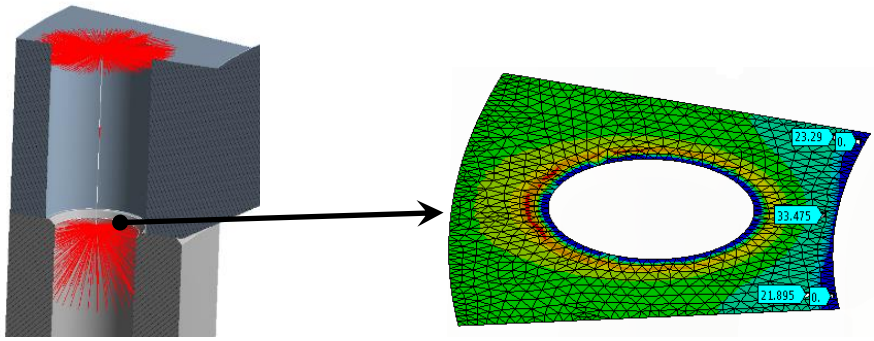

Figure 12: Effect of rigid MPCs on mesh stiffness and the resulting pressure distribution with Class II model

2.4.3 Class III

In this class, the bolt is represented by a solid volume body. Through the bolt material properties, the bolt compliance is represented in the FE-model by the relevant constitutive equations. Contact in the bolt head bearing area is well represented, and no artificial stiffness are introduced. Assessment of joint slip and tendency to self-loosening can be carried out.

The resilience of the bolt depends on the bolt diameter. A simple approximation is to use a uniform diameter based on the thread minor diameter (d_3). If there is a shank, it can be modelled with the bolt nominal diameter. Further details on this topic are described in 2.4.6.

Preparing a Class III model requires some more effort than with Class II, especially for MBJs with a large number of bolts. However, in some cases it still may be beneficial to use a Class III model.

2.4.4 Class IV

For this class, the bolt is modelled in detail down to the correct radius in the bottom of the threads, and contact conditions are applied to all thread surfaces. The strength of this class is assessment of micro behaviour and stress concentrations, and will not be practical to use with VDI 2230 verifications or in a large scale load analysis. The required simulation and modelling efforts are very high.

2.4.5 Comparison of Model Classes

Table 5 compares the different model classes, and how central model parameters are represented.

Table 5: Comparison of FE-model classes [Pt.2 – Table 2]

Model class:	**I**	**II and III**	**IV**
Modelling of the BJ			
Effort	low	medium	high
Idealisation of the bolt	not modelled	simplified	modelled in detail
Contact conditions in the interface	not modelled	modelled	modelled
Preload	without	with	with
Required parameters from VDI 2230 Part 1 – relevant section number is indicated			
Compliance of the bolt δ_S	5.1.1	5.1.1 / included in the model	included in the model
Compliance of the plates δ_P	5.1.2	included in the model	included in the model
Load application factor n	5.2.2	included in the model	included in the model
Tightening factor α_A	5.4.3	5.4.3	5.4.3
Amount of embedment f_Z	5.4.2.1	5.4.2.1	5.4.2.1

2.4.6 Bolt Diameter

There are three natural bolt diameters to use when modelling the bolt: nominal diameter (d), thread minor diameter (d_3), and diameter based on the analytic bolt resilience (d_δ).

A diameter based on the thread minor diameter is the most simple option, and provides a fairly realistic bolt resilience.

The diameter based on analytic bolt resilience can be calculated according to Eq.(18), and require that the analytic resilience is known. Calculation of this is described in [Pt.1–5.1.1].

[Pt.2 - Eq.79]

$$A_\delta = \frac{l_k}{E_S \cdot \delta_S} \quad , \quad d_\delta = \sqrt{\frac{\pi}{4} \cdot A_\delta} \tag{18}$$

$$I_\beta = \frac{l_k}{E_S \cdot \beta_S} \tag{19}$$

For Class II beams, there is a possibility to define a “user integrated” cross section for the beam with separate definition of cross section area and areal moment of inertia. Those properties can be calculated according to (18) and (19) from the analytic axial and bending resilience. With this option, it is ensured that both axial and bending properties of the beam correspond to the analytic resiliencies.

2.4.7 Validity in Resilience Representation

The resilience representation in the joint is of importance and affect the “load factor” in the FE-model. How the workload is distributed between relieving the clamped plates and increasing the load in the bolt.

The mesh has to be refined in the clamping solid volume to have an accurate representation of the clamping solid and the clamped parts resilience. The representation of clamping solid also affect the clamping pressure distribution in the interface in the model.

Both the bending and axial resilience of the bolt in the FE-model can be inaccurate. With respect to the bolt loads, the most conservative is that the FE-bolt is too stiff. The bolt will then absorb higher axial load and bending moment than what might be realistic. Note that this also can affect the load limit for joint opening. The uncertainty can be quantified by performing a sensitivity study, or by comparing with analytic values.

For traditional joints with high preload, and where the bolt is much more resilient than the clamped plates, the additional bolt loads are often small. In such cases, the effect of inaccurate bolt resilience representation can be less critical.

3 DQW CRAB CAVITIES HELIUM VESSEL ANALYSIS

The scope of this chapter is to investigate how VDI 2230 has been combined with FEA for a practical case. It will introduce the Crab Cavities Helium vessel, and its role in the context of LHC (Large Hadron Collider) and the High Luminosity upgrade. Then, the analysis of the bolted joints will be presented and used as basis to identify challenges, and how those challenges could be countered.

3.1 INTRODUCTION TO THE CRAB CAVITIES

3.1.1 LHC

At CERN, particles are accelerated to 99.9999991% the speed of light and to a kinetic energy of 7 TeV[1] [8]. The acceleration happens through 5 accelerator steps, as illustrated in Figure 13. For acceleration of protons, a small bunch of Hydrogen atoms are ionized, and accelerated in LINAC 2 to 30% the speed of light. Then the BOOSTER, PS, SPS, and LHC accelerate the particle bunches to the maximum energy levels.

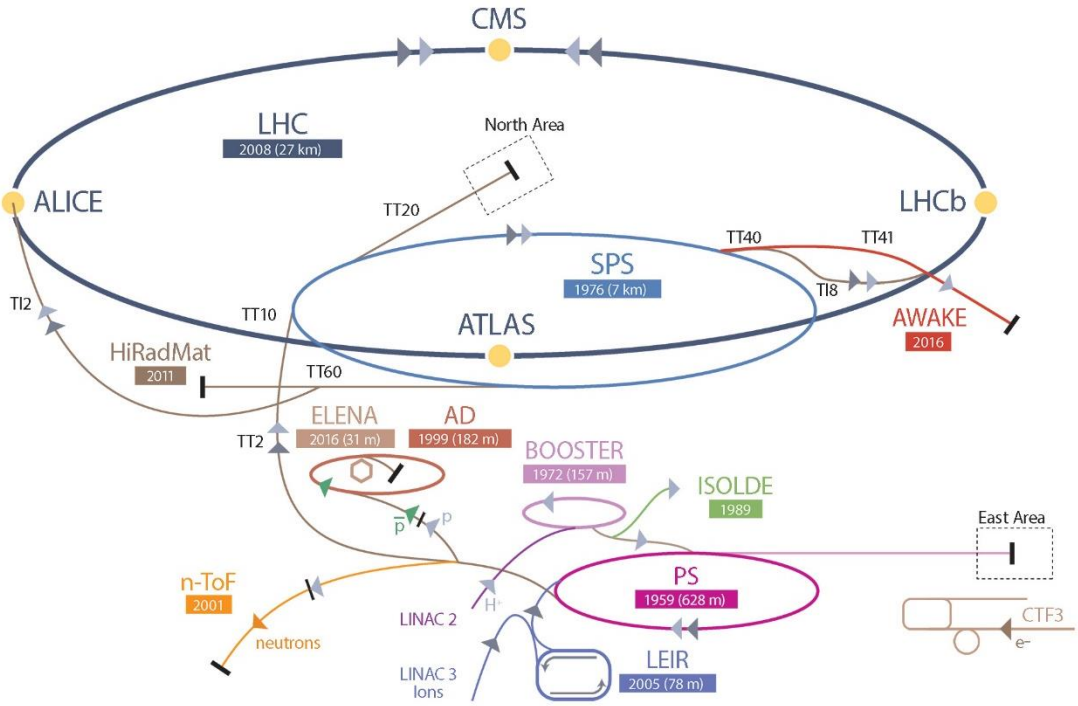

Figure 13: The CERN accelerator complex © CERN

The *Large Hadron Collider* (LHC) is one of the largest scientific instruments ever built. It has a circumference of about 27 km, and is located 100m underground in average. Magnetic fields from superconducting dipole magnets curve the particle trajectories, and electromagnetic resonators (RF-cavities) accelerate the particles. There are two proton beams circulating in opposite directions, and the design capacity is 2808 bunches per proton beam. Each bunch contain $1.2 \cdot 10^{11}$ protons, and circulate 11 245 rotations per second. One bunch is 30 cm long (1 ns), and has a diameter of one millimetre when far from the collision point. Before collision, they are squeezed to about 20 micro-meters in diameter. There are about 7.5m between the bunches (25 ns), and the beam is kept within +/- 7mm traveling through LHC. The particles

[1] 1 eV = $1.6 \cdot 10^{-19}$ Joule. Thus 14 TeV = $22.4 \cdot 10^{-7}$ Joule. 1 TeV equals the energy of a flying mosquito.

travel in UHV (Ultra-high Vacuum, 10e-10 mbar), and the beam pipe is cooled to 1.9K (-271.3℃) by superfluid Helium.

3.1.2 Collisions and Luminosity

At four locations around LHC, the two particle beams are crossed to collide particles. These collisions are probed by the detectors ATLAS, CMS, ALICE and LHCb, as seen in Figure 14. Since the particle beams travel in opposite directions, the collision energy is 14 TeV.

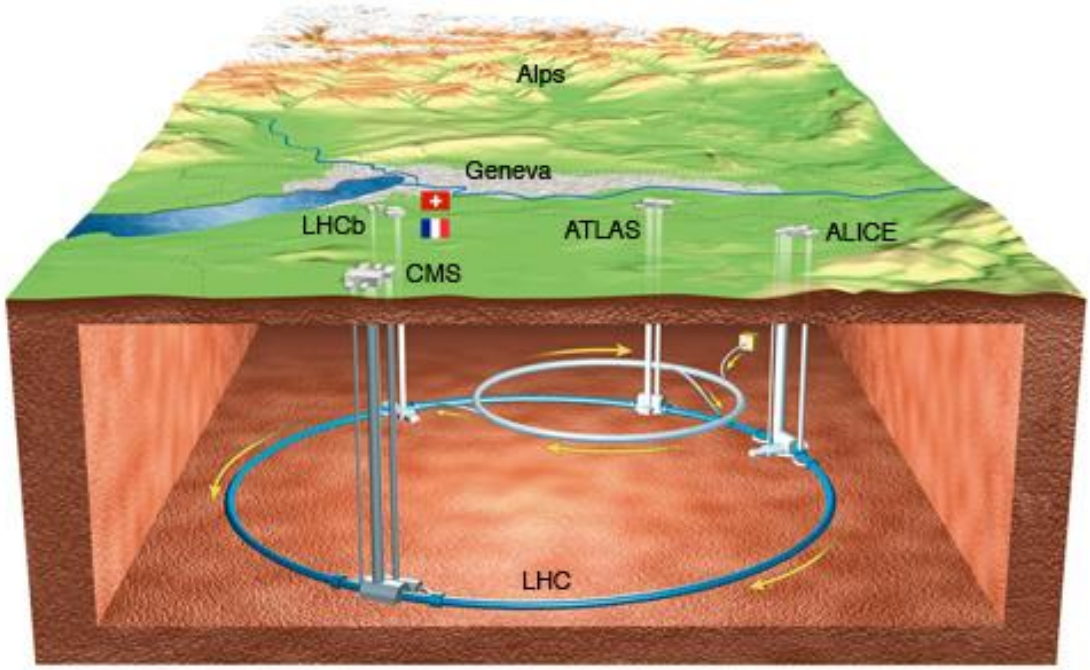

Figure 14: Location of detectors around LHC © CERN

The detectors track secondary particles from the collisions, and study processes that vary with collision energy and are often rare. Therefore, the goal is to have high collision energy, and a large number of collisions.

There are about 100 billion particles in each bunch, but there is a very low probability of collisions. The average number of collisions for each bunch crossing is 40, resulting in a total of 1 billion collisions per second. The amount of collisions per time unit (rate) can be expressed as *luminosity*. The integrated luminosity will then be the total number of collisions. To make statistically significant discoveries, the integrated luminosity must be as high as possible. Some parameters that influence the number of collisions are: number of particles in each bunch, number of bunches, frequency of bunch rotations, and beam cross section.

3.1.3 HL-LHC and Crab Cavities

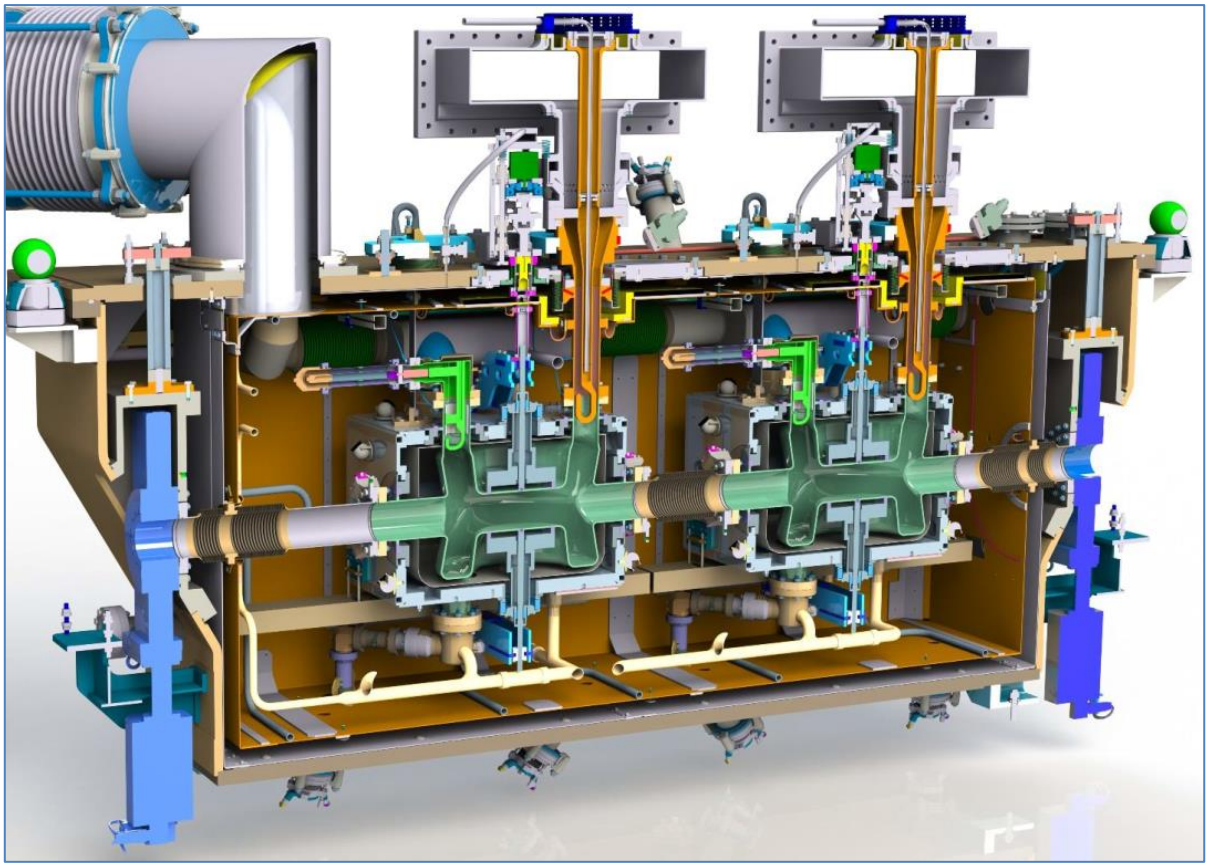

Figure 15: Cryomodule with two DQW Crab Cavities ©CERN

To increase the luminosity of LHC, a large upgrade of the performance is planned. The new configuration is known as *High Luminosity* LHC (HL-LHC), and will rely on a number of key innovations to push the accelerator technology beyond its present limits. HL-LHC will increase the luminosity by a factor of five beyond the original design value, and the integrated luminosity by a factor of ten [9]. One of those key innovations are RF-deflectors, compact superconducting cavities for beam rotation, often referred to as Crab Cavities (Figure 15 and Figure 16).

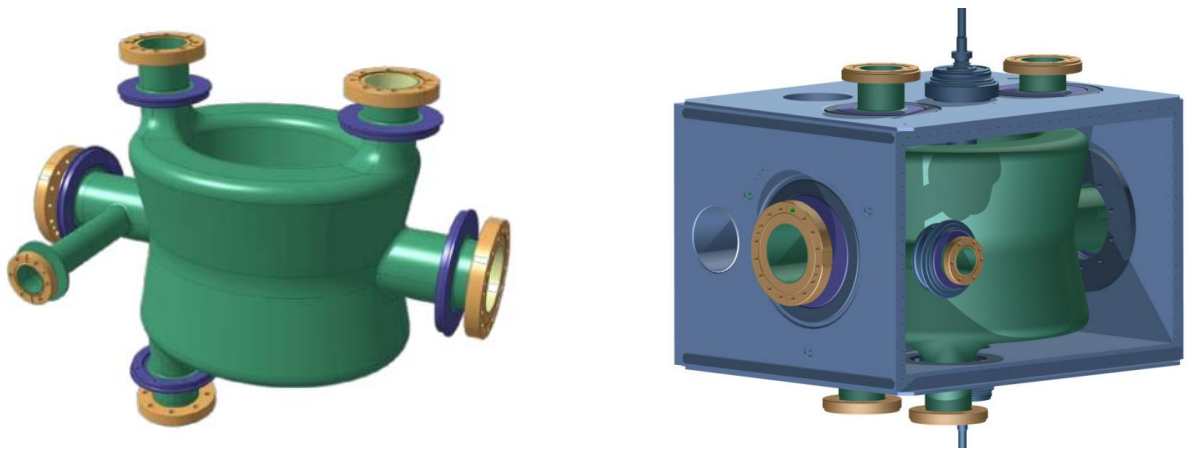

Figure 16: DQW Crab Cavity, bare (left) and in He-vessel (right) ©CERN

At the collision point, bunches cross as shown in Figure 17, having a certain crossing angle. A significant increase in the probability for collisions and gain in luminosity can be obtained from achieving a more head-on crossing, like seen in centre of Figure 17. To achieve that, Crab Cavities are to be placed on both sides of the collision points. A time-dependent transverse kick from the Crab Cavities is used to rotate the bunches to impose head-on collisions at the impact point. After the collision point, a second cavity reverses the rotation before the bunches continue the path in LHC.

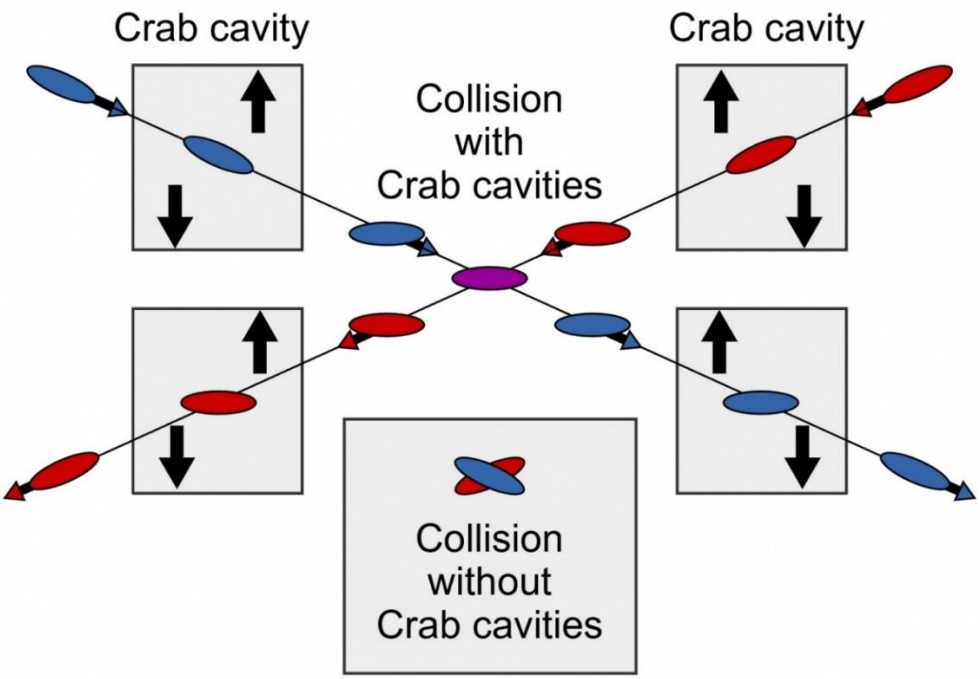

Figure 17: Visualisation of how Crab Cavities rotate bunches before and after collision point ©CERN

There are two crab cavity concepts: DQW (Double Quarter Wave, vertical) and RFD (RF Dipole, horizontal). The most relevant cavity for this report is the DQW Crab Cavity. December 2017, one prototype cryomodule with two DQW cavities were assembled (Figure 18), and are supposed to be tested in SPS in 2018. The long-term plan is that 8 cryomodules shall be installed in LHC during LS3 (Long Shutdown 3) in 2024-2026.

Figure 18: Two Helium vessels for DQW Crab Cavities during assembly in 2017 ©CERN

3.2 Helium Vessel for DQW Crab Cavities

The DQW Crab Cavity is made of Niobium, which has superconducting properties when its temperature is < 9.25K. To achieve such temperatures, it must be submerged into superfluid Helium at 2K. To minimize the required volume of Helium and to maximize heat extraction from the cavity, a Helium vessel was designed to enclose the cavity and contain the Helium.

The development of prototype cavities is detailed in several papers [10-12], and the design evolution of the vessel is detailed in a report by N. Kuder [13]. The strength assessment for the DQW Crab Cavity and Helium vessel is presented in another report [14].

The He-vessel has the outer dimensions 573x488x390, weighs 120kg or 180 kg with the cavity included. It contains 30l of Helium and is designed for an internal operating pressure (PS) of 1.8 bar (abs). The test pressure[2] is 2.6 bar (abs), which is 1.43xPS. This is the maximum pressure the vessel must be able to withstand [10].

The Helium tank has a structural role and is rigidly connected to the Stainless-Steel cavity ports. Thus, one goal of the design has been to minimize the loads acting on the cavity from the vessel. To minimize the loads on the Niobium cavity during cool-down from room temperature (293K) to cold (2K), it was decided that the He-Vessel plates should be made of Titanium Grade 2, which is in the same thermal contraction range as Niobium. The integrated thermal contraction is about 1.5 mm/m when cooled from 300K to 2K.

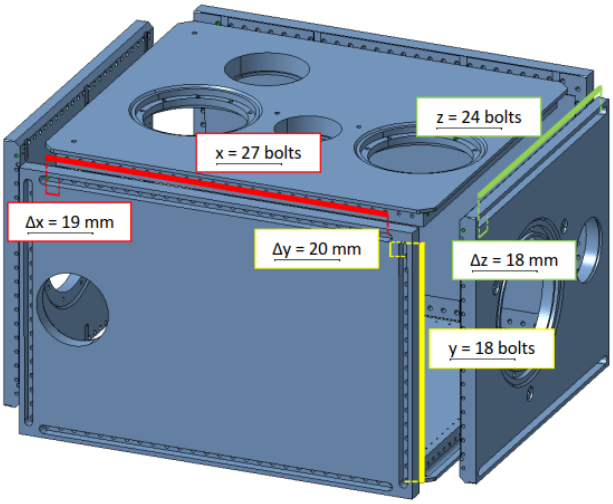

Figure 19: Helium vessel and bolted joints [14]

In the initial design, the six plates of the Helium vessel were joined together by welds. This design was discarded due to high deformations resulting from the welding process, and the high requirements for precision in the connections to the cavity. The final design concept was that the vessel should be joined together by bolted joints (Figure 19), and that additional fillet welds should ensure leak-tightness. This is an unconventional concept, and there was no experience at CERN or other available sources with this concept. No known standards or guidelines provide specific rules or recommendations for such pressure vessels. Therefore, the design and verification of the He-vessel were innovative work, and efforts was made to perform a thorough and conservative analysis. It was decided to use the calculation guideline VDI 2230 to aid the analysis.

[2] According to EN 13445 – Unfired Pressure Vessels

3.2.1 Joint Design

The three joint designs that are present on the He-vessel are displayed in Figure 20. The joint rows are numbered, showing the location of the joints on the vessel. All the joints are tapped thread joints (TTJ). Two of the joints has an overlap edge. Fillet welds are applied to ensure leak tightness in the joints. As seen in Figure 22, the bolt heads are countersunk into a groove in the plate. This grove is covered by a cover that is welded and serves as an additional barrier to prevent leakage of Helium.

The bolt size is M6x20, and there are 276 bolts in total. The bolt material is Titanium Grade 5 because of its high proof stress, and to have a similar thermal contraction to the Titanium Grade 2 plates. This reduce preload losses from differential thermal contraction. The bolts have a outgassing hole in the centre with diameter Ø1.75, to allow potential trapped Helium to evacuate.

The clamping length is 13mm. For the prototype vessel, SCHNORR preload washers (10-6.4-1) made of Bronze are applied under the bolt head.

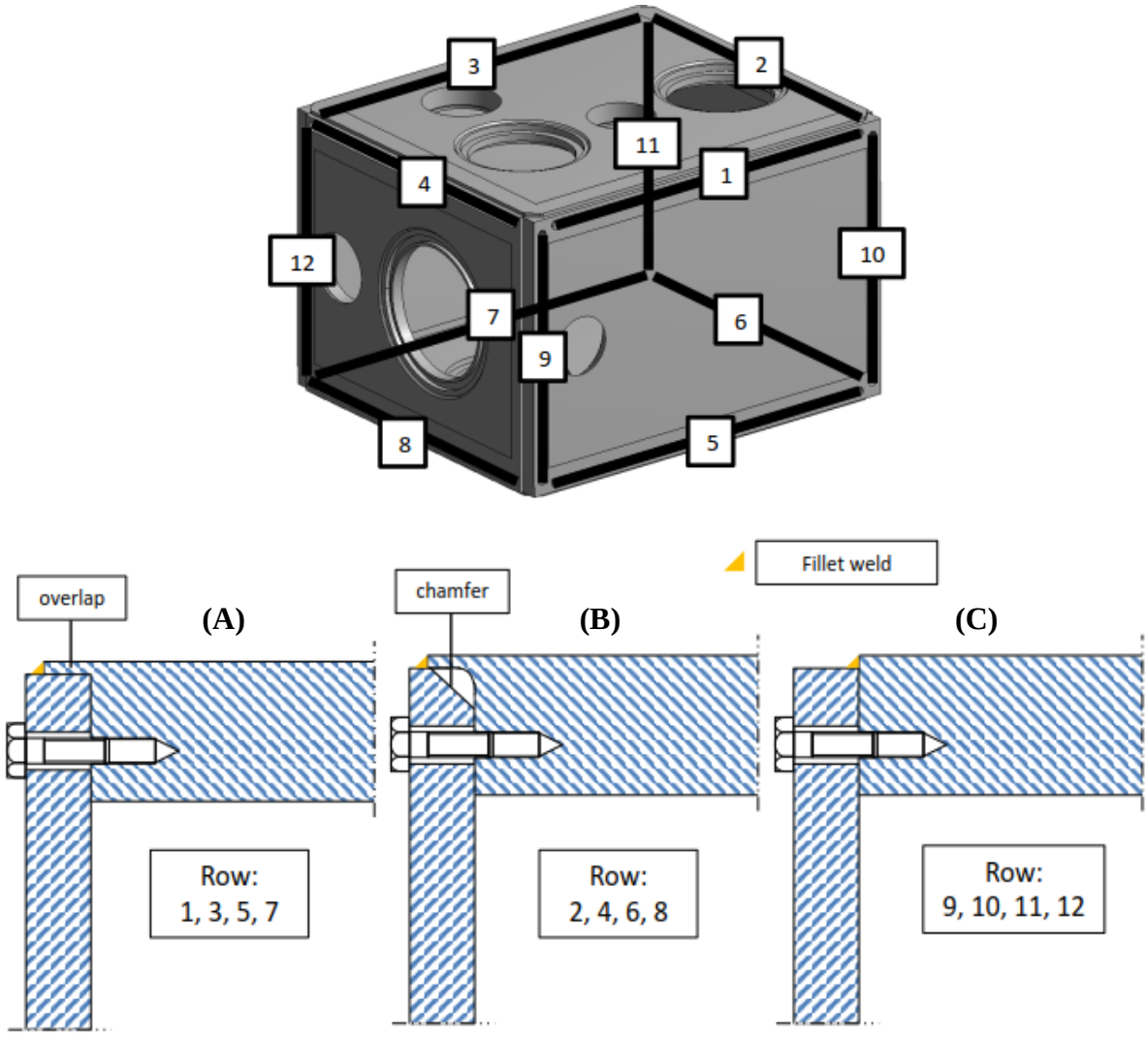

Figure 20: The three joint concepts on the He-vessel, with fillet welds for leak-tightness [14]

3.3 Helium Vessel Bolt Analysis

In this section the bolt analysis of the He-vessel [14] is presented, and challenges in the assessment and in combining VDI 2230 and FEA are identified and discussed (RQ1). This is used as basis in answering how the challenges can be met and avoided in the future (RQ2).

3.3.1 Boundary and Load Conditions

The analysis is carried out for the boundary and load conditions shown in Figure 21, and listed in Table 6. The loads on the model is: self-weight under normal gravity, internal Helium pressure, and a load on the helium vessel plates from a 0.12mm pre-tuning deformation of the cavity.

The He-vessel is attached to a support structure, which give realistic support response for the vessel. The Niobium cavity stiffness is represented in the model. Room temperature has been assumed for the analysis, since the material properties are weakest at this temperature.

The bolts are preloaded to 4.5 kN, which were selected to provide an acceptable level of work stress during maximum loading. It is stated in the report [10] that it was not clear from relevant codes how the preload should be defined.

Frictionless contact is applied in the clamping interfaces, as it was assumed that this would provide a conservative approach, where the bolt would have to withstand axial, shear, and bending loads.

Simulations has been performed with and without the fillet welds. The simulation results relevant for the bolt analysis is when the welds are not present, as the bolted joints alone must ensure the complete structural integrity of the vessel.

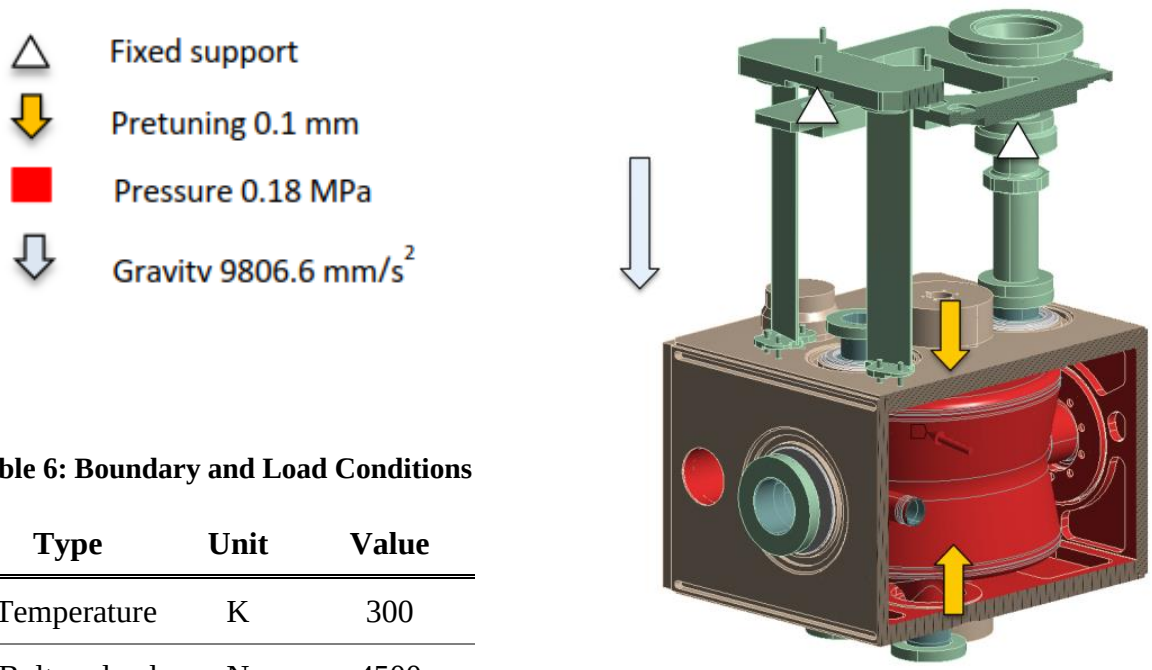

Figure 21: BCs of He-vessel FE-model [14]

Table 6: Boundary and Load Conditions

Type	Unit	Value
Temperature	K	300
Bolt preload	N	4500

3.3.2 Bolt Representation in FE-analysis

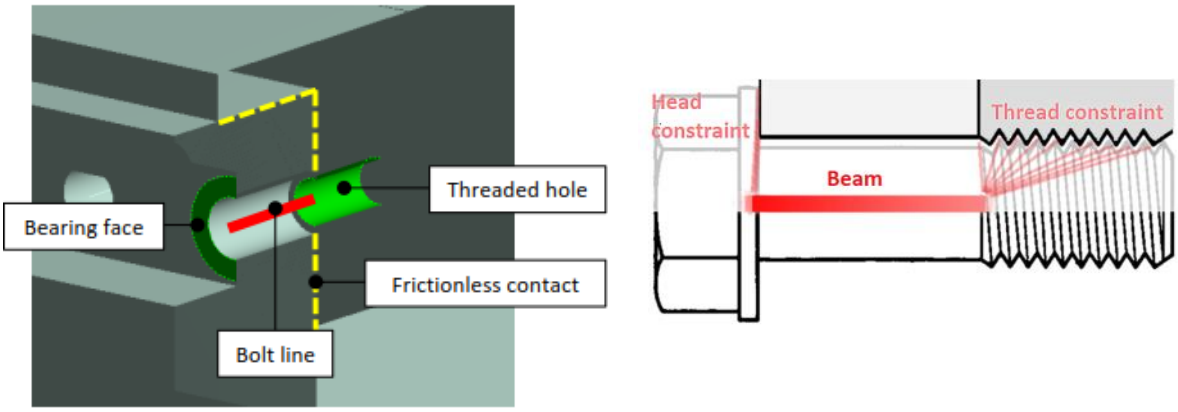

Figure 22: Bolt representation in the FE-model according to VDI 2230 Class II [14]

The bolts are represented by beams, according to VDI 2230 Class II. They are connected with Multi-Point Constraints (MPCs) in the bolt bearing face area and in the threaded hole, as illustrated in Figure 22. The beam properties used are listed in Table 7, and has been calculated according to Eq. (18) from the analytically calculated axial resilience (δ_S) and bending resilience (β_S). The analytic resiliensies consideres the outgassing hole in the center of the bolt, and the resilience contribution from the bolt head and thread engagement. The bolt material is defined to be Titanium, with an elastic modulus of $E = 110\ GPa$.

Table 7: Beam properties for M6 bolt

Length [mm]	Area [mm^2]	I_x [mm^4]	I_y [mm^4]	J [mm^4]
13	9.86	16.92	16.92	33.84

3.3.3 Analysis of Results and Verifications

Bolt loads

Table 8 list the extracted loads, calculated stress, and safety factors. In the original table, there are two separate columns for simulations with and without fillet welds. As stated above, only the results from the simulation without welds are relevant for the bolt analysis.

The maximum bolt load is 4.65 kN, and the additional bolt load resulting from the applied workload is F_{SA} = 150N. The equivalent stress is calculated to be 620 MPa, and is calculated from the axial and shear load, bending moment, and residual tightening torque. Thus, a modified version of the VDI 2230 working stress equation has been used. According to the standard VDI 2230 working stress calculation, shear and bending stress is not included. The resulting safety factor against yield in the bolt has been calculated to be $S_F = 1.34$.

Table 8: Loads extracted from FEA and calculated bolt stress, adapted from [14]

Name	Symbol	Unit	Value
Preload	F_M	[N]	4500
Max axial bolt load	$F_{S\max}$	[N]	4650
Max bending moment	M_{Sbo}	[Nmm]	3430
Max shear force	$F_{Q\max}$	[N]	525
Equivalent stress	$\sigma_{red.B}$	[MPa]	620
Proof stress Ti gr.5	$R_{p0,2}$	[MPa]	830
Safety factor	S_F	-	1.34

Figure 23 show the axial bolt load distribution in Row 1 of the Helium vessel. It is clear that there is an uneven workload distribution, and that the most highly loaded bolts are in the middle. This illustrate that for this case, assuming uniform load distribution would be inaccurate. However, the force difference is only about 30N and would not have any significant impact in this case.

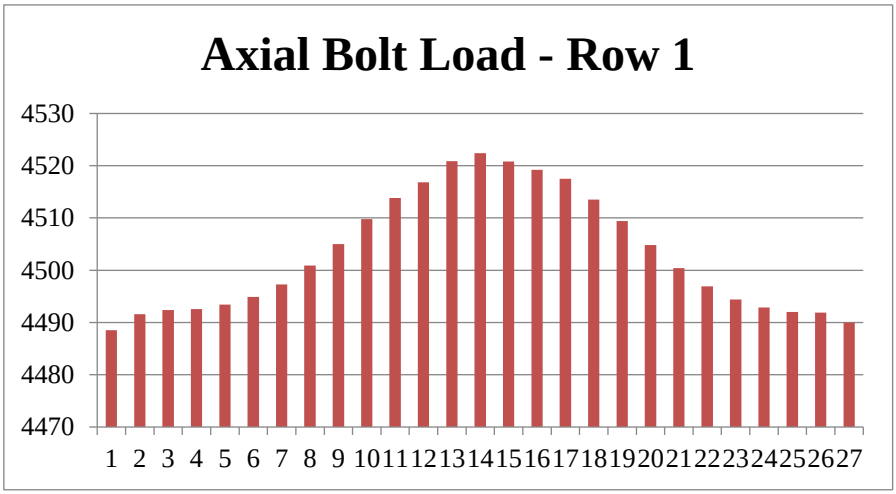

Figure 23: Axial bolt load distribution in Row 1

As there is no friction in the contact area, sliding is allowed and the shear force in the bolt is a result of the relative displacement between the clamped plates. This gives rise to the bending moment in the beam, which is analytically calculated in (20). Comparing this analytic bending moment to the moment extracted in Table 8, it is clear that the shear load is the source of the bending moment. This bending moment gives rise to the bolt bending stress, which is 270 MPa and 39% of the equivalent stress.

$$M_{Sb} = \left(F_Q \cdot \frac{l_K}{2} \right) = \left(525N \cdot \frac{13mm}{2} \right) = 3412.5Nmm \tag{20}$$

The torsional stress from residual tightening torque is 155 MPa and 22.6% of the work stress. It is according to VDI 2230 practice to include this in the calculation of working stress, but it should be noted that there is significant uncertainty related to this value.

The report concludes: "*The stress for the bolts considering the worst loading condition is acceptable. They will operate within the elastic limit.*"

Clamping pressure

A verification of the clamping conditions has been performed by analysing the pressure distribution for all the 12 clamping areas. Two of them are shown in Figure 24. Blue colour indicates very low to zero pressure, and red indicate maximum pressures.

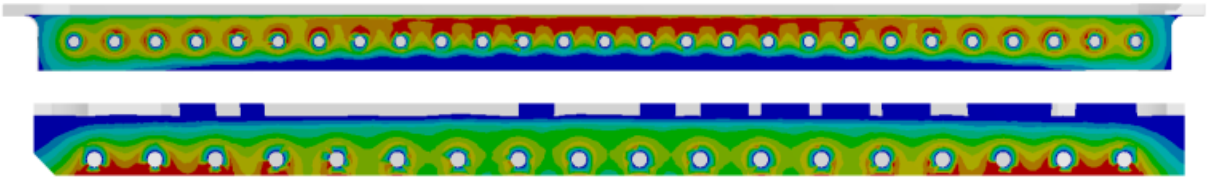

Figure 24: Resulting pressure distribution in bolt Row 1 (top) and Row 10 (lower)

Continuity of clamping pressure in the interfaces is required to prevent leakage, and normally joint opening should not occur. In this case, care should be made that superfluid Helium, which has zero viscosity and can penetrate the smallest glitches, does not reach the tapped threads.

There is continuity in pressure between the bolts. In Row 10, the pressure distribution is relatively uniform, and there are only small signs of joint opening in the corners. In Row 1, there is joint opening towards the middle bolts. This can be related to the bolt load distribution in Figure 23.

The report concludes: "…*the pressure contacts are evaluated and examined to find the probable openings and overall behaviour of the plates. The helium vessel will secure the leak-tightness.* "

3.3.4 Discussion of Bolt Assessment

In this section, the bolt analysis is discussed, and challenges related to combining VDI 2230 with FE-analysis are outlined.

Friction in the Clamping Interface

In principle, bolts should not experience shear or bending, and slipping in the joint is considered a failure. The bolt should provide preload, so that the joint through clamping pressure and friction achieve a friction grip and is able to transfer the workloads and behave as a continuous solid. Thus, the joint should be designed to avoid slipping, and the main stress acting in the bolt is normal stress (tension).

In the analysis, an approach that assumes a "worst case scenario" has been used. This scenario includes having no friction in the clamping interfaces, which gives rise to slipping and associated shear and bending loads. All the load components in the bolt are included in the calculation of combined stress. This verifies that the bolt is able to withstand all the loads that can act on the bolt and resembles a "failure scenario".

One challenge with this approach is that it can encourage a low preload, to reduce the combined stress and increase the bolt stress safety factor. However, having a low preload reduce the friction grip of the joint and increase the chance of joint slipping and "failure" to occur.

By following a standard VDI 2230 approach, emphasis is put on having a high preload and verifying that no slipping occurs. In this case, only axial load and residual tightening torque is included in the calculation of bolt stress. VDI 2230 also propose to calculate a shear safety factor for a scenario where slipping is present.

In terms of bolt stress, the “worst case” approach is conservative since it includes shear and bending stress. However, since it favours low preload, taking a more standard VDI 2230 approach can in many cases be more beneficial. This will encourage a high preload and give a higher friction grip capacity in the joint. Friction should then also be included in the FE-analysis, and it should be verified that slipping is not occurring.

It can be noted that joint slip also is of importance when identifying the loads on the fillet welds, as slipping can increase the loads significantly.

Joint Opening

According to the standard VDI 2230 approach, joint opening should be avoided and is a prerequisite for the validity of the analytic calculations. However, FEA expands that validity range with allowing for more detailed analysis of the bolt loads and clamping pressure distribution.

In the He-vessel analysis the clamping pressure has been assessed and it is concluded that the sealing function of the joint is fulfilled. Partial joint opening is present in some locations, and it is pointed out that this is related to the uneven bolt load distribution. It is not known if, or to which degree non-linear bolt load development (prying) is present. The validity of the pressure distribution and bolt loads depends on the mesh size in the clamping solid and interface surface mesh refinement, and is not known.

Uncertainty in preload

In the analysis, one preload level has been applied in the simulation that verifies both bolt stress and clamping pressure. According to VDI 2230, there will be tightening uncertainty and preload losses, which results in a minimum and maximum preload. The verification of bolt stresses should then be carried out with the maximum preload, and verification of clamping requirements with the minimum preload.

Operating Pressure

The analysis has been carried out for a nominal operating pressure (PS) of 1.8 bar (abs). The bolted joints should be designed and verified for the maximum workload to ensure the structural integrity in the extreme loading case. VDI 2230 does not treat how the maximum workload should be defined, but according to one standard [15] the vessel should be designed for the test pressure of 2.6 bar (abs). Which pressure to use depend on considerations about which safety factor that is required from the design, and the probability of operating pressures above nominal values.

3.3.5 Selection of Preload

One of the challenges in design and verification of the bolted joints of the He-vessel was selecting the bolt preload. The first guess of preload were based on the assumption that the bolt would have to be preloaded with the same load as the bolt workload. However, when the preload were selected to match the bolt workload, the bolt load became even higher in the next simulation. This new bolt load were then applied as preload, and it resulted in a iterative process where the preload were defined by the bolt load of the previous simulation.

This behaviour has been recreated in a simulation, and the loads are presented in Figure 25. It can be seen that in the first simulation, the workload is 4.3 kN. In simulation 2, the preload is set to be 4.3 kN, but the bolt load becomes 5.3 kN. For simulation 2, the additional bolt load is 893 N. In the next simulation, the preload is set to be 5.3kN. What can be seen is that as the preload increase (>6 kN), the additional bolt load decrease and approaches 160-200 N. The preload level where this happen is higher than the initial estimate of 4.3 kN which were based on the workload.

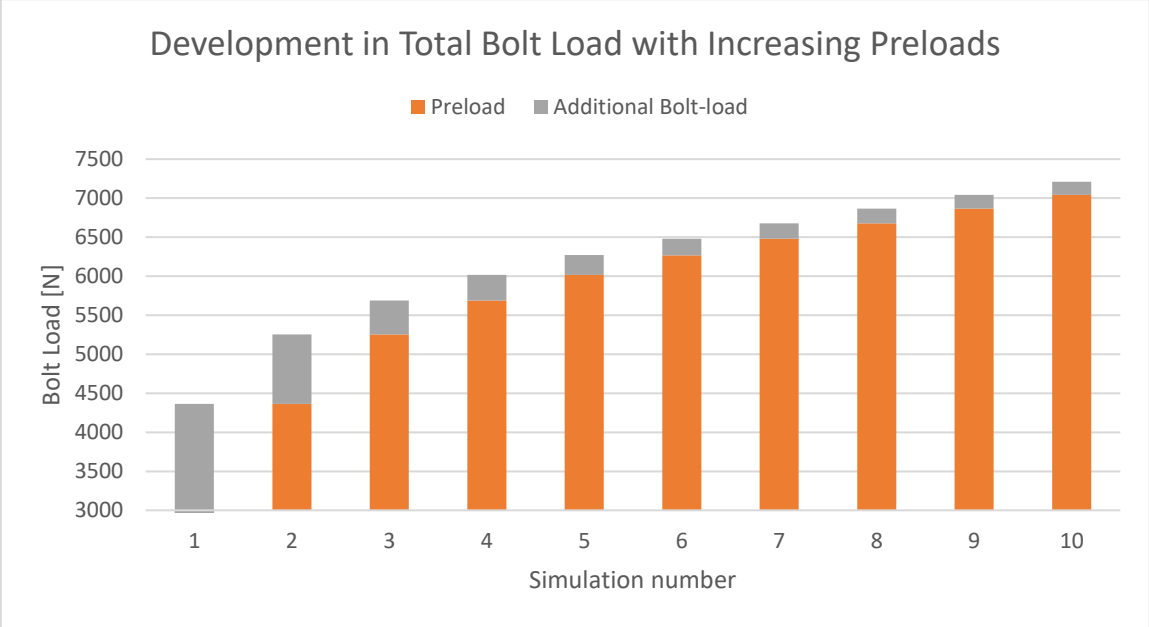

Figure 25: Development in Total Bolt Load with Increasing Preloads

This behavior led to some confusion and uncertainty about how to best identify an appropriate level of preload. It was expected that prying had a role in the described behavior, but not exactly to which extent the preload influenced the presence of prying.

3.4 RQ1: Challenges in Analysis of Bolted Joints

Based on the discussion of the analysis (3.3.4) and the description of preload selection (3.3.5), this section summarises some central challenges in combining VDI 2230 and FE-analysis for the case of the Crab Cavities Helium vessel.

Some challenges related to the “worst case scenario” approach by assuming no friction in the clamping interface and including all load components in calculation of the combined stress are discussed. It is pointed out that taking a more standard VDI 2230 approach with friction in the interface and emphasis on avoiding joint slip will encourage a higher preload, and can in some

cases be more beneficial. Verifications must then be performed in the analysis that no slipping will occur.

Partial joint opening is present in some locations, but the sealing function is fulfilled. To improve the use of FEA in such assessments, methods to identify if prying is present could be clarified, along with aspects of validity.

In the analysis, one preload level has been applied in the verification of clamping pressure and bolt stress. According to VDI 2230 there is uncertainty in the preload, and verifications of bolt stress and clamping pressure should be verified for the max and min preload level respectively.

There was some challenges in the selection of preload, as demonstrated by the preload iterations. Prying were expected to have some role, but it was not known to which extent the level of preload influenced the presence of prying.

Altogether, the above identify challenges in how FEA and VDI 2230 has been combined in the Helium vessel bolt analysis and answers the first research question. It also serves as constructive feedback on the analysis and outline relevant learning points. These findings are used as basis for the suggestions and recommendations for a potential revision of the analysis given in Ch. 6, and in answering RQ2.

3.5 RQ2: HOW CAN THE CHALLENGES BE MET?

With the challenges outlined above in mind, the next question is how they can be met and avoided in the future?

The guideline VDI 2230 contains answers to many of the challenges, but not in a straight forward and clear way. It is a detailed and thorough guideline, and it can be challenging to catch the fundamental principles and verification concepts. The second part of the guideline cover FEA aspects in general, but it does not provide a simple and easy to use workflow defining how a combined analysis should be performed. For a user with little experience with VDI 2230 to reach the required level of knowledge to perform such an assessment would be time consuming and require high efforts.

To lower the threshold for combining VDI 2230 with FE-analysis, making it simple to apply and to achieve high quality in the analysis, the following support material is suggested:

Analysis Approach - The typical difference in traditional analytic VDI 2230 approach and FEA based analysis should be emphasized and made clear.

Simplified Workflow - This should provide a structured approach to bolt analysis, and include all the basic elements like selection of preload, setup of FEA and BCs, how analytic calculations and FEA results should be combined, and descriptions of verification strategies. To simplify the calculations, a Mathcad template that matches the workflow steps should be prepared.

Guide - This should be related to the suggested workflow steps, and provide detail descriptions, know how, best practices, discuss aspects of validity, and provide relevant references.

Examples of Application - For some cases, the simplified workflow and calculations should be demonstrated so they can serve as examples of how FEA can be used in analysis of bolted joints.

Seminar - A seminar could be prepared to educate relevant personnel about use of FEA in analysis of bolted joints. It should provide a thorough introduction to VDI 2230 and the simplified workflow.

Studies of Prying - Studies should be performed to understand how it is related to additional bolt loads and joint opening, and how it affected by the preload level. How it can be identified and avoided should also be made clear.

The combination of the above suggested support material are believed to help the readers to avoid the challenges in the He-vessel bolt analysis, and that the wish for having the material presented in a format so can benefit the engineering department at CERN is achieved in a good way.

The prying studies are presented in Ch. 4, and the workflow and associated support material are presented in Ch. 5.

4 INVESTIGATIONS INTO PRYING

The scope of this chapter is to investigate "Prying". To describe what it is, why and when it is relevant, how it can be encountered, and aspects related to FE-analysis. This includes a brief investigation to assess the impact of preload on prying. The focus is not to dive too much into equations, but to describe the basics and draw some practical conclusions.

The main source of information about prying is the chapter: *Behavior of the Joint Loaded in Tension* from a book by *John H. Bickford* [16].

4.1 WHAT IS PRYING?

Pying is from the verb "*pry*", and is defined (Oxford Advanced American Dictionary):

> *"to use force to separate something from something else*"

Prying is a non-linear effect on the bolt load that is important to understand to perform proper design and verification of BJs. It is an effect that comes into play when the workload is applied eccentric from the bolt center axis, and not concentric. Then, a moment is introduced in the joint, and under the right conditions an additional reaction force is generated in the clamping interface. To maintain moment equilibrium in the joint, the bolt has to withstand the additional prying load, as seen in Figure 26 (A). It can also be seen that a deformation angle is imposed on the bolt head. In Figure 26 (B), the clamped plate is very stiff and can be assumed to be rigid. This nearly removes the prying load, and the eccentric workload is in practice applied as a concentric load on the bolt.

Prying affect the bolt stress in two significant ways:

1) By an additional axial prying load due to the lever arm principle and moment equilibrium.
2) By imposing an angle deformation on the bolt head, introducing bending moment in the bolt.

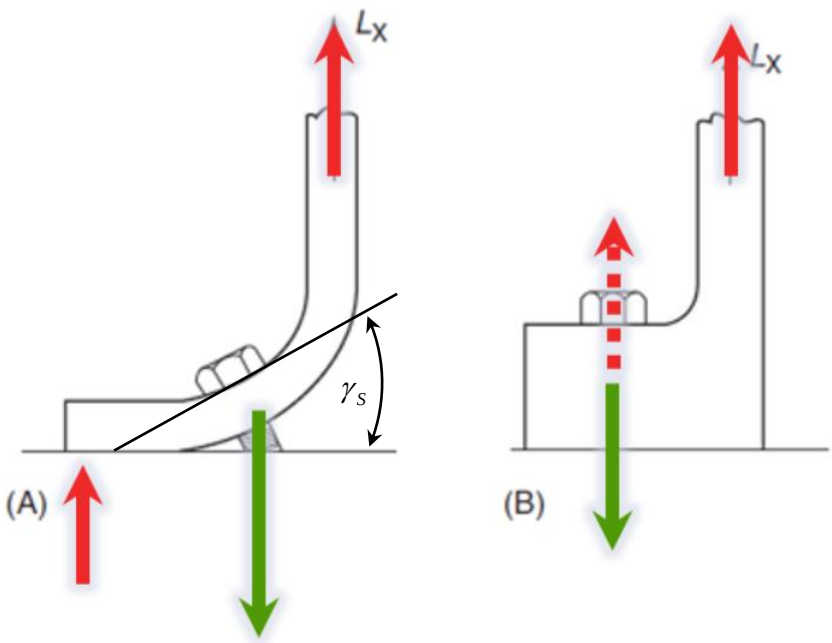

Figure 26: Prying action in a flexible and a rigid joint [16]

Factors that affect prying is the stiffness of the clamped plates from both material and geometry, the distance of eccentricity for the applied workload, and magnitude of the preload relative to the workload.

Description

For a standard joint with concentric work load, the additional bolt load is defined by Eq. (8). This is a linear equation, and the additional bolt load increase linearly with the applied workload. This graph can be recognized in Figure 28 as curve a). This curve continue until the compressed clamping solid is relieved, joint opening occur, and the residual clamping force in the interface (F_{KR}) becomes zero. For such joints, that will happen at a critical workload. When that happens, the bolt has to carry all the workload and bolt failure is likely to occur.

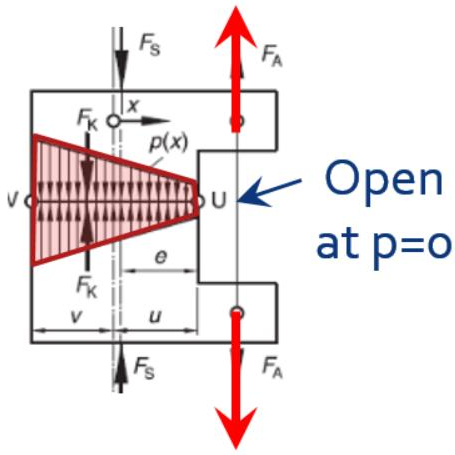

Figure 27: Pressure distribution in the clamping interface

For a joint where the load is applied as an eccentric workload, the development is slightly different. At a critical workload, partial joint opening will start to occur at one side of the clamping interface, as seen in Figure 27. When that happens, the compressed clamping solid is partially relieved, and the bolt has to carry an increasing amount of the bolt workload. This development in additional bolt load versus working load can be recognized in Figure 28, from point b) to point e). The curve c) is the bolt load when the clamping solid is completely relieved, and the full prying load is effective.

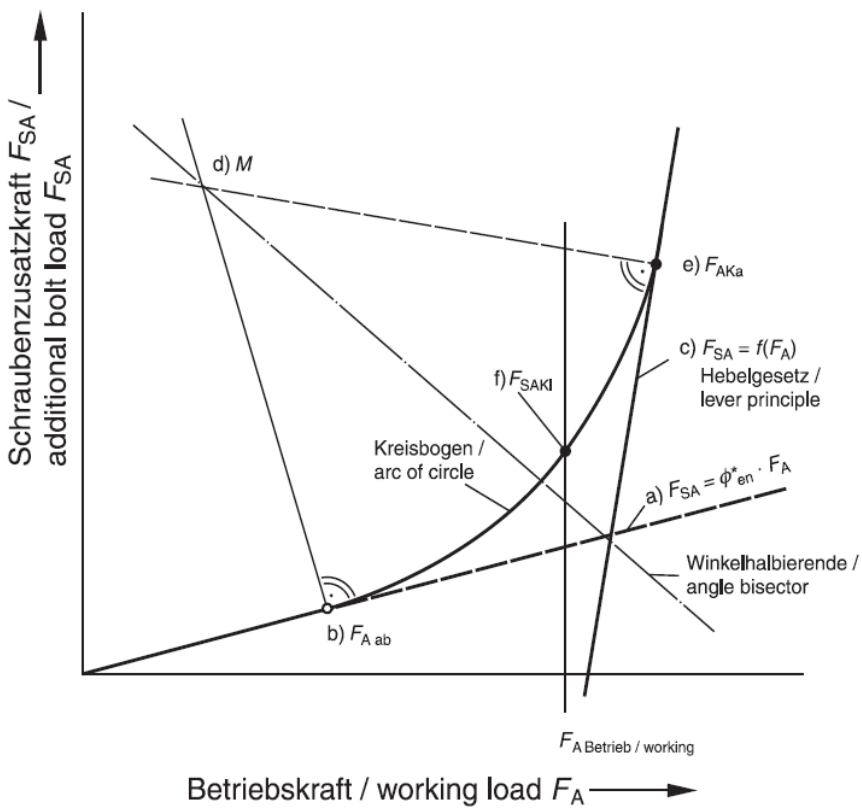

Figure 28: Additional bolt load development for an opening joint [Pt.1 - Figure D1]

There is limited treatment of prying in VDI 2230 [17]. The effect on the clamped parts resilience from eccentric load-application and clamping are to some degree considered by modified resilience and load factors, like: Φ^*_{en}. In [Pt.1–Annex D], analytic methods are suggested for how the additional prying load due to joint opening can be estimated. These methods are not practical to apply and rely on analytic assumptions and calculation quantities with large uncertainties. For the analytic VDI 2230 approach to be valid, it has to be assumed that the joint is not going to open.

Prying and FEA

Some of the advantages with FE-analysis is that the actual geometry and compliance, preload, and clamping pressure are represented. This makes it possible to avoid the analytic limitations and assess the presence and effect of prying in the joint with good accuracy.

There are two main stages: before and after joint opening. With FEA, the bolt load can be plotted as the workload increase. In Figure 29, the bolt load in a joint is plotted for five different levels of preload. The dotted line is the bolt workload as a function of the global workload. In Stage 1, before joint opening, the load development is linear and predictable. In Stage 2, partial joint opening is occurring, and the bolt load increases rapidly. When designing a bolted joint, the goal is to stay in Stage 1. Graphs like the ones below can be used to identify the required level of preload to stay in Stage 1 for a given workload.

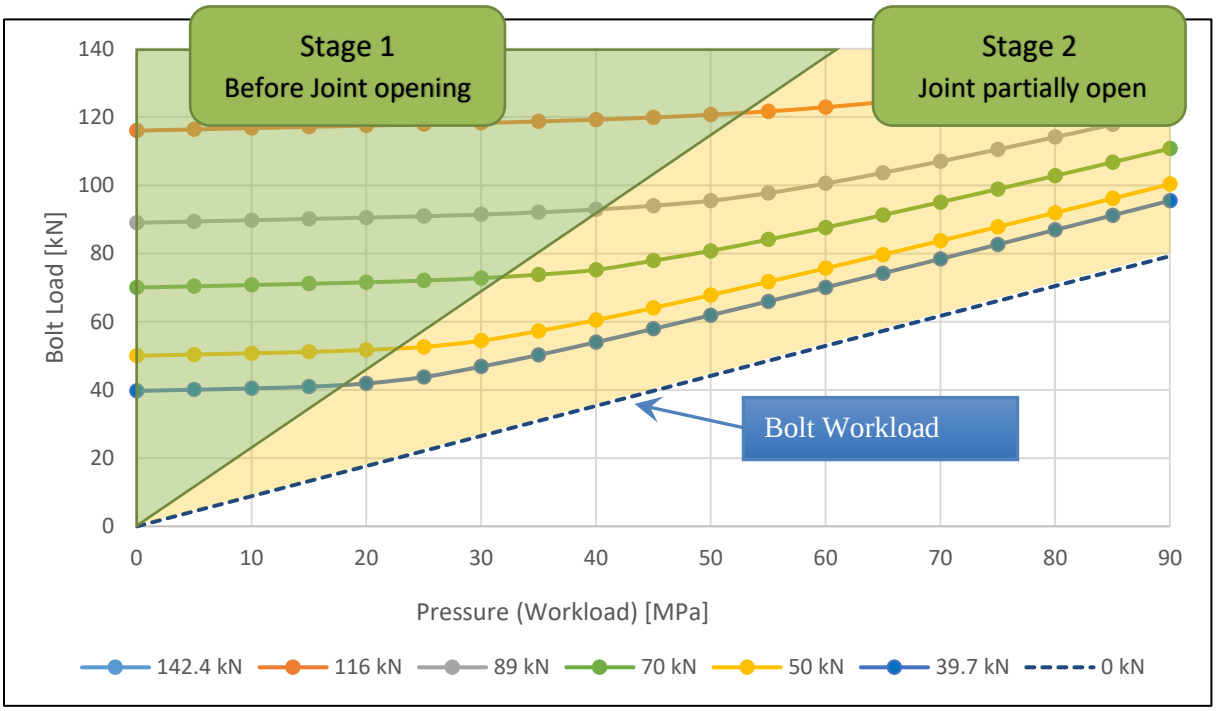

Figure 29: Bolt load before and after joint opening for five levels of preload

4.2 WHY AND WHEN IS IT RELEVANT?

In a large organization like CERN where there is a lot of custom design, soft materials like Titanium are used, many of the BJs are exposed complex loads, vacuum and temperatures as low as 2K, and proper function is critical - it is important to have control of the joint performance and bolt loading to provide a safe design.

By using analytic calculation approaches, the bolt loads can easily be underestimated due to the limitations of these methods. Distributed pressures and strains are challenging to account for by analytic methods. Thus, prying might not be identified and properly accounted for. This is especially the case for complex geometries, complex pressure states, and large clamping interfaces. In such cases, joint opening and prying loads can be difficult to predict.

If prying loads are present in the design, small changes in global workload can result in large changes in the bolt load. So, if there is uncertainty in the global workload, that can have large consequences for the bolt load. With dynamic loads, this can give large stress amplitudes and related fatigue challenges.

4.3 HOW SHOULD IT BE ENCOUNTERED?

In general, prying should be avoided. That can be done by verifying that prying is not present in the joint. Methods to assess if joint opening and prying are present, are presented in 5.4.11. If prying is present, two things can be done. The first is to account for it in the stress verifications, making sure the joint will handle the additional loads. The second is to modify the joint design or preload level to avoid prying.

To account for prying loads, a FEA based assessment of the joint must be performed. Prying loads are then included in the bolt load, and the verification can be performed based on realistic loads.

To avoid prying and joint opening by design, the stiffness in the joint should be high enough that it will behave in a rigid manner. That can be achieved by using design guidelines, or design by analysis methods using FEA.

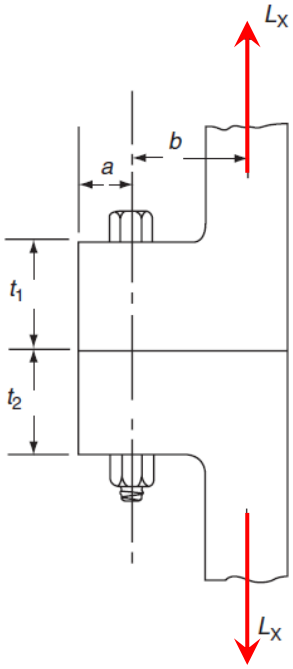

Figure 30: Important parameters for joint stiffness [16]

With reference to Figure 30, the effect of prying can be minimized by increasing the thickness *t* and distance *a*, and reducing distance *b*. The elastic modulus of the clamped parts also affect the resilience of the joint as seen in Eq.(4), and the load on the bolt through the load factor as Eq.(7) show. Thus, clamped plates of soft materials such as Titanium or Aluminum require stiffer geometry to behave in a rigid manner.

4.4 FEA-Study of Preload Influence on Prying

4.4.1 Scope

By performing some experimental FE-simulations, the scope is to exemplify and investigate the influence of preload on prying. To goal is to acquire information about how prying can be identified, and how to assess if the level of preload is sufficient to avoid prying.

4.4.2 Setup and Boundary Conditions

The simulation geometry, FEA model, and analytic calculations according to VDI 2230 are presented in ***Appendix C***. The most relevant details for this investigation is repeated here.

The single bolted joint in Figure 31 is extracted from a MBJ Blind Flange, and has a Class III representation of a M16 bolt. The bolt diameter is uniform and based on the thread minor diameter (d_3=13.55mm). The bolt and clamped parts material are Steel.

Frictionless contacts are applied to the side surfaces to represent symmetric boundary conditions. Friction has been applied in the clamping interface, with a friction coefficient of $\mu_T = 0.15$.

The internal pressure is applied on the Top Cap internal surfaces, and are in the range of 0-100 MPa. This results in a maximum axial work load (F_{Amax}) on each bolt of 88.5kN. The load is applied in 20 sub-steps of 5 MPa (4.42kN), which gives a good resolution on the graphs.

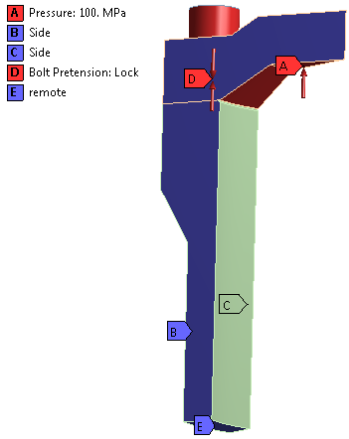

Figure 31: Geometry used in Prying analysis

4.4.3 Results and Analysis

Below, different diagrams display results that illustrate the impact of preload on the bolt load as the global workload increase. The "0kN" graphs are when no preload is applied and is the workload acting on the bolt. Since there is contact in the clamping interface, prying loads are represented.

The preload levels used in the simulations are based on analytic calculation quantities. According to the VDI 2230 calculations for this case (***Appendix C-2***), the resulting allowed assembly preload for the internal pressure of 22MPa is $F_{Mzul} = 142.4kN$. This is included in the diagrams as a red cross. Taking the tightening uncertainty into consideration, the minimum applied preload is 89kN. Considering all preload losses, the preload will be a bit lower than this, $F_{Mmin} = 63kN$. The required preload to avoid joint opening is calculated to be $F_{Kerf} = 39{,}7\ kN$, again for the internal pressure of 22MPa.

Maximum Bolt Load

The first plot (Figure 32) show the development in maximum bolt load as the global workload increase. The global workload (pressure) translates into the bolt workload, given by the blue dotted line. The initial preload levels are easy to identify from the starting points of the curves. For low workloads, all curves rise with a low and constant slope. At about 20-25 MPa, the lowest preloaded bolt experiences an increase in the bolt load. As the workload continue to increase, this happen to all bolts. Towards the maximum global workload, the load curves appear to become parallel with the bolt workload.

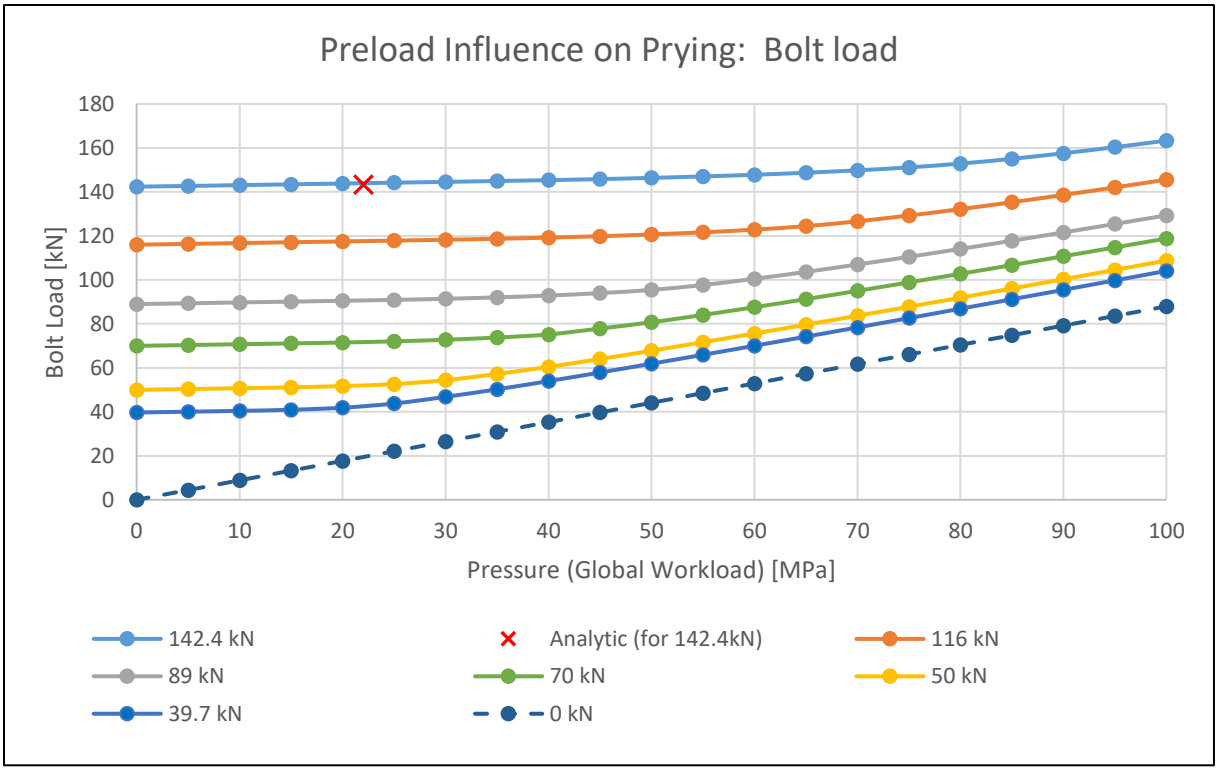

Figure 32: Maximum bolt loads for various preload levels

Additional Bolt Load

To better compare the load developments, Figure 33 plot the additional bolt loads as the global workload increase. The additional bolt load is obtained by subtracting the preload from the maximum bolt load ($F_{SA} = F_{Smax} - F_V$).

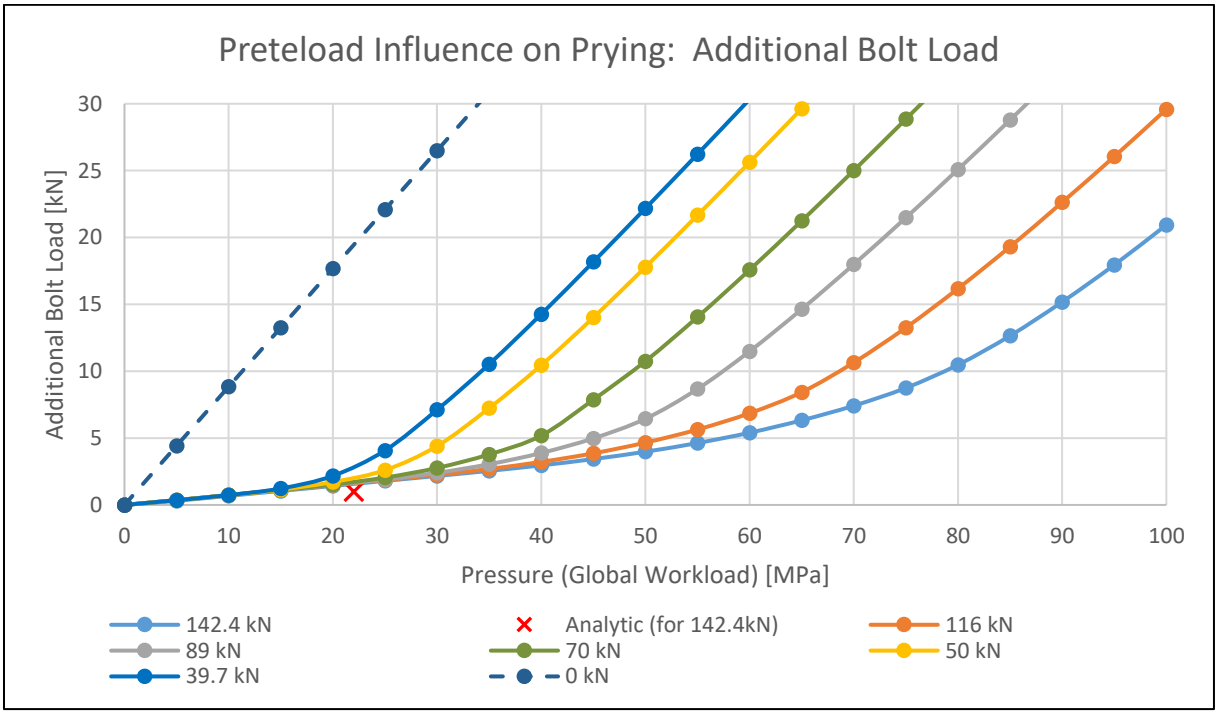

Figure 33: Additional bolt load for various preload levels

Comparing the additional bolt loads, they all coincide and increase in a linear manner up to a global workload of about 20 MPa. Then, the lowest preloaded bolt experiences a rapid increase in the bolt load. This increase is the effect of prying. As the global workload increase, prying becomes present in all the bolts. The trend is clear: for low preloads, prying occurs at lower workloads than for more highly preloaded bolts. The higher preload, the more workload can be applied before prying occur.

For the joint preloaded to the required clamp load (39,7kN) to prevent opening at a global workload of 22 MPa, opening appear to occur with about 20 MPa internal pressure. Thus, the analytic estimate is quite close to the FEA results.

One interesting observation is that the radius of curvature on the graphs, before they straighten out, increase as the preload increase. One explanation can be, based on the theory of Figure 28, that the curved part of the graph is when the clamping solid is partially relieved. When the preload is low, not much workload is required to relieve the clamping solid, and the radius of curvature is small. When the preload is higher, it takes much more workload to fully relieve the clamping solid, and the radius of curvature become large. Hence, the workload range for fully relieving a clamping solid, and associated radius of curvature increase as the preload the joint increase.

Joint Opening

In Figure 34, the relative displacement of the edges in the clamping interface are plotted (described in 5.4.11), and show the joint opening as edge separation in millimeters. The joint complies with the limit criteria G, so the clamping solid reaches the edge of the clamping interface. Thus, edge separation is expected to be related to partial relief of the clamping solid and the presence of prying loads.

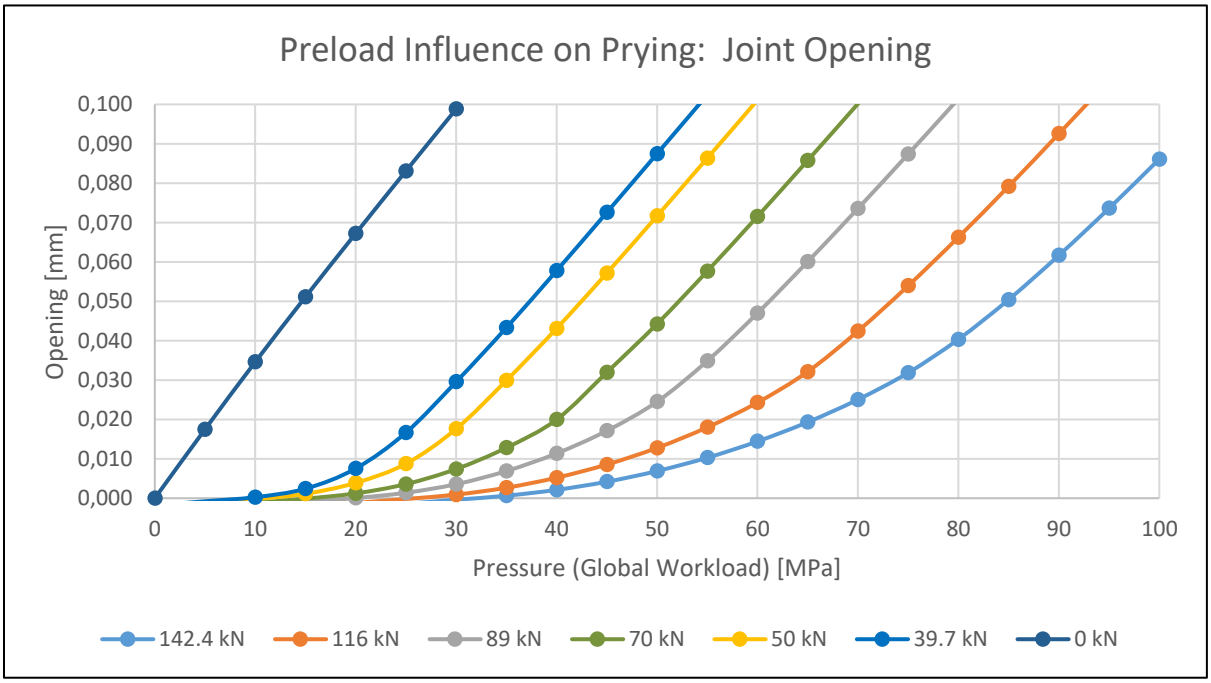

Figure 34: Joint opening for various preload levels

Comparing the joint opening and additional bolt load graphs, the resemblance is striking. The joints with low preload open at lower global workloads than the more highly preloaded joints.

There is also a good correlation between the global workload where joint opening is occurring, and where prying load becomes present. Before joint opening, the bolt loads are low and behave in a linear manner. When the joint opens, prying loads significantly increase the bolt load.

For the lowest preload simulation (39,7kN), prying occurs at about 20 MPa global workload. This corresponds well with when joint opening start to become significant. It also corresponds well with the analytic calculations that predicted this level of preload as the required clamp load to prevent joint opening at an internal pressure of 22 MPa.

One outcome of the correlation between joint opening and prying, is that joint opening can be used to predict prying. If the limit criteria G is fulfilled and there is joint opening, there is probably prying. On the other hand, if there is no opening, there is no prying. This knowledge can be useful when performing verifications of joint performance, assessing if prying is present.

4.5 DISCUSSION

4.5.1 Validity of Simulations

The validity of the joint opening data depends on the mesh refinement in the bolt, clamping interface, and clamping solid volume. The refinement is believed to be sufficient in this case, but no sensitivity studies are performed. However, the refinement is the same for all simulations, so the data should be qualitatively valid.

The interface edge separation displacements are an average of the total curve length, which can introduce some inaccuracies. A more detailed assessment of the clamping pressure in the interface could support the joint opening estimate and give a better understanding of the degree of opening in the clamping interface.

The global workload (pressure) used in the preload simulations are higher than what is realistic. The thread capacity and clamped parts stress level for the different materials would be limiting factors. For tapped Aluminum threads, the thread-strip limit is 87.6kN. However, using this large global workload, the trends and prying mechanisms are demonstrated in a good way.

The correlation between joint opening and prying are expected to be related to the limit criteria G. If a joint does not comply with this limit criteria, joint opening does not have to imply that prying is present. Further assessments would then have to be made to identify if prying is present. However, it can be stated that if joint opening does not occur, prying is not present.

4.5.2 Preload Iterations

Looking back at the preload iterations in 3.3.5 and Figure 25 with the knowledge of prying from this chapter in mind, it is clear that for the lowest levels of preload, prying was present and were the reason for the high additional workloads. For the higher preloads, the additional workload was relatively small and did not change much as the preload changed. For these preloads, it can be assumed that no prying was present. Thus, prying is the source of the behavior described for the preload iterations.

The preload iterations illustrate in a good way that the preload level can affect the presence of prying.

4.5.3 Appropriate Level of Preload

To assess if the level of preload in a joint is sufficient to avoid prying, the bolt load curve for the minimum probable preload level can be analyzed. The minimum preload is when preload losses and tightening uncertainty are subtracted from the allowed assembly preload, as Eq. (28) show. The bolt load curve should demonstrate linear behavior within the relevant global workload range.

In Figure 35 for a global workload of 40 MPa, the green the area shows acceptable preload levels where the bolt load is linear. For lower preloads, in the red area, non-linear behavior can be observed within the relevant workload range, which is not desirable.

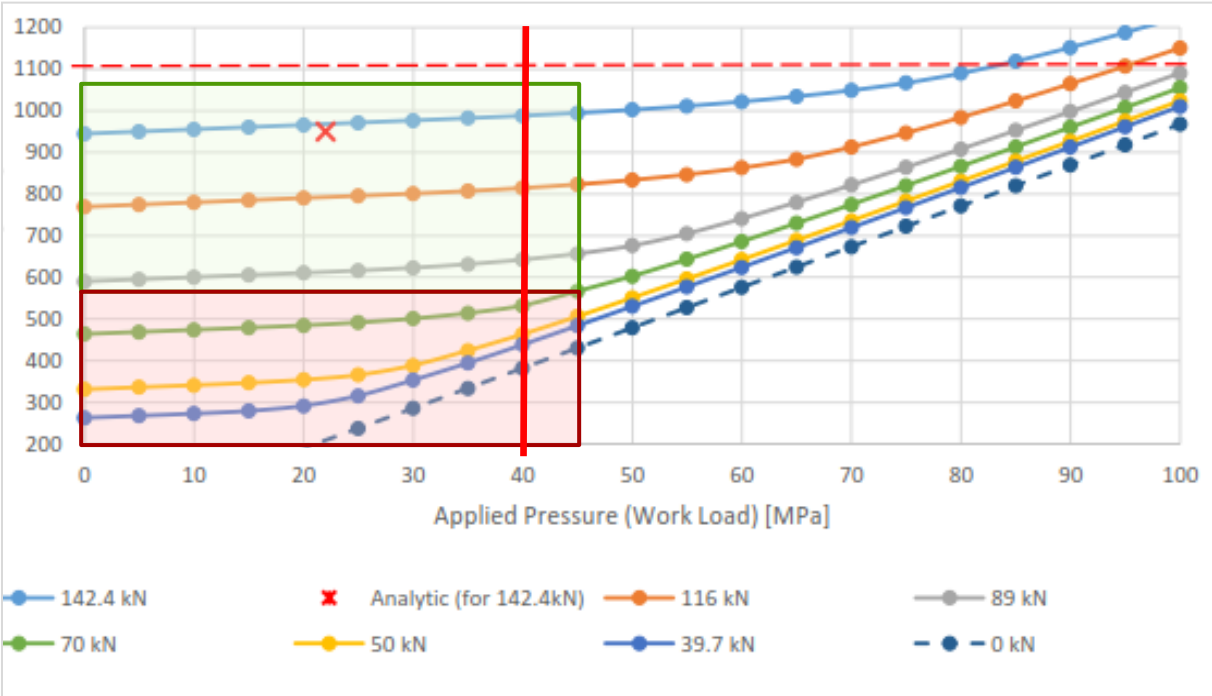

Figure 35: Strategy to assess preload level and presence of prying

4.5.4 VDI 2230 Approach

The VDI 2230 strategy is to avoid joint opening, and to apply a preload that utilize most of the bolt capacity. What has been presented in this chapter supports this to be a reasonable strategy. By avoiding joint opening, prying challenges are avoided. By utilizing most of the bolt capacity (90%) with the allowed assembly preload, the resulting minimum preload will be as high as possible for that joint. That gives a higher acceptance for unforeseen preload losses, and a larger safety against joint opening and prying if the joint is exposed to higher workloads than expected.

However, it is not economic to oversize the bolts if there is a large number of bolts. So, if the safety against opening is much larger than what it has to be, a smaller bolt size can be tested. It is possible to identify the minimum clamp load at the joint opening limit (F_{KA}) for a given workload with FEA. This can serve as a reference to establish a safety factor against joint opening, or to guide selection of a suitable bolt diameter. This does however require some additional efforts and well planned FEA setup, because prying loads can easily corrupt the

identification of preload level in the simulation. In-stead of identifying the exact clamp load at the joint opening limit, it might be simpler and more time efficient to just test a smaller bolt size and perform a verification simulation with it.

But it must be remembered that bolt assessment is no exact science, and there are many uncertainties and sources of error that are challenging to fully account for. Thus, in some cases it might be better to oversize slightly, than trying to be precise and have the risk of too small margins.

4.6 SUMMARY

In this chapter, important knowledge about prying and the influence of preload are presented. What prying is, why and when it is relevant, and how it can be encountered are answered, before a brief study show how preload affect joint opening and prying loads.

Prying introduces higher loads on the bolt that what might be expected from analytic calculations. This can have unfortunate consequences, and in general prying should be avoided. The possibility to represent joint opening and prying loads has come forth as a large advantage of using FEA over analytic methods.

The main findings of the study are:

- When joint opening occurs (within limit G), the clamping solid is relived, and prying loads become present in the bolt.

- Joint opening and prying are highly dependent on the level of preload. If the preload is high, the joint will accept a high workload before the joint open and prying loads arise.

- If there is no joint opening, there is no prying. This can be used in FEA verification of joint performance.

Based on the findings, verification that no prying is present for the minimum preload should be included in the FEA workflow. A good first approach is to check if the joint remains closed, as it can rule out any prying loads. If joint opening in present, it must be verified that no non-linearities are present for the relevant workload range.

If prying is present, actions can be made to avoid it by increasing the preload or making the joint geometry more stiff. Alternatively, the prying loads can be accounted for in the stress calculations.

5 FEA AIDED ASSESSMENT OF BOLTED JOINTS

This chapter provides a complete analysis framework for bolted joints, and detail how FEA and the analytic guideline VDI 2230 can be combined in a simple way to perform high quality assessment of bolted joints. That is done through first comparing analytic and FEA based approaches, and presenting a basic workflow in 13 steps which describe the interaction between analytic calculations, CAD modelling, and FEA analysis. A calculation template to aid the analysis is introduced, and how to handle non-critical joints are described. A Guide then provide further details that are relevant for each of the steps. Some further verifications are presented, before two case examples demonstrates the basic workflow. In the end, a seminar that is prepared to educate about assessment of bolted joints and the simplified workflow are included.

5.1 ANALYSIS APPROACH

The analytic VDI 2230 approach are described in Ch. 2.3. Two approaches for combining FEA and VDI 2230 are listed in Table 9. Strategies to identify parameters for the *Analytic FEA* approach are described in VDI 2230 Pt. 2.

To best utilize the strengths of FEA and the possibilities in the FEA software, a *Semi Analytic FEA* approach is most beneficial. It is by using this approach that the limitations of the analytic approach can be omitted, and the efficiency and quality reward of using FEA can be fully achieved.

Table 9: Two approaches for combining FEA and VDI 2230

Analytic FEA (A-FEA)	The analytic procedure is used, and FEA assist identification of calculation parameters. E.g., Distance of load eccentricity, resilience, load introduction factor,…
Semi Analytic FEA (SA-FEA)	The analysis structure is altered to optimize the workflow. Some simulation input parameters defined by analytic calculations. FEA is performed with representative geometry and bolts. Verifications are performed in FEA software or by analytic calculations using extracted loads.

Figure 36 compares the analytic and SA-FEA approaches. It can be seen that the major differences are in step 4 to 6. In the analytic procedure, Step 4 includes many time-consuming calculations. The outcome is a minimum required assembly preload, that ensure that the clamping requirements are fulfilled. Then, in Step 5 the min/max required preloads are calculated. The allowed assembly preload must be higher than the max required preload. In this way, the clamping requirements are verified. In Step 6, further verifications are performed before tightening torque is calculated and the joint is approved or not. If the calculations at any time shows that the safety margins are too small, the bolt diameter or strength has to be increased. This may affect some of the calculations in Step 4-6, which then will have to be re-done. This can be quite time consuming.

In the SE-FEA approach, the max/min assembly preloads are calculated based on the estimated bolt diameter and are used as input for the FE-analysis. Resilience, load introduction factor and other analytic quantities are represented in the FE-model. For the max preload simulation, the

Figure 36: Comparison of Analytic and Semi Analytic FEA workflows

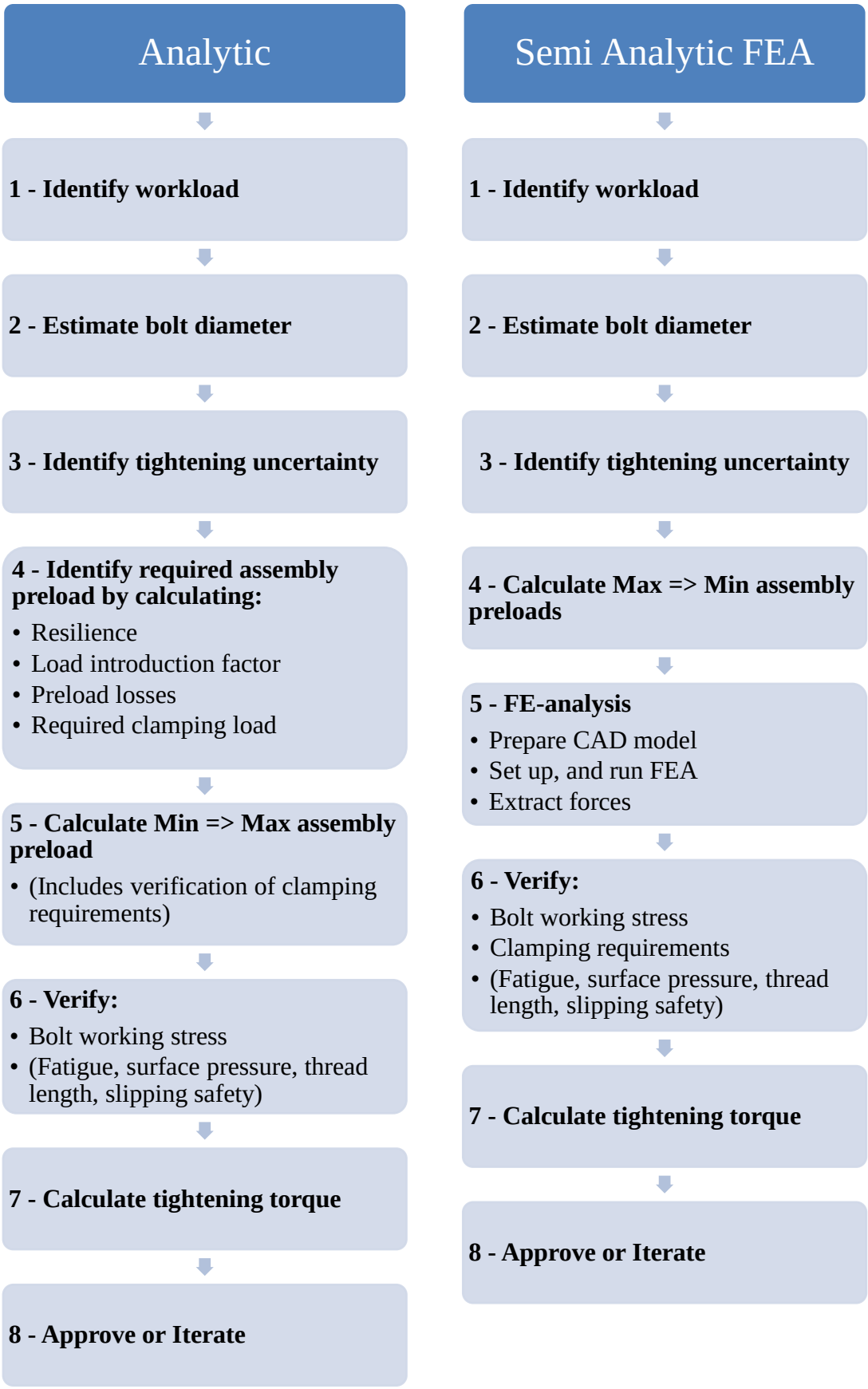

bolt working stress is verified. For the minimum preload simulation, the clamping requirements are verified. If any changes are required, the simulations must be updated and re-run.

5.1.1 Advantages of Semi Analytic FEA approach

By optimizing and streamlining the interaction between FEA and VDI 2230, an efficiency reward can be gained. It also gives confidence that the analysis is performed correctly, avoiding making simple mistakes. By keeping the workflow basic and simple, the threshold for using it is also lowered.

In general, by using FEA many of the limitations of the analytic procedure is avoided. Representation of the bolt and clamped parts resilience and load introduction factor is included. Eccentricity in load application, and the compliance of the geometry is also represented. Load distribution in MBJs are better than what can be obtained with analytic methods. Thus, the quality of the analysis is increased.

5.2 BASIC FEA WORKFLOW

In Table 10, a basic workflow that has been developed for combining FE-analysis and VDI 2230 are presented. It contains has the main categories: Pre-calculations and Dimensioning, FE-analysis, and Analysis of Results. The goal has been to keep it general and easy to use, so users with little experience in a simple way can perform high quality assessments of bolted joints according to the VDI 2230 methodology. After the workflow is presented, the analysis concept and calculation template are introduced.

Use of this workflow assumes good knowledge of the relevant FEA software. *ANSYS Workbench 17.2* has been used for this project, which includes some practical functionality such as bolt preload definition and contact status control.

The assumed initial state for applying the workflow in Table 10 is specified in step S0.

Table 10: Basic FEA Workflow for analysis of bolded joints according to VDI 2230

	Description
S0	**Initial state** A CAD-model of the relevant geometry is available, and according to design rules and experience, a guess has been made about the bolt size, number, and distribution of bolts. The analysis case and relevant details like geometry and workloads should be described in the report.
Pre-calculations and Dimensioning	
S1	**Workload** The workload can be determined by analytic calculations, or FE-analysis.

S2	**Estimation of Nominal Bolt Diameter** The nominal bolt diameter is based on the bolt workload, and can be estimated from VDI 2230 Pt.1 Table A7. If other bolt materials than Steel is used, a bolt with equivalent load capacity can be used: $$d_2 \geq \sqrt{\frac{R_{p0.2.Bolt_1}}{R_{p0.2.Bolt_2}} \cdot (d_1)^2}$$
S3	**Tightening Factor** The tightening factor is linked to the precision of the tightening method and tool used for assembly, and can be estimated via VDI 2230 Pt. 1 Table A8.
S4	**Maximum Assembly Preload** The allowed assembly preload can be calculated from the formula below using the proof strength of the bolt and a utilization factor. For Steel bolts, assuming a utilization factor $\nu = 0.9$ (90%), VDI 2230 Pt.1 Tables A1–A4 can be used to quickly identify the allowed assembly preload. Coefficients of friction can be obtained from [Pt.1-Table A5-A6] or [18, 19]. $$\sigma_{red.Mzul} = \nu \cdot R_{p0.2\min}$$ $$F_{M\max} = F_{Mzul} = A_S \cdot \frac{\sigma_{red.Mzul}}{\sqrt{1+3\left[\frac{3d_2}{2d_0}\left(\frac{P}{\pi \cdot d_2}+1.155\mu_{G\min}\right)\right]^2}}$$
S5	**Minimum Assembly Preload** The minimum preload is determined from the max preload and the tightening factor. Estimated preload losses can be included to obtain a more realistic minimum preload. $$F_{M\min} = \frac{F_{Mzul}}{\alpha_A} - (\text{preload losses})$$
FE-Analysis	
S6	**Simplify and Prepare CAD Geometry** Simplify and prepare a CAD-model that corresponds to Class II or III. The minor thread diameter d_3 can be used as bolt diameter. Other diameters can be used to manipulate the bolt resilience. For Class III, the bolt and tapped threads must have a corresponding diameter.
S7	**Prepare and Run FE-analysis** ➢ Create two static structural simulations for max/min assembly preloads, with shared Engineering Data, Geometry, and FE-Model. ➢ Define correct material properties for the bolt and clamped parts. ➢ Apply BCs, Loads, Contacts, and Create Mesh ○ Apply maximum workload in both simulations to get max bolt load, and min clamping pressure. ○ Apply bonded contact (Class III), or MPC connection (Class II) in the tapped thread area. Friction should be applied in the clamping interface.

	○ Mesh the bolt with HEX elements. Note: The mesh in the clamping interface and clamping solid volume should be refined to achieve a realistic pressure distribution and clamped parts resilience.
S8	**Extract Values from the FE-analysis** The values below can be extracted from the FE-analysis. <table><tr><th>F_{Mmin} - Minimum Assembly Preload</th><th>F_{Mmax} - Maximum Assembly Preload</th></tr><tr><td>F_{Mmin} – Actual preload (F_{KR} – Residual clamping force)</td><td>F_{Mmax} – Actual preload F_{Smax} – Maximum bolt load M_{Sbo} – Maximum bolt moment</td></tr></table>
Analysis of Results	
S9	**Verification of Work Stress (R8)** Calculate the bolt work stress based on the extracted loads and identify the safety factor. ➢ S_F - Safety factor for exceeding yield limit
S10	**Verification of Clamping Requirements (R12)** Verify the joint clamping requirements by controlling joint opening, clamping pressure, residual clamp load, slipping, and/or prying. FEA software specific functionality and tools may be used. Check the guide (Ch.5.4) for further descriptions.
S11	**Calculation of Tightening Torque (R13)** Calculate the tightening torque required to reach the allowed assembly preload F_{Mzul}. $$M_A = F_{M.zul}\left(0{,}16P + 0{,}58d_2 \cdot \mu_{G\min} + \frac{D_{K.\min}}{2}\mu_{K\min}\right)$$
S12	**Approve or Iterate** If the clamping requirements and bolt work stress has sufficient margins, the BJ is approved. If not, possible actions are described in the guide (Ch.5.4). Redo the procedure from **S3**.

NB! In this Basic Workflow, verification aspects like: preload losses (R4), fatigue (R9), pressure under the bolt head (R10), thread length of engagement (R11), and stress level in the clamped parts are not treated.

5.2.1 Analysis Concept

A graphical representation of the analysis and verification concept of the basic workflow is provided in Figure 37. The minimum (F_{Mmin}) and maximum (F_{Mmax}) assembly preloads are displayed in the joint diagram, with associated forces and deformations. The source of two different assembly preload levels are tightening uncertainty and preload losses. The maximum workload (F_{Amax}) is applied for both preloads.

For the maximum preload, the maximum bolt load F_{Smax} must stay below the minimum bolt proof load $F_{p0.2min}$. The gap between them determines the bolt safety margin.

For the minimum preload, the minimum residual clamping load F_{KRmin} must remain higher than the clamping requirement F_{Kerf}. This gap determines the clamping safety margin.

In short, the extreme cases with the worst combination of possible assembly preload and applied workload are analyzed. When the bolted joint provides sufficient safety margin for the extreme cases, the bolted joint will according to the analysis and associated assumptions be considered to be approved.

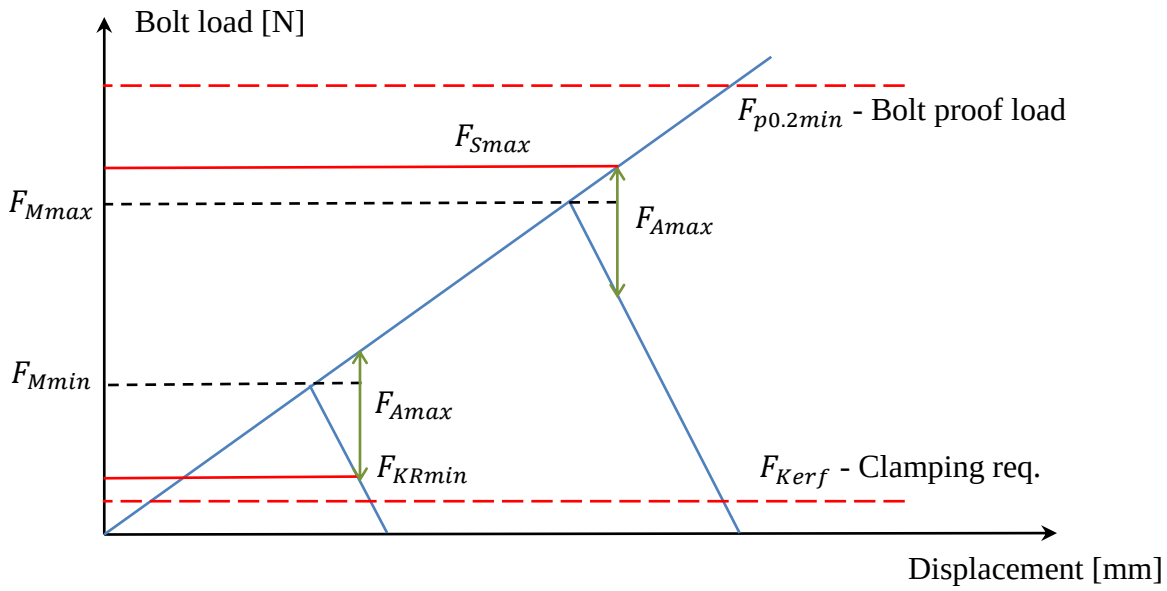

Figure 37: Joint diagram with the analysis concept of the basic workflow analysis.

5.2.2 Calculation Template

In ***Appendix A***, a calculation template that matches the Basic Workflow is attached. The file has been prepared in *PTC Mathcad Prime V4.0*, a common software for engineering calculations, and is attached in digital and printed format. The intension is that the template can be used as a basis, and adapted to the calculation case in question by the user. Use of the template can improve the efficiency of the analysis, and give significant time savings.

The template matches the steps in the Basic Workflow. Input parameters are highlighted in blue (Figure 38), and are used to calculate required calculation quantities and outputs according to VDI 2230. Some of these are used in setup of the FE-analysis, and in verification of bolt stress and clamping. The template allows for simple modification of the basic parameters, like if the bolt size or strength is changed, automatically updating all calculation quantities and output parameters.

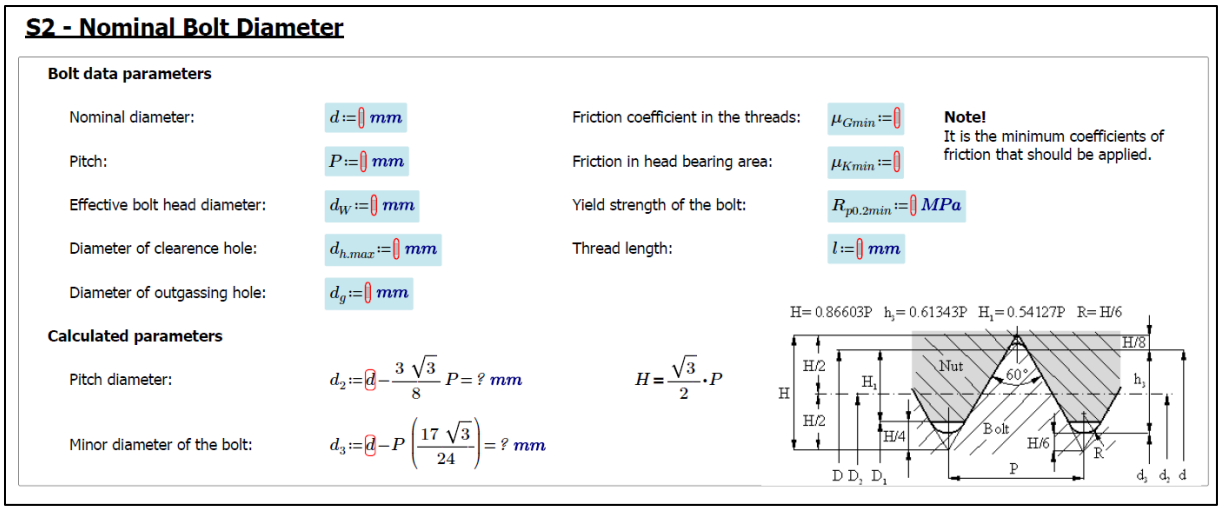

Figure 38: Extract of step S2 from the Basic Workflow calculation template in *Appendix A*

An advantage of using Mathcad templates is the possibility to have simple programming loops, as displayed in Figure 39. The left is used to calculate a parameter that is determined differently for different values of the input parameter. The right one is a verification loop that simplifies criteria checking in the calculations.

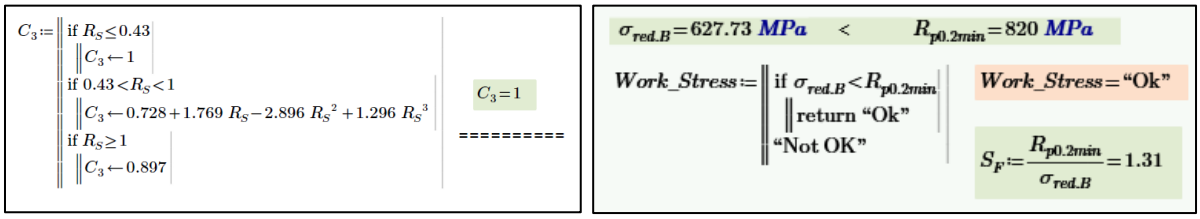

Figure 39: Two examples of programming in bolt assessment calculations

5.3 Non-critical Joints

Joints under static conditions, with no working loads and no need for a specific preload may be defined as non-critical joints. The only requirements might be that they should not come loose, and not break during tightening. Such joints may be used to fix components, covers, thermalisation points, sensors, or similar.

There is no need for detailed analysis of such joints. However, there are some factors that can affect the tightening torque, like bolt strength and coefficients of friction. To aid the calculation of tightening torque for specific non-critical bolts, a Mathcad calculation template has been prepared in ***Appendix B***.

The input parameters are the proof stress of the bolt, and the coefficient of friction in the threads and under the bolt head. The output values are listed in a table, as seen in Figure 40, with tightening torques and associated preloads for bolt range M3-M12. These values are provided for 30%, 50%, 75%, 90% and 100% utilisation of the bolt proof stress.

Two standards provide data about the minimum breaking torque for Steel [20] and Stainless Steel [21] bolts. These values can be used as reference values for the maximum tightening torques.

Tightening Torques M3-M12 Bolts

Basic parameters

Friction in threads:	**0,2**
Friction in head bearing:	**0,2**
0.2% proof stress:	**640** MPa

Tightening Torques & Corresponding Assembly Preloads - Standard Bolts											
		Utilization of Bolt Capacity									
	Stress section	*100 %*		*90 %*		*75 %*		*50 %*		*30 %*	
Bolt	mm^2	*Nm*	*kN*	*Nm*	*kN*	*Nm*	*kN*	*Nm*	*kN*	*Nm*	*kN*
M3	5,0	2,0	*2,5*	1,8	*2,3*	1,5	*1,9*	1,0	*1,3*	0,6	*0,8*
M4	8,8	4,5	*4,4*	4,1	*3,9*	3,4	*3,3*	2,3	*2,2*	1,4	*1,3*
M5	14,2	9,0	*7,1*	8,1	*6,4*	6,7	*5,3*	4,5	*3,6*	2,7	*2,1*
M6	20,1	15,6	*10,1*	14,0	*9,1*	11,7	*7,6*	7,8	*5,0*	4,7	*3,0*
M8	36,6	37,9	*18,4*	34,2	*16,6*	28,5	*13,8*	19,0	*9,2*	11,4	*5,5*
M10	58,0	75,1	*29,3*	67,6	*26,4*	56,3	*22,0*	37,6	*14,7*	22,5	*8,8*
M12	84,3	129,9	42,7	116,9	38,5	97,4	32,1	64,9	21,4	39,0	12,8

Figure 40: Table with tightening torques and associated preloads for M3-M12 bolts

In case of a TTJ joints, it is important to verify that the tapped threads length of engagement is sufficient. Check 5.5.4 for further details.

Coefficients of Friction

Typical coefficients of friction can be found in [Pt.1-Table A5]. The CERN MME Mechanical Lab has test facilities for identifying coefficients of friction for specific combinations of bolt, clamped parts, and lubrications. For Steel bolts and a range of standard coefficients of friction, tightening torques and associated preloads can be found in [Pt.1-Table A1-A4] for 90% utilisation of the bolt capacity.

Note that there is a risk associated with using wrong coefficients of friction. Factors such as oxidation and flattening of involved surfaces can influence the friction coefficient, so it deviates from the expected value. If the coefficient of friction is large, small changes can have large effects on the achieved preload. If the friction is higher than assumed, the resulting preload will be lower than expected. If the friction is lower than assumed, the preload will be higher than expected. If the last happens, the bolt might break due to the increased axial load.

Thus, if there is uncertainty associated with the friction, it is better to use the minimum coefficients of friction in the threads and under the bolt head when calculating the tightening torque.

One strategy can be to use lubrication to ensure low friction, which also give minimal consequences if there is uncertainty in the friction. That is not a possible at CERN, since lubrication is not acceptable in many cryogenic applications. One possibility however is to use silver coating, and perform mechanical measurements of the resulting coefficient of friction.

Bolt Loosening

Preload losses can occur from surface flattening in the threads and under the bolt head. This can lead to significant preload losses if the clamping length is small (stiff bolt). According to VDI 2230, the clamping length is recommended to be according to (21) for the joint to provide proper safety against bolt loosening. In the case of vibrations, retraining elements [Pt.1-Table A14] can be used to reduce the risk of loosening.

$$l_k / d \geq (3...5) \tag{21}$$

5.4 GUIDE FOR BASIC FEA WORKFLOW

This Guide contains supplementary details for the Basic FEA Workflow in Ch. 5.2, and is intended to assist in performing FEA analysis of bolted joints. It provides descriptions of calculations, verifications, and useful references. However, it is not an all-inclusive self-standing guide and it is assumed that VDI 2230 is available to the user, and that the user has good knowledge about the relevant FEA software.

It is important to be aware that even though analytic limitations are avoided by using FEA, there are some aspects of validity with FE-analysis that is important to aware of. Therefore, aspects of validity are discussed where relevant. In the end of the section, the importance of testing is underlined.

[Pt.1–Table A9] provides useful information about properties for common materials, and useful dimensions for Hexagon Head Bolts [22], Hexagon Socked Head Cap Screws [23], and clearance holes [24] can be found in relevant references.

5.4.1 S0: Initial State

It is assumed that there is a CAD-model of the relevant geometry available, designed according to basic rules and experience. A preliminary guess of the bolt size, number of bolts, and distribution of bolts must be made. Two approaches are:

1) **Unknown bolt size** - To perform an initial guess about bolt size, spacing and number of bolts, iterations of the steps S1 and S2 can be performed.

2) **Bolt size is known** - Step S1 and S2 can be skipped. However, it might still be interesting to carry out the steps S1 and S2 to compare the estimated bolt diameter to the actual bolt diameter. This can serve as a first indication of the suitability of the bolt selected.

The analysis case and relevant details like geometry and workloads should be described in the report.

5.4.2 S1: Workload

To estimate the nominal bolt diameter, the maximum workload on the bolt must be known. For MBJs, there are different strategies for load determination. Table 11 list four strategies that can be used to identify bolt workloads. The analytic methods of *Rigid Body Mechanics* and *Elastomechanics* for determination of workload in MBJs are described in [Pt. 2-Ch.6].

Table 11: Strategies for determination of bolt workloads

	Strategy	Description	+/-
WL 1	*Analytic*	Assuming rigid bodies and uniform distribution, or that the transverse load is proportional to the distance from the centre, the workload can be identified by simple analytic force and moment equilibrium calculations	Can in some cases underestimate the bolt workload May not be applicable for complex geometries and loads

WL 2	*Class I*	Using bonded contact in the interface, the reaction forces in the interface can be extracted and by assuming uniform distribution, divided on the relevant bolts	The assumption of uniform distribution may not be completely valid, but with complex loads and geometries it can give a good first estimate
WL 3	*Spot-welds*	By applying spot-welds in the bolt locations, relative load distribution is represented, and the most highly loaded bolt can be identified	The actual load distribution may not be perfectly accurate, but more accurate than assuming uniform distribution. Asymmetric geometric conditions and prying can be represented with this approach
WL 4	*Class II, no preload*	By performing a Class II simulation using beams without preload and with frictionless contact, similar to WL 3, the most highly loaded bolt can be identified Rigid beams may be used	Same as for WL 3 Since slipping can occur, and the beams have a certain resilience, the load distribution can be affected

Maximum Workload

A joint is designed to withstand axial (F_A) and/or transverse (F_Q) loads. If both are present, VDI 2230 suggests to use the dominant load according to Eq. (22) when estimating the nominal diameter. The maximum global workload, and most unfortunate combination of loads must be applied to the structure to obtain the maximum bolt workload. A safety factor can be applied to the global workload to account for uncertainties. This can be determined by codes and standards, or company practice and experience.

$$\max\left(F_{A\max}, \frac{F_{Q\max}}{\mu_{T\min}}\right) \tag{22}$$

F_{Amax} is the maximum axial bolt workload, F_{Qmax} is the maximum transverse load, and μ_{Tmin} is the minimum friction in the interface.

As a result of designing the joint for the dominant load, it will also have a certain resistance for the other load component. Thus, if designed for an axial load, the clamping will provide a certain friction grip to resist transverse loads, and opposite. Verifications are made in step S10 to ensure that sufficient clamping pressure is present for the worst combination of loads.

Concentric or Eccentric Workload

If it is known that prying loads are included in the bolt workload, the joint can be said to be *concentric* instead of *eccentric* in step **B2** when estimating bolt diameter. In this way, the eccentric or prying conditions will not be accounted for twice and result in overestimating the bolt size.

Unit Load Approach

The standard way to identify the bolt workload is to apply the full global workload, and obtain the working loads according to the strategies listed in Table 11. In some cases however, for simple MBJs without prying effects, a unit load can be applied as global workload. Then the percentage distribution of the unit load to the bolts becomes clear in a simple way, and can be used to estimate bolt loads for other global workloads.

However, this assumes a linear relation between global load and bolt load development. As seen with prying, that might not always be the case, and this approach does not capture non-linear bolt load development.

Validity of Workload

When identifying the workload, no preload is present and friction grip in the clamping interface is not represented. If the bolt representation is not rigid, the bolts have a certain resilience. These two factors affect the global compliance of the assembly, and can affect the load distribution.

Because of this, it can be expected that the bolt workloads and global load distribution will be different when preload, and friction in the clamping interface is present. This illustrates the importance of the verification steps S9 and S10.

5.4.3 S2: Estimation of Nominal Bolt Diameter [Pt.1 – R0]

[Pt.1-Table A7] provides a practical guide to perform a qualified guess to estimate the nominal bolt diameter, based on the bolt workload. The workload is scaled in discrete steps based on many different factors, such as loading mode, eccentric or concentric conditions for loading or clamping, and tightening method. Then a nominal diameter is suggested for different strength grades of Steel bolts.

Using this table, there is a higher chance of choosing the correct nominal diameter the first time. However, there are large uncertainties in the estimate, so it is important to verify the bolt performance.

Note that if the bolt workload already includes prying loads, *concentric* can be chosen instead of *eccentric* in step **B2**.

Non-Steel bolts

For different reasons, bolts of other materials than Steel may be used. That might be to have improved corrosion properties, match thermal contraction properties of the clamped plates, or to improve the joint by having a more resilient (soft) bolt.

The most simple approach is to convert the nominal diameter for the Steel bolt resulting from the above selection guide, to a bolt size of the new material having an equivalent proof load capacity. The diameter of the non-steel bolt is calculated according to Eq. (26).

The bolt proof load is defined in (23). It can then be stated that the proof strength of the two bolts should be the same, as (24) show.

$$F_{p0.2} = R_{p0.2} \cdot A_S \approx R_{p0.2} \cdot \frac{\pi}{4} d^2 \tag{23}$$

$$F_{p0.2.Bolt_1} = F_{p0.2.Bolt_2} \tag{24}$$

Based on (23) and (24), the following relation can be made:

$$R_{p0.2.Bolt_1} \cdot \frac{\pi}{4} \cdot (d_1)^2 = R_{p0.2.Bolt_2} \cdot \frac{\pi}{4} \cdot (d_2)^2 \tag{25}$$

Thus, the diameter of an equivalent bolt diameter can be calculated:

$$d_2 \geq \sqrt{\frac{R_{p0.2.Bolt_1}}{R_{p0.2.Bolt_2}} \cdot (d_1)^2} \tag{26}$$

Elongation Before Fracture

When selecting bolt strength, it is important to be aware of the ductility and elongation before fracture properties of the bolt. The stronger and harder the bolt is, the less elongation is accepted before the bolt fracture, as Figure 41 show.

For a high strength bolt where a lot of the strength is utilized, little yielding is allowed and overloading can easily lead to fracture of the bolt and joint failure. Because of this, high grade bolts should be used with care.

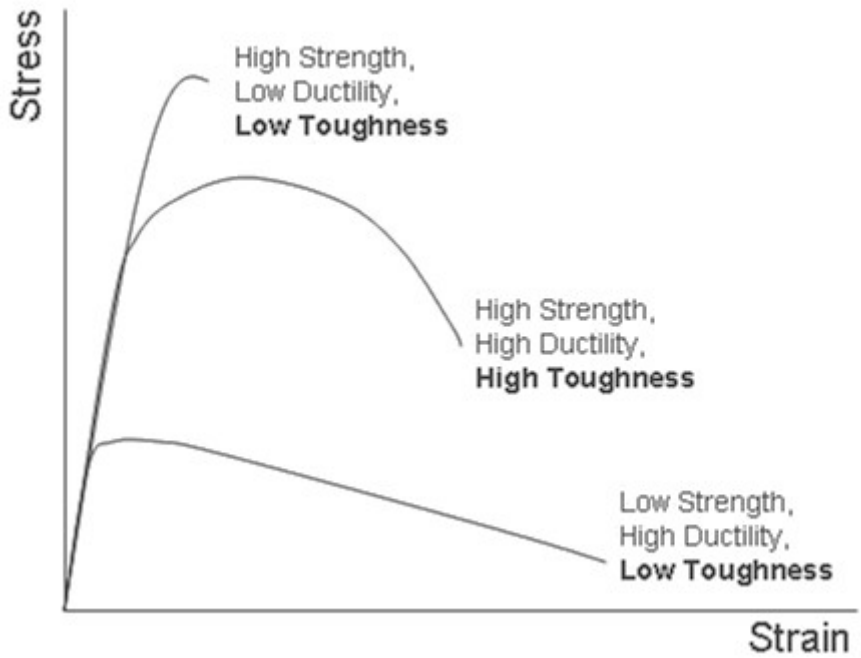

Figure 41: Typical stress-strain curves for various material strengths

5.4.4 S3: Tightening Factor [Pt.1 – R1]

The tightening factor is based on the tightening uncertainty associated with different tightening methods. Factors affecting the uncertainty is friction, accuracy in measurement and reading, and the resilience of the joint.

A thorough guide to tightening methods and uncertainties are provided in [Pt.1–Table A8]. Some typical values are listed in Table 12.

Table 12: Typical tightening factor ranges for typical tightening methods

α_A	**Method**
1.0	Yield controlled tightening
1.1 – 1.2	Elongation control or ultrasound monitoring
1.2 – 1.4	Rotation angle controlled tightening Hydraulic frictionless tightening
1.4 – 2.5	Torque controlled tightening
2.5 – 4	Impact wrench, impulse driver, by hand

To reduce the tightening uncertainty and achieve a higher minimum assembly preload for a given bolt, a more precise tightening method should be used. By using tightening angle, the effect of friction is neglected, which is a large source of uncertainty. The uncertainty can also be reduced by having a more resilient bolt by material selection, cross section, or larger clamping length

Another source of tightening uncertainty to be aware of that is not treated in VDI 2230, is the impact of tightening sequence for MBJs. If tightening is not performed according to recommendations [25], single bolts can experience large preload losses that is challenging to predict.

5.4.5 S4: Maximum Assembly Preload [Pt.1 – R7]

The allowed assembly preload (F_{Mzul}) for a given bolt is calculated according to Eq. (27). The maximum axial and torsional stress during assembly are used in the equation to identify the allowed preload. The allowed bolt stress ($\sigma_{red.Mzul}$) is based on the minimum bolt proof strength ($R_{p0.2min}$), and a utilization factor (ν). It can be noted that the proof strength of the bolt may be typically 85-95% of the yield strength.

$$\sigma_{red.Mzul} = \nu \cdot R_{p0.2\min}$$

(R7/2)

$$F_{M\max} = F_{Mzul} = A_S \cdot \frac{\sigma_{red.Mzul}}{\sqrt{1+3\left[\frac{3d_2}{2d_0}\left(\frac{P}{\pi \cdot d_2}+1.155\mu_{G\min}\right)\right]^2}} \tag{27}$$

For Steel bolts and a utilisation factor of 0.9 (90%), the tables [Pt.1–Table A1-A4] has listed allowed assembly preloads for a range of bolts and standard coefficients of friction. Coefficients of friction can be obtained from [Pt.1–Table A5-A6] or [18, 19].

Note the remarks about coefficient of friction provided on page 50.

Utilization Factor

For critical joints, a high utilisation factor is generally recommended. VDI 2230 suggest using $\upsilon = 0.9$. That is because a high utilisation and high preload gives a higher acceptance of preload losses, better resistance against bolt loosening, and reduces the risk of joint opening and unpredictable prying loads.

Having a high utilisation factor may be counter intuitive, as it is based on having a high stress level in the bolt, giving a lower bolt stress safety factor. However, due to the reasons above, the overall safety is higher with high utilisation.

Table 13: Bolt properties according for Steel and Stainless-Steel bolts [21, 26]

Steel Group		***Steel***			***Stainless Steel (Austenitic)***		
Steel grade					A1, A2	A3, A4	A5
Property class		**8.8**	**10.9**	**12.9**	**50**	**70**	**80**
Tensile strength	R_m [MPa]	800	1000	1200	500	700	800
Stress at 0,2% permanent strain	$R_{p0,2}$ [MPa]	640	940	1080	210	450	600
Elongation at fracture	A_5	12 %	9 %	8 %	0,6 d	0,4 d	0,3 d
Shear ratio	τ_B / R_m	0,65	0,62	0,60	0,80	0,72	0,68

5.4.6 S5: Minimum Assembly Preload

The minimum assembly preload is the lowest probable preload, and is determined from the maximum assembly preload as Eq.(28) show. The two preload levels are illustrated in Figure 37. If preload losses are estimated (5.5.2), they can be included to obtain a more realistic and conservative minimum preload.

$$F_{M\,\min} = \frac{F_{M\,\max}}{\alpha_A} - (\text{preload losses}) \tag{28}$$

5.4.7 S6: Simplify and Prepare CAD Geometry

The CAD geometry must be simplified and prepared for the FE-analysis. Which model class (bolt representation) to use must be decided. The different classes are presented in Ch. 2.4.

Class I and IV are not suitable for simulations with preload, and for verification of joint performance. Class II with beam representation and Class III with volume body representation of the bolt (Figure 42) have different advantages and disadvantages.

Setting up a Class II model is more simple than a Class III model, but it can give a more stiff bolt representation than Class III. That is because of the MPC joints connecting the beam to the clamped parts. For TTJs, this can also affect the validity of the pressure distribution in the clamping interface. Class III requires modelling of a volume body representing the bolt, and can give a more accurate representation of the joint compliance. The bolt resilience for both classes can be manipulated with the bolt diameter used in the the model.

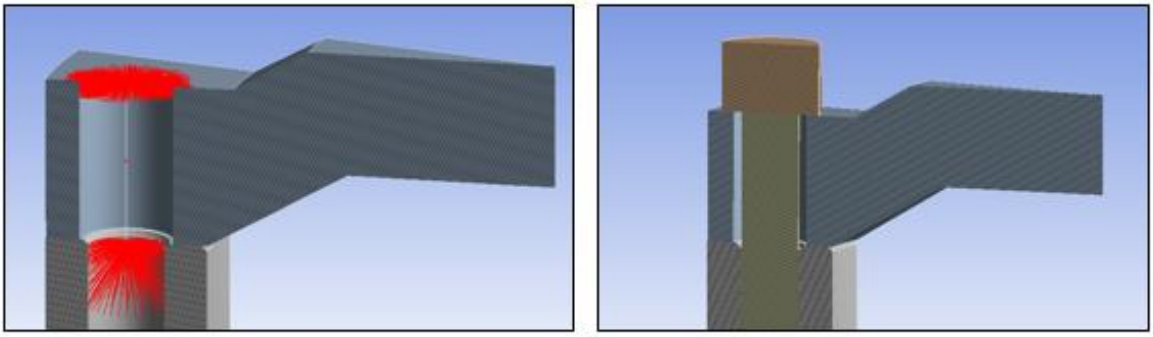

Figure 42: Class II and Class III bolt representation

Bolt Diameter

The most simple is to use a uniform diameter, based on thread minor diameter d_3. However, as described in 2.4.6., a more accurate representation can be achieved by basing the diameter on the analytic resilience.

For Class III bolts with a shank, the threads can be represented with the thread minor diameter and the shank by the nominal diameter d, as seen in Figure 43. For TTJs if using Class III, the tapped thread diameter must have the same diameter as the bolt. The bolt head diameter d_W can be identified in the relevant standards.

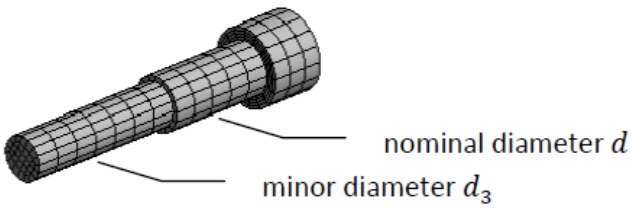

Figure 43: Class III representation of bolt

Extracting a SBJ

If the model and loading is symmetric, it is possible to extract a SBJ from the MBJ to simplify the analysis, as Figure 44 show. This might give sufficient representation to verify the joint performance.

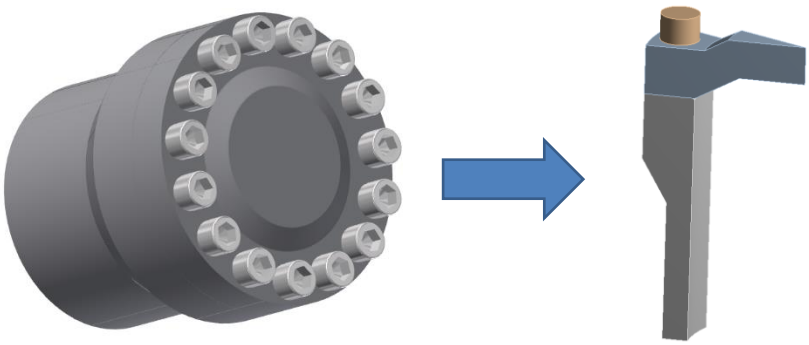

Figure 44: Extraction of SBJ from a MBJ

5.4.8 S7: Prepare and Run FE-analysis

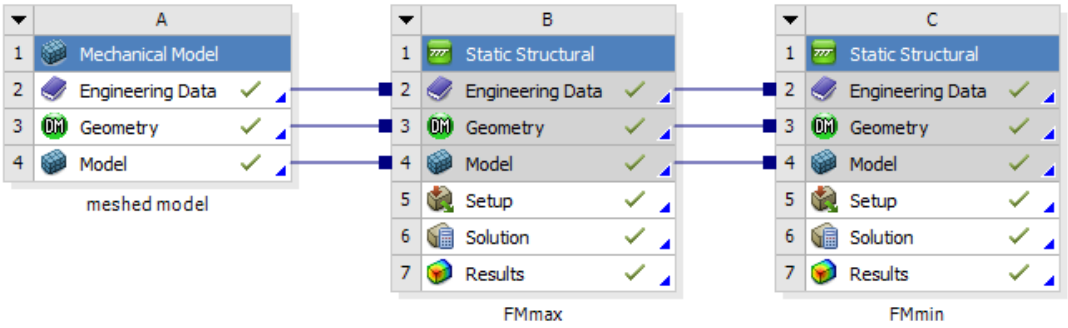

Figure 45: Simulation setup in ANSYS with Max and Min preload

Two simulations must be performed, one for each preload state. Model geometry, material data and mesh can be shared, as Figure 45 show.

Material data

Define correct material properties and apply correct materials to all parts of the assembly. Note that some properties can be temperature dependent. [Pt.1–Table A9] provides a good overview of common materials and their properties at room temperature.

Mesh

If the bolt has a Class III representation, the bolt must be meshed with HEX elements, e.g. using "Multizone Meshing". A poor mesh can give inaccurate results.

Normal mesh considerations should be used on the complete model to ensure correct component or assembly compliance. The mesh in the clamping solid volume should be refined to have the complete deformation cone represented. This is important to achieve the correct resilience of the clamped parts in the model, and to get a realistic representation of the pressure in the clamping interface.

Note that in [Pt.2-p.71], it is stated that the clamping pressure is represented with sufficient realism only for large clamping lengths, and with TBJs. That is related to proper formation of deformation cones, and stiffness introduced from the threads close to the clamping interface in TTJs.

Boundary Conditions and Contact

The model should have realistic boundary conditions and supports. Realistic friction should be applied in the clamping interface, so friction grip and its effect of the compliance is represented and assessment if slipping occur can be performed.

Load

The maximum global workload, and most unfortunate combination of loads must be applied so the bolted joint can be designed and verified for the maximum bolt workload.

As stated in Table 15, strategy "2" can be used, and a higher workload than the design workload can be applied. In this way, the joint performance can be demonstrated and verified with a workload safety factor. Codes and standards can define required safety factors on the workload. According to one code, *EN 13445 Unfired Pressure Vessels* [15], the test pressure for pressure vessels is 1.43x the nominal operating pressure.

Sub-steps

Normally, the solver automatically detects the need for sub-steps that is required for the simulation to converge. Sometimes however, a higher resolution of the data points might be beneficial to track the load development, like when verifying prying behaviour. Then, sub-steps can be defined to achieve the desired resolution.

5.4.9 S8: Extract Values from the FE-analysis

The forces and moments in Table 14 can be extracted from the simulations. The actual preloads should be extracted to verify that the correct preload level is acheived. The residual clamping force can be extracted and compared against joint or gasket requirements. The maximum bolt load and moment is used in verification of the bolt work stress.

Note that when extracting forces and moments from surfaces, the nodal forces for that surface are summarized. This is a potential source of error, and should be done with care.

Table 14: Values to be extracted from the simulations

F_{Mmin} - Minimum Assembly Preload	**F_{Mmax} - Maximum Assembly Preload**
F_{Mmin} – Achieved preload (F_{KR} – Residual clamping force)	F_{Mmax} – Achieved preload F_{Smax} – Maximum bolt load M_{Sbo} – Maximum bolt moment

5.4.10 S9: Verification of Work Stress [Pt.1 – R8]

Analytic calculation of the work stress is considered to be more accurate than analysing the stress in the FEA model. From the maximum bolt loads extracted, the work stress can be calculated according Eq. (29). This is a modified version of the working stress equation where the bending stress is included. The criteria in (30) must be fulfilled, and the safety factor can be calculated according to Eq. (31).

(R8/4)
$$\sigma_{red.B} = \sqrt{\left(\frac{F_{S\max}}{A_S} + \frac{M_{Sbo}}{W_S}\right)^2 + 3\left(k_t \cdot \tau_{\max}\right)^2} \tag{29}$$

(R8/5-1)
$$\sigma_{red,B} < R_{p0.2\min} \tag{30}$$

(R8/5-2)
$$S_F = \frac{R_{p0,2\min}}{\sigma_{red,B}} \geq 1,0 \tag{31}$$

The bolt proof load can be obtained from Table 13, experimental testing, or other sources. If the bolt is exposed to different operating temperatures, the lowest proof load should be used. The safety factor is in many cases expected to be in the range of 1.05 to 1.2.

Torsional Stress

According to VDI 2230, it assumed that there will be residual torsional stress in the bolt from the tightening torque applied during assembly. VDI 2230 recommends to include 50% of the torsional stress ($k_t = 0.5$). Note that there is high uncertainty related to this value.

Bending Stress

The bending stress contribution to work stress should be analysed, and not be significant. That is because stress concentrations in the threads and under the bolt head can magnify the peak bending stress 3 to 5 times [27]. This can lead to low cycle fatigue challenges, or static bolt failure. High bending stress might also indicate that slipping or prying is present.

The bending stress is not included in the original equation because VDI 2230 assumes that in most cases for highly preloaded bolts where the bolt and clamped parts are made of Steel, the bolt is much more resilient (softer) than the clamped parts ($\delta_S \gg \delta_P$) and will not be experience to high bending moments. For custom designs however, where the clamped parts can be made of Titanium which has half the E-modulus of Steel, bending moments might be present.

5.4.11 S10: Verification of Clamping Requirements [Pt.1 - R12]

There are many approaches to verifying the clamping requirements. What to verify, and which approach to use depends on the case in question. In general, no joint opening is a good indication and rule out prying challenges. If joint opening is present, or for specific clamping requirements, further verifications should be performed.

Two strategies to identify safety factors by the aid of FE-analysis are listed in Table 15. Below, aspects concerning verification of clamping pressure, slipping and prying is described. Clamping requirements are always verified for the minimum preload that is likely to be present.

For all methods, the validity depends on the numerical representation of friction, mesh size in the bolt and deformation solid, and mesh refinement in the clamping interface. Also note that preload losses like embedding and differential thermal contraction is not included in the basic workflow, which could further lower the minimum preload.

Table 15 : Safety factor strategies for FE-analysis of bolted joints

#	Name	Description
1	***Preload Safety Factor***	The workload and minimum preload is applied. Then the preload is reduced until joint opening, slipping, or the wanted sealing pressure occurs. The resulting preload ratio give a safety factor.
2	***Workload Safety Factor***	The minimum preload is applied. Then the workload is applied, and increased above nominal workload until joint opening, slipping, or the wanted sealing pressure occurs. The resulting workload ratio give a safety factor.

An alternative to identifying the exact safety factor is to define a minimum safety factor and verify the joint performance at this safety factor.

Clamping Pressure and Joint Opening

The clamping pressure can be investigated to assess the continuity in pressure between the bolts and pressure distribution across the clamping interface. As stated in 2.2.6, the clamping solids should interact with each other in MBJs, and cover the whole clamping interface width (comply with limit criteria G).

A stress plot of the joint cross-section along the bolt axis (Figure 46) can also be useful to assess the range of the clamping solid, both in terms of opening and pressure continuity in MBJs, depending on the orientation of the cross-section.

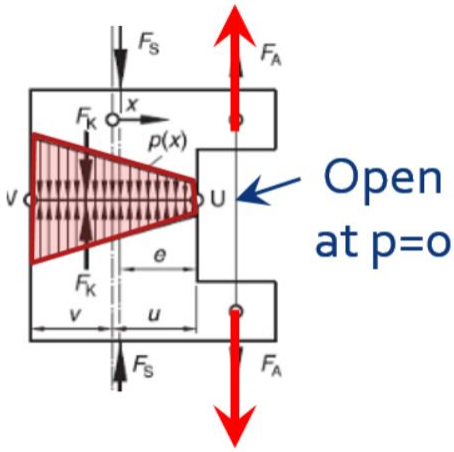

Figure 46: Pressure distribution in the interface, and joint opening.

Joint opening can indicate that the clamping solid is relieved, and that prying might be present. That will be the case if the limit criteria G is fulfilled, Eq. (13), and the pressure at the edge of the interface drops to zero, as Figure 46 illustrate.

If joint opening is not present, there is little chance of prying loads. Therefore, checking joint opening can be a simple first approach to controlling the clamping requirements.

One technique to assess joint opening is to plot the relative deformation of the two interface edges, as illustrated in Figure 47. From the graph, it is clear when the edges separate and partial joint opening is initiated.

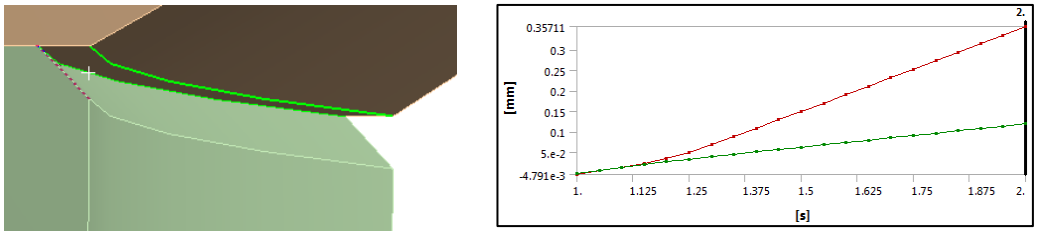

Figure 47: Plot of relative deformation for two edges on the clamping interface

ANSYS has a built-in functionality where the "contact status" can be probed, as shown left in Figure 48. This will let the user know if the faces are sticking, are near, or are sliding.

As shown right in Figure 48, the pressure magnitude and distribution can be analyzed. Blue areas are where there is zero pressure, and the joint is opened. For such an assessment, it can be useful to have a reference pressure distribution with only the preload applied.

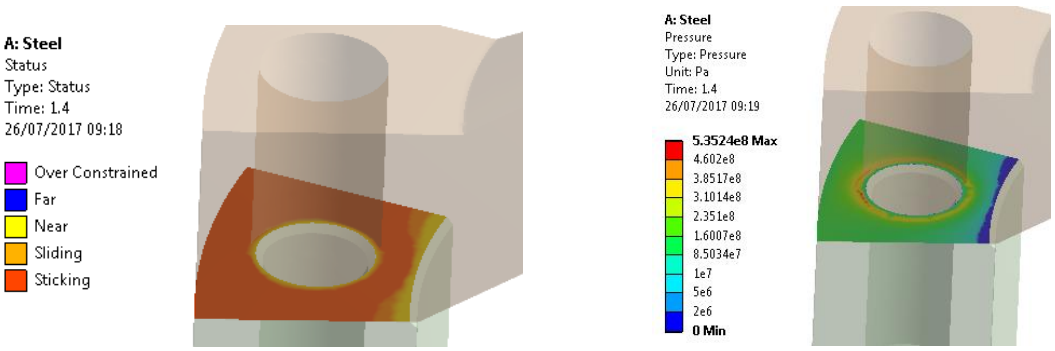

Figure 48: Assessment of joint opening with "status" and surface pressure plots

Slipping

There are multiple techniques to analyse if slipping occur in a joint. One is to have friction in the clamping area, and use the integrated ANSYS functionality and check the "status" in the clamping interface or "slipping distance", as shown in Figure 49. Another approach is to probe and plot the shear loads of the bolts. If there are any sudden load developments, it might indicate that slipping is initiated.

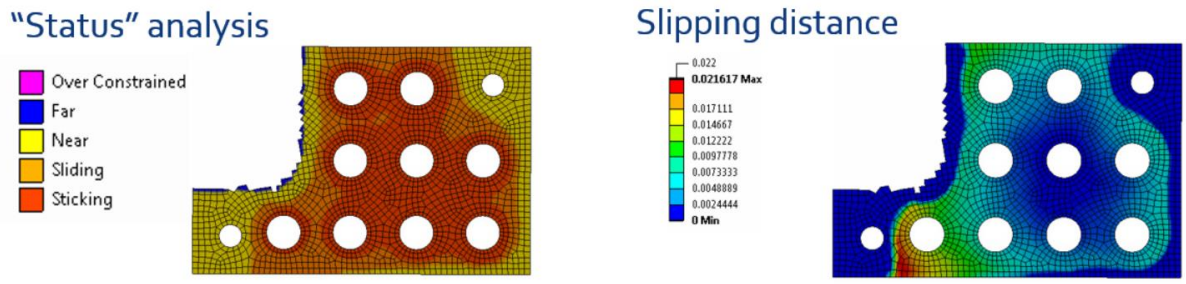

Figure 49: ANSYS plots for assessment of slipping

Analytic approaches can be made according to [Pt.1–R12] and [Pt.2–R12 p.99] to identify a safety factor against slipping (S_G). The transverse loads can be identified from having a bonded interface and probing the reaction loads, or from performing a Class II or III simulation with frictionless conditions and probe the bolt loads. The shear loads on the most highly loaded bolt can be extracted, and used in the analytic verification calculations. Note that the validity aspects of load distribution mentioned in "Validity of Workload" applies in this case.

Prying

What prying is, how it can be encountered, and the influence of preload is treated in Ch.4. In most cases, the goal is to verify that prying is not present in the joint. A typical development in additional bolt load for a certain preload level, as the workload is applied, is demonstrated in Figure 50. This characteristic development applies to both axial loads and bending moments if prying is present in the joint.

In the example case demonstrated in Figure 50, the joint is verified for a workload of 40 MPa, with a workload safety factor of 1.25. In the green area, the load development is linear and predictable. In the red area, partial joint opening is occurring, and the load is non-linear and challenging to predict.

When verifying that no prying is present, the workload must be in the green area. For this preload level, the bolt will experience linear and predictable loads up to the global workload of 50 MPa. Note that this curve will change for other preload levels.

To ensure the validity of the verification, the data points defined through sub-steps should have a sufficient resolution.

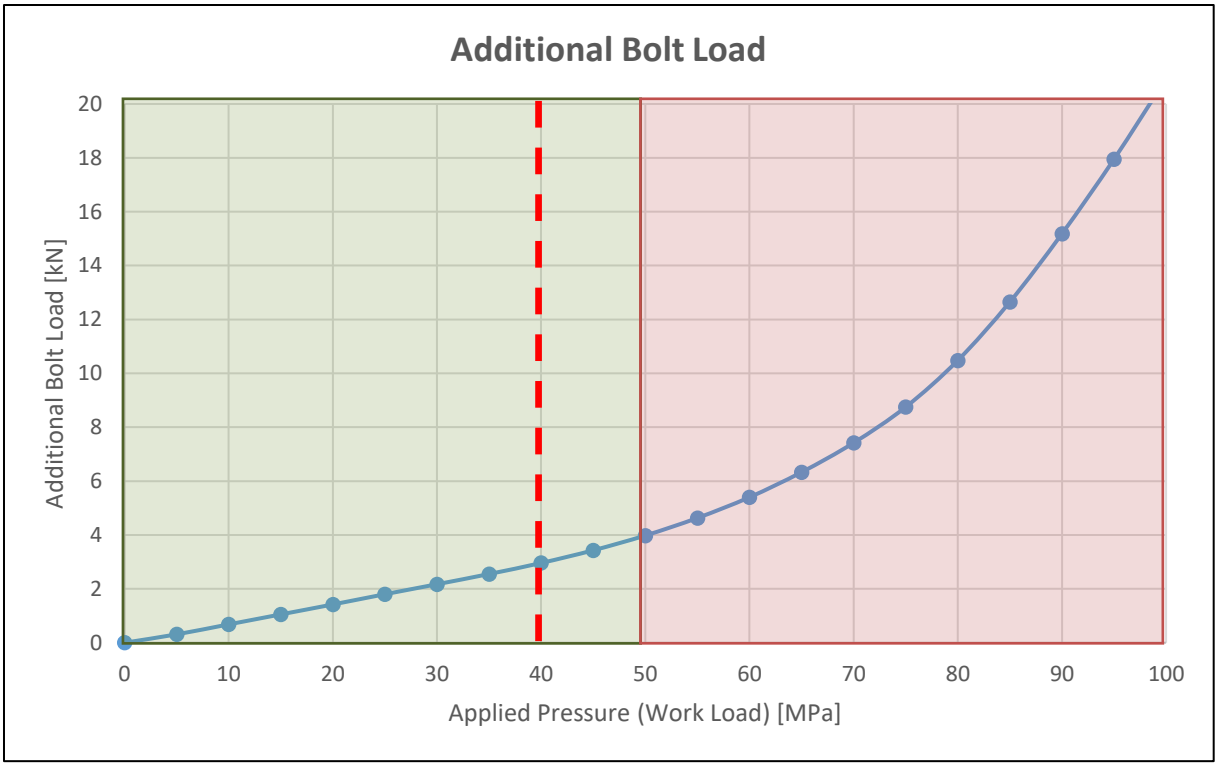

Figure 50: Bolt load development for a joint with prying

5.4.12 S11: Calculation of Tightening torque [Pt.1 – R13]

The tightening torque is calculated according to Eq. (32). It can be noted that the tightening torque is defined to reach the allowed assembly preload (F_{Mzul}).

(R13/1)

$$M_A = F_{M.zul}\left(\underbrace{0{,}16P + 0{,}58d_2 \cdot \mu_{G.\min}}_{\text{thread}} + \underbrace{\frac{D_{K.\min}}{2}\mu_{K.\min}}_{\text{bolt head area}}\right) \tag{32}$$

5.4.13 S12: Approve or iterate

If the clamping requirements and bolt work stress is approved by sufficient margin, the basic analysis is completed, and the BJ is approved. However, further verifications according section 5.5 can be performed to consider fatigue, preload losses, and thread length of engagement.

If not approved, possible actions are listed below, and the analysis must be revised from **S3**:

- Increase the maximum assembly preload
  - Adjust utilisation factor
  - Reduce thread friction
  - Increase bolt strength
  - Select a larger nominal bolt diameter

- Increase the minimum assembly preload
  - Increase the maximum assembly preload
  - Reduce preload losses
  - Reduce tightening uncertainty

If prying is present, the minimum preload should be increased. The design can also be modified to stiffen the geometry, as detailed in section 4.3. Further details of improving joint design is given in [Pt.1-Figure 37] and detailed in [Pt.1-Ch.6]. A list of measures to increase the service reliability of BJs is provided in [Pt.1-A13], including how the bolt loading and stress can be reduced and how the stressability of the bolt can be increased. The actions are described terms of geometry, material and assembly.

5.4.14 Testing and Verification

There are many questions that can be asked about the accuracy in a FE-analysis: Are the coefficients of friction correct? Are all non-linear phenomena captured? Are all boundary conditions represented correctly? Are the contacts correctly represented? Are the numerical representation of contacts and friction in the FE-analysis correct?

No certainty about the joint performance can reached before physical testing has been carried out under realistic conditions. After the test, critical bolts should be inspected for plastic deformations like reduced cross section, or increased length. Significantly reduced loosening torque is a clear indication of unexpected preload losses.

5.5 FURTHER ASSESSMENTS

Some calculation quantities and verification aspects are left out of the Basic FEA Workflow to simplify it. This section briefly describes the most relevant aspects that are left out, and how they can be included in the analysis. Some of the further assessments are demonstrated in ***Appendix C-2*** and Part 2 of ***Appendix F***.

5.5.1 Analytic Calculation Quantities

For some of the following calculations, it is required that the resilience of the joint is known. This can be determined with FEA according to the methods described in [Pt.1–7.3.1], or calculated by the analytic methods described in [Pt.1-R3].

5.5.2 Preload Losses [Pt.1 – R4]

Two sources of preload losses accounted for by the analytic VDI 2230 procedure is embedding and differential thermal expansion. Identification of these quantities require some efforts, but increase the accuracy of the bolted joint analysis. When the preload losses is estimated, they can be included in Eq.(28) to provide a more realistic minimum assembly preload.

Embedding

Embedding or relaxation is local deformations that occur during assembly or loading. The amount of embedding depends on the number of surfaces that interacts and the surface roughness. Guide values are provided in [Pt.1-Table 5], and the preload loss is calculated according to Eq. (33).

(R4/1)

$$F_Z = \frac{f_Z}{\delta_S + \delta_P} \tag{33}$$

According to a NASA report, the preload loss due to embedding can be expected to be 5% of the maximum assembly preload [28]. This can serve as a quick estimate.

Differential thermal expansion

If the joint is exposed to thermal changes and the thermal expansion properties of the bolt and clamped parts are different, it can result in increased or reduced bolt loads. If the plate contracts more than the bolt, the preload will be reduced. If the bolt contracts more than the plate, the bolt load is increased. The change in preload can be calculated according to Eq. (34).

The change in bolt load from differential thermal expansion should be included in the maximum bolt load in Eq.(29) if the preload increase, and as a preload loss in Eq.(28) if the bolt load decrease.

$$\Delta F'_{Vth} = \frac{l_K \cdot \left(\alpha_S \cdot \Delta T_S - \alpha_P \cdot \Delta T_P\right)}{\delta_S \frac{E_{SRT}}{E_{ST}} + \delta_P \frac{E_{PRT}}{E_{PT}}} \tag{34}$$

Changes in bolt load due to thermal changes can also be identified from a separate thermal FE-analysis, where the thermal material properties are defined.

To reduce the effect of differential thermal expansion, the material of the bolt and the clamped parts can be selected to have the same coefficient of thermal expansion.

5.5.3 Fatigue [Pt.1 – R9]

If the workload is dynamic, the alternating stresses can be calculated with Eq. (35) using the extracted axial load and bending moment for maximum and minimum workload. This gives a stress amplitude that can be compared against fatigue the relevant fatigue limits. VDI 2230 contains relevant reference values for Steel bolts.

[Pt.1 – Eq.93]

$$\sigma_{SAb} = \frac{F_{SA}}{A_S} + \frac{M_{SA}}{W_S} \tag{35}$$

5.5.4 Tapped Thread Length [Pt.1 – R11]

For TTJ joints, it can be important to verify that the tapped threads length of engagement is sufficient. A common rule is that the tapped thread length of engagement should be 1.5 times the nominal bolt diameter ($m_{eff} = 1.5 \cdot d$). With longer thread length of engagements, there is a risk that the thread can become jammed. A quick guide for Steel bolts and different tapped thread materials are provided in Figure 51.

Detailed calculation of the minimum thread length of engagement can be performed according to [Pt.1-R11] and [Pt.1-5.5.5].

Material of components		Length of engagement l_e [2] according to property class of screw			
		3.6 / 4.6	4.8...6.8	8.8	10.9
Steel with R_m N/mm²	≤ 400	0.8 · d	1.2 · d	–	–
	400...600	0.8 · d	1.2 · d	1.2 · d	–
	> 600...800	0.8 · d	1.2 · d	1.2 · d	1.2 · d
	> 800	0.8 · d	1.2 · d	1.0 · d	1.0 · d
Cast iron		1.3 · d	1.5 · d	1.5 · d	–
Copper alloys		1.3 · d	1.3 · d	–	–
Light metals [1]	Cast Al alloys	1.6 · d	2.2 · d	–	– [3]
	Pure aluminium	1.6 · d	–	–	– [3]
	Al alloy, hardened	0.8 · d	1.2 · d	1.6 · d	– [3]
	not hardened	1.2 · d	1.6 · d	–	– [3]
Soft metals, plastics		2.5 · d	–	–	–

[1] For dynamic loads the specified value of l_e must be increased by approx. 20%. *Source: Roloff / Matek*
[2] Fine pitch threads require approx 25% greater lengths of engagement.
[3] For higher strength screws, the shear strength of the internal thread material as calculated in VDI 2230 must be taken into account.

Figure 51: Guide for recommended lengths of tapped thread engagement [29]

5.6 Case Examples

Two example cases with bolted joints has been solved using the Basic FEA Workflow. The cases are different from each other, and demonstrate different techniques and analysis aspects. The scope is that they can serve as practical examples of the workflow applied, and provide guidance in how such analysis can be performed.

5.6.1 Blind Flange Analysis Example

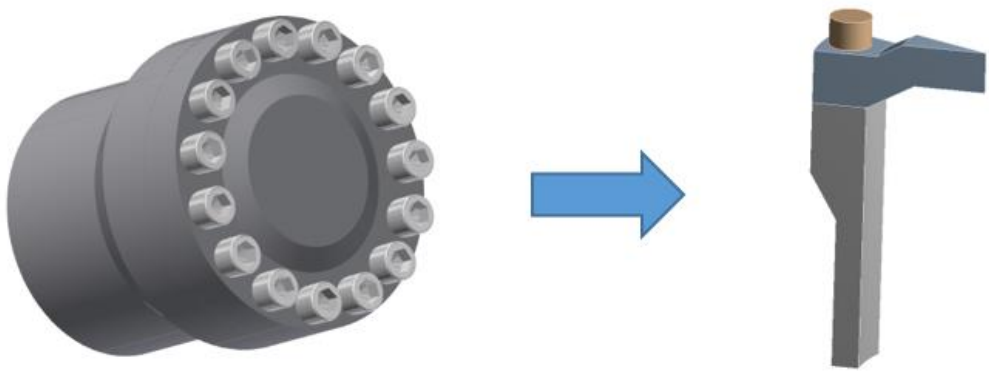

Figure 52: Blind Flange Analysis Example

A SBJ is extracted from the Blind Flange MBJ, as seen in Figure 52, and a Class III representation of the bolt is used. The bolt is eccentrically loaded from internal pressure in the cylinder. Verifications of the bolt working stress and clamping pressure is performed.

The analysis rapport is attached in ***Appendix C-1a***, and the Mathcad calculations in ***Appendix C-1b***.

This same case has also been solved by the analytic VDI 2230 procedure. It can be used as a reference to compare the approaches, and it demonstrates calculation of analytic quantities. The report is attached in ***Appendix C-2a***, and the Mathcad calculations in ***Appendix C-2b***.

5.6.2 Bolted Tuner Analysis Example

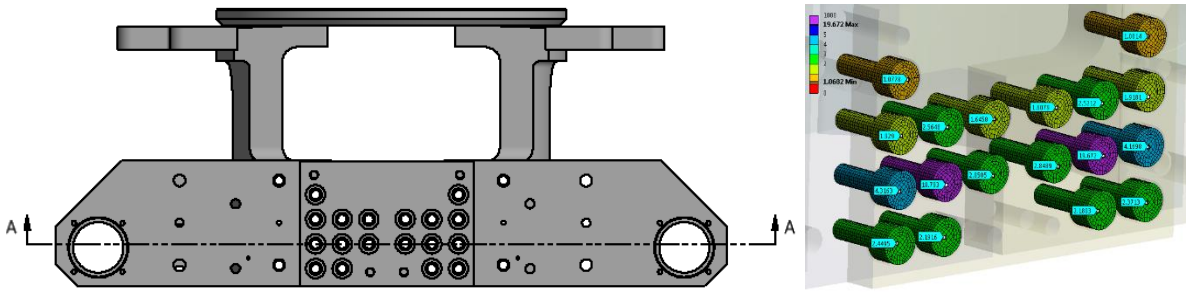

Figure 53: Bolted HG Cavity Tuner subjected to MBJ slipping analysis

This is an analysis that were performed for the practical case of a bolted tuner (Figure 53) for the High Gradient (HG) Cavities. The main scope of the analysis was to assess if slipping would occur in the joint, while subjected to the maximum tuning load.

Different approaches and techniques are used to assess MBJ slipping. The report is attached in ***Appendix D-1***, and the associated Mathcad calculations are attached in ***Appendix D-2***.

5.7 SEMINAR ABOUT FEA & VDI 2230

To transfer knowledge about how to use FEA in analysis of bolted joints according to VDI 2230 to relevant personnel, a seminar has been prepared and attached in ***Appendix E***. The seminar format allows interaction and discussion about relevant topics, and is a practical way to introduce the topic. The presentation has 43 slides, and includes the following main topics:

1. Basic Concepts of Bolted Joints and VDI 2230
2. Combining FEA and VDI 2230
3. Further Calculations and Verifications
4. Improvements of Bolted Joint Design
5. Support Material and References
6. Summary

Aspects like how to estimate the bolt diameter from workload, calculate preload, and how to verify bolt stress and clamping conditions are included in the presentation. The scope is also to emphasize the importance of joint design, and how different factors can influence the joint performance. After the seminar, the participants should feel confident with the use of VDI 2230 and FEA in design and verification of BJs. Thus:

- Know central terms and principles in VDI 2230
- Know how FEA and VDI 2230 can be combined
- Get introduced to further VDI 2230 calculations and verifications
- Know how to improve the joint design and performance
- Know where to look for more information

The seminar was held for a group of engineers in the engineering department at CERN in December 2017. The time allocated were 1.5hr, with 1hr for presentation and 30 minutes for discussion. This was a bit too short time, and for the future it is recommended to have the presentation in 3x45 minutes, and to include brief discussions after each of the chapters.

The seminar can also be adapted to focus on some of the topics, or to serve as a shorter introduction by removing some of the topics.

6 REVISED CRAB CAVITY HE-VESSEL ANALYSIS

After the prototypes are tested and before the series production is initiated, there is a possibility to review the design and structural analysis of the He-vessel and bolted joints. This chapter takes basis in the initial He-vessel analysis and provide suggestions and recommendations for this potential review.

6.1 SUGGESTIONS AND RECOMMENDATIONS

Inspection of Prototype Vessel Bolts

According to the recommendations in 5.4.14, the bolts from the prototype He-vessel should be inspected. Plastic deformations of the bolts and low loosening torques can indicate unexpected preload losses. An external inspection of the vessel can identify gaps or cracked sealing welds, which can indicate joint slipping. If any deviations are identified, this can serve as useful input for the revised analysis.

Workflow in New Analysis

If a revised analysis is performed, it should follow the Basic FEA Workflow and recommendations provided in the Guide (Ch.5.4). In addition, preload losses should be considered and included in the calculations. By doing this, many of the challenges outlined in section 3.4 would be cared for. It will ensure:

- Two levels of preload from tightening uncertainty and preload losses
- Friction in the clamping interface, giving realistic bolt loads and allowing verification of slipping
- Analysis of prying loads
- Good validity of the FEA results

Possible Improvements

Some possible improvements of bolted joints in general are referred to in 5.4.13. Relevant modifications might be to increase the clamping length to increase the bolt resilience and lower the load factor. That will give lower additional bolt loads, reduce preload losses, and improve the resistance against loosening. The plate thickness is 23mm, but because of the groove and sealing cap the clamping length is 13mm. If the design is changed, the plate thickness could in principle allow for a larger clamping length.

If prying loads and joint opening is problematic, actions can be made to improve the stiffness of the clamped plate and increase the preload. To increase the minimum assembly preload in the current design, a more precise tightening method can be used, or the maximum preload can be increased.

The joint designs could also be studied in detail to understand how they perform, and to identify potential improvements. The joint concepts are shown in Figure 20, and two joint drawings are displayed in Figure 54. It could be interesting to investigate the influence of the 7mm large chamfer in joint B on prying loads and pressure in the interface, and how the 5mm lip interacts with the plates. In joint C, the bolt is eccentrically positioned in the clamping interface, and there is only a small edge (1.75mm) between the bolt and the edge of the interface. How this influences the clamping pressure distribution and bolt loads could be of interest.

If joint slipping turns out to be a challenge, one solution could be to add shear pins in strategic positions. That could be a simple way to rule out slipping.

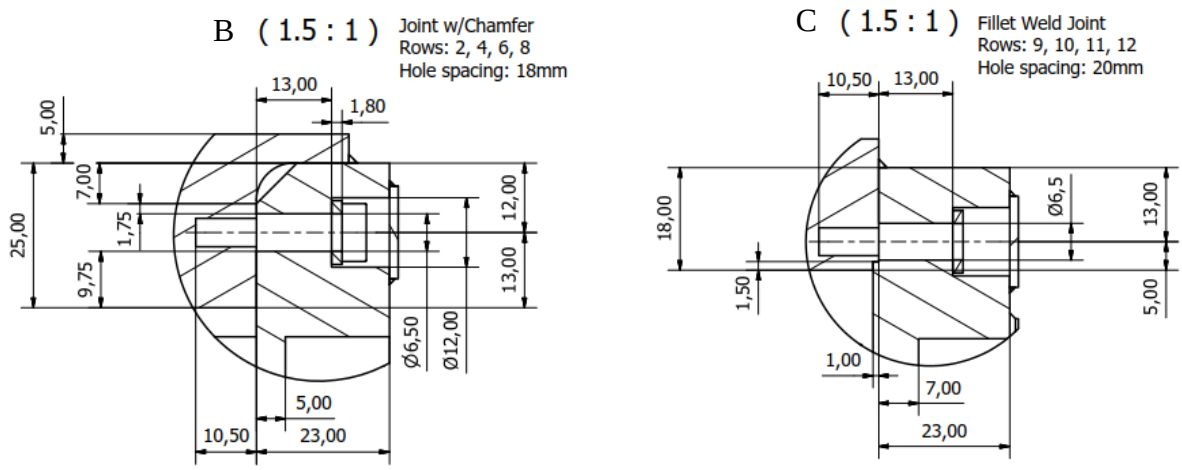

Figure 54: Detail drawings of joint type B and C

Simplified Simulations

There are some techniques that can be used to simplify the simulations. For the He-vessel structural analysis, it can be assumed that the bolded joints will manage to provide the complete structural integrity, and that no slipping will occur. In the simulation, all clamping interfaces can then be bonded.

For the analysis of the bolted joints, the most critical clamping area in terms of slipping, joint opening, and bolt workload can be identified. The other clamping areas, which are not determined to be critical for the assessment can be bonded. This can reduce the computing time, and still provide an accurate analysis. However, attention must be paid to how this affect the global compliance, load distribution, and slipping characteristics. E.g., the boundary conditions must not prevent the critical joint from slipping.

Another technique that can be used to learn about the qualitative performance of the joints is to create a SBJ model of the actual joint geometry, as in Figure 55. With this simple model, FE-simulations require small computational efforts. They will provide information about the joint characteristics and allow for quick iterations. The initial design can serve as a reference, and the effect of small design changes and different preload levels on bolt loads, slipping, and joint opening can be investigated. Such a model might not be representative enough to provide a final verification of the multi body joint, but it can provide useful qualitative information.

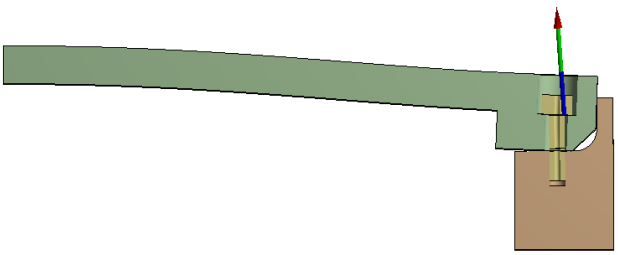

Figure 55: SBJ extracted from He-vessel

Overall Design Concept

If the bolted He-vessel is qualified from the prototype testing, a brief review of the analysis and calculations might be sufficient to provide confidence enough to initiate the series production.

However, if any challenges with leak tightness, fractured fillet welds, or loose bolts emerges, a more comprehensive review might be needed. One option could then be to modify the design of the bolted joints. Another option in that case, in the authors opinion, would be to revisit the initial design concept with a welded vessel. That is because there are some fundamental challenges with the bolted joint concept:

- Bolted joints are not optimal for permanent installations. Over time, unexpected relief in preload can occur from load cycles and relaxation in the surfaces and material. This is not easily recreated in short term testing. If the preload degrades, this can lead to increasing loads on the fillet welds, which they might not be designed to handle, and can result in leaks.

- Installed bolts should be available for inspection, so their performance can be verified over time. This is not so easy for the He-vessel bolts, which are covered by welded covers, packed with MLI[3], and assembled in a cryo-vessel. Therefore, potential bolt failure might not be identified in an initial phase, and the failure can evolve and lead to larger consequences.

- With a very large number of bolts (276), there is a high statistical chance that some unexpected conditions during tightening, in friction or tightening method, can cause the installation preload to deviate more than expected. This can have influence on the bolt load, and be a source of failure.

It should also be noted that for the He-vessel, the consequence of failure is significant. The vessel is out of reach, and a failure or leakage could in the worst case jeopardize the LHC performance. Therefore, the uncertainty regarding the structural integrity of the He-vessel and bolted joints should be minimized as much as possible.

A welded vessel would be more permanent, and not have the same risk of degradation in performance over time. In principle, it can be a more permanent and safe concept. There were some challenges with the welded vessel concept, and reasons why it was discarded in the first place. But in the case a comprehensive review of the bolted joints is needed, these reasons could be revisited, and perhaps overcoming these challenges might be easier than improving the design of the bolted joints.

A compromise could be to have some of the joints completely welded, and some joints bolted. It could also be investigated if some of the joints could be made self-sealing, where the internal pressure assists the sealing function.

[3] Multilayer Insulation – used as thermal insulation in cryogenic systems to block for heat radiation

6.2 REVISED CALCULATIONS

The calculations associated with the He-vessel analysis has been reviewed and adapted to the "Basic FEA Workflow" calculation template in ***Appendix F***. There was no room within the framework of this project to redo the complete He-vessel simulations, so the same bolt loads used in the initial analysis has been re-used in the calculations. If new bolt loads are obtained from future simulations, the calculations can easily be modified in the attached Mathcad file. Calculations has also been performed to according to "Further Assessments" in 5.5 to identify preload losses and assessing the strength of the tapped threads. All input parameters must be checked before the results are used.

7 DISCUSSION

7.1 GOAL ACHIEVEMENT

The first research question was answered by presenting the He-vessel analysis and the assessment of the bolted joints. This illustrated the significance of the bolt assessment and placed it in the larger context of LHC and CERN. Taking basis in this analysis also demonstrated in a good way which challenges that can arise and proved the need for improved descriptions of how FEA can aid analysis of bolted joints.

The second research question asked how the challenges could be met and avoided in the future. It was suggested to study prying, since it is a topic that is important to understand to perform safe design and verification of bolted joints. It was also suggested to develop support material that could be used in future analysis of bolted joints, so similar challenges could be avoided.

Next, the study of prying is carried out, and the relevant support material that has been developed is presented. Aspects of validity are mentioned where relevant throughout the support material, so it is easy to achieve a high analysis quality. A priority has been that the findings and material are presented in a format where it easily can be applied and benefit the engineering department at CERN.

The author considers the thesis in total to answer the research questions and goals of the thesis in a good way, and think it will serve as a useful resource for applying FEA in design and verification of bolted joints according to VDI 2230 in the future.

7.2 RESEARCH ACTIVITIES

It has been challenging to pinpoint the most relevant investigations, and to define the aspects of most interest to present in this thesis. The intension was never to make a self-standing guideline, since VDI 2230 is very thorough and describe many aspects and concepts about analysis of bolted joints in a good way. The scope has more been to provide a description of how the interaction between FEA and VDI 2230 can be streamlined and performed as efficient as possible. By doing that, the scope was that it should be simple to obtain a certain standard on the analysis, making it easy to have control of the validity and to achieve a good quality. Therefore, the idea was that the material should provide a practical introduction, outlining the major steps, and provide relevant information about them. This has been the central elements when choosing what to investigate, and what to present in the thesis.

Another challenge has been to balance being generic and being specific. Being generic is challenging because there is many possible variations and configurations of bolted joints, so it would be confusing and impossible to try and cover all. Being too specific could reduce the value of the material, making it impossible to transfer to other cases. It is believed that a suitable balance has been found, and that the methodology and concepts are described with adequate detail, also providing examples of application and relevant references for the user to customize it to own needs.

During the MSc project work and preparations for the thesis, many questions about combining FEA and assessment of bolted joints has been identified and investigated [5, 6]. The first report goes into detail about the analytic calculations of VDI 2230, and basic principles of FEA representation and analysis. This report identified topics of interest for further investigations

and provided the basis for the second report. This second report has the format of a research log where relevant topics and questions are investigated for each chapter.

In retrospect, the research activities leading up to the thesis were quite wide and not all created direct value. The scope of the thesis was to some degree defined early, but the boundaries of the research activities were not narrowed down accordingly. Therefore, in principle the thesis in its current state could have been reached earlier. However, going wide in the beginning and then narrowing down made the thesis better. It contributed to the knowledge and experience foundation of the author, making it possible to prepare the support material in this thesis.

To ensure high relevance of the thesis and support material, discussions with colleagues and supervisors has been essential. The Basic FEA Workflow, with associated descriptions and calculation support material were developed through solving actual cases, and from performing iterations to optimize the workflow and contents.

7.3 Productivity Paradox and Simulation Driven Design

To put this thesis, and the work to streamline interaction between FEA and the analytic guideline VDI 2230 in a broader perspective, a reference can be made to the productivity paradox, and the later developments and trends in simulation driven design.

With the introduction of electricity in the 1890s, a chain of innovations was initiated. Significant increase in productivity from electric motors did however not emerge until almost 40 years after their introduction into factories [30]. In the 1920s, factories had group drives (Figure 56) driven by mechanical power derived from steam or water. When the electric motors came, they replaced the initial power source of the group drive. It was not until they figured out that all the machines could be driven by separate small electric motors, unit drives, that the full productivity potential was achieved. The factory layout no longer had to be dictated by the placement of power transmitting shafts and rods. The factories were redesigned, and the machines were distributed throughout the factory.

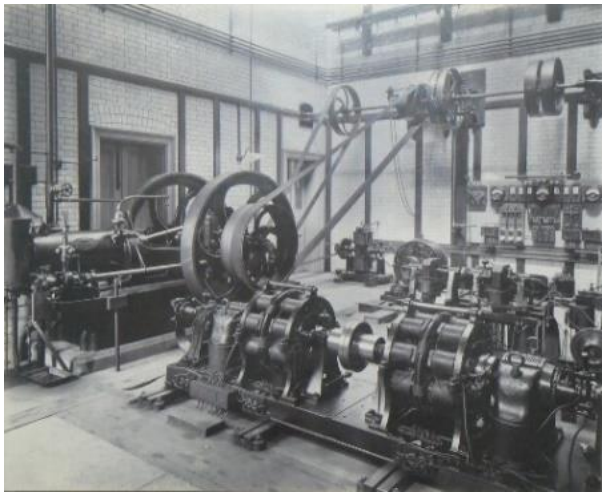

Figure 56: Group drive

This example shows that it is important to understand how new technology should be used to realize its full potential – often it is not by replacing the old technology with new technology, but by rearranging and optimizing the complete framework and how it is applied.

With the introduction of computers, questions concerning how they best can be utilized to increase productivity has been raised [31]. It is referred to as a productivity paradox, because computerization does not automatically increase productivity, like with the introduction of the electric motor in factories. But if it is used as an essential component of a broader system of structural changes, it can increase productivity. The interpretation of structural change in this regard is to put the computer resource into a framework where interaction with other elements are specified and optimized.

Most design now days are made as 3D-models in CAD software. This has made it simple to perform FE-analysis to assess the structural integrity. However, such workflows are often sequential. What simulation driven design means, and the Basic FEA Workflow demonstrates, is that there can be rapid interaction between CAD and FE-analysis in design and verification process. When this is structured in a streamlined and optimized workflow, this is the key to realizing the productivity and quality reward that comes from using computer assisted assessment of bolted joints, and how the "factory" can be reorganized to extract the full potential.

7.4 FUTURE RESEARCH

This section provides suggestions for potential improvements of the thesis, and outline possible ways to extend the contents.

7.4.1 Improve the FEA Workflow

The FEA workflow and associated support material (Ch.5) contains the most relevant information about FEA aided assessment of bolted joints and could be extracted from the thesis to serve as a single standing report. This can make it easier to use, and allow for revisions and improvements of the contents based on user feedback and experiences. This can make the information more relevant, and more available.

More research can also be done into FEA representation of bolted joints, and the effect of simulation parameters such as mesh size, type, refinement, and more. This can improve the recommendations in the guide, and serve as "Best Practices"

As the workflow in the future is applied to various engineering cases, an overview with references to the relevant reports and a brief description of the cases could be prepared. In that way, they can expand the "Case Examples" and serve as practical examples of how the workflow is applied, and demonstrate different analysis approaches. This overview could be included in the separate report suggested above.

7.4.2 Approach of Other Standards

It could be interesting to collect information about how bolted joints are handled by different relevant standards, like *BPVC*[4] and *EN 13445 Unfired Pressure Vessels* [15]. Aspects of interest would be to identify which stress levels that are allowed for the bolts, material constraints, equations for bolt load and preload, and estimation of nominal bolt diameter.

There are also other guidelines that provide useful recommendations and best practices [28, 32-34]. They could be used to supplement and improve the suggested FEA workflow and support material.

7.4.3 Definition of Preload with FEA

A topic that has been investigated by the author in this MSc project, but excluded from the thesis has been the use of FEA to define clamping requirements, required preload and estimation of nominal bolt diameter. This can be done for the relevant joint design, materials, and for a given global workload. This kind of approach would be close to the analytic VDI 2230

[4] ASME Boiler and Pressure Vessel Code

procedure, using FEA to define calculation parameters as described in Table 9 (Analytic FEA approach).

In the research, the scope was to check if this type of approach could be more simple and time saving than the Semi Analytic FEA approach. According to the preliminary results, significant time savings or reduction in simulation efforts were not identified. For unexperienced users, it could also be easy to get lost in the details. Therefore, this research was excluded from this thesis, and it was decided it was better to fully focus on the Basic FEA Workflow. But even though it was excluded from this thesis, it could still be interesting to continue the research and investigate and clarify alternative workflows and analysis approaches. It is possible that they could give some advantages for some cases.

8 SUMMARY

In the engineering department at CERN (EN-MME), accelerator components with bolted joints are frequently developed. As use of FEA (Finite Element Analysis) aided design is becoming more widespread, questions have been raised about how to best apply FEA in design and verification of bolted joints.

First, the specific case of a bolt analysis for the Crab Cavities Helium vessel, a part of the HL-LHC upgrade, is investigated. Challenges in combining FEA and VDI 2230 are identified and provides the basis for the following investigations.

Next, investigations into prying are performed, a relevant source of non-linear bolt loads and unpredictable load development, to understand the phenomenon and the influence of preload.

A complete analysis framework is then proposed, which consist of a streamlined Basic FEA Workflow, associated calculation templates, details about more advanced verifications, a detailed guide with best practices and references, examples where the analysis framework has been applied, and seminar slides that can be used to educate relevant personnel.

The basic workflow suggested takes basis in the analytic VDI 2230 workflow, but is adapted to optimize the interaction between CAD modelling, FE-analysis, and analytic calculations. The Mathcad calculation template matches the steps in the workflow, and simplifies the calculations.

In the end, specific suggestions and recommendations for a potential revision of Helium vessel bolt analysis are provided.

Altogether, the goal has been to leverage the threshold for using FEA in analysis of bolted joints according to VDI 2230, and achieving quality and productivity rewards. The thesis and associated support material could serve as a resource on the topic, and should benefit the engineering department at CERN and other potential users.

In the discussion, the project is put in a broader perspective stating that the full benefits are not achieved by just replacing analytic steps with computer aided steps. Only by structuring and optimizing the interaction between CAD, FEA and analytic calculations, the full rewards can be achieved.

The thesis provides a good basis for further research. In the discussion, possible improvements and ways forward are described:

- Extract Ch. 5 to a self-standing report that can be revised based on user experiences and feedback. Future assessment using the suggested workflow can be referenced to as examples of application.
- Investigate how relevant standards handle bolted joints, to identify allowed stress levels, relevant equations, estimation of preload, and more.
- Investigate alternative approaches in other calculation guidelines and best practices to improve the suggested workflow and associated material.
- Investigate how FEA can be used to define the required preload, clamping requirements and more, as parts of alternative analysis approaches.

References

[1] CERN. (2016). *About CERN*. Available: www.home.cern/about

[2] *Systematic calculation of highly stressed bolted joints; Joints with one cylindrical bolt*, VDI 2230 Part 1, 2014.

[3] *Systematic calculation of highly stressed bolted joints; Multi bolted joints*, VDI 2230 Part 2, 2014.

[4] J. H. Bickford, *Introduction to the Design and Behavior of Bolted Joints, Fourth Edition* (Dekker Mechanical Engineering). CRC Press, 2007.

[5] J. Apeland, "Assessment of Bolted Joints According to VDI 2230 Using Finite Element Analysis," Project Thesis, Engineering Design and Materials, NTNU, Trondheim, 2016.

[6] J. Apeland, "Studies into Application of FEA in Assessment of Bolted Joints," EDMS 1770646, 2017, Available: https://edms.cern.ch/document/1770646.

[7] Y.-L. Lee and H.-C. Ho, "Chapter 12 - Design and Analysis of Metric Bolted Joints: VDI Guideline and Finite Element Analysis," in *Metal Fatigue Analysis Handbook* Boston: Butterworth-Heinemann, 2012, pp. 461-513.

[8] "LHC - The Guide ", CERN 2017, Available: https://cds.cern.ch/record/2255762.

[9] G. Apollinari, I. Béjar Alonso, O. Brüning, M. Lamont, and L. Rossi, *High-Luminosity Large Hadron Collider (HL-LHC): Preliminary Design Report* (no. CERN Yellow Reports: Monographs). Geneva: CERN, 2015.

[10] K. Artoos *et al.*, "Compact Crab Cavity Cryomodule: Deliverable: D4.4," CERN-ACC-2015-0130, Oct 2015, Available: https://cds.cern.ch/record/2059225.

[11] F. Carra *et al.*, "Crab Cavity and Cryomodule Development For HL-LHC," presented at the 17th International Conference on RF Superconductivity (SRF2015), Whistler, BC, Canada, 2015.

[12] C. Zanoni *et al.*, "Design of Dressed Crab Cavities for the HL-LHC Upgrade," in *17th International Conference on RF Superconductivity (SRF2015)*, Whistler, BC, Canada, 2015, pp. 1284-1288.

[13] N. Kuder, "History of Development of DQW Dressed Cavity Design," EDMS 1708890, 2016, Available: https://edms.cern.ch/document/1708890.

[14] N. Kuder, "DQW Dressed Cavity Strength Assessment," EDMS 1549819, 2016, Available: https://edms.cern.ch/document/1549819.

[15] *Unfired Pressure Vessels - Part 3: Design*, EN 13445-3, 2014.

[16] J. H. Bickford, "Behavior of the Joint Loaded in Tension " in *Introduction to the Design and Behavior of Bolted Joints, Fourth Edition* (Dekker Mechanical Engineering: CRC Press, 2007).

[17] P. Agatonović, "Structural Integrity Analysis of Multi-Bolted Connections Using the Innovative Beam Model," *Structural Interity and Life*, vol. 11, no. 3, pp. 147-156, 2011.

[18] M. Guinchard, "Tightening Tests: Evaluation of the Friction Coefficient for Several Configurations of Inox," EDMS 1184393, 2012, Available: https://edms.cern.ch/document/1184393.

[19] R. Beardmore. (2013). *Various Coefficients of Friction*. Available: http://www.roymech.co.uk/Useful_Tables/Tribology/co_of_frict.htm

[20] *Mechanical Properties of Fasteners, Part 7: Torsional test and minimum torques for bolts and screws with nominal diameters 1mm to 10mm*, ISO 898-7, 1992.

[21] *Mechanical Properties of Corrosion Resistant Stainless-Steel Fasteners, Part 1: Bolts, screws and studs*, ISO 3506-1, 1997.

[22] *Hexagon Head Bolts - Product Grades A and B*, ISO 4014, 1999.

[23] *Hexagon Socket Head Cap Screws*, ISO 4762, 2004.

[24] *Fasteners - Clearance Holes for Bolts and Screws*, ISO 273, 1979.

[25] "Bolt Tightening ", vol. 8, Tohnici Torque Handbook [Online]. Available: https://www.tohnichi.com/torque-technical-data.htm.

[26] *Mechanical Properties of Fasteners made of Carbon Steel and Alloy Steel*, ISO 898-1, 2013.

[27] T. F. Lehnhoff and B. A. Bunyard, "Bolt Thread and Head Fillet Stress Concentration Factors," *Journal of Pressure Vessel Technology*, vol. 122, no. 2, pp. 180-185, 2000.

[28] NASA, "Criteria for Preloaded Bolts," NSTS 08307, 1998.

[29] Böllhoff, "The Manual of Fastening Technology ", vol. 5 Available: https://eshop.boellhoff.de/out/media/pdf/normteile/The-Manual-of-Fastening-EN-8100.pdf.

[30] P. A. David, "The dynamo and the computer : an historical perspective on the modern productivity paradox," *The American economic review*, vol. 80, no. 2, pp. 355-361, 1990.

[31] E. Brynjolfsson and L. M. Hitt, "Beyond the Productivity Paradox: Computers are the catalyst for bigger changes," *Communications of the ACM*, vol. 41, no. 8, p. 49, 1998.

[32] K. H. Brown, C. W. Morrow, S. Durbin, and A. Baca, "Guideline for Bolted Joint Design and Analysis: Version 1.0," Sandia National Laboratories SAND2008-0371, 2008, Available: www.osti.gov/scitech/servlets/purl/929124.

[33] R. T. Barrett, "Fastener Design Manual," NASA Reference Publication 1228, 1990.

[34] J. A. Chambers, "Preloaded Joint Analysis Methodology for Space Flight Systems," NASA Technical Memorandium 106943, 1995.

APPENDIX A: Basic FEA Workflow Calculation Template

APPENDIX B: Tightening Torque Template for Non-Critical Bolts

APPENDIX C: Blind Flange Analysis Example

C-1a Blind Flange Case Report

C-1b Calculations for Blind Flange Case

C-2a Blind Flange with Analytic VDI 2230 Procedure

C-2b Calculations for Blind Flange with Analytic VDI 2230 Procedure

APPENDIX D: Bolted Tuner Analysis Example

D-1 HG Cavity Bolted Tuner Analysis

D-2 Analytic Calculations for Tuner Analysis

APPENDIX E: VDI 2230 and FEA Seminar Presentation

APPENDIX F: Revised Calculations for HE-Vessel Joints

APPENDIX A

BASIC FEA WORKFLOW CALCULATION TEMPLATE

Calculation Template for Basic FEA Workflow

Analysis performed by: Name **Date of Analysis:** Month, 201#

Analysis revision: v# **EDMS Reference:** -

Color codes: **Input parameters** **Calculation quantities** **Results** **Functions** **Criteria check**

S1 - Workload

Run FE-analysis of perform analytic calculations to identify the maximum workload.

Maximum Workload: $F_{A.max} := \square\ N$

==========

S2 - Nominal Bolt Diameter

Bolt data parameters

Nominal diameter: $d := \square\ mm$

Pitch: $P := \square\ mm$

Effective bolt head diameter: $d_W := \square\ mm$

Clearence hole diameter: $d_h := \square\ mm$

Friction coefficient in the threads: $\mu_{Gmin} := \square$

Friction in head bearing area: $\mu_{Kmin} := \square$

Proof strength of the bolt: $R_{p0.2min} := \square\ MPa$

Note!
Minimum coefficients of friction must be applied.

Calculated parameters

Pitch diameter: $d_2 := d - \frac{3\sqrt{3}}{8} P = ?\ mm$

$H = \frac{\sqrt{3}}{2} \cdot P$

Minor diameter of the bolt: $d_3 := d - P\left(\frac{17\sqrt{3}}{24}\right) = ?\ mm$

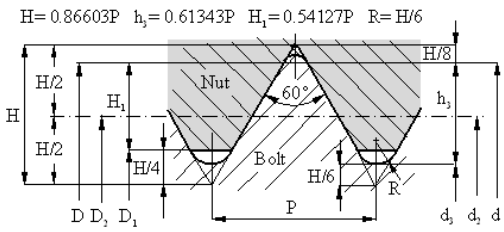

S3 - Tightening Factor

Torque wrench: $\alpha_A := \square$

S4 - Max Assembly Pretension

Calculation quanteties

Stress diameter: $d_S := 0.5\ (d_2 + d_3) = ?\ mm$

Stress area: $A_S := \frac{\pi}{4}\ (d_S)^2 = ?\ mm^2$

Parameters

Bolt capacity utililization factor: $\nu := 0.9$ VDI 2230 suggest: 0.9

Calculations

Allowed assembly stress: $\sigma_{Mzul} := \nu\ R_{p0.2min} = ?\ MPa$

Maximum permitted assembly preload:

$$F_{Mzul} := A_S \frac{\nu\ R_{p0.2min}}{\sqrt{1 + 3\left(\frac{3}{2}\frac{d_2}{d_S}\left(\frac{P}{\pi\ d_2} + 1.155\ \mu_{Gmin}\right)\right)^2}}$$

ans. $F_{Mzul} = ?\ kN$

==========

S5 - Min Assembly Pretension

Minimum assembly preload: $F_{Mmin} := \frac{F_{Mzul}}{\alpha_A}$

ans. $F_{Mmin} = ?\ kN$
==========

S6 - Simplify and Prepare CAD-geometry

S7 - Prepare and Run FE-analysis

Parameters

Coefficient of friction in the head bearing area: $\mu_{Kmin} = ?$

Calculation of theoretical beam parameters:

Minor diameter area: $A_{d3.g} := \frac{\pi}{4} \left(d_3^2\right) = ?\ mm^2$

Minor second area areal moment of inertia: $I_{d3.g} := \frac{\pi}{64} \left(d_3^4\right) = ?\ mm^4$

Torsional stiffness: $J := \frac{\pi}{32} \left(d_3^4\right) = ?\ mm^4$

S8 - Results and Analysis

Max assembly preload

Acheived preload: $F_{Vmax} := \square\ kN$

Max bolt load: $F_{Smax} := \square\ kN$

Max bolt bending moment: $M_{Sbo} := \square\ N\ mm$

Min assembly preload

Acheived preload: $F_{Vmin} := \square\ kN$

Clamping force in the interface: $F_{KR} := \square\ kN$

S9 - Work Stress

Note: In this calculated work-stress, bending stress is included. That is not the case for the standard VDI 2230 equation.

Parameters

Residual torque factor: $k_t := 0.5$ VDI 2230 suggest: 0.5

Calculation quanteties

Bending modulus: $W_S := \frac{\pi}{32} \left(d_S^3\right) = ?\ mm^3$

Thread moment: $M_G := F_{Mzul} \cdot \frac{d_2}{2} \cdot \left(\frac{P}{\pi\ d_2} + 1.155\ \mu_{Gmin}\right) = ?\ N\ m$

Polar moment of inertia: $W_p := \frac{\pi}{16} \cdot \left(d_S^3\right) = ?\ mm^3$

Calculations

Normal stress: $\sigma_{zb.max} := \frac{F_{Smax}}{A_S} + \frac{M_{Sbo}}{W_S} = ?\ MPa$

Torsional stress: $\tau_{max} := \frac{M_G}{W_p} = ?\ MPa$

Working stress: $\sigma_{red.B} := \sqrt{\sigma_{zb.max}^2 + 3\left(k_t \cdot \tau_{max}\right)^2} = ?\ MPa$

Bending stress

$\sigma_{Sbo} := \frac{M_{Sbo}}{W_S} = ?\ MPa$

Bending stress contribution to work stress

$\Delta\sigma_{Sbo.p} := \frac{\sigma_{Sbo}}{\sigma_{red.B}} = ?$

Assessment

Criteria: $\sigma_{red.B} = ?\ MPa$ < $R_{p0.2min} = ?\ MPa$

$Work_Stress := \begin{cases} \text{if } \sigma_{red.B} < R_{p0.2min} \\ \quad \text{return "Ok"} \\ \text{"Not OK"} \end{cases}$

$Work_Stress = ?$

Safety factor: $S_F := \dfrac{R_{p0.2min}}{\sigma_{red.B}} = ?$

==========

S10 - Clamping Requirements

S11 - Tightening Torque

Average head friction diameter: $D_{Km} := \dfrac{d_W + d_h}{2} = ?\ mm$

Tightening Torque: $M_A := F_{Mzul} \cdot \left(0.16\ P + 0.58\ d_2\ \mu_{Gmin} + \dfrac{D_{Km}}{2}\ \mu_{Kmin}\right) = ?\ N\ m$

==========

S12 - Approve or Iterate

==========
APPROVED
==========

==========
NOT APPROVED
==========

Summary of Key Results

Calculation step	Results			
S1 - Workload	Maximum axial load:	$F_{A.max} = ?$		
S2 - Nominal Bolt Diameter	$d = ?\ mm$	$P = ?\ mm$		
S3 - Tightening Factor	$\alpha_A = ?$			
S4 - Max Assembly Pretension	$\mu_{Gmin} = ?$ $\nu = 0.9$ $F_{Mzul} = ?\ kN$	$\sigma_{Mzul} = ?\ MPa$		
S5 - Min Assembly Pretension	$F_{Mmin} = ?\ kN$			
S6 - Simplify and Prepare CAD-geometry				
S7 - Prepare and Run FE-analysis	$\mu_{Kmin} = ?$			
S8 - Extracted Results	$F_{Vmax} = ?\ kN$ $F_{Vmin} = ?\ kN$	$F_{Smax} = ?\ kN$ $F_{KR} = ?\ kN$	$M_{Sbo} = ?\ N\ m$	
S9 - Work Stress	$\sigma_{red.B} = ?\ MPa$	< $R_{p0.2min} = ?\ MPa$	$S_F = ?$	$Work_Stress = ?$
S10 - Clamping requirements				
S11 - Tightening Torque	$M_A = ?\ N\ m$			
S12 - Approve or Iterate	========== **APPROVED** ==========	========== **NOT APPROVED** ==========		

APPENDIX B

TIGHTENING TORQUE TEMPLATE FOR NON-CRITICAL BOLTS

Tightening Torques for M3 - M12

Calculations prepared by: Name **Date of Analysis:** Month 201#

EDMS Reference: EDMS 1840088

Input parameters

Yield strength of the bolt: $R_{p0.2min} := 640\ MPa$

Friction coefficient in the threads: $\mu_{Gmin} := 0.2$

Friction coefficient in the head bearing area: $\mu_{Kmin} := 0.2$

Bolt capacity utililization factors: $\nu := \begin{bmatrix} 1 \\ 0.90 \\ 0.75 \\ 0.50 \\ 0.30 \end{bmatrix}$

Head dia. from: ISO 4014 - Hexagon head bolts
Clearence hole: ISO 273-m

d (mm)	P (mm)	d_W (mm)	d_h (mm)	d_g (mm)
3	0.5	5.07	3.4	0
4	0.7	5.74	4.5	1
5	0.8	6.74	5.5	1.2
6	1	8.74	6.6	1.6
8	1.25	11.47	9	2
10	1.5	14.47	11	3
12	1.75	16.47	13.5	3

d = Nominal diameter
P = Thread pitch
d_W = Min. bolt head dia
d_h = Clearance hole
d_v = Venting hole diameter

Allowed assembly stress $\sigma_{Mzul} := \nu\ R_{p0.2min} = \begin{bmatrix} 640 \\ 576 \\ 480 \\ 320 \\ 192 \end{bmatrix} MPa$

Calculation quanteties

Pitch diameter: $d_2 := d - \frac{3\sqrt{3}}{8} P$

$d_2 = \begin{bmatrix} 2.68 \\ 3.55 \\ 4.48 \\ 5.35 \\ 7.19 \\ 9.03 \\ 10.86 \end{bmatrix} mm$

Bolt minor thread dia.: $d_3 := d - P\left(\frac{17\sqrt{3}}{24}\right)$

$d_3 = \begin{bmatrix} 2.39 \\ 3.14 \\ 4.02 \\ 4.77 \\ 6.47 \\ 8.16 \\ 9.85 \end{bmatrix} mm$

Stress diameter: $d_S := 0.5\ (d_2 + d_3)$

$d_S = \begin{bmatrix} 2.53 \\ 3.34 \\ 4.25 \\ 5.06 \\ 6.83 \\ 8.59 \\ 10.36 \end{bmatrix} mm$

Stress area: $A_S := \frac{\pi}{4}(d_S)^2$

$A_S = \begin{bmatrix} 5.03 \\ 8.78 \\ 14.18 \\ 20.12 \\ 36.61 \\ 57.99 \\ 84.27 \end{bmatrix} mm^2$

Modified stress area: $A_{S.g} := \frac{\pi}{4}\left(d_S{}^2 - d_g{}^2\right)$

$A_{S.g} = \begin{bmatrix} 5.03 \\ 7.99 \\ 13.05 \\ 18.11 \\ 33.47 \\ 50.92 \\ 77.20 \end{bmatrix} mm^2$

Average head friction diameter $D_{Km} := \frac{d_W + d_h}{2}$

$D_{Km} = \begin{bmatrix} 4.24 \\ 5.12 \\ 6.12 \\ 7.67 \\ 10.24 \\ 12.74 \\ 14.99 \end{bmatrix} mm$

Functions

Maximum permitted assembly preload:

$$F_{Mzul}(\nu, A) := \overrightarrow{A \frac{\nu\ R_{p0.2min}}{\sqrt{1 + 3\left(\frac{3}{2}\frac{d_2}{d_S}\left(\frac{P}{\pi\ d_2} + 1.155\ \mu_{Gmin}\right)\right)^2}}}$$

Tightening Torque:

$$M_A(F) := \overrightarrow{F \cdot \left(0.16\ P + 0.58\ d_2\ \mu_{Gmin} + \frac{D_{Km}}{2}\ \mu_{Kmin}\right)}$$

Calculations for standard bolts (Collapsible area)

Calculations for vented bolts (Collapsible area)

Note:

- If the friction is lower than what is assumed, the resulting assembly preload will be higher than what is listed above, when tightened to the specified torque.
- If the bolt head diameter is larger than what is assumed, a slightly lower assmebly preload will be acheived.
- The strength of tapped threads are not considered in this analysis. For short length of engagement or soft materials, additional verifications should be performed.
- If spring washers are applied, the maximum spring force should be compared to the acheived preloads above. If the preload is higher, the washer is flattened.

Tightening Torques M3-M12 Bolts

Basic parameters

Friction in threads:	**0,2**
Friction in head bearing:	**0,2**
0.2% proof stress:	**640** MPa

Tightening Torques & Corresponding Assembly Preloads - *Standard Bolts*

		Utilization of Bolt Capacity									
	Stress section	***100 %***		***90 %***		***75 %***		***50 %***		***30 %***	
Bolt	**mm^2**	***Nm***	***kN***	***Nm***	***kN***	***Nm***	***kN***	***Nm***	***kN***	***Nm***	***kN***
M3	5,0	2,0	*2,5*	1,8	*2,3*	1,5	*1,9*	1,0	*1,3*	0,6	*0,8*
M4	8,8	4,5	*4,4*	4,1	*3,9*	3,4	*3,3*	2,3	*2,2*	1,4	*1,3*
M5	14,2	9,0	*7,1*	8,1	*6,4*	6,7	*5,3*	4,5	*3,6*	2,7	*2,1*
M6	20,1	15,6	*10,1*	14,0	*9,1*	11,7	*7,6*	7,8	*5,0*	4,7	*3,0*
M8	36,6	37,9	*18,4*	34,2	*16,6*	28,5	*13,8*	19,0	*9,2*	11,4	*5,5*
M10	58,0	75,1	*29,3*	67,6	*26,4*	56,3	*22,0*	37,6	*14,7*	22,5	*8,8*
M12	84,3	129,9	42,7	116,9	38,5	97,4	32,1	64,9	21,4	39,0	12,8

Tightening Torques & Corresponding Assembly Preloads - *Bolts with outgassing hole*

		Utilization of Bolt Capacity									
	Stress section	***100 %***		***90 %***		***75 %***		***50 %***		***30 %***	
Bolt	**mm^2**	***Nm***	***kN***	***Nm***	***kN***	***Nm***	***kN***	***Nm***	***kN***	***Nm***	***kN***
~~**M3**~~	~~5,0~~	~~2,0~~	~~*2,5*~~	~~1,8~~	~~*2,3*~~	~~1,5~~	~~*1,9*~~	~~1,0~~	~~*1,3*~~	~~0,6~~	~~*0,8*~~
M4	8,0	4,1	*4,0*	3,7	*3,6*	3,1	*3,0*	2,1	*2,0*	1,2	*1,2*
M5	13,1	8,3	*6,6*	7,4	*5,9*	6,2	*4,9*	4,1	*3,3*	2,5	*2,0*
M6	18,1	14,0	*9,1*	12,6	*8,2*	10,5	*6,8*	7,0	*4,5*	4,2	*2,7*
M8	33,5	34,7	*16,9*	31,2	*15,2*	26,0	*12,6*	17,3	*8,4*	10,4	*5,1*
M10	50,9	66,0	*25,8*	59,4	*23,2*	49,5	*19,3*	33,0	*12,9*	19,8	*7,7*
M12	77,2	119,0	39,2	107,1	35,2	89,3	29,4	59,5	19,6	35,7	11,7

Suggested Lengths of Tapped Threads

Material of components		Length of engagement l_e[2] according to property class of screw			
		3.6 / 4.6	4.8...6.8	8.8	10.9
Steel with R_m N/mm²	≤ 400	0.8 · d	1.2 · d	–	–
	400...600	0.8 · d	1.2 · d	1.2 · d	–
	> 600...800	0.8 · d	1.2 · d	1.2 · d	1.2 · d
	> 800	0.8 · d	1.2 · d	1.0 · d	1.0 · d
Cast iron		1.3 · d	1.5 · d	1.5 · d	–
Copper alloys		1.3 · d	1.3 · d	–	–
Light metals[1]	Cast Al alloys	1.6 · d	2.2 · d	–	–[3]
	Pure aluminium	1.6 · d	–	–	–[3]
	Al alloy, hardened	0.8 · d	1.2 · d	1.6 · d	–[3]
	not hardened	1.2 · d	1.6 · d	–	–[3]
Soft metals, plastics		2.5 · d	–	–	–

[1] For dynamic loads the specified value of l_e must be increased by approx. 20%.

Source: Roloff / Matek

[2] Fine pitch threads require approx 25% greater lengths of engagement.

[3] For higher strength screws, the shear strength of the internal thread material as calculated in VDI 2230 must be taken into account.

APPENDIX C

BLIND FLANGE ANALYSIS EXAMPLE

C-1a	**Blind Flange Case Report**
C-1b	**Calculations for Blind Flange Case**
C-2a	**Blind Flange with Analytic VDI 2230 Procedure**
C-2b	**Calculations for Blind Flange with Analytic VDI 2230 Procedure**

APPENDIX C-1A BLIND FLANGE CASE

This is an analysis of the bolted joints for a Blind Flange, and demonstrates the "Basic FEA Workflow". The associated calculations are presented in ***Appendix C-1b***. The same case, solved with the analytic VDI 2230 procedure is presented in ***Appendix C-2***.

S0: INITIAL STATE

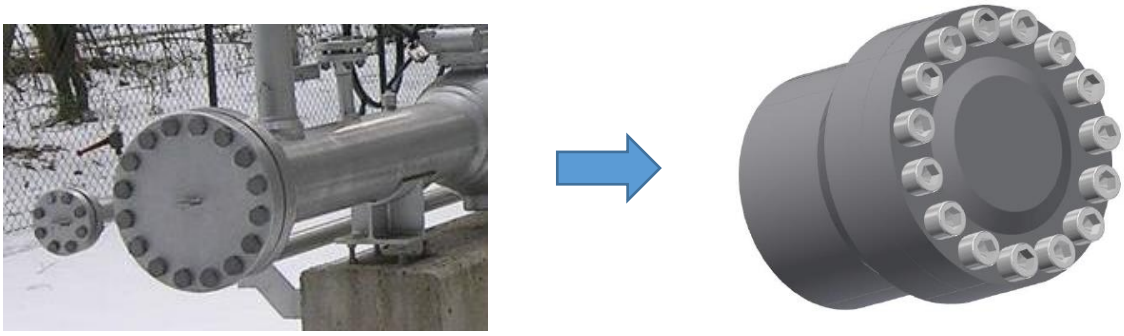

Figure 1: Blind Flange Bolt CASE design

The geometry is provided by the designer, as seen in Figure 1. It is a blind flange, and the rest of the system is not of interest for this analysis. There is a pressure in the system that pulsate between two pressure levels. The number and distribution of bolts has been guessed. The bolts are determined to be Hexagon socket head cap type.

Due to the symmetry, it is decided to simplify the assessment and extract one single bolt from the multi bolted joint.

Pre-calculations and Dimensioning

S1: WORKLOAD

An analytic approach to determine the bolt work load F_A has been used in (1), assuming rigid bodies. Relevant data is listed in Table 1.

Table 1: Design data

Number of bolts	$i = 15$	Defined
Max / min internal pressure	$p_{max} = 22MPa \,/\, p_{min} = 8MPa$	Defined
Internal Cylinder Diameter	$D_{Zi} = 130mm$	Defined

Analytic calculation of workload:

$$F_{A_{\max/\min}} = \frac{\pi}{4 \cdot i} \cdot D_{Zi}^2 \cdot p_{\max/\min} \quad \text{giving} \quad \underline{\underline{\begin{matrix} F_{A_{\max}} = 19{,}5 \\ F_{A_{\min}} = 7.1 \end{matrix} kN}} \qquad (1)$$

S2: Nominal Bolt Diameter

According to the bolt size estimation guide in [Pt.1-Table A7], the bolt chosen is: **M16x60-12.9**. The estimation steps are shown in Table 2. Relevant bolt data are listed in Table 3.

Table 2: Preliminary dimensioning procedure

Step	*Evaluation*	*Result*
A	$F_{A_{max}} < 25kN$	25 kN
B	+ two steps for dynamic and eccentrically applied load	63 kN
C	+ one step for using a torque wrench	100 kN
D	Strength grade 12.9 give nominal diameter:	16 mm

Table 3: Data for M16x60 – 12.9 bolt

Parameter	Sym.	Value	Unit	Source
Bolt material		Steel		
E-modulus	E	205	GPa	
0.2% Proof strength of the bolt	$R_{p0.2}$	1100	MPa	Class 12.9
Nominal diameter	d	16	mm	
Thread Pitch	P	2	mm	[Pt.1-Table A12]
Pitch Diameter	d_2	14.701	mm	[Pt.1-Table A11] / Calc.
Minor Diameter	d_3	13.546	mm	[Pt.1-Table A12] / Calc.
Effective head diameter	d_W	22	mm	ISO 4762
Bolt head height	k	16	mm	ISO 4762
Bolt length	l	60	mm	Defined
Clearance hole diameter	d_h	17.5	mm	ISO 273 - medium
Thread Coefficient of Friction	μ_{Gmin}	0.1	-	[Pt.1-Table A5-A6]
Friction in Head Bearing Area	μ_{Kmin}	0.1	-	[Pt.1-Table A5-A6]

S3: Tightening Factor

Using [Pt.1-Table A8] for friction coefficient class B, knowing a precision torque wrench will be used and choosing a high value in the allowed range give the tightening factor $\alpha_A = 1.6$.

(R1/1)

$$\alpha_A = \frac{F_{M\,\max}}{F_{M\,\min}} = 1,6 \qquad (2)$$

S4: Maximum Assembly Preload

By defining how much of the bolt capacity that should be utilized during assembly through the utilization factor ν, a maximum permitted assembly preload is obtained. The associated data is found in Table 4.

Table 4: Data associated with calculation of the maximum assembly pretension

Utilization factor	υ	0.9		Defined
Stress Area	A_S	156,7	mm^2	[Pt.1-Table A11] / Calc.
Maximum Permitted Assembly Preload	$\boldsymbol{F_{Mzul}}$	**142.5**	$\boldsymbol{kN}$	Calculated

S5: Minimum Assembly Preload

Taking the tightening uncertainty into account, the lowest preload after assembly should be the minimum assembly preload listed in Table 5.

Table 5: Data and Results Min Assembly Pretension

Minimum Assembly Preload	$\boldsymbol{F_{M.min}}$	**89**	$\boldsymbol{kN}$	Calculated

FE-Analysis

S6: Simplify and Prepare CAD geometry

A simplified CAD model is prepared. The data required for modelling is listed in Table 3. The bolt is represented by a Class III model, with diameter based on the thread minor diameter (d_3). The tapped thread hole dimeter is modified to have a corresponding diameter.

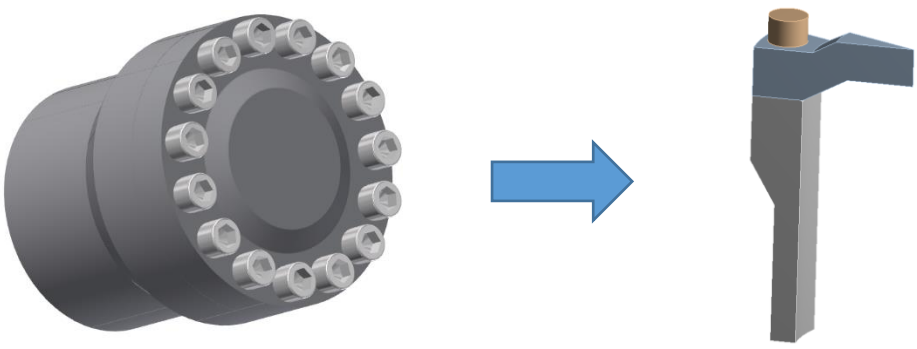

Figure 2: SBJ extracted from a MBJ

S7: Prepare and Run FE-analysis

The material properties are defined and applied to all parts. The meshed model can be seen in Figure 3. The bolt is meshed with HEX elements. The mesh is refined in the clamping interface.

In Figure 4, the boundary conditions are shown. On the cut sides of the model, frictionless boundary conditions are applied to represent the symmetric conditions. In the tapped threads are, the bolt is bonded. In the clamping interface and the head bearing area, friction-contact is applied with the coefficient of friction μ_{Tmin} (Table 6) has been applied. Pressure is applied to internal surfaces, and the bolt is preloaded.

Table 6: Data needed for FE-simulation

Contact Coefficient of Friction	μ_{Tmin}	0.2	-	[Pt.1-Table A5-A6]

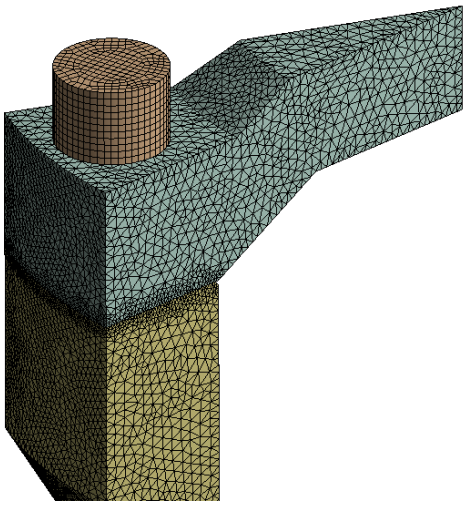

Figure 3: Meshed model

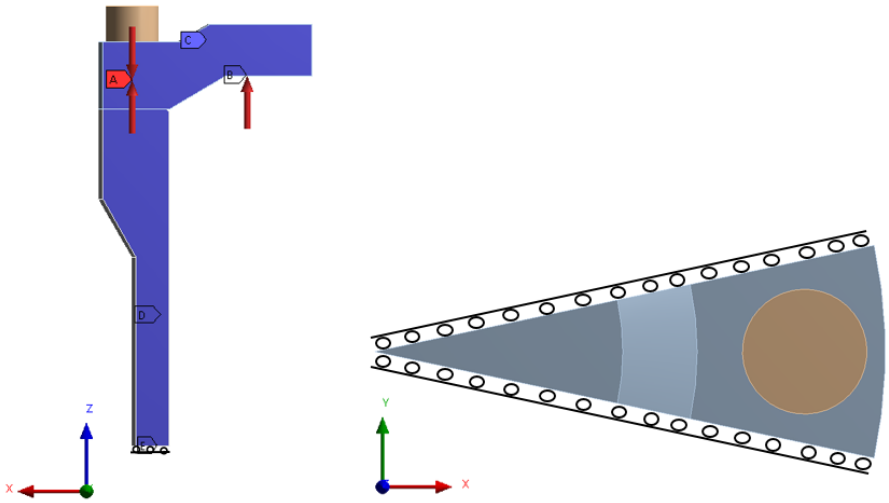

Figure 4: Boundary conditions of the model and applied loads

S8: Extract values from the FE-analysis

The results from the simulation is listed in Table 7. They are used for later calculations and verifications.

Table 7: Extracted values from FE-analysis

Actual max preload	F_{Vmax}	142.5	kN
Max bolt load	F_{Smax}	143.7	kN
Bolt moment	M_{Sbo}	7.5	Nm
Workload	F_A	19.46	kN
Actual min preload	F_{Vmin}	89	kN
Residual clamping force	F_{KR}	70.8	kN

Analysis of Results

S9: Work Stress

The work stress is calculated, and found to provide a safety factor against yield of 1.1.

Table 8: Calculated values from FE-analysis

Work Stress	$\sigma_{red.B}$	979.6	MPa	Calculated
Amount bending stress		2.8	%	
Bolt Yield Safety Factor	S_F	1.12		Calculated

S10: Clamping Requirements

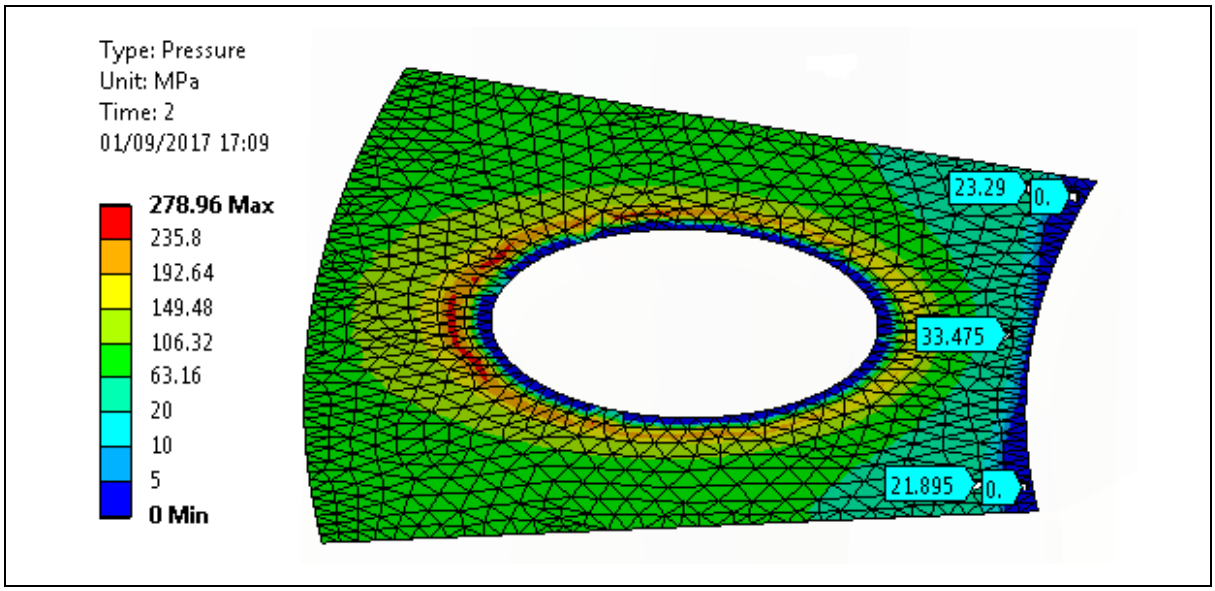

Figure 5: Pressure in the clamping interface with max load and minimum pretension

In Figure 5, the residual clamping pressure resulting from the minimum assembly preload simulation is shown. The pressure distribution looks good, and the amount of opening is minimal. From this, it is concluded that there is a small chance of prying, and that the clamping requirements are fulfilled.

Joint Function	OK	Visual inspection

S11: Tightening Torque

The tightening torque is calculated and presented in Table 9.

Table 9: Data and Results Max Assembly Pretension

Average Head Friction Area	D_{Km}	19.75	mm	Calculated
Tightening Torque	M_A	307.9	Nm	Calculated

S12: Approve or Iterate

Based on this analysis, the bolted joint is approved.

Approved

Calculations for FEA-assessment of Blind Flange Case

Analysis performed by: Jørgen Apeland **Date of Analysis:** 01/09/2017

Analysis revision: v1 **According to procedure:** BASIC FEA Workflow

S1 - Workload

Number of bolts: $i := 15$

Inner diameter of Cylinder: $D_{Zi} := 130\ mm$

Internal pressure in cylinder: $\begin{bmatrix} p_{max} \\ p_{min} \end{bmatrix} := \begin{bmatrix} 22 \\ 8 \end{bmatrix} MPa$

Workload: $\begin{bmatrix} F_{A.max} \\ F_{A.min} \end{bmatrix} := \frac{\pi}{4 \cdot i} \cdot (D_{Zi})^2 \cdot \begin{bmatrix} p_{max} \\ p_{min} \end{bmatrix}$ **ans.** $\begin{bmatrix} F_{A.max} \\ F_{A.min} \end{bmatrix} = \begin{bmatrix} 19.47 \\ 7.08 \end{bmatrix} kN$

==========

S2 - Nominal Bolt Diameter

Bolt data parameters

Note: The minimum coefficients of friction must be applied.

Nominal diameter: $d := 16\ mm$

Pitch: $P := 2\ mm$

Effective bolt head diameter: $d_W := 22\ mm$

Diameter of clearence hole: $d_h := 17.5\ mm$

Friction coefficient in the threads: $\mu_{Gmin} := 0.1$

Friction in head bearing area: $\mu_{Kmin} := 0.1$

Yield strength of the bolt: $R_{p0.2min} := 1100\ MPa$

Calculated parameters

$$H = \frac{\sqrt{3}}{2} \cdot P$$

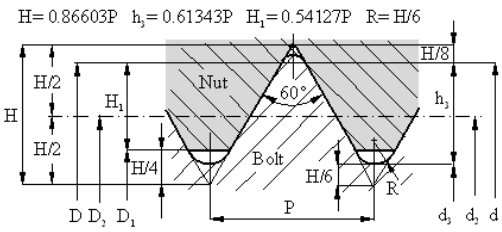

Pitch diameter: $d_2 := d - \frac{3\sqrt{3}}{8} P = 14.701\ mm$

Minor diameter of the bolt: $d_3 := d - P\left(\frac{17\sqrt{3}}{24}\right) = 13.546\ mm$

S3 - Tightening Factor

Torque wrench: $\alpha_A := 1.6$

S4 - Max Assembly Pretension

Calculation quanteties

Stress diameter: $d_S := 0.5\ (d_2 + d_3) = 14.12\ mm$

Stress area: $A_S := \frac{\pi}{4} (d_S)^2 = 156.7\ mm^2$

Parameters

Bolt capacity utililization factor: $\nu := 0.9$

Calculations

Allowed assembly stress: $\sigma_{Mzul} := \nu\ R_{p0.2min} = 990\ MPa$

Maximum permitted assembly preload:

$$F_{Mzul} := A_S \frac{\nu\ R_{p0.2min}}{\sqrt{1 + 3\left(\frac{3}{2}\frac{d_2}{d_S}\left(\frac{P}{\pi\ d_2} + 1.155\ \mu_{Gmin}\right)\right)^2}}$$

ans. $F_{Mzul} = 142.5\ kN$

==========

S5 - Min Assembly Pretension

Minimum assembly preload: $F_{Mzul.min} := \frac{F_{Mzul}}{\alpha_A}$

ans. $F_{Mzul.min} = 89.1\ kN$

==========

S6 - Simplify and Prepare CAD-geometry

S7 - Prepare and Run FE-analysis

Parameters

Coefficient of Friction in the clamping interface: $\mu_{Tmin} := 0.2$

Coefficient of friction in the head bearing area: $\mu_{Kmin} = 0.1$

S8 - Results and Analysis

Max assembly preload

Acheived preload: $F_{Vmax} := 142.5\ kN$

Max bolt load: $F_{Smax} := 143.7\ kN$

Max bolt bending moment: $M_{Sbo} := 7.5\ N\ m$

Workload: $F_A := 19.47\ kN$

Min assembly preload

Acheived preload: $F_{Vmin} := 89\ kN$

Clamping force in the interface: $F_{KR} := 70.8\ kN$

S9 - Work Stress

Parameters

Residual torque factor: $k_t := 0.5$

Calculation quanteties

Bending modulus: $W_S := \frac{\pi}{32} d_S^{\ 3} = 276.59\ mm^3$

Thread moment: $M_G := F_{Mzul} \cdot \frac{d_2}{2} \cdot \left(\frac{P}{\pi\ d_2} + 1.155\ \mu_{Gmin} \right) = 166.4\ N\ m$

Polar moment of inertia: $W_p := \frac{\pi}{16} \cdot d_S^{\ 3} = 553.18\ mm^3$

Calculations

Axial stress: $\sigma_{zb.max} := \frac{F_{Smax}}{A_S} + \frac{M_{Sbo}}{W_S} = 944.34\ MPa$

Torsional stress: $\tau_{max} := \frac{M_G}{W_p} = 300.73\ MPa$

Working stress: $\sigma_{red.B} := \sqrt{\sigma_{zb.max}^{\ 2} + 3\ (k_t \cdot \tau_{max})^2} = 979.6\ MPa$

Bending stress

$\sigma_{Sbo} := \frac{M_{Sbo}}{W_S} = 27.12\ MPa$

Bending stress contribution to work stress

$\Delta\sigma_{Sbo.p} := \frac{\sigma_{Sbo}}{\sigma_{red.B}} = 2.77\%$

Assessment

Criteria: $\sigma_{red.B} = 979.59\ MPa$ < $R_{p0.2min} = 1100\ MPa$

Safety factor: $S_F := \frac{R_{p0.2min}}{\sigma_{red.B}} = 1.12$

==========

S10 - Clamping Requirements

S11 - Tightening Torque

Average head friction diameter: $D_{Km} := \frac{d_W + d_h}{2} = 19.75\ mm$

Tightening Torque: $M_A := F_{Mzul} \cdot \left(0.16\ P + 0.58\ d_2\ \mu_{Gmin} + \frac{D_{Km}}{2}\ \mu_{Kmin}\right) = 307.9\ N\ m$

==========

S12 - Approve or Iterate

=========
APPROVED
=========

Additional Calculations

Additional bolt load: $F_{SA} := F_{Smax} - F_{Vmax} = 1.2\ kN$

Load factor: $\Phi_{FE} := \frac{F_{SA}}{F_A} = 0.062$

Summary of Key Results

Calculation step	Results		
S1 - Workload	$\begin{bmatrix} p_{max} \\ p_{min} \end{bmatrix} = \begin{bmatrix} 22 \\ 8 \end{bmatrix} MPa$	$\begin{bmatrix} F_{A.max} \\ F_{A.min} \end{bmatrix} = \begin{bmatrix} 19.5 \\ 7.1 \end{bmatrix} kN$	
S2 - Nominal Bolt Diameter	$d = 16\ mm$	$P = 2\ mm$	
S3 - Tightening Factor	$\alpha_A = 1.6$		
S4 - Max Assembly Preload	$\mu_{Gmin} := 0.1$ $\nu := 0.9$ $F_{Mzul} = 142.5\ kN$	$\sigma_{Mzul} = 990\ MPa$	
S5 - Min Assembly Preload	$F_{Mzul.min} = 89.1\ kN$		
S6 - Simplify and Prepare CAD geometry	$d_3 = 13.55\ mm$		
S7 - Prepare and Run FE-analysis	$\mu_{Tmin} = 0.2$	$\mu_{Kmin} = 0.1$	
S8 - Extracted Results	$F_{Vmax} = 142.5\ kN$ $F_{Vmin} = 89\ kN$	$F_{Smax} = 143.7\ kN$ $F_{KR} = 70.8\ kN$	$M_{Sbo} = 7.5\ N\ m$ $F_A = 19.47\ kN$
S9 - Work Stress	$\sigma_{red.B} = 979.6\ MPa$ <	$R_{p0.2min} = 1100\ MPa$ ==========	$S_F = 1.12$
S10 - Clamping requirements			
S11 - Tightening Torque	$M_A = 308\ N\ m$		
S12 - Approve or Iterate	========== **APPROVED** ==========		
Additional Calculations	$F_{SA} = 1200\ N$	$\Phi_{FE} = 0.06$	

Blind Flange with Analytic VDI 2230 Procedure

Case Description

This case is based on example B5 in VDI 2230 Part 1, but geometry details and parameters has been changed. The case to be analysed is a blind flange (Figure 1), with the function as an inspection hatch for a pressurized system. In operation, there is a pulsating internal pressure. 15 tapped thread joints (TTJ) holds the cap attached to the cylinder, and the scope is to design and verify that the bolts can withstands the operating pressure, without opening in the interface. The bolts are to be tightened with a precession torque wrench.

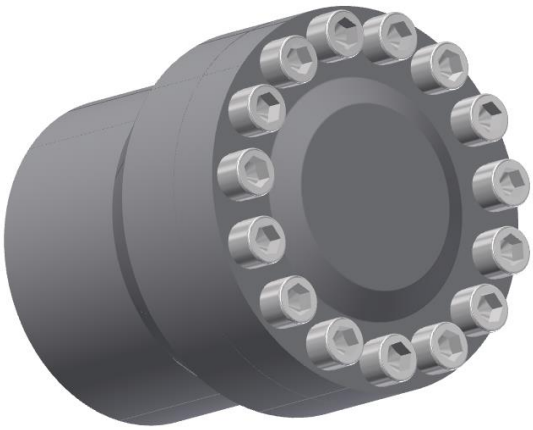

Figure 1: CASE model

CASE Parameters

The case data are stated in Table 1. The 15 bolts are placed around the edge, equally spaced. Since it is symmetric, it allows for simplification of the case geometry into 15 equally sized parts. The geometry, with all relevant dimensions are shown in Figure 2. Some central geometry parameters are listed in Table 2, together with symbols and a description of the parameter. The material data of *S355 JO* is listed in Table 3.

Table 1: CASE data

Cap / Cylinder material	S355 JO	Plain structural steel
Tightening	Precision torque wrench	
Number of bolts	$i = 15$	Hexagon socket head cap screws
Strength grade	12.9	
Interface roughness	$R_Z = 16 \mu m$	Surfaces of head bearing area
Max / min internal pressure	$p_{\min} = 8MPa,\ \ p_{\max} = 22MPa$	

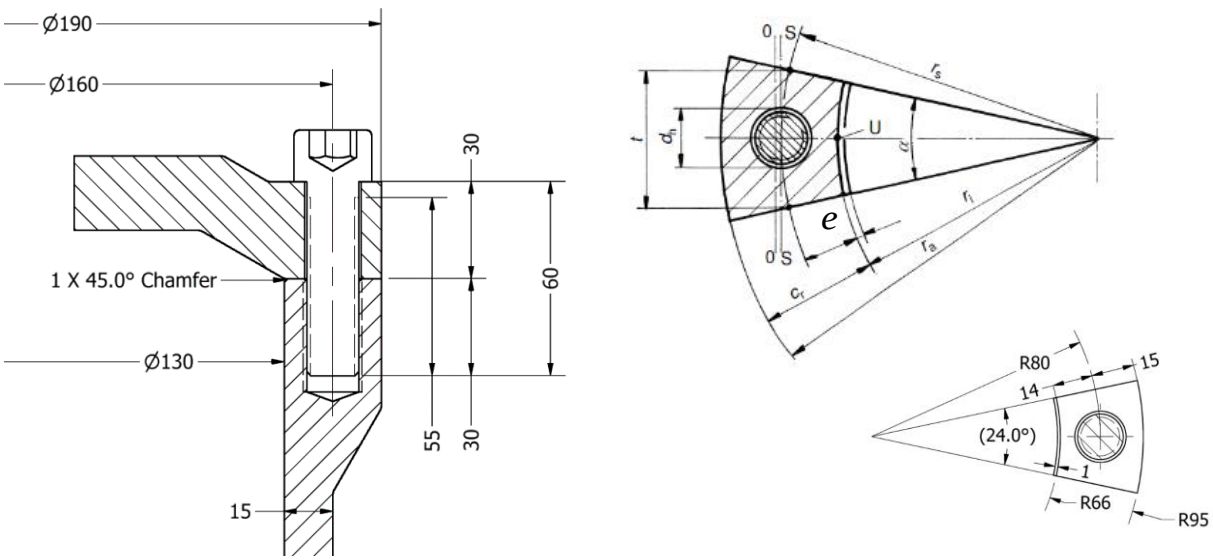

Figure 2: CASE section

Table 2: Geometry data

Description	***Sym.***	***Value***	***Unit***
Outside diameter of cap and cylinder	D_a	190	mm
Cylinder inside diameter	D_{Zi}	130	mm
Pitch circle diameter	D_{ST}	160	mm
Clamp length	l_K	30	mm
Length, side at risk of opening	e	14	mm
Width of the interface	c_T	29	mm

Table 3: Material data according to table A9 [Pt.1-Annex A]

Material		$S355\ JO$	
Tensile strength	$R_{m.\min}$	490	MPa
0,2% proof stress	$R_{p0,2.\min}$	325	MPa
Shear strength	$\tau_{B.\min}$	390	MPa
Lim. Surface pressure	p_G	760	MPa
E-modulus	E	205000	MPa
Density	ρ	7,85	kg / dm^3

ANALYTIC CALCULATIONS

The analytic calculations have been solved according to the procedure described in VDI 2230 Part 1. The calculation steps together with a brief description, the most relevant formulas, and the results are presented. The **(Rx/y)** formulas refer to the formulas defined in the verification procedure. The complete calculations are found in the attached MathCAD calculations in ***Appendix C-2b***.

R0: NOMINAL DIAMETER

Working load

Based on the internal pressure, the max and minimum working loads $F_{A\max/\min}$ are calculated according to (1).

$$F_A = \frac{\pi}{4 \cdot i} \cdot D_{Zi}^2 \cdot p \qquad \text{giving} \qquad \begin{matrix} F_{A\max} \\ F_{A\min} \end{matrix} = \begin{matrix} 19{,}5 \\ 7.1 \end{matrix} kN \tag{1}$$

Assuming the cap is flexible, the load is introduced on one side of the bolt, thus being subjected to eccentric loading.

Preliminary dimensioning

According to the preliminary dimensioning procedure [Pt.1-Table A7], the nominal diameter is found to be 16mm (Table 4). This procedure is a quick way to make a qualified estimate based on some critical conditions: Dynamic or static loading, tightening method, and if concentric or eccentric loading are present.

Table 4: Preliminary dimensioning procedure

Step	***Evaluation***	***Result***
A	$F_{A_{\max}} < 25kN$	$25kN$
B	+ two steps for dynamic and eccentrically applied load	$63kN$
C	+ one step for using a torque wrench	$100kN$
D	Strength grade 12.9 give nominal diameter:	$16mm$

Evaluation criteria: Validity range

Then, a check for compliance with the validity range is performed (2), making sure that the width of the interface area c_T is smaller than the limiting size of the interface area G'. A check at the side at risk of opening give that the distance on the interface e, from the bolt axis to the edge at risk of opening is below half the minimum limiting size (3). The interface design complies with the validity range.

(R0/1) $$c_T = 29mm \ < \ G' = d_W \cdot \begin{bmatrix} 1.5 \\ 2 \end{bmatrix} \tag{2}$$

(R0/2) $$e = 14mm \ < \ \frac{G'_{\min}}{2} = 17{,}4mm \tag{3}$$

Bolt data

A Hexagon socket head cap screw ISO 4762 M16x60–12.9 bolt is selected, and according to [Pt.1-Table A11] and [7-10], the dimensions shown in Figure 3 and listed in Table 5 apply.

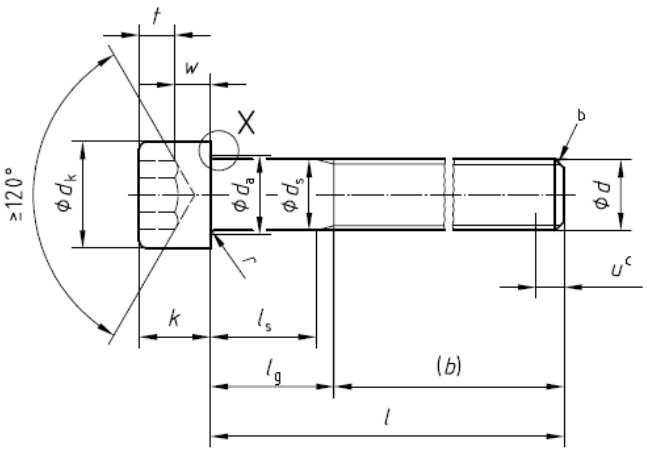

Figure 3: Bolt dimensions [8]

Table 5: Bolt dimensions

ISO 4762-M16x60-12.9 [8]			
Head diameter	d_K	24	mm
Effective head diameter	d_W	23,17	mm
Bolt shank diameter	d_S	16	mm
Nominal bolt length	l	60	mm
Thread length	b	44	mm
Length to effective thread $(l_{nom} - b)$	l_g	16	mm
Bolt shank length $(l_g - 5P)$	l_S	6	mm
Data from [Pt. 1-Table A11]			
Load at minimum yield point [10]	$F_{0,2\min}$	173	kN
0,2% minimum yield limit for the bolt	$R_{S.p0.2.\min}$	1100	MPa
Pitch	P	2	mm
Pitch diameter	d_2	14,701	mm
Cross section at d_3	A_{d_3}	144,1	mm^2
Minor diameter	d_3	13,55	mm
Stress cross section	A_S	157	mm^2
Clearance hole diameter [7]	d_h	17,5	mm

R1: TIGHTENING FACTOR

Using [Pt.1-Table A8] for friction coefficient class B, knowing a precision torque wrench will be used and choosing a high value in the allowed range give the tightening factor (4).

(R1/1)

$$\alpha_A = \frac{F_{M\max}}{F_{M\min}} = 1,6 \tag{4}$$

R2: REQUIRED MINIMUM CLAMP LOAD

The required minimum clamp load F_{Kerf} has to satisfy (5). Since there is no transverse load or any acting moments, $F_{KQ} = 0$. There is no extra sealing requirement, so $F_{KP} = 0$. However, prevention of opening has to be considered, and the minimum clamp force at the opening limit F_{KA} has to be calculated (6). The results are presented in Table 6.

(R2/4)

$$F_{Kerf} \geq \max\left(F_{KQ}; F_{KP} + F_{KA}\right) \tag{5}$$

(R2/3)

$$F_{Kerf} \geq \left(F_{KA} = F_{A_{\max}} \frac{A_D\left(a \cdot u - s_{sym} \cdot u\right)}{I_{BT} + s_{sym} \cdot u \cdot A_D} \right) \tag{6}$$

Calculation approach

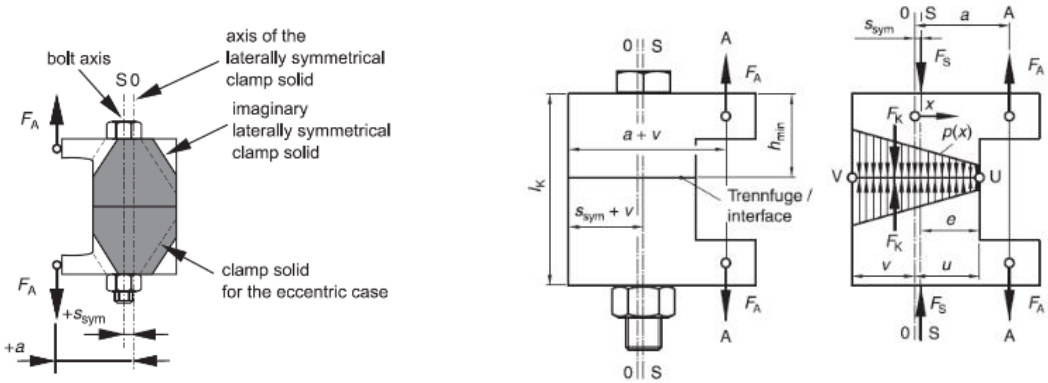

Figure 4: Calculation model with calculation parameters [Pt.1-Figure 4 & Figure 25]

To find F_{KA}, the parameters of (6) had to be calculated. The approach is to create a centred imaginary laterally symmetrical clamp solid consisting of a cone and sleeve, shifted with the distance s_{sym} from the eccentric**.** Knowing s_{sym} give u. Then the distance from the centre of the new cone to where the axial load is applied, a, is found based on a Class I simulation giving the cross-section forces and moments. Then the areal moment of inertia I_{BT}, and the surface of the interface area A_D is calculated. All values are now known, and the clamping requirement F_{Kerf} is calculated.

Parameters and results

Table 6: R2 analytic values

Sym.	*Value*	*Unit*	*Description*
F_{Kerf}	$\geq 39,7$	kN	Clamp load required for sealing functions and prevention of one-sided opening at the interface
F_{KA}	$39,7$	kN	Minimum clamp load at the opening limit
$F_{A_{max}}$	$19,5$	kN	Axial load directed in the bolt axis direction
A_D	$737,3$	mm^2	Sealing area of interface
a	$13,5$	mm	Distance of the substitutional line of action of the axial load F_A from the axis of the imaginary laterally symmetrical deformation body
u	$12,2$	mm	Distance of the edge bearing point V from the axis of the imaginary laterally symmetrical deformation body
s_{sym}	$-1,8$	mm	Distance of the bolt axis from the axis of the imaginary laterally symmetrical deformation body
I_{BT}	$67791,4$	mm^4	Areal moment of inertia of the interface area

R3: LOAD FACTOR AND RESILIENCIES

Finding the load factor Φ, which is the relation between the work load F_A and the additional bolt load F_{SA} (7), requires information about the resilience of the clamped parts δ_P and the bolt δ_S. The proportion of the work-load that relieves the clamped parts is calculated from (8). For the case of eccentric clamping and loading, the load introduction factor n is also included and the load factor Φ^*_{en} is found (9). All the results are presented in Table 7.

(R3/1)
$$\Phi = \frac{F_{SA}}{F_A} \tag{7}$$

(R3/2)
$$F_{PA} = (1-\Phi)F_A \tag{8}$$

(R3/4)
$$\Phi^*_{en} = n \cdot \frac{\delta_P^{**}}{\delta_S + \delta_P^{**}} \tag{9}$$

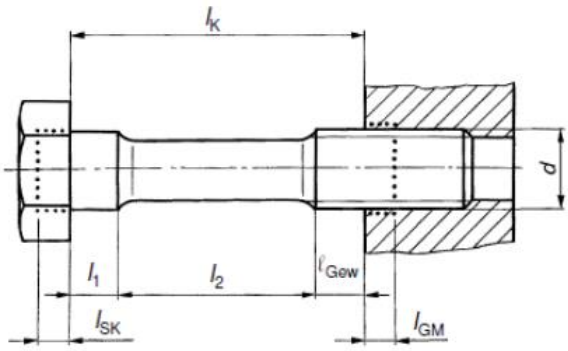

Figure 5: Bolt resilience dimensions [Pt.1-Figure 6]

Calculation approach

First, the resilience of all the parts of the bolt (Figure 5) is calculated, and combined to the bolt resilience δ_S. Then the bending resilience of the bolt β_S is calculated, since it later is needed to calculate the alternating stresses. To calculate the resilience of the clamped parts, the form and size of the substitutional deformation body is calculated (Figure 6). Then the resilience of the deformation sleeve δ_P^H, and of the deformation cone δ_P^V is calculated and combined, giving the resilience of the clamped parts δ_P. Due to the eccentric clamping and loading, the compensated values δ_P^* and δ_P^{**} are calculated. In the end, the load introduction factor n is found, based on [Pt.1-Figure 22 & Table 2]. The SV2 is the best fit, and n is obtained.

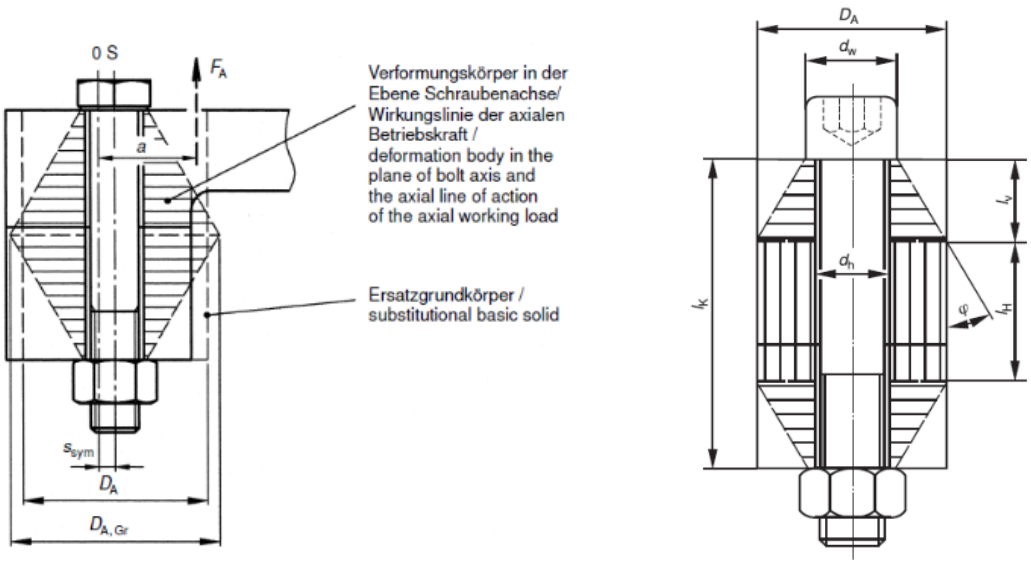

Figure 6: Parameters related to the substitutional deformation body [Pt.1-Figure 8]

Parameters and results

Table 7: R3 analytic values

Sym.	*Value*	*Unit*	*Description*
Φ_{en}^*	0,051	ul	Load factor for eccentric clamping and eccentric load introduction via the clamped parts
δ_S	$1{,}4 \cdot 10^{-3}$	mm/kN	Elastic resilience of the bolt
β_S	0,107	$1/kNm$	Elastic bending resilience of the bolt
δ_P^{**}	$2{,}0 \cdot 10^{-4}$	mm/kN	Elastic resilience of the clamped parts or eccentric clamping and eccentric loading
n	0,27	ul	Load introduction factor for describing the effect of the introduction point of F_A on the displacement of the bolt head
$F_{PA.\max}$	18,5	kN	Proportion of the axial load which changes the loading of the clamped parts, additional plate load
$F_{SA.\max}$	1,002	kN	Axial additional bolt load

R4: PRELOAD CHANGES

To compensate for the embedding resulting from the high assembly and operational loads, the resulting loss in force F_Z has to be calculated (10). The amount of embedding is based on the surface roughness, and suggested deformations f_Z are found in [Pt.1-Table 5].

(R4/1)

$$F_Z = \frac{f_Z}{\delta_S + \delta_P} \tag{10}$$

Parameters and results

Table 8: R4 analytic values

Sym.	*Value*	*Unit*	*Description*
F_Z	4,8	kN	Loss of preload resulting from embedding during operation
f_Z	8	μm	Plastic deformation because of embedding

R5: MINIMUM ASSEMBLY PRELOAD

The minimum required assembly preload $F_{M.\min}$ is calculated, taking into account different changes in the preload and assuming the greatest possible relief of the joint (11). The clamping requirement F_{Kerf}, relief in the clamped parts due to the maximum work load F_{PA}, and loss of preload due to embedding is considered. The change in preload due to thermal expansion $\Delta F'_{Vth}$ is not relevant in this case. The results are listed in Table 9.

(R5/1)

$$F_{M.\min} = F_{Kerf} + \underbrace{\left(1 - \Phi^*_{en}\right) F_{A.\max}}_{F_{PA}} + F_Z + \Delta F'_{Vth} \tag{11}$$

Parameters and results

Table 9: R5 analytic values

Sym.	*Value*	*Unit*	*Description*
$F_{M.\min}$	63	kN	Required minimum assembly preload which can occur at $F_{M.\max}$ because of a lack in precision in the tightening technique and maximum friction
F_V	58,2	kN	General preload, without embedding effect

R6: MAXIMUM ASSEMBLY PRELOAD

Taking into account the expected uncertainty and scatter determined in (4), the maximum assembly preload needed to ensure the clamping requirements are fulfilled is calculated (12). The result is presented in Table 10.

(R6/1)

$$F_{M.\max} = \alpha_A \cdot F_{M.\min} \tag{12}$$

Parameters and results

Table 10: R6 analytic values

Sym.	*Value*	*Unit*	*Description*
$F_{M.\max}$	100,8	kN	Maximum assembly preload for which a bolt must be designed, so that, despite lack of precision in the tightening technique and the expected embedding during operation, the required clamp load in the joint is produced and maintained.

R7: ASSEMBLY STRESS & LOAD

The assembly stress $\sigma_{red,M}$ resulting from the preloading $F_{M.\max}$ must be checked against the allowed assembly stress $\sigma_{red,Mzul}$ (13). That is done by checking that the assembly preloading $F_{M.\max}$ is below the maximum allowed assembly force F_{Mzul} (14). This value can also be obtained from [Pt.1-Table A1-A4]. The result is given in Table 11, and evaluation against the criteria is done in (16). The different preload values are identified and compared to the bolt strength in Figure 7.

(R7/1)
$$\sigma_{red,Mzul} = \nu \cdot R_{p0,2\min} \tag{13}$$

(R7/2)
$$F_{Mzul} = A_0 \frac{\nu \cdot R_{p0,2\min}}{\sqrt{1+3\left[\frac{3}{2}\frac{d_2}{d_0}\left(\frac{P}{\pi \cdot d_2}+1{,}155\mu_{G\min}\right)\right]}} \tag{14}$$

(R7/3)
$$F_{M\max} \le F_{Mzul} \tag{15}$$

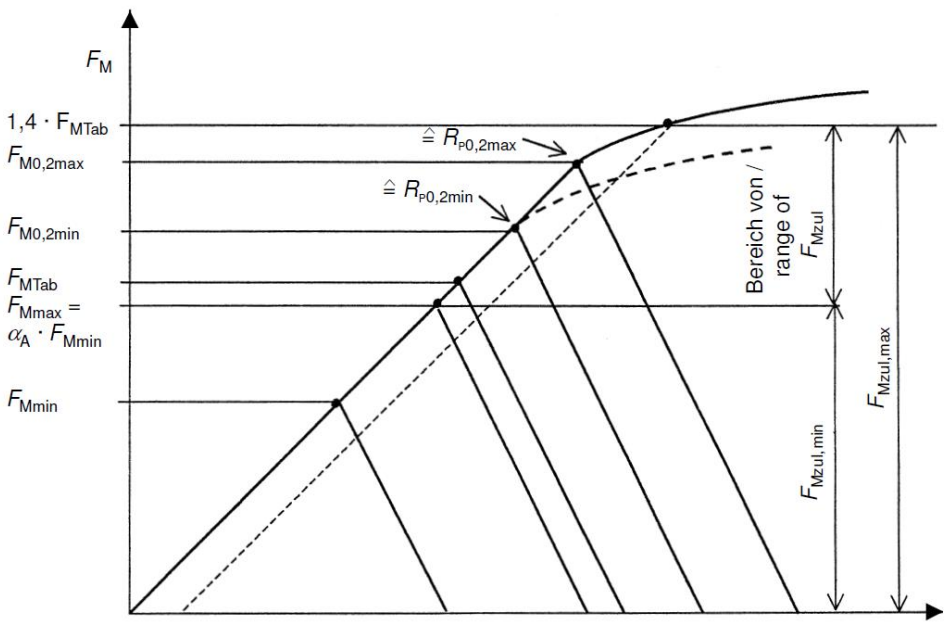

Figure 7: Permissable assembly preload [Pt.1-Figure 33]

Calculation Approach

The allowed assembly stress $\sigma_{red,M}$ is found using a utilization factor of $\nu = 0.9$ on the minimum yield point $R_{p0,2\min}$ (13). Based on the allowed assembly stress, the equivalent maximum allowed assembly force F_{Mzul} is calculated (14). The requirement states that the maximum assembly preloading $F_{M.\max}$ must be smaller than the maximum allowed assembly force F_{Mzul}.

Result

$$F_{M.\max} = 100,8kN \quad < \quad F_{M.zul} = 142,4kN \tag{16}$$

Table 11: R7 analytic values

Sym.	*Value*	*Unit*	*Description*
$F_{M.zul}$	$142,4$	kN	Permissible assembly preload

R8: WORKING STRESS

The maximum stress in the bolt during operation, $\sigma_{red,B}$, has to be checked not to exceed the proof stress of the bolt, $R_{S.p0.2.\min}$ (19). The results from the calculation are presented in Table 12.

(R8/1)
$$F_{S.\max} = F_{M.zul} + \underbrace{\Phi^*_{en} \cdot F_{A.\max}}_{F_{PA}} - \Delta F_{Vth} \tag{17}$$

(R8/4)
$$\sigma_{red.B} = \sqrt{\sigma^2_{z.\max} + 3\left(k_t \cdot \tau_{\max}\right)^2} \tag{18}$$

(R8/5-1)
$$\sigma_{red,B} < R_{p0.2\min} \tag{19}$$

(R8/5-2)
$$S_F = \frac{R_{p0,2\min}}{\sigma_{red,B}} \geq 1,0 \tag{20}$$

Calculation Approach

The maximum force in the bolt is calculated according to (17), which is used to calculate the normal stresses $\sigma_{z.\max}$. Then the torsional stresses of the threads from the tightening process is calculated, $\tau_{\max}$, coming from the tightening moment on the threads (M_G) required to achieve a pretension of F_{Mzul}. It is assumed that half the torsional stress ($k_t = 0,5$) will remain throughout operation. The reduced stress during operation $\sigma_{red,B}$ is calculated (18), and compared to the allowed stress (19) or by establishing a safety factor (20).

Parameters and results

Table 12: R8 analytic values

Sym.	*Value*	*Unit*	*Description*
$\sigma_{red.B}$	$949,5$	MPa	Comparative stress in the working state
S_F	$1,2$	ul	Safety margin against exceeding the yield point
$F_{S.\max}$	$143,4$	kN	Max bolt load
$\sigma_{z.\max}$	$913,4$	MPa	Max tensile stress in the bolt based on $F_{S.\max}$
$\tau_{\max}$	$299,5$	MPa	Torsional stress in the thread as a result of tightening torque on the thread

R9: ALTERNATING STRESS

Since the load is pulsating, the bolt will be exposed to alternating stresses. For the case of eccentricity, the stress amplitude σ_{ab} has to be compared to the fatigue limit for bolts rolled before heat treatment σ_{ASV}. The results are presented in Table 13.

(R9/2)

$$\sigma_{ab} = \frac{\sigma_{SAb0} - \sigma_{SAbu}}{2} \tag{21}$$

$$\sigma_{SAb} = \left[1 + \left(\frac{1}{\Phi^*_{en}} - \frac{s_{sym}}{a}\right)\frac{l_K}{l_{ers}} \cdot \frac{E_S}{E_P} \cdot \frac{\pi \cdot a \cdot d_S^3}{8 \cdot \bar{I}_{Bers}}\right]\frac{\Phi^*_{en} \cdot F_A}{A_S} \tag{22}$$

$$F_A = \begin{matrix} F_{A.\max} \\ F_{A.\min} \end{matrix} \Rightarrow \begin{matrix} \sigma_{SAbo} \\ \sigma_{SAbu} \end{matrix} \tag{23}$$

(R9/3)

$$\sigma_{ab} < \sigma_{ASV} \tag{24}$$

(R9/4)

$$S_D = \frac{\sigma_{ASV}}{\sigma_{ab}} \geq 1,0 \tag{25}$$

Calculation Approach

The max (σ_{SAbo}) and minimum (σ_{SAbu}) stress states (23), are calculated using (22). That equation use some of the geometry, stiffness and loading parameters. The substitutional bending length of the bolt l_{ers} is calculated based on the bending resilience of the bolt, β_S. The stress amplitude is calculated according to (21), and compared to the fatigue limit σ_{ASV} (24) or by the safety factor S_D (25).

Relevant parameters and results

Table 13: R9 analytic values

Sym.	*Value*	*Unit*	*Description*
σ_{ab}	$10,9$	MPa	Continuous alternating stress acting on the bolt during eccentric clamping and loading
S_D	$4,2$	ul	Safety margin against fatigue failure
σ_{ASV}	$46,2$	MPa	Stress amplitude of the endurance limit of the bolts rolled before heat treatment
l_{ers}	$36,2$	mm	Substitutional bending length for a bolt
$\bar{I}_{Bers}$	$5,6 \cdot 10^4$	mm^4	Substitutional areal moment of inertia for the deformation body, subtracted the areal moment of inertia of the bolt hole

R10: SURFACE PRESSURE

The surface pressure in the bearing area, between the bolt head and the cap, is checked against the maximum material surface pressure (26), or by finding a safety factor S_P (27). If exceeded, creep may pose a threat. The results are listed in Table 14. Only the assembled state is considered, since that is where the forces are largest.

(R10/1)

$$p_{M\,\max} = \frac{F_{Mzul}}{A_{p\,\min}} \leq p_G \tag{26}$$

(R10/4)

$$S_P = \frac{p_G}{p_{M\,\max}} \tag{27}$$

Parameters and results

Table 14: R10 analytic values

Sym.	*Value*	*Unit*	*Description*
p_G	760	MPa	Maximum permissible pressure under the bolt head
S_P	$0,97$	ul	Safety margin against surface pressure
$p_{M.\max}$	$786,3$	MPa	Surface pressure in the assembled state
$A_{p.\min}$	$181,1$	mm^2	Minimum bolt head bearing area

R11: LENGTH OF ENGAGEMENT

To make sure the thread length of engagement is sufficient, a calculation of the thread capacity is compared the effective thread length. The results are listed in Table 15.

Calculation Approach

First, the thread is identified as critical (28). Then, a diagram [Pt.1-Figure 36] gives the specific length of thread engagement required, m_{eff}. Then it is checked that the effective thread length of engagement is larger than the required length (29).

$$R_S = 0.604 \quad < \quad 1 \quad \Rightarrow \quad \text{Thread is critical} \tag{28}$$

$$m_{effvorh} = 26\text{mm} \quad > \quad \text{m}_{eff} = 16{,}8mm \tag{29}$$

Parameters and results

Table 15: R11 analytic values

Sym.	*Value*	*Unit*	*Description*
R_S	0,604	ul	Strength ratio
m_{eff}	16,8	mm	Effective length of thread engagement
$m_{effvorh}$	26	mm	Allowed length of thread engagement

R12: SAFETY MARGIN AGAINST SLIPPING

This step is omitted, since shearing is not relevant.

R13: TIGHTENING TORQUE

As the final step, the tightening torque is calculated. Results are listed in Table 16.

(R13/1)

$$M_A = F_{M.zul}\left(\underbrace{0{,}16P + 0{,}58d_2 \cdot \mu_{G.\min}}_{\text{thread}} + \underbrace{\frac{D_{K.\min}}{2}\mu_{K.\min}}_{\text{bolt head bearing}}\right) \tag{30}$$

Calculation Approach

The tightening torque M_A can be calculated from (30), or since it is based on the permitted assembly preload $F_{M.zul}$, found in [Pt.1-Table A1].

The following coefficients of friction is assumed: $\mu_{G.\min} = \mu_{K.\min} = 0{,}1$

Parameters and results

Table 16: R13 analytic values

Sym.	*Value*	*Unit*	*Description*
M_A	309	Nm	Tightening torque during assembly for preloading a bolt to $F_{M.zul}$
D_{Km}	20,3	mm	Effective diameter for the friction moment at the bolt head

CONCLUSION AND SUMMARY OF KEY RESULTS

The analytical calculations of the case defined in section 0, has resulted in the recommended use of bolt: **ISO 4762-M16x60–12.9**, rolled before heat treatment. The BJ design has been verified, and the most relevant results are summarized in Table 17.

Table 17: Summary of analytic values

Calculation step	Sym.	Value	Unit
R0: Nominal Diameter	$F_{A_{\max}}$	$19,5$	kN
	$F_{A_{\min}}$	7.1	kN
	d	16	mm
R1: Tightening Factor	α_A	$1,6$	ul
R2: Required Minimum Clamp Load	F_{Kerf}	$\geq 39,7$	kN
R3: Load factor and resiliencies	Φ^*_{en}	$0,051$	ul
	δ_S	$1,4 \cdot 10^{-3}$	mm/kN
	δ^{**}_P	$2,0 \cdot 10^{-4}$	mm/kN
	$F_{SA.\max}$	$1,002$	kN
	$F_{PA.\max}$	$18,5$	kN
R4: Preload changes	F_Z	$4,8$	kN
R5: Minimum assembly load	$F_{M.\min}$	63	kN
	F_V	$58,2$	kN
R6: Maximum assembly load	$F_{M.\max}$	$100,8$	kN
R7: Assembly stress & load	$F_{M.zul}$	$142,4$	kN
R8: Working stress	$\sigma_{red.B}$	$949,5$	MPa
	S_F	$1,2$	ul
	$F_{S.\max}$	$143,3$	kN
R9: Alternating stress	σ_{ab}	$10,9$	MPa
	S_D	$4,2$	ul
R10: Surface pressure	S_P	$0,97$	ul
	$p_{M.\max}$	$786,3$	MPa
R11: Length of engagement	$m_{effvorh}$	26	mm
R12: Safety margin against slipping	-	-	-
R13: Tightening torque	M_A	309	Nm

Blind Flange Calculations with Anaytic VDI 2230 Procedure

This analytic calculation are based on the calculation procdure defined in VDI 2230, and are associated with Appendix C-2a.

A summary of key results are found on page 8.

Parameters

Internal pressure in cylinder: $\begin{bmatrix} p_{max} \\ p_{min} \end{bmatrix} := \begin{bmatrix} 22 \\ 8 \end{bmatrix} MPa$ $\quad p := \begin{bmatrix} p_{max} \\ p_{min} \end{bmatrix}$

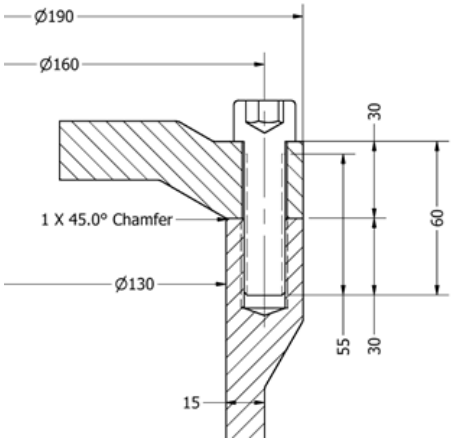

Geometry data

$D_{ST} := 160\ mm$

$D_{Zi} := 130\ mm$

$D_a := 190\ mm$

$c_T := 29\ mm$

$e := 14\ mm$

$chamf := 1\ mm$

$d_h := 17.5\ mm$

$l_K := 30\ mm$

$l := 60\ mm$

$b := 44\ mm$

$l_g := l - b = 16\ mm$

$l_s := l_g - 5\ P = 6\ mm$

Data for M16x60-12.9 bolt

$i := 15$

$d := 16\ mm$

$F_{0.2min} := 173\ kN$

$P := 2\ mm$

$d_2 := 14.701\ mm$

$A_{d3} := 144.1\ mm^2$

$A_S := 157\ mm^2$

$d_K := 24\ mm$

$d_W := 23.17\ mm$

$d_S := 16\ mm$

$d_3 := \sqrt{\frac{4\ A_{d3}}{\pi}} = 13.55\ mm$

$d_S := \sqrt{\frac{4\ A_S}{\pi}} = 14.14\ mm$

Material data: S355 JO

$R_{m.min} := 490\ MPa$

$R_{M.p0.2.min} := 325\ MPa$

$\tau_{B.min} := 390\ MPa$

$p_G := 760\ MPa$

$E := 205\ GPa$

$\rho := 7.85\ \frac{kg}{dm^3}$

$\begin{bmatrix} E_S \\ E_P \end{bmatrix} := \begin{bmatrix} E \\ E \end{bmatrix}$

$R_{mM} := R_{m.min}$

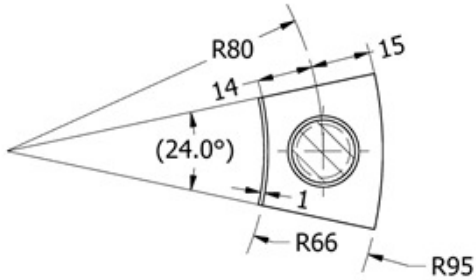

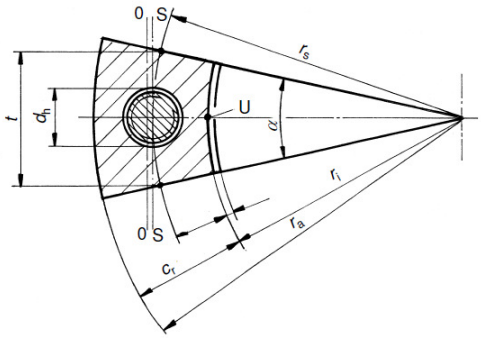

R0 - Nominal diameter $\quad R_{S.p0.2.min} := \frac{F_{0.2min}}{A_S} = 1102\ MPa$

$$\begin{bmatrix} F_{A.max} \\ F_{A.min} \end{bmatrix} := \frac{\pi}{4 \cdot i} \cdot (D_{Zi})^2 \cdot p = \begin{bmatrix} 19.5 \\ 7.1 \end{bmatrix} kN \qquad F_A := \begin{bmatrix} F_{A.max} \\ F_{A.min} \end{bmatrix}$$

$$G' := d_W \begin{bmatrix} 1.5 \\ 2 \end{bmatrix} = \begin{bmatrix} 34.8 \\ 46.3 \end{bmatrix} mm \quad > \quad c_T = 29\ mm$$

$$e = 14\ mm \quad < \quad \frac{G'}{2} = \begin{bmatrix} 17.4 \\ 23.2 \end{bmatrix} mm$$

R1: Tightening factor

$\alpha_A := 1.6$

R2: Required Minimum Clamp Load

Substitutional outside diameter of the basic solid

$D'_{A.I} := D_{ST} = 160\ mm$

Limiting outside diameter

$D_{A.R} := 2\ (c_T - e) = 30\ mm$

Lower bearing area diameter (inside)

$d_{Wu} := 2\ e = 28\ mm$

Average bearing area diameter

$d_{Wm} := \frac{d_W + d_{Wu}}{2} = 25.6\ mm$

$$\beta_L := \frac{l_K}{d_{Wm}} = 1.2 \qquad y := \frac{D'_{A.I}}{d_{Wm}} = 6.3 \qquad \varphi_D := \operatorname{atan}\left(0.362 + 0.032\ \ln\left(\frac{\beta_L}{2}\right) + 0.153\ \ln(y)\right) = 0.6$$

Limiting diameter on the inside

$D_{AGr.I} := d_{Wu} + l_K\ \tan(\varphi_D) = 46.8\ mm$

Average diameter of inside and cap edge side

$$D_{m.A.I} := \frac{D_{AGr.I} + d_{Wu}}{2} = 37.4\ mm$$

Small cone component

$$D_{m.A.R} := D_{A.R} = 30\ mm$$

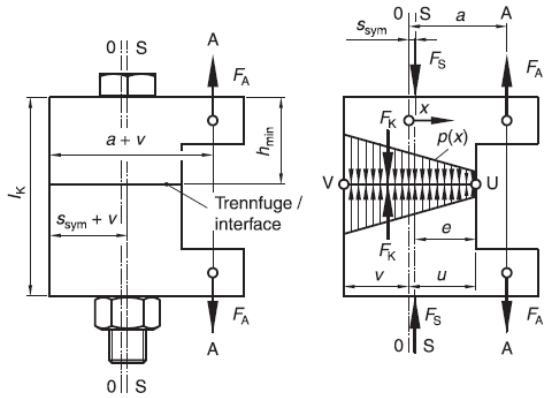

Average diameter of the complete substitutional sleve

$$D_{Am} := \frac{D_{A.R} + D_{m.A.I}}{2} = 33.7\ mm \qquad v := \frac{D_{Am}}{2} = 16.8\ mm$$

Check sign rules in table 4, VDI2230 pt. 1.
CASE III - for the displacement of the deformation body into a symmetrical position.

$$s_{sym} := c_T - e - v = -1.8\ mm \qquad u := e + s_{sym} = 12.2\ mm$$

To determine the eccentricity a of the load introduction, a FE-simulation according to **Class I** was performed:

Force reaction: $F_{KI} := 19462\ N$

$F_{sim.Q} := 6842.5\ N$

Moment reaction:

$M_{KI} := 2.6309\ 10^5\ N\ mm$

$F_{KI} = 19462\ N$

Note - Very similar to: $F_{A.max} = 19467\ N$

$$a := \frac{M_{KI}}{F_{KI}} = 13.5\ mm$$

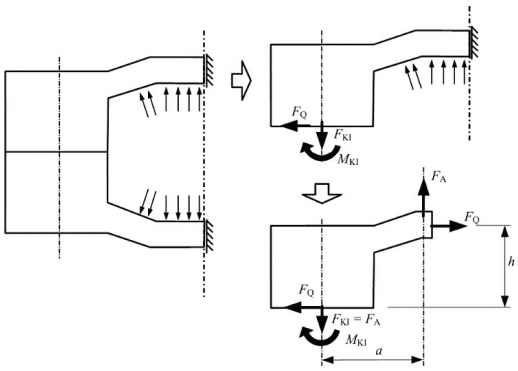

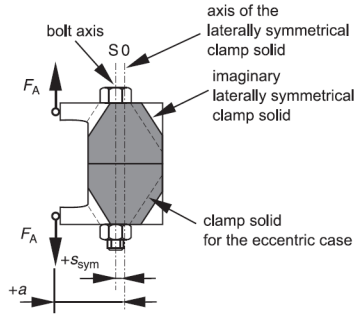

Figure 4. Model for determining s_{sym} for an eccentrically clamped joint from an imaginary concentrically clamped joint

Outer radius

$$r_a := \frac{D_a}{2}$$

Effective internal radius

$$r_i := \frac{D_{Zi}}{2} + chamf$$

Radius to bolt axis

$$r_s := \frac{D_{ST}}{2}$$

Spacing

$$t := \frac{\pi\ D_{ST}}{i} = 33.5\ mm$$

The interface area is: $A_D := \frac{\pi}{i}\left(r_a^{\ 2} - r_i^{\ 2}\right) - \left(\frac{\pi}{4}\ d_h^{\ 2}\right) = 737.34\ mm^2$

Areal moment of inertia for the interface segment: $I_{BT} := \frac{t\ c_T^{\ 3}\ \left(r_a^{\ 2} + 4\ r_a \cdot r_i + r_i^{\ 2}\right)}{36\ r_s \cdot \left(r_a + r_i\right)} = 67791.4\ mm^4$

The requesite clamp load is thus:

$$F_{Kerf} \geq F_{KA} := F_{A.max} \cdot \frac{A_D \cdot \left(a\ u + s_{sym}\ u\right)}{I_{BT} + s_{sym}\ u\ A_D} = 39.7\ kN$$

$$F_{Kerf} := F_{KA}$$

==========

R3: Load factor and resiliences

Axial resilience of the bolt are calculated:

$l_G := 0.5 \cdot d \qquad l_M := 0.33\ d \qquad l_{SK} := d\ 0.4 = 6.4\ mm$

$l_{Gew} := l_K - l_g = 14\ mm \qquad I_{d3} := \frac{\pi}{64}\ d_3^{\ 4} = \left(1.7 \cdot 10^3\right)\ mm^4$

$\delta_G := \frac{l_G}{E_S \cdot A_{d3}} = \left(2.7 \cdot 10^{-7}\right)\ \frac{mm}{N} \qquad A_N := \frac{\pi}{4}\ d^2$

$\delta_M := \frac{l_M}{E_P \cdot A_N} = \left(1.3 \cdot 10^{-7}\right)\ \frac{mm}{N} \qquad I_N := \frac{\pi}{64}\ d^4$

$\delta_{GM} := \delta_G + \delta_M = \left(4 \cdot 10^{-7}\right)\ \frac{mm}{N}$

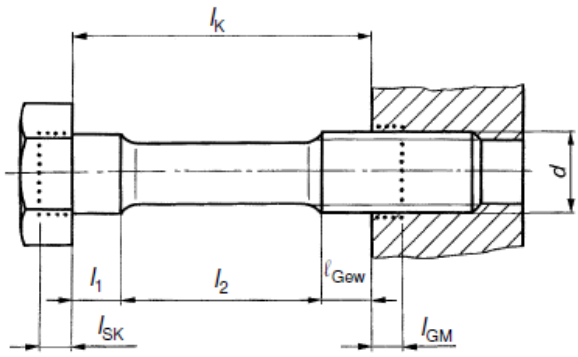

Unengaged loaded part of the thread

$$\delta_{Gew} := \frac{l_{Gew}}{E_S \cdot A_{d3}} = \left(4.7 \cdot 10^{-7}\right) \frac{mm}{N}$$

$$\delta_1 := \frac{l_g}{E_S \cdot A_N} = \left(3.9 \cdot 10^{-7}\right) \frac{mm}{N}$$

$$\delta_{SK} := \frac{l_{SK}}{E_S \cdot A_N} = \left(1.6 \cdot 10^{-7}\right) \frac{mm}{N}$$

$$\delta_S := \delta_{SK} + \delta_1 + \delta_{Gew} + \delta_{GM} = \left(1.4 \cdot 10^{-6}\right) \frac{mm}{N}$$

Bending resiliences:

$$\beta_{Gew} := \frac{l_{Gew}}{E_S \cdot I_{d3}} = \left(4.1 \cdot 10^{-8}\right) \frac{1}{N\ mm}$$

$$\beta_{SK} := \frac{l_{SK}}{E_S \cdot I_N} = \left(9.7 \cdot 10^{-9}\right) \frac{1}{N\ mm}$$

$$\beta_G := \frac{l_G}{E_S \cdot I_{d3}} = \left(2.4 \cdot 10^{-8}\right) \frac{1}{N\ mm} \qquad \beta_M := \frac{l_M}{E_P \cdot I_N} = \left(8 \cdot 10^{-9}\right) \frac{1}{N\ mm}$$

$$\beta_{GM} := \beta_G + \beta_M = \left(3.2 \cdot 10^{-8}\right) \frac{1}{N\ mm}$$

$$\beta_1 := \frac{l_g}{E_S \cdot I_N} = \left(2.4 \cdot 10^{-8}\right) \frac{1}{N\ mm}$$

$$\beta_S := \beta_{SK} + \beta_1 + \beta_{GM} + \beta_{Gew} = \left(1.1 \cdot 10^{-7}\right) \frac{1}{N\ mm}$$

Substitutional length for a cylindrical bolt: $l_{ers} := \beta_S \cdot E_S \cdot I_{d3} = 36.2\ mm$

For the clamped parts, form and size of the substitutional deformation body of the present TTJ is determined.

$$D'_{Ai} := 2\left(t - \frac{d_h}{2}\right) = 49.5\ mm \qquad D'_{A.I} = 160\ mm$$

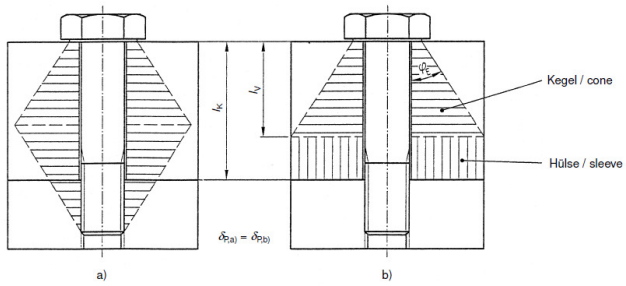

Bild 9. Zylindrische ESV
a) Ersatzverformungskegel
b) Berechnungsmodell

Figure 9. Cylindrical TTJ
a) substitutional deformation cone
b) calculation model

Substititional outside diameter of the basic solid

$$D'_A := \frac{D'_{A.I} + 2\left(c_T - e\right) + \left(2\ t - d_h\right)}{3} = 79.8\ mm$$

$$\beta_L := \frac{l_K}{d_W} = 74.2\ deg \qquad y := \frac{D'_A}{d_W} = 3.4$$

Substitutional cone angle

$$\varphi_E := \operatorname{atan}\left(0.348 + 0.013\ \ln\left(\beta_L\right) + 0.193\ \ln\left(y\right)\right) = 30.5\ deg$$

ref. p. 45 - eq. 39 $w := 2$ for TTJ

Limiting diameter

$$D_{A.Gr} := d_W + w \cdot l_K \cdot \tan\left(\varphi_E\right) = 58.6\ mm$$

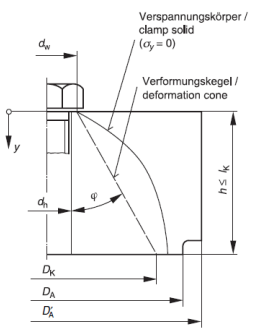

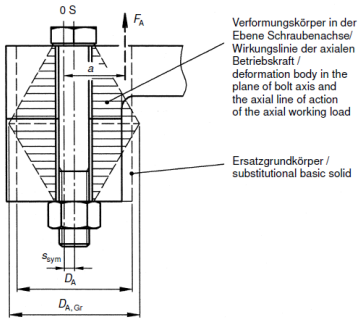

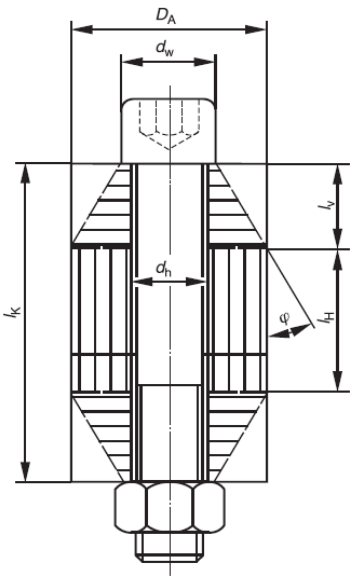

Substitutional outside diameter at the interface: $D_A := \frac{(2\ t - d_h) + 2\ e + 2\ (c_T - e)}{3} = 35.8\ mm$

See that $D_{A.Gr} = 58.6\ mm > D_A = 35.8\ mm$

The substitutional deformation body consist of cone and sleve.

The following applises for the resilience of the substitutional cone, with the cone height:

$$l_V := \frac{D_A - d_W}{2\ \tan(\varphi_E)} = 10.7\ mm$$

$$\delta_{V.P} := \frac{\ln\left(\frac{(d_W + d_h)\cdot(d_W + 2\ l_V\ \tan(\varphi_E) - d_h)}{(d_W - d_h)\cdot(d_W + 2\ l_V\ \tan(\varphi_E) + d_h)}\right)}{E_P \cdot d_h \cdot \pi \cdot \tan(\varphi_E)} = (1.4\cdot 10^{-7})\ \frac{mm}{N}$$

The remaining substitutional sleve has the height:

$$l_H := l_K - \frac{2\ l_V}{w} = 19.3\ mm$$

$$\delta_{H.P} := \frac{4\ l_H}{E_P \cdot \pi \cdot (D_A{}^2 - d_h{}^2)} = (1.2\cdot 10^{-7})\ \frac{mm}{N}$$

$$\delta_P := \delta_{V.P} + \delta_{H.P} = (2.6\cdot 10^{-7})\ \frac{mm}{N}$$

Resilience for eccentric loading & clamping

$$I_{V.Bers} := 0.147 \cdot \frac{(D_A - d_W)\cdot d_W{}^3 \cdot D_A{}^3}{D_A{}^3 - d_W{}^3}$$

Substitutional cone: $I_{VE.Bers} := I_{V.Bers} + s_{sym}{}^2 \cdot \frac{\pi}{4}\ D_A{}^2$

Substitutional sleeve: $I_{H.Bers} := \frac{(2\ t - d_h)\cdot c_T{}^3}{12}$

Substitational areal moment of inertia: $I_{Bers} := \frac{l_K}{\frac{2\ l_V}{w \cdot I_{VE.Bers}} + \frac{l_H}{I_{H.Bers}}} = (6\cdot 10^4)\ mm^4$

$$\delta'_P := \delta_P + \frac{s_{sym}{}^2 \cdot l_K}{E_P \cdot I_{Bers}} = (2.7\cdot 10^{-7})\ \frac{mm}{N}$$

$$\delta''_P := \delta_P + \frac{a \cdot s_{sym} \cdot l_K}{E_P \cdot I_{Bers}} = (2\cdot 10^{-7})\ \frac{mm}{N}$$

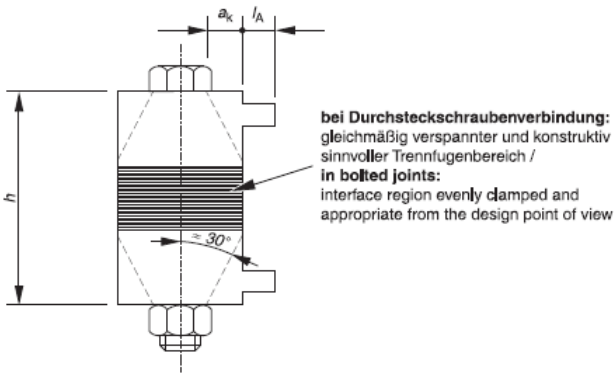

Determining KEF n by Table 2: (most unfavorable variant)

$$a_k := a - s_{sym} - \frac{d_W}{2} = 3.8\ mm$$

$$r := \frac{a_k}{l_K} = 0.1 \qquad \frac{l_A}{l_K} = 0$$

The connecting solid start at the line of action of F_A. In table 2, use SV2

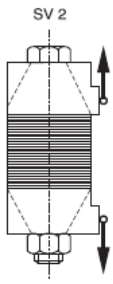

Linear interpolation $n := 0.3 + 0.04\ \frac{0.13 - 0.3}{0.5 - 0.3} = 0.266$ n = load introduction factor

Load factor

$$\Phi'_{en} := n \cdot \frac{\delta''_P + \delta_M}{\delta'_P + \delta_S} = 0.0515$$

Additional bolt load

$$F_{SA.max} := F_{A.max} \cdot \Phi'_{en} = (1\cdot 10^3)\ N$$

Additional plate load

$$F_{PA.max} := F_{A.max} \cdot (1 - \Phi'_{en}) = 18.5\ kN$$

R4 - Preload changes

From Table 5, embedding from $Rz := 16\ \mu m$ is $2\ \mu m$ for an inner interface, $3\ \mu m$ for for head bearing area and $3\ \mu m$ for the thread contact, thus:

$f_Z := 8\ \mu m$

With eg. **(R4/1)**

$$F_Z := \frac{f_Z}{\delta_S + \delta_P} = 4.8\ kN$$

R5 - Minimum assembly preload
eq. **(R5/1)**

$F_{Kerf} = 39.7\ kN$ $\quad F_{A.max} = 19.5\ kN$ $\quad F_Z = 4.8\ kN$

$F_{M.min} := F_{Kerf} + \left(1 - \Phi'_{en}\right) F_{A.max} + F_Z$ $\quad F_V := F_{Kerf} + \left(1 - \Phi'_{en}\right) F_{A.max}$

$F_{M.min} = 63\ kN$ $\quad F_V = 58.2\ kN$

R6 - Maximum assembly preload
eq. **(R6/1)**

$$F_{M.max} := \alpha_A \cdot F_{M.min} = 100.8\ kN$$

R7 - Assembly stress

according to Table A1, with $\mu_{G.min} := 0.1$

$F_{M.zul} = F_{M.Tab}$ $\quad F_{M.max} = 100.8\ kN$ < $F_{M.zul} := 142.4\ kN$

R8 - Working stress
eq. **(R8/1)**

$$F_{S.max} := F_{M.zul} + \Phi'_{en} \cdot F_{A.max} = 143.4\ kN$$

$$\sigma_{z.max} := \frac{F_{S.max}}{A_S} = 913.4\ MPa$$

$$M_G := F_{M.zul} \frac{d_2}{2} \left(\frac{P}{\pi \cdot d_2} + 1.155 \cdot \mu_{G.min} \right) = 166.2\ N\ m$$

$$W_P := \frac{\pi}{16} \cdot \left(d_S\right)^3 = 554.9\ mm^3$$

$$\tau_{max} := \frac{M_G}{W_P} = 299.5\ MPa$$

eq. **(R8/4)** $\quad k_t := 0.5$

$$\sigma_{red.B} := \sqrt{\sigma_{z.max}^{\ 2} + 3\ \left(k_t\ \tau_{max}\right)^2} = 949.5\ MPa$$

Checking that maximum working stress is below the minimum yield stress of the bolt.
$\sigma_{red.B} = 949.5\ MPa$ < $R_{S.p0.2.min} = 1101.9\ MPa$

Safetyfactor against yielding are:

$$S_F := \frac{R_{S.p0.2.min}}{\sigma_{red.B}} = 1.2$$

R9 - Alternating stress

Amplitude of alternating stress ref. eq. (9/2):

Surface areal moment of inertia:

$$I'_{Bers} := I_{Bers} - \frac{\pi}{64} d_h^{\,4} = \left(5.6 \cdot 10^4\right)\ mm^4$$

Bending resilience of the clamped parts:

$$\beta_P := \frac{l_K}{E_P\ I'_{Bers}} = \left(2.6 \cdot 10^{-6}\right) \frac{1}{N\ m}$$

Bending moment absorbed by the bolt:

$$M_{Sb} := \frac{\beta_P}{\beta_S}\left(1 - \frac{s_{sym}}{a}\ \Phi'_{en}\right) F_A\ a = \begin{bmatrix} 6.5 \\ 2.4 \end{bmatrix} N\ m$$

$$\sigma_{SAb} := \left(1 + \left(\frac{1}{\Phi'_{en}} - \frac{s_{sym}}{a}\right) \frac{l_K}{l_{ers}} \cdot \frac{E_S}{E_P} \cdot \frac{\pi \cdot a \cdot d_S^{\,3}}{8 \cdot I'_{Bers}}\right) \frac{\Phi'_{en} \cdot F_A}{A_S} = \begin{bmatrix} 34.2 \\ 12.4 \end{bmatrix} MPa \quad \begin{bmatrix} \sigma_{SAbo} \\ \sigma_{SAbu} \end{bmatrix} := \sigma_{SAb}$$

$$\sigma_{ab} := \frac{\sigma_{SAbo} - \sigma_{SAbu}}{2} = 10.9\ MPa$$

Permissable continous alternating stress for bolts rolled before heat treatment

$$\sigma_{ASV} := 0.85\left(\frac{150}{d'} + 45\right) MPa = 46.2\ MPa \qquad l_{ers} := \beta_S \cdot E_S \cdot I_{d3} = 36.2\ mm$$

The amplitude are smaller then tha allowed stress amplitude

$$\sigma_{ab} = 10.9\ MPa < \quad \sigma_{ASV} = 46.2\ MPa$$

The safetyfactor against fatigue are

$$S_D := \frac{\sigma_{ASV}}{\sigma_{ab}} = 4.2$$

R10 - Surface pressure

$$A_{p.min} := \frac{\pi}{4}\left(d_W^{\,2} - d_h^{\,2}\right) = 181.1\ mm^2$$

Assembled state: $p_{M.max} := \frac{F_{M.zul}}{A_{p.min}} = 786.3\ MPa$

The surface pressure are not below the allowed surface pressure. A washer should be used to reduce the surface pressure.

$$p_{M.max} = 786.3\ MPa \quad > \quad p_G = 760\ MPa$$

$$S_P := \frac{p_G}{p_{M.max}} = 0.97$$

Working state omitted, since: $\Delta F_{Vth} = 0$ and $F_Z > F_{SA.max}$

R11 - Length of engagement

acc. to eq. (199)

$$D_2 := d_2 \qquad D_1 := 14.2\ mm \qquad R_{mS} := R_{S.p0.2.min} = \left(1.1 \cdot 10^3\right) MPa \qquad R_{mM} = 490\ MPa$$

$$R_S := \frac{d \cdot \left(\frac{P}{2} + (d - D_2) \cdot \tan(30\ deg)\right)}{d \cdot \left(\frac{P}{2} + (d_2 - D_1) \cdot \tan(30\ deg)\right)} \cdot \frac{R_{mM}}{R_{mS}} = 0.604 < \quad 1 \quad \Rightarrow$$

The thread is critical

$$\tau_{B.min} = 390\ MPa$$

$$m_{eff} := 1.05 \cdot d = 16.8\ mm \qquad m_{gesvorh} := l - l_K = 30\ mm$$

$$m_{effvorh} := m_{gesvorh} - 2\ P = 26\ mm$$

$$m_{effvorh} = 26\ mm \quad > \quad m_{eff} = 16.8\ mm$$

p. 101

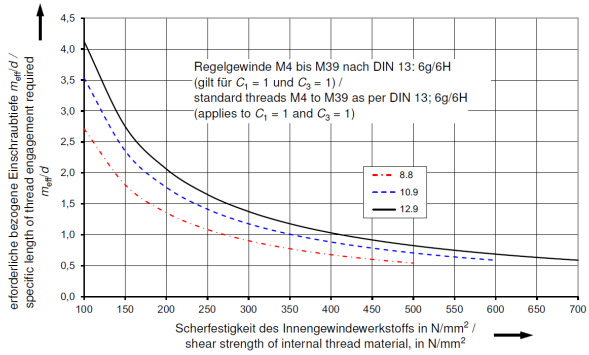

R12 - Safety margin against slipping

Omitted

R13 - Tightening torque

$$\mu_{K.min} := \mu_{G.min} \qquad D_{Km} := \frac{(d_W - d_h)}{2} + d_h = 20.3\ mm$$

$$M_A := F_{M.zul} \cdot \left(0.16\ P + 0.58\ d_2 \cdot \mu_{G.min} + \frac{D_{Km}}{2} \cdot \mu_{K.min}\right) = 311.8\ N\ m$$

Table A1: $M_A := 309\ N\ m$
==========

Summary of Key Results

Calculation step	Main output	Sub parameters
R0 - Nominal diameter	$\begin{bmatrix} F_{A.max} \\ F_{A.min} \end{bmatrix} = \begin{bmatrix} 19.5 \\ 7.1 \end{bmatrix} kN$ $G' = \begin{bmatrix} 34.8 \\ 46.3 \end{bmatrix} mm \quad > \quad c_T = 29\ mm$ $e = 14\ mm \quad < \quad \frac{G'}{2} = \begin{bmatrix} 17.4 \\ 23.2 \end{bmatrix} mm$	$I_{BT} = 67791.4\ mm^4$
R1: Tightening factor	$\alpha_A = 1.6$	
R2: Required Minimum Clamp Load	$F_{Kerf} \geq F_{KA}$ $F_{Kerf} = 39.7\ kN$	$s_{sym} = -1.8\ mm$ $\quad a = 13.5\ mm$ $u = 12.2\ mm$ $\quad F_{KA} = 39.7\ kN$
R3: Load factor and resiliences	$\delta_S = (1.4 \cdot 10^{-3})\ \frac{mm}{kN}$ $\quad \delta_P = (2.6 \cdot 10^{-4})\ \frac{mm}{kN}$ $\beta_S = 0.107\ \frac{1}{kN\ m}$ $\quad \delta'_P = (2.7 \cdot 10^{-4})\ \frac{mm}{kN}$ $\Phi'_{en} = 0.051$ $\quad \delta''_P = (2 \cdot 10^{-4})\ \frac{mm}{kN}$	$n = 0.27$ $F_{PA.max} = 18.5\ kN$ $F_{SA.max} = 1.002\ kN$
R4 - Preload changes	$F_Z = 4.8\ kN$	$f_Z = 8\ \mu m$
R5 - Minimum assembly preload	$F_{M.min} = 63\ kN$ $F_V = 58.2\ kN$	$F_{Kerf} = 39.7\ kN$ $F_{A.max} = 19.5\ kN$ $F_Z = 4.8\ kN$
R6 - Maximum assembly preload	$F_{M.max} = 100.8\ kN$	
R7 - Assembly stress	$F_{M.max} = 100.8\ kN < \quad F_{M.zul} = 142.4\ kN$	
R8 - Working stress	$\sigma_{red.B} = 949.5\ MPa < R_{S.p0.2.min} = 1101.9\ MPa$ $S_F = 1.2$	$F_{S.max} = 143.4\ kN$ $\sigma_{z.max} = 913.4\ MPa$ $\tau_{max} = 299.5\ MPa$
R9 - Alternating stress	$\sigma_{ab} = 10.9\ MPa < \sigma_{ASV} = 46.2\ MPa$ $S_D = 4.2$	$\sigma_{ab} = 10.9\ MPa$ $I'_{Bers} = (5.6 \cdot 10^4)\ mm^4$ $l_{ers} = 36.2\ mm$
R10 - Surface pressure	$p_{M.max} = 786.3\ MPa < p_G = 760\ MPa$ $S_P = 0.97$	
R11 - Length of engagement	$R_S = 0.6 \quad < \quad 1$ => Thread is critical $m_{effvorh} = 26\ mm > m_{eff} = 16.8\ mm$	
R12 - Safety margin against slipping	Omitted	
R13 - Tightening torque	$M_A = 309\ N\ m$	

Additional calculations:

$$F_{KR.min} := \frac{F_{M.zul}}{\alpha_A} - F_Z - F_{PA.max} = 65.8\ kN \qquad F_{Kerf} = 39.7\ kN \qquad F_{KA} = 39.7\ kN \qquad S_C := \frac{F_{KR.min}}{F_{KA}} = 1.65$$

APPENDIX D

BOLTED TUNER ANALYSIS EXAMPLE

D-1 **HG Cavity Bolted Tuner Analysis (EDMS 1716574)**

D-2 **Analytic Calculations for Tuner Analysis**

HG Cavity Tuner Bolted Joint Analysis

Analysis performed by:	Jørgen Apeland	***Date of Analysis:***	September 2017
Analysis revision:	V2	***EDMS Reference:***	1716574
According to procedure:	BASIC FEA Workflow		
Mathcad calculation:	Appendix D-2 Analytic Calculations for Tuner Analysis		

BASIC FE-ASSISTED ANALYSIS

This is an analysis of the bolted joint on the HG Cavity Tuner. The scope of this analysis is to assess if slipping occur under operational loads, and define tightening specifications. The assessment is performed according to a simplified procedure based on VDI 2230.

S0: INITIAL STATE

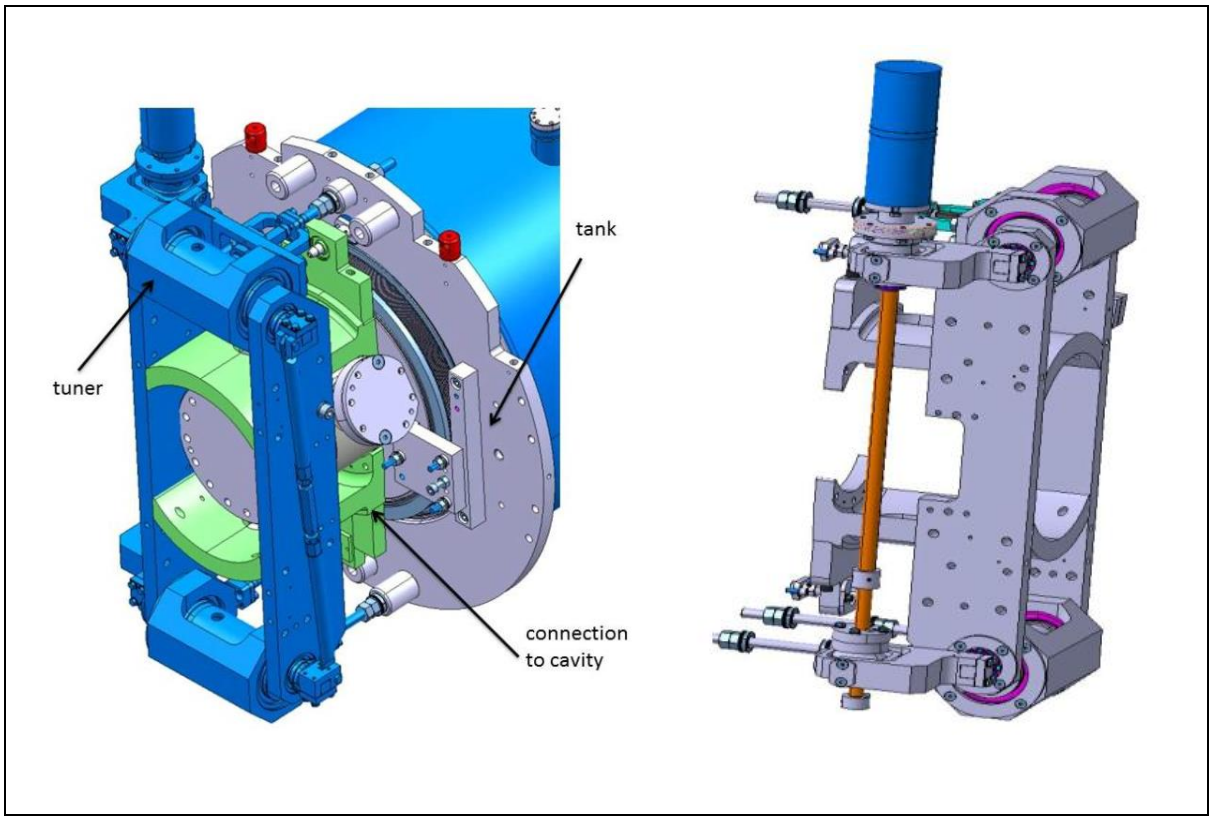

Figure 1: Tuner geometry without bolted joint

The initial tuner geometry is presented in Figure 1. In Figure 2, the tuner geometry with bolted joint is shown. There are 4 separate bolted joints, with 9 bolts in each. The total number of bolts are 36. The bolts are determined by the designer to be: **ISO 4762 M8x20-A4**, Austenitic Stainless Steel of **property class 70**. The tuner is made of **AISI 316** Stainless Steel.

For this analysis, the eight alignment/shear pins are neglected.

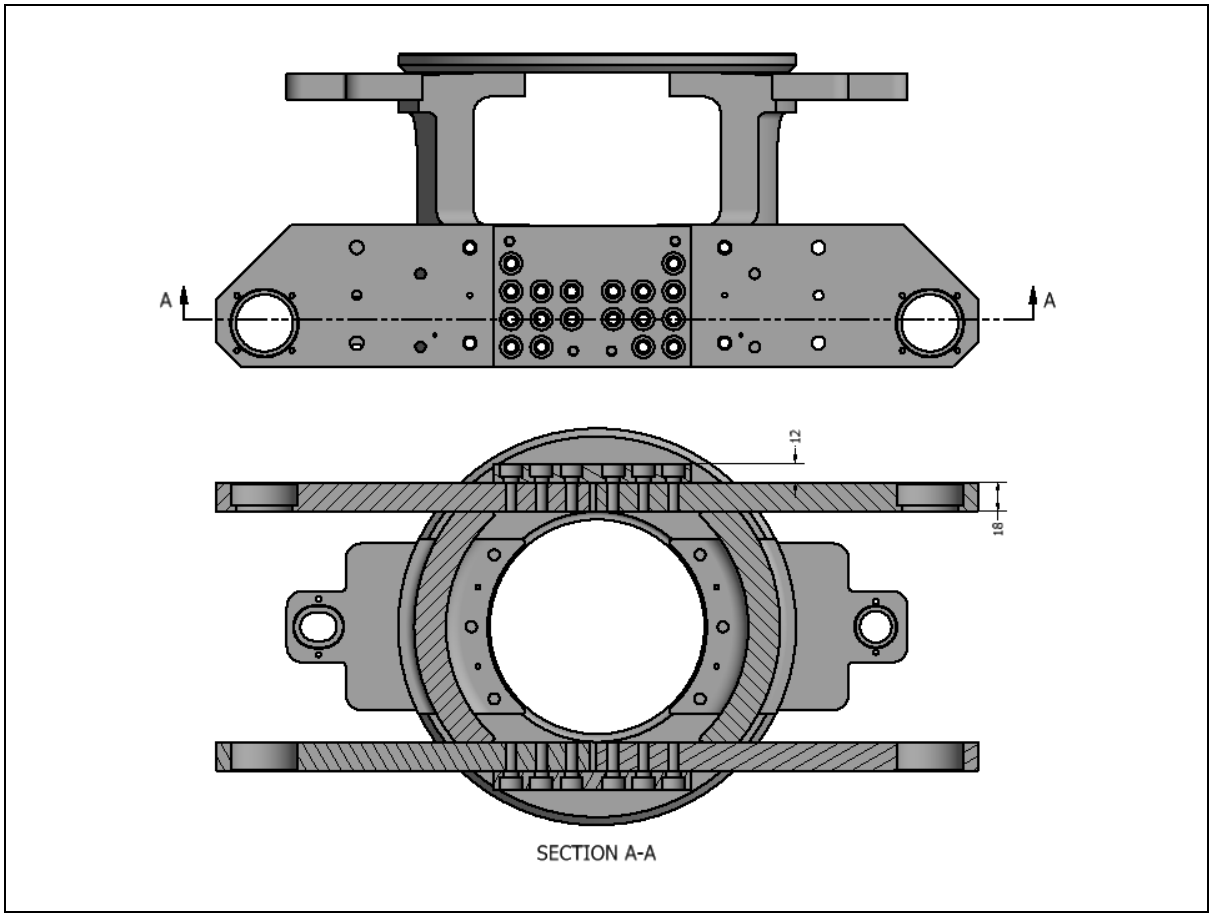

Figure 2: Tuner geometry with bolted joint

Based on an analysis of the HG Cavity and tank [1], the stiffness of the tank is found to be 130 kN/mm, and the cavity to be 4 kN/mm. The cavity deformation range is +/- 1mm, thus 2mm in total. Assuming the tank is stiff, due to the much higher stiffness, a 2mm deformation of the cavity will introduce 8 kN of load on the tuner. Including a small safety factor (1.25), assuming 2.5 mm deformation, the load on the tuner is 10 kN. The friction in the clamping interface has been assumed to be 0.2.

The most important data is summarised in Table 1.

Table 1: Design and workload data

Bolt type	ISO 4762 M8x20 A4 Class 70
Number of bolts	$n_S = 9 \qquad n_{S.tot} = n_S \cdot 4 = 36$
Tuner material	AISI 316 Stainless Steel
Friction in the clamping interface	$\mu_{T\min} = 0.2$
Max Tuner Workload	$F_{A.max} = 10\ kN$

Pre-calculations and Dimensioning

S1: WORKLOAD

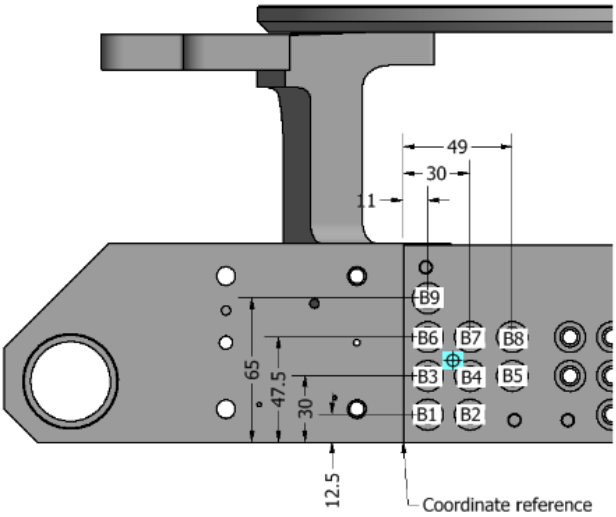

Figure 3: Naming of bolts and bolt positions

In Figure 3, the bolts for one of the four BJs are named and positioned. In the associated Mathcad document (***Appendix D-2***), the center of the bolt pattern and the radius to each bolt is identified. The critical bolt is "B9", and is positioned 32.7mm from the bolt pattern center.

Through a Class I simulation, having the clamping interface bonded, a reaction moment about the bolt pattern center were extracted, and found to be $M_Z = 123Nm$. From analytic equations, the following quantities are calculated:

Assuming:

Coefficient of friction in the interface: $\mu_{T\min} = 0.2$

Minimum required safety factor: $S_{G.req} = 1.2$

Transverse force on critical bolt: $F_{Q\max} = 902.6N$

Minimum req. clamp load: $F_{KQ} = \dfrac{S_G \cdot F_{qM\max}}{\mu_{T\min}} = 5.4kN$

The analytic approach assumes rigid bodies, and that the reactive forces of the bolting points are divided proportionally to their distance from the centroid. The outermost bolt(s) are defined as critical, and are the subject of verification.

Based on this calculation, the minimum preload to satisfy the required transverse load-carrying capacity is **5.4kN,** when not considering preload losses.

From a simulation with frictionless conditions in the interface and bonded contacts in the head bearing area, the maximum transverse load is found to be **1.85kN.** This is twice as high

as the load obtained from analytic calculations. This load is however expected to be too high, due to unrealistic load distribution in the joint when friction is not present.

S2: NOMINAL BOLT DIAMETER

For Standard Steel Bolts

According to the bolt-size estimation guide in [Pt.1-Table A7], knowing the maximum transverse load on the bolt F_{qMmax}, the bolt has to be: **M8 – 8.8**. The estimation steps are shown in Table 2.

For the transverse load resulting from a FE-analysis with frictionless contact in the interface, the estimated nominal diameter would be 12mm.

Table 2: Preliminary dimensioning procedure for analytic load

Step	*Evaluation*	*Result*
A	$F_{Q_{max}} < 1000N$	1 kN
B	+ four steps for static or dynamic transverse load	6.3 kN
C	+ one step for using a torque wrench	10 kN
D	Strength grade 8.8 give nominal diameter:	8 mm

For Bolts of Other Materials

The bolt will be of Stainless Steel, so two approaches can be taken:

1. **Verify that the yield stress of a similar SS bolt will be the same**

   $R_{p0.2}$ of A4-70 is 450 MPa < 640 MPa of Steel class 8.8

   Thus, the Stainless Steel bolt is weaker than the bolt suggested by [Pt.1 – Table A7]. The nominal diameter should therefore be larger than what the procedure suggest.

2. **Identify a new SS bolt size based on the same capacity as the steel bolt.**

$$F_{Steel} = F_{SS}$$
$$R_{p0.2.Steel} \cdot A_{Steel} = R_{p0.2.SS} \cdot A_{SS}$$
$$640MPa \cdot \frac{\pi}{4} \cdot (8mm)^2 = 450MPa \cdot \frac{\pi}{4}(d_{SS})^2$$
$$d_{SS} = \sqrt{\frac{640MPa \cdot (8mm)^2}{450MPa}}$$
$$\underline{\underline{d_{SS} = 9.5mm}}$$

According to this calculation, to achieve the same capacity in the Stainless Steel bolt as the one suggested by VDI 2230 Table A7, The bolt should have the size M10.

Based on the above estimates, the bolt should have been larger. However, since M8 is specified, this bolt will be kept for the following analysis.

Bolt and Clamped Parts Data

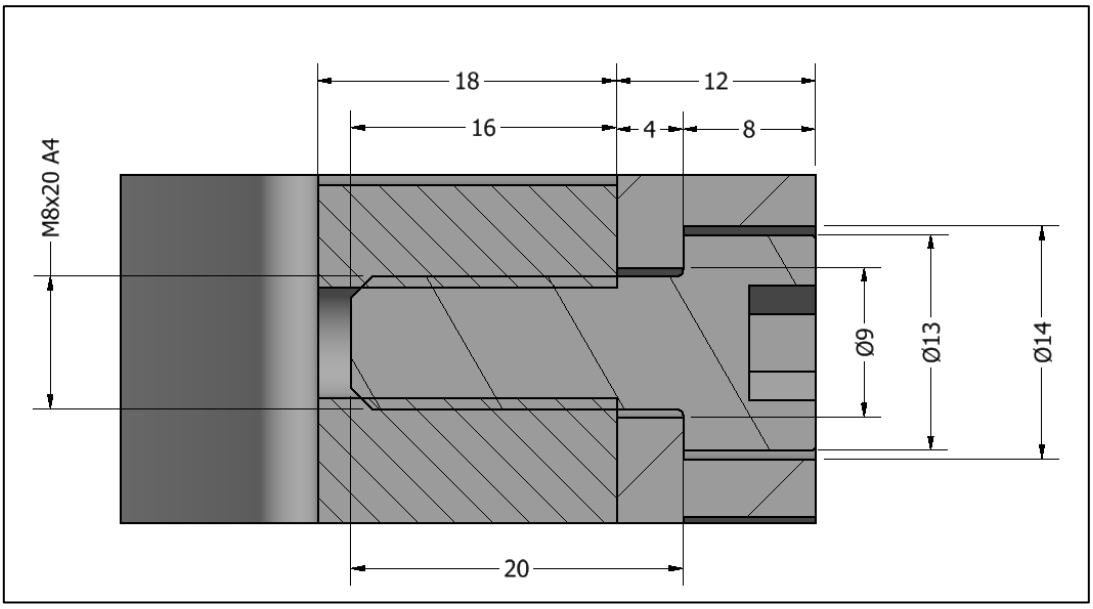

Figure 4: Cross-section of bolted connection

A cross-section of the bolted connection is shown in Figure 4. The bolt data is presented in Table 3, and the clamped parts data in Table 4.

Table 3: Bolt data

Parameter	Sym.	Value	Unit	Source
Bolt material	Stainless Steel A4-70			[Pt.1-Table A9]
E-modulus	E	200	GPa	EDMS 1530740
Tensile strength of bolt	R_m	700	MPa	BOSSARD
0.2% Proof strength of the bolt	$R_{p0.2}$	450	MPa	BOSSARD
Nominal diameter	d	8	mm	Defined
Thread Pitch	P	1.25	mm	[Pt.1-Table A12]
Pitch Diameter	d_2	7.188	mm	[Pt.1-Table A11] / Calc.
Minor Diameter	d_3	6.466	mm	[Pt.1-Table A12] / Calc.
Effective head diameter	d_W	12.33	mm	ISO 4762
Bolt head height	k	8	mm	ISO 4762
Bolt shank length	l_S	20	mm	Defined
Clearance hole diameter	d_h	9	mm	ISO 273 - medium
Thread Coefficient of Friction	μ_{Gmin}	0.2	-	[Pt.1-Table A5-A6]
Friction in Head Bearing Area	μ_{Kmin}	0.2	-	[Pt.1-Table A5-A6]

Table 4: Clamped parts data

Parameter	Sym.	Value	Unit	Source
Clamped parts material	AISI 316 Stainless Steel / 1.4401			
E-modulus	E	200	GPa	[Pt.1-Table A9]
Tensile strength	$R_{m\,min}$	530	MPa	[Pt.1-Table A9]
0.2% Proof strength	$R_{p0.2}$	220	MPa	[Pt.1-Table A9]
Friction in the interface	μ_{Tmin}	0.2		

S3: Tightening Factor

Using [Pt.1-Table A8] for friction coefficient class B, knowing a precision torque wrench will be used, and choosing a high value in the allowed range give the tightening factor $\alpha_A = 1.6$.

(R1/1)

$$\alpha_A = \frac{F_{M\max}}{F_{M\min}} = 1,6 \quad (1)$$

S4: Maximum Assembly Pretension

By defining how much of the bolt capacity that should be utilized during assembly through the utilization factor υ, a maximum permitted assembly preload is obtained. The associated data is found in Table 5. Knowing the bolt might be too small, a high utilization is chosen.

Table 5: Data associated with calculation of the maximum assembly pretension

Utilization factor	υ	0.9		Defined
Stress Area	A_S	36.6	mm^2	[Pt.1-Table A11] / Calc.
Maximum Permitted Assembly Preload	$\boldsymbol{F_{Mzul}}$	**11.7**	$\boldsymbol{kN}$	Calculated

S5: Minimum Assembly Pretension

Taking the tightening uncertainty into account, the lowest preload after assembly should be the minimum assembly preload listed in Table 6.

Table 6: Data and Results Min Assembly Pretension

Minimum Assembly Preload	$\boldsymbol{F_{Mzul.min}}$	**7.3**	$\boldsymbol{kN}$	Calculated

FE-analysis

S6: Simplify and Prepare CAD Geometry

In this step, a simplified FE-model is prepared and small holes are removed. All relevant data is listed in Table 3 and Figure 4.

The bolt is represented by a Class III model, with diameter based on the minor diameter (d_3). The tapped thread hole-dimeter correspond to the bolt diameter.

S7: Prepare and Run FE-analysis

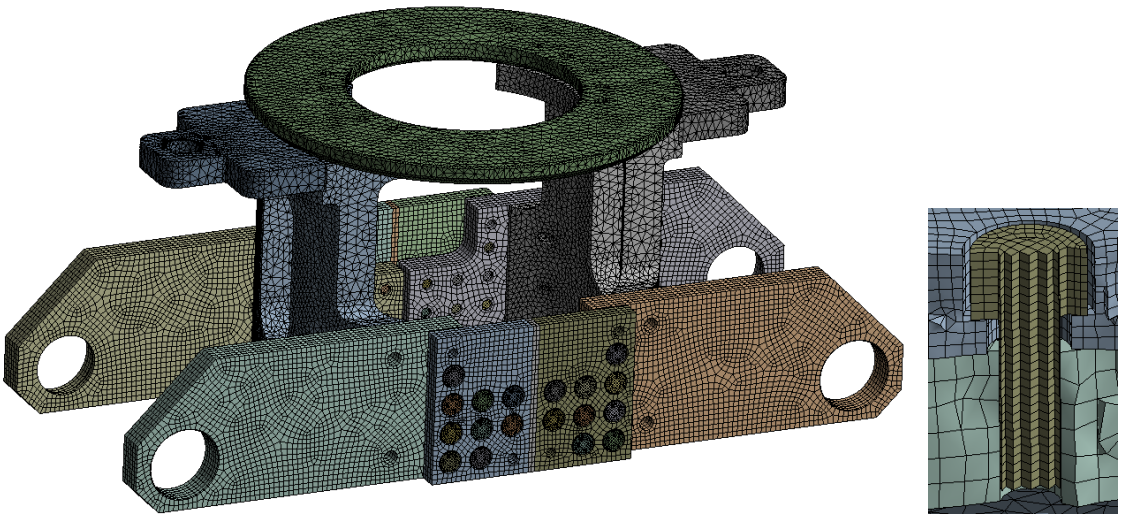

Figure 5: CAD geometry, FE-model, and contact conditions

The model has 323 000 elements (Table 5), mainly Hex20 and Tet10. The bolt is meshed with Hex elements (Figure 6). The clamping plate is split in two to allow simple extraction of moment for each BJ connection.

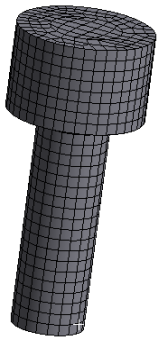

Figure 6: Bolt mesh

The correct E-modulus on the bolt and tuner bodies are applied. In the clamping interface and in the head bearing area, friction-contact is applied with the coefficient of friction μ_{Tmin}. All other contacts are bonded.

In the first load-step, the preload is applied. In the second step, the actual workload of 10kN of axial force are applied to the tuner. In a third step, 20kN are applied as a maximum case to initiate slipping.

Revolute joints are applied to represent the four bearings (Figure 7). For these joints, only rotation about the Z-axis are allowed. All other degrees of freedom are fixed.

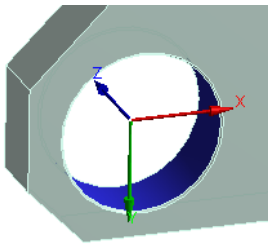

Figure 7: Revolute joint

When setting up the model, the following functions are very useful to save time:

- Named selections
- Object generator

S8: Extract Values from the FE-analysis

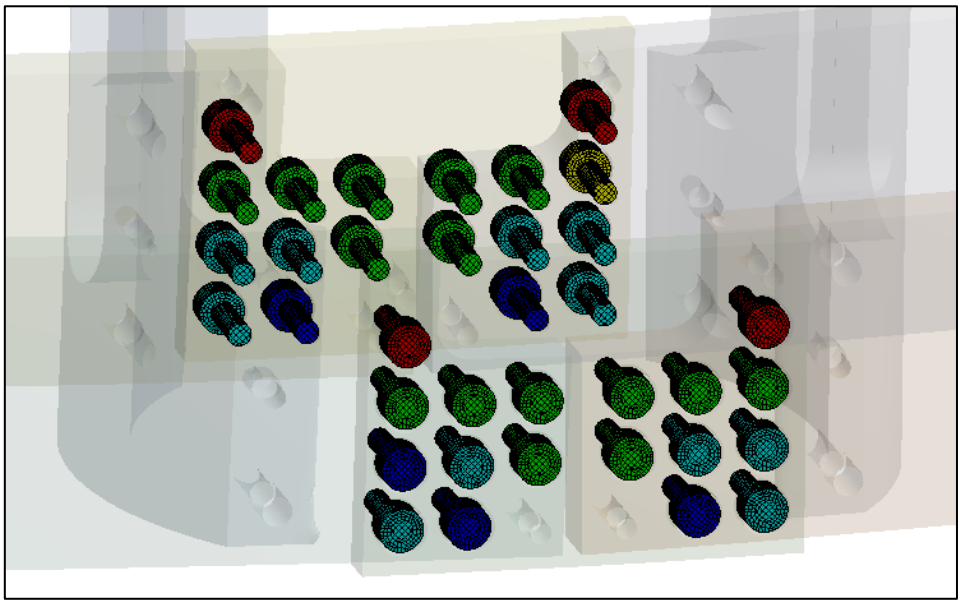

Figure 8: Using the bolt tool, the workload can be visualised.

From Figure 8 it is clear that the bolt loading is quite symmetric, and that the B9-bolts that are most highly loaded. The results with 10kN applied workload is listed in Table 7.

The residual clamping-force in the interface is divided by number of bolts.

Table 7: Extracted values from FE-analysis

Maximum Assembly preload	Max preload for M8x20-A4 70: **1B-2**			
Max achieved preload	F_{Vmax}	11.70	kN	Extracted FEA
Max bolt load	F_{Smax}	11.75	kN	
Max bolt moment	M_{Sbo}	1.8	Nm	
Minimum Assembly Preload	Min preload for M8x20-A4 70: **1B-2**			
Actual preload	F_{Vmin}	7.29	kN	Extracted FEA
Max work-moment on BJ	M_Z	131	Nm	
Residual clamping force	$F_{KR.min}$	7.31	kN	

Analysis of Results

S9: Work Stress

Since no axial loads are applied, stress verification in assembly state is sufficient, and calculation of the working stress can be omitted. To have a reference value, it is calculated in this situation.

Table 8: Calculated values from FE-analysis

Work Stress	$\sigma_{red.B}$	413	MPa	Calculated
Amount bending stress		14	%	
Bolt Yield Safety Factor	S_f	1.09		Calculated

S10: CLAMPING REQUIREMENTS

In this step, the clamping requirement that no slipping should occur assessed. First, an analytic approach is done. Then, an assessment is performed using the functionality in ANSYS, before results using CADFEM is presented. In the end, the different results are compared, before a conclusion is made.

Analytic calculations

Using the extracted moment of the clamping interface, $M_{Z.max}$, the following safety factor against slipping can be identified:

$$S_G = \frac{F_{V\min} \cdot \mu_{T\min}}{F_{qM.nax}} = 1.52 \qquad \underline{\underline{S_G > 1.2}}$$

According to this calculation, the slipping resistance is higher than the occurring transverse force at the most highly loaded bolt. With maximum preload, the safety factor is 2.43 for this bolt.

If slipping should occur, the following safety factor for shearing of the bolt can be calculated:

$$S_A = \frac{\tau_B \cdot A_S}{F_{qM.\max}} = 19.2 \qquad \underline{\underline{S_A > 1.1}}$$

Preload losses

Preload losses are not considered in this analysis. Since both bolt and clamped parts are of similar material, the thermal coefficient of expansion is similar, so no preload loss are expected from cooling the components to 2K.

Embedding might occur however. The values in VDI 2230 are based on ordinary Steel, and would for this joint be $f_Z = 8\mu m$

The resulting preload loss depend on the resilience of the joint. Two estimates are performed, suggesting preload losses of 4.4kN and 3kN. That would result in safety against slipping of 0.6 and 0.9 respectively.

Embedding could have a critical impact on the joint function. However, there is uncertainty about actual embedding for Stainless Steel, and it will depend on surface finish.

Two alternatives to reduce the effect of embedding are to use Heavy Duty spring washers, or to introduce a counter bore (Figure 9). That will increase the resilience of the joint, and reduce the resulting preload loss from embedding.

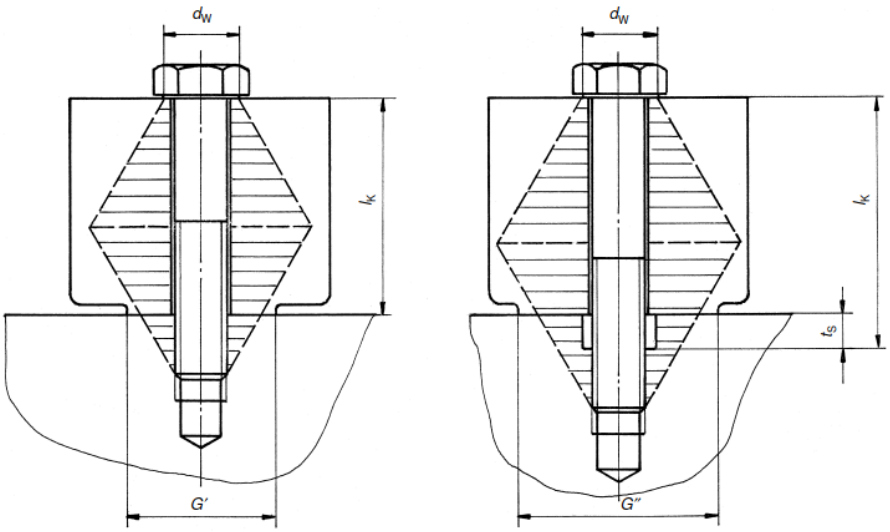

Figure 9: Effect of introducing counter-bore

Increased thread friction

Another uncertainty is the friction in the threads, interface, and in the head bearing area. If the friction in the threads and head bearing area increase to 0.3, applying the recommended tightening torque will result in preloads of max/min = 8kN / 5kN. The safety factor against slipping would in this case be S_G=1.04.

ANSYS Assessment

Table 9: Legends for result plots

Surface pressure	Status	Sliding distance
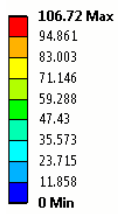		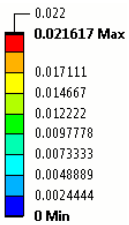

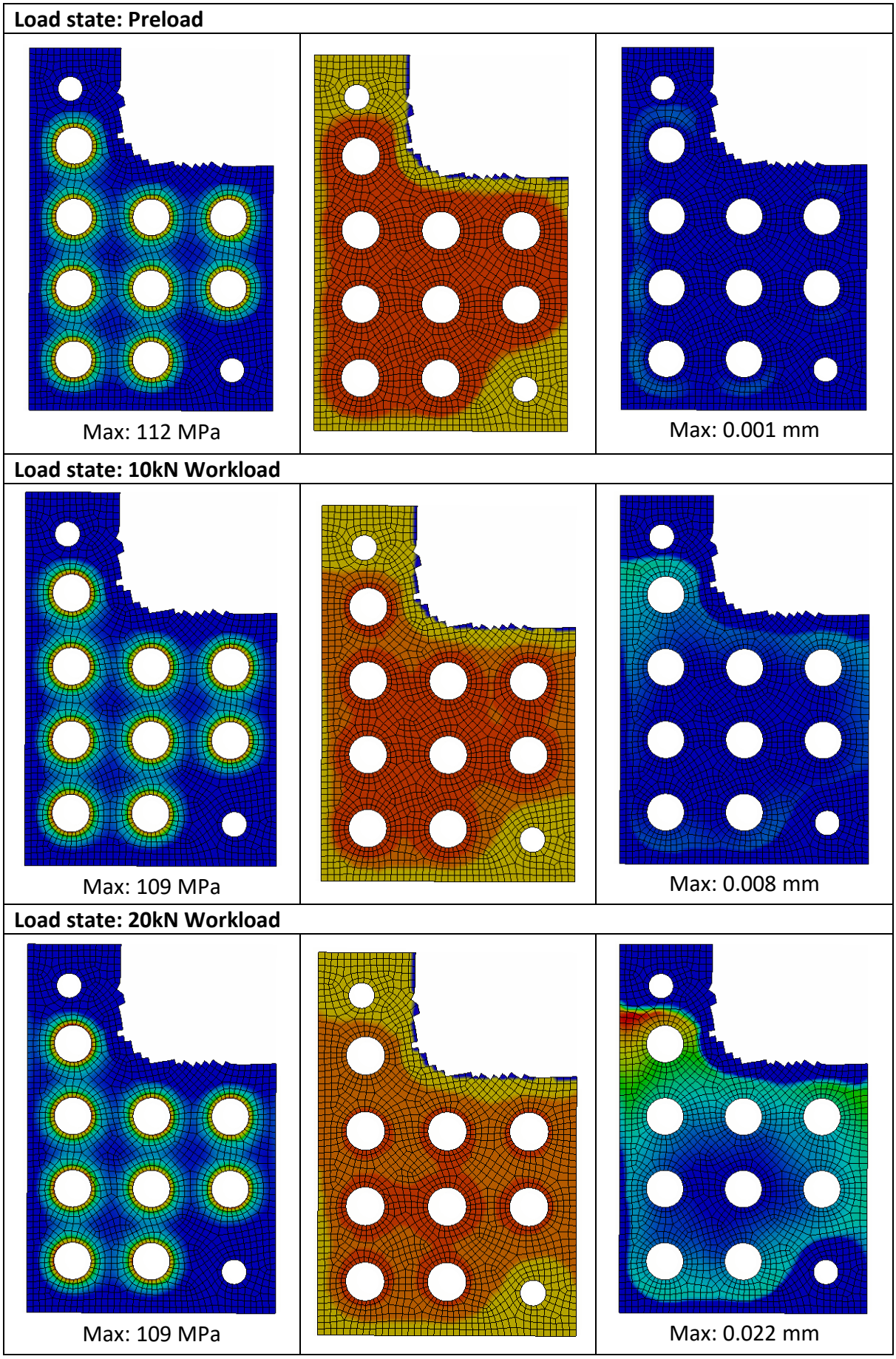

Figure 10: Surface pressure, status, and sliding distance

In Figure 10, investigations of the clamping interface using ANSYS functionality has been performed. The following observations can be made:

- The pressure resulting from the deformation cones slightly interact, and appear to be well positioned.

- There is no significant change in the pressure distribution with applied workload.

- No slipping occur when only preload are applied, and only negligible sliding distance are present.

- For 10kN workload, the status plot indicate that in general, no slipping occur in the deformation cone areas. Some slipping is present in the outermost areas, and the upper left bolt (B9) is most highly affected by slipping. The slipping distance plot confirm this, but the slipping distance is still negligible.

- For 20kN workload, slipping is occurring in the joint. The middle bolt is not affected, but slipping is occurring on the outer bolts. The maximum slipping distance are in the range of 0.02 mm. This is not much, but with the high level of slipping, such slipping can accumulate with multiple load cycles.

Based on the ANSYS analysis, only acceptable levels of slipping occur for the 10kN workload scenario, and it is concluded that the joint should withstand such a workload.

CADFEM Assessment

Figure 11 show the slipping safety factors for the different bolts, and the results are summarised in Table 10. It is clear that bolt B9 is the most exposed bolt, and the factor is lower than the 1.2 recommended by VDI 2230. The other bolts have factors from 1.6 and up, and are fine. Note that torsion about the bolt axis are excluded.

The exact reason for the difference to the analytic safety factor is unknown, but contributing factors might be:

- Better representation of elastic effects and load distribution between the bolts in FEA.
- The analytic approach rely on some assumptions and simplifications.
- Mesh-size effects in the FE-analysis and numerical inaccuracies.

Table 10: Safety factors with 10kN Workload

Safety factor S_G	Bolts
1.08	B9
1.6 – 1.9	B6, B8
2.2 – 2.8	B1, B2, B5, B7
4.3	B3
18.8	B4

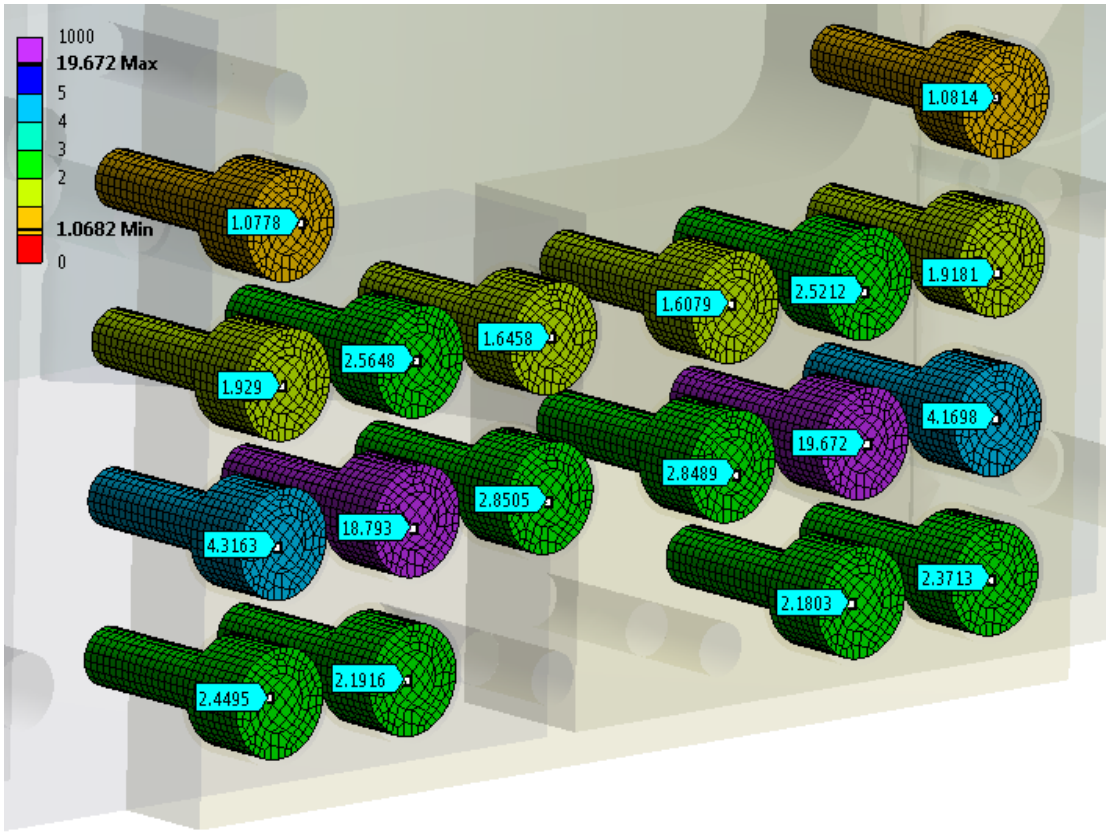

Figure 11: CADFEM-plot of slipping safety factors with 10 kN workload and minimum preload (7.3kN)

Pressure Under the Bolt Head

Based on the limiting surface pressure, and the highest bolt load, a verification of the pressure under the bolt head has been carried out (Table 11).

Table 11: Surface Pressure under the Bolt Head

Limiting surface pressure	p_G	630	MPa	Calculated
Safety factor	S_p	3	-	Calculated

S11: Tightening Torque

The tightening torque is calculated, and listed in Table 12.The minimum breaking torque for this bolt is 32 Nm (ISO 3506).

Table 12: Data and Results Max Assembly Pretension

Average Head Friction Area	D_{Km}	10.67	mm	Calculated
Tightening Torque	M_A	24.5	Nm	Calculated

S12: Approve or Iterate

Several approaches has been made to assess if slipping will occur in the joint. In the analysis, a tightening uncertainty of 1.6 are applied, resulting in max/min preload of 11.7kN / 7.3kN respectively. The actual workload from 2mm cavity deformation is 8kN. In this analysis, a small workload safety factor is applied in assuming 2.5mm cavity deformation resulting in 10kN workload. In S1, an estimate is made that the minimum preload should stay above at-least 5.4kN to achieve a satisfying safety factor. All the analysis are carried out for the minimum preload case and with a workload of 10kN. The results are summarized in Table 13.

Table 13: Summary of Slipping Assessments

Analytic Slipping Safety Factor	S_G	1.5	-	Calculated
Analytic Shearing Safety Factor	S_A	19.2	-	Calculated
ANSYS assessment	-	Ok		ANSYS inspection of Status and slipping distance
CADFEM assessment	S_G	1.08	-	Semi-analytic (FEA and calc.)

All assessment indicate that the B9 bolt and surrounding area is critical. Due to the fact that there will be a guide pin located close to bolt B9, a safety factor against slipping slightly lower than recommended 1.2, but still above 1 is considered to be sufficient. If slipping occur, the safety against bolt shear is 19.2.

Further preload-losses are mentioned and assessed. Since the bolt is quite short and have a small elongation when assembled, embedding might pose a risk of reliving a large amount of the preload. There is however some uncertainty about embedding behaviour for Stainless Steel. A suggested action is to apply heavy-duty force washers for the bolts.

Preload-loss due to thermal contraction are assumed not to have any influence on the preload.

An argument can be made that the considered preload loss due to tightening uncertainty (-38% / -4.4kN) is quite high, and that the preload most likely will be higher than what is applied in this analysis. Thus, this margin could also include some risk for additional preload losses

With the mentioned aspects in mind, making a total assessment of the joint functionality, it is concluded that for the defined tightening conditions the joint will not slip, and does fulfil the requirements of the joint.

Approved

ADDITIONAL RESULTS

REQUIRED LENGTH OF THREAD ENGAGEMENT

It is found that the internal thread is the critical thread. With the present thread engagement (16mm), the thread stripping force is **100kN**, while the breaking load of the free loaded bolt thread is **25.6kN**. Thus, the bolt will beak before the tapped thread. The minimum thread length of engagement is **6.6mm.** The full calculations can be found in ***Appendix D-2***.

GEOMETRY

Solid Tuner	**Tuner with Bolted Joints (BJs)**
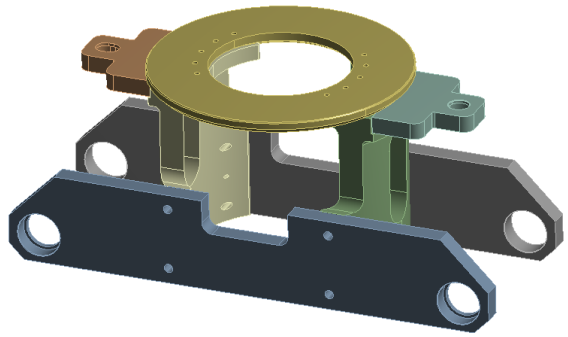	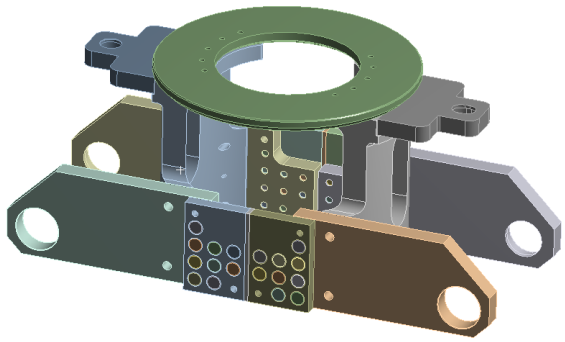

GLOBAL DEFORMATION – FOR 10KN

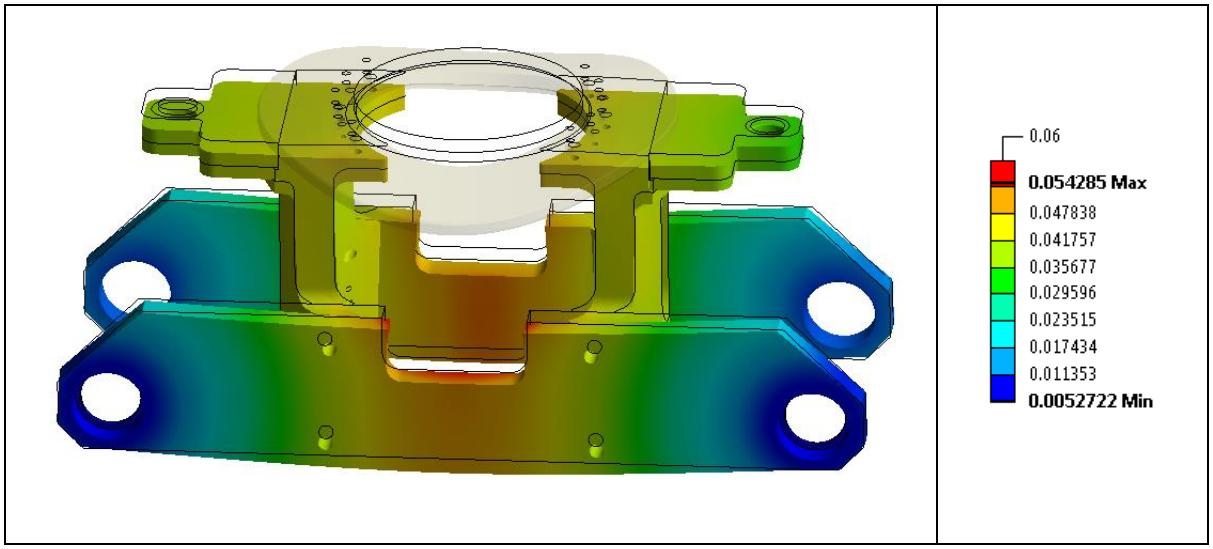

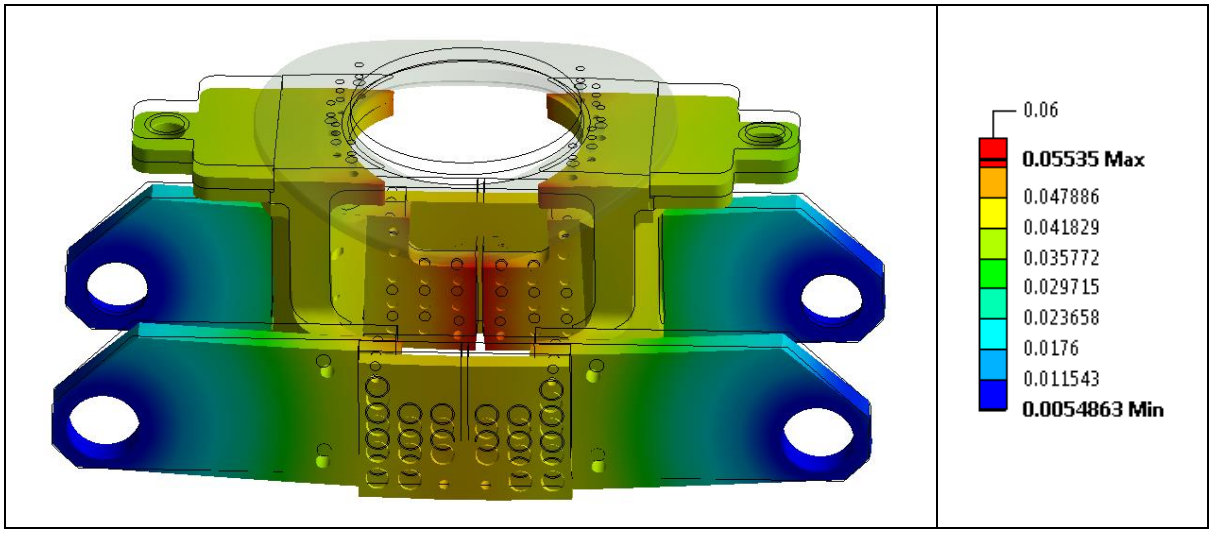

Comments: The deformations for this load level is very similar. The top circular plate is not included, since the actual connection to the cavity might introduce some additional stiffness to it. It is of highest relevance to assess how the rest of the body deforms.

GLOBAL STRESS

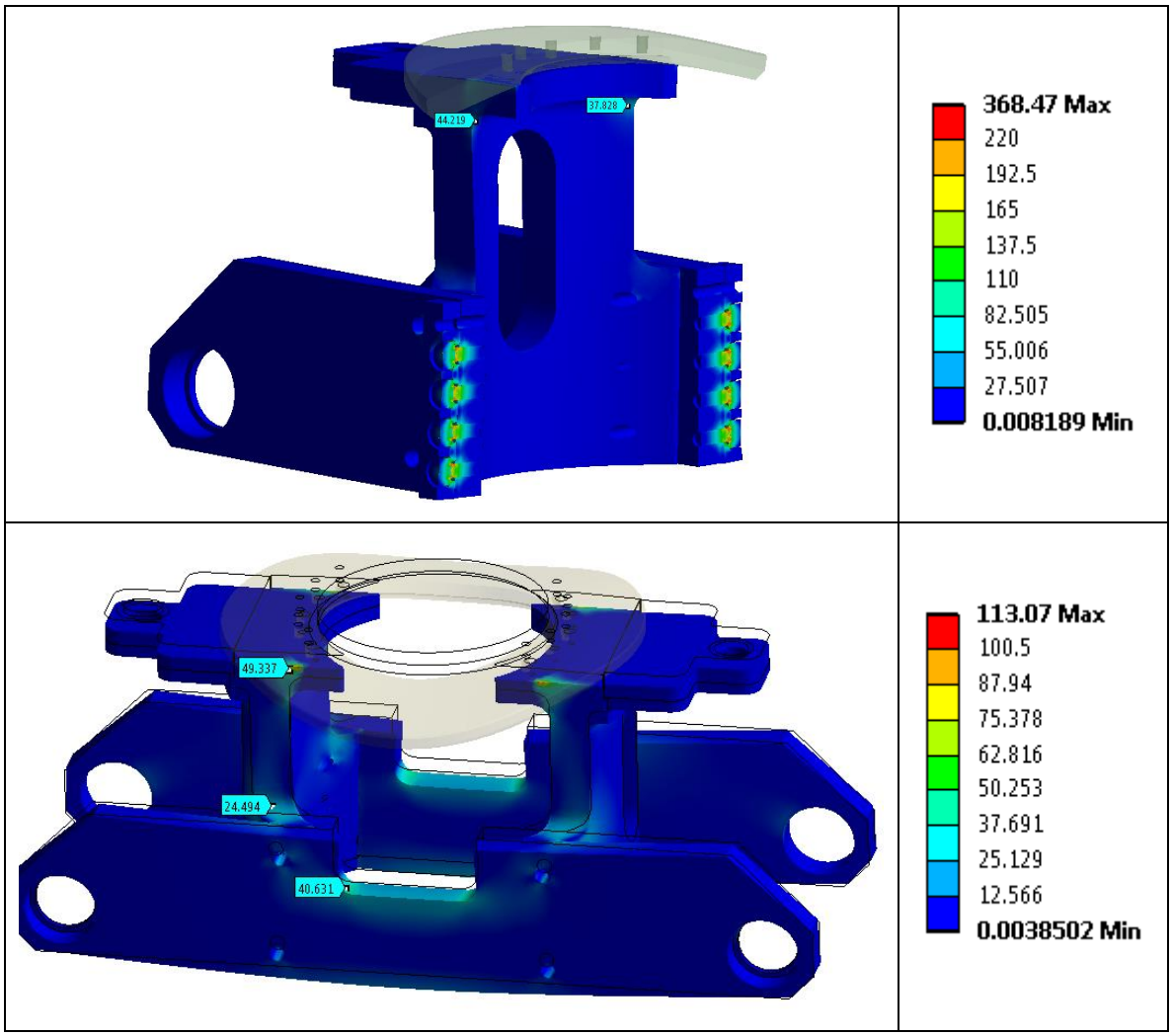

Comments: The stress level in the tuner body is generally low, with peaks of about 50 MPa. The proof stress of the material are 220MPa. Some higher stresses arise in the BJs, but verifications of the bolt stress level are performed analytically.

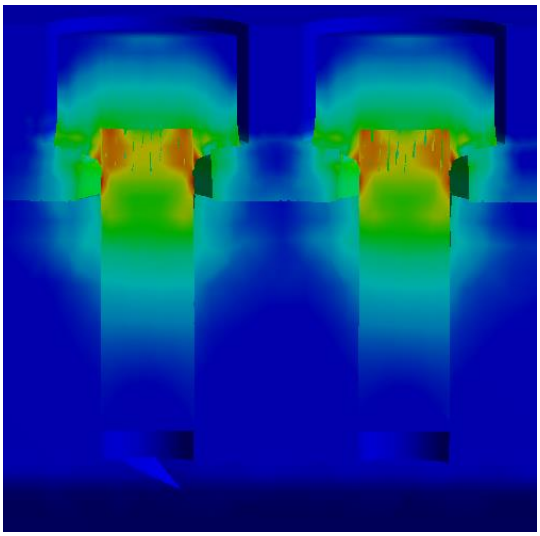

Figure 12: Stress distribution in the bolts

AXIAL DEFORMATION AND RELATIVE STIFFNESS

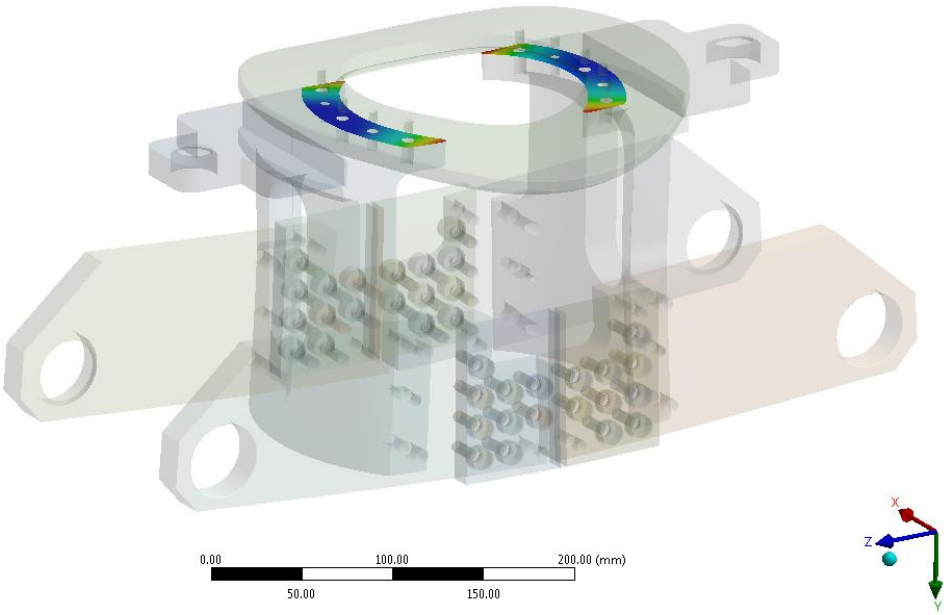

By obtaining the axial deformations of the highlighted area for both the solid and bolted Tuner, information about relative axial stiffness are extracted. The minimum deformation values are extracted, to have the most realistic and comparable results.

The stiffness are found to be 0.0042 mm/kN, up to a workload of 10kN.

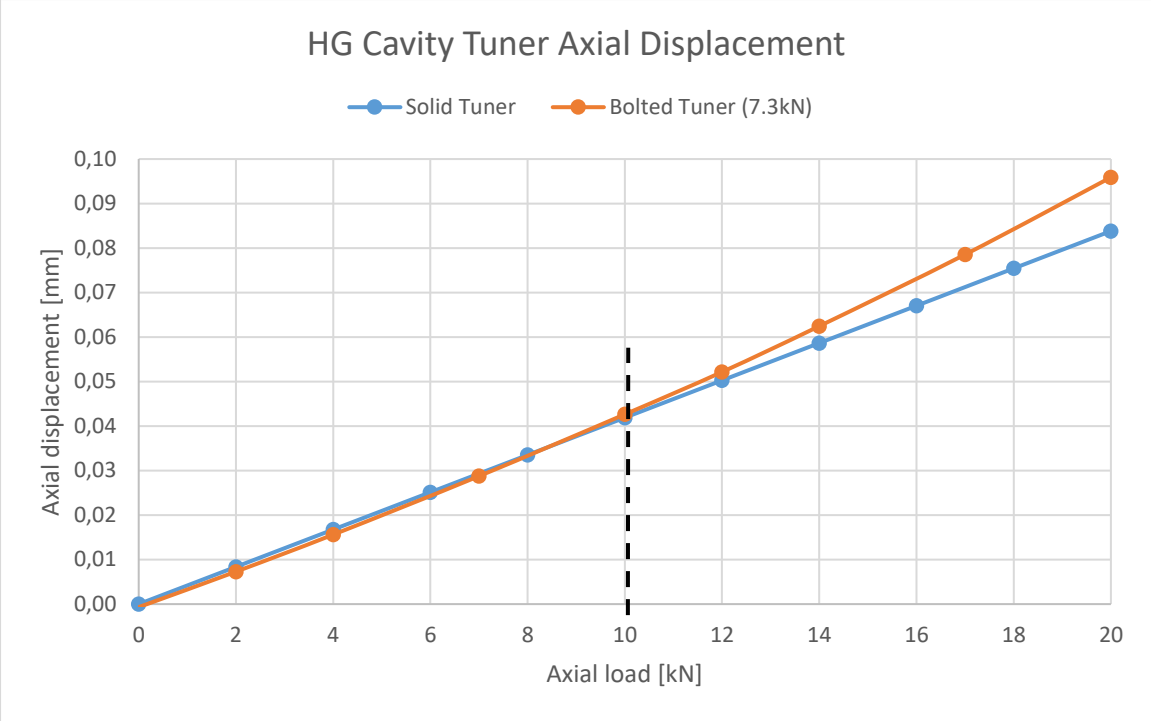

Comments: The deformation characteristics of the two tuners are very similar until 10kN workload. Above that, the solid tuner continues linearly. The bolted tuner then has larger deformation pr. Unit load, resulting in a non-linear curve. It is assumed that it is slipping in the joint that leads to this behaviour.

SPECIFIC PROBES

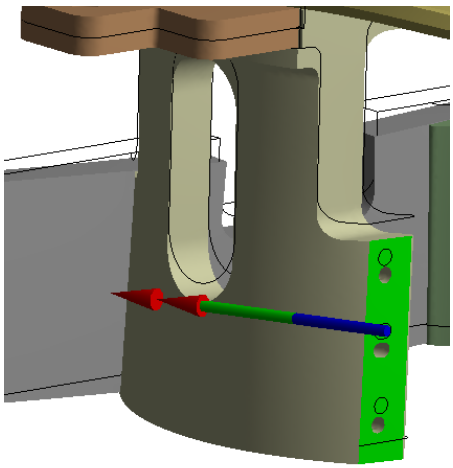

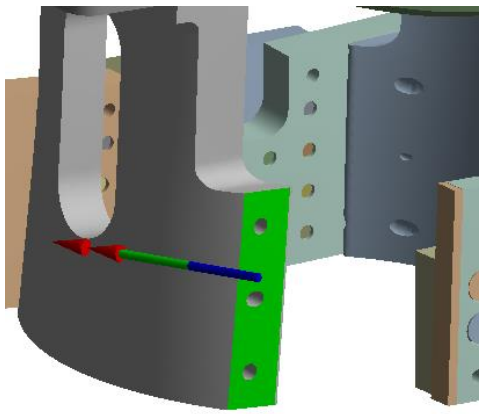

One other point on the Tuner that might be critical, is the connection highlighted above. For the solid and bolted tuner, the moment to be carried through the contact are **97 Nm** and **102 Nm** respectively.

If this connection only rely on a preloaded bolt-connection and no slipping should occur, an additional verification should be carried out. This applies to both the solid and the bolted Tuner. In the model, it appears as the plan has been to use two M8 bolts.

From a basic analytic calculation, it has been found that the bolt will have to minimum be preloaded with 10.2 kN, which could be managed by a M8 bolt at 90% utilisation. However, due to tightening uncertainty a M10 bolt should be used, providing 18.6 kN preload.

Using stronger bolts for this BJ could also be an alternative that has not been assessed.

Tightening Torques M4-M12 Bolts

Basic parameters

Friction in threads:	**0.2**
Friction in head bearing:	**0.2**
0.2% proof stress:	**450** MPa

Tightening Torques & Corresponding Assembly Preloads - Bolts without venting hole

		Utilization of Bolt Capacity									
	Stress section	100%		90%		75%		50%		30%	
Bolt	mm^2	Nm	kN	Nm	kN	Nm	kN	Nm	kN	Nm	kN
M4	8.8	3.2	3.1	2.9	2.8	2.4	2.3	1.6	1.5	1.0	0.9
M5	14.2	6.3	5.0	5.7	4.5	4.7	3.8	3.2	2.5	1.9	1.5
M6	20.1	11.0	7.1	9.9	6.4	8.2	5.3	5.5	3.5	3.3	2.1
M8	36.6	26.7	13.0	24.0	11.7	20.0	9.7	13.3	6.5	8.0	3.9
M10	58.0	52.8	20.6	47.5	18.6	39.6	15.5	26.4	10.3	15.8	6.2
M12	84.3	91.3	30.1	82.2	27.1	68.5	22.5	45.7	15.0	27.4	9.0

MODAL ANALYSIS

The modal analysis provide information about relative stiffness, and for which deformations the model is weakest. Realistic representation and response from BCs are important, and contact with other components can affect the probability of these deformations to occur.

Mode	**Solid tuner**	**Bolted tuner**
1	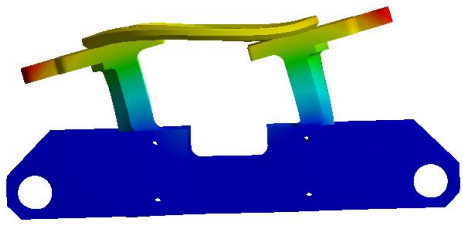	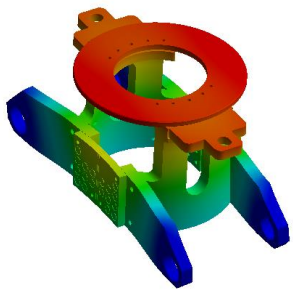
	462 Hz	**398 Hz**
2	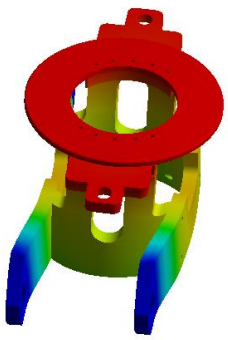	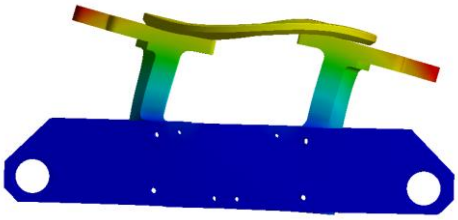
	466 Hz	**512 Hz**

3	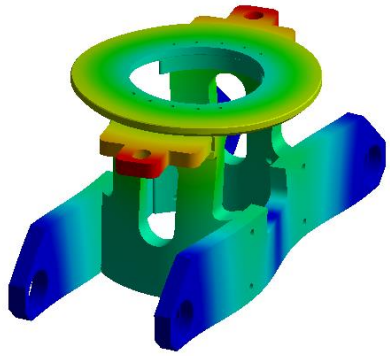	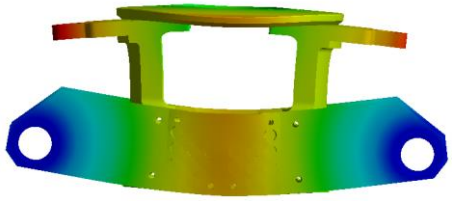
	779 Hz	**629 HZ**
4	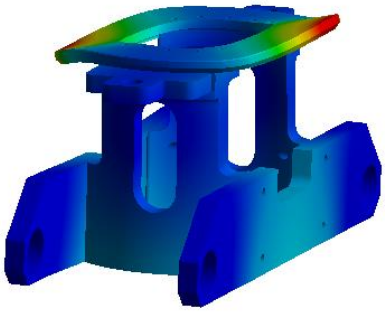	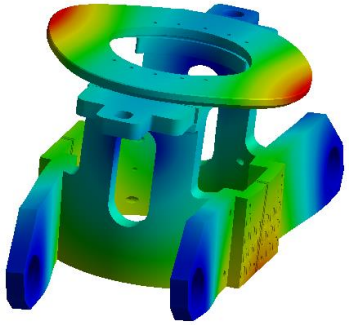
	884 Hz	**719 Hz**
5	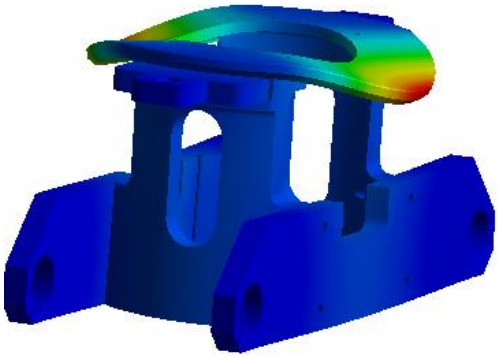	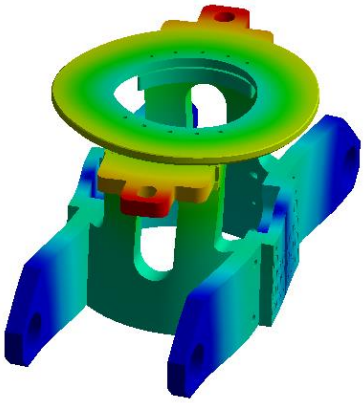
	912 Hz	**813 Hz**
6	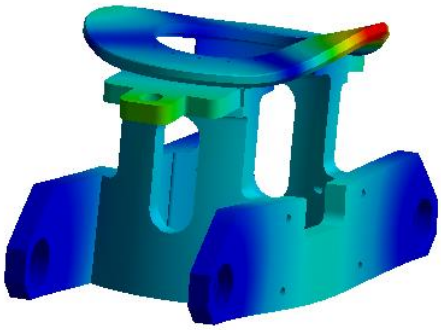	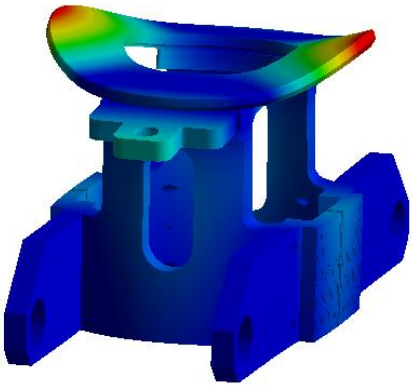
	1170 Hz	**1149 Hz**

SUMMARY

An FE-analysis and associated calculations has been carried out for the HG Cavity Tuner to assess if slipping occur, define tightening specifications, and to compare the relative stiffness to a solid tuner without bolted joints. The assessment is performed according to a simplified procedure based on VDI 2230.

FINDINGS

- An initial estimate according to VDI 2230 suggest that an M10 bolt should have been used.

- The max / min preload is found to be 11.7kN / 7.3kN with 90% utilisation of the bolt proof strength.

- Bolt B9 is the most highly loaded. The minimum safety factors are: 1.5 from analytic calculation, and 1.08 from the CADFEM assessment. This is when using a safety factor of 1.25 on the applied workload. Thus, no slipping will occur.

- The tightening torque is 24.5 Nm.

- The stiffness of the bolted and the solid tuner is the same, as long as no slipping occur.

IMPROVEMENTS:

- To achieve a higher preload, improving the friction grip capacity of the joint, the bolts could be changed to M10, or a higher strength grade could be chosen.

- The joint is not very resilient, since the clamping length is only 4mm. This results in large preload loss from possible embedding. To improve this situation, adding a counter-bore has been suggested, increasing the clamping length. The minimum required thread length of engagement has been found to be 6.6mm.

- Another BJ, consisting of two M8 bolts has been identified. A quick assessment suggest that the nominal diameter should be M10 for these bolts, or M8 bolts with a higher quality than Class 70.

REFERENCES

[1] M. Esposito, "Mechanical & Thermal calculations for the SPL cavity and tank," EDMS 1219955, 2012.

Calculations for FEA-assisted Analysis of HG Cavity Tuner

Analysis performed by:	Jørgen Apeland	**Date of Analysis:**	September 2017
Analysis revision:	v4	**According to procedure:**	BASIC FEA Workflow
Calculation case:	Bolted Tuner	**EDMS Reference:**	EDMS 1716574

S1 - Workload

Number of bolts: $n_S := 9$ $\quad n_{S.tot} := 4\ n_S = 36$

Moment on single BJ: $M_Z := 123\ N\ m$ — Obtained from a Class I simulation, extracting the moment in the clamping interface with centre defined as below.

Friction in the interface: $\mu_{Tmin} := 0.2$ — http://www.roymech.co.uk/Useful_Tables/Tribology/co_of_frict.htm

Identification of Bolt Pattern Center and Relative Bolt Position

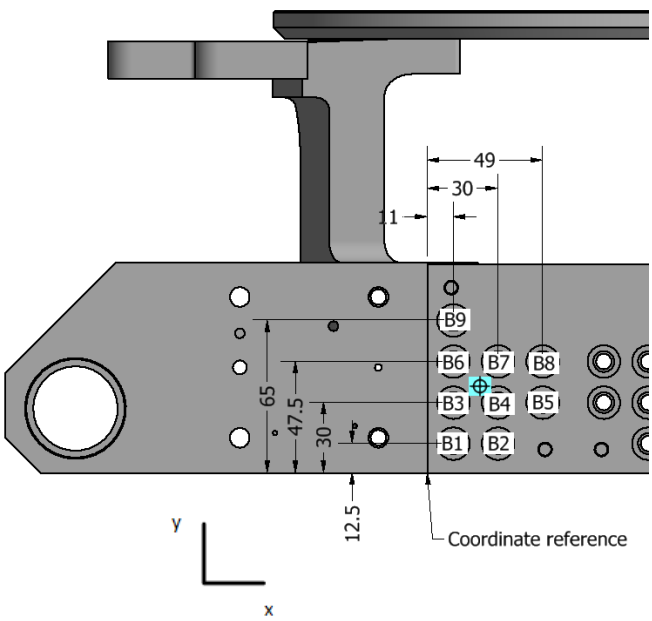

B	x (mm)	y (mm)
1	11	12.5
2	30	12.5
3	11	30
4	30	30
5	49	30
6	11	47.5
7	30	47.5
8	49	47.5
9	11	65

Location of center point:

$X := \text{mean}(x) = 25.78\ mm$

$Y := \text{mean}(y) = 35.83\ mm$

Relative location of center point:

$X_C := x - X \qquad Y_C := y - Y$

Radius to each bolt:

$r_C := \sqrt{X_C^{\ 2} + Y_C^{\ 2}}$

$$X_C = \begin{bmatrix} -14.78 \\ 4.22 \\ -14.78 \\ 4.22 \\ 23.22 \\ -14.78 \\ 4.22 \\ 23.22 \\ -14.78 \end{bmatrix} mm \qquad Y_C = \begin{bmatrix} -23.33 \\ -23.33 \\ -5.83 \\ -5.83 \\ -5.83 \\ 11.67 \\ 11.67 \\ 11.67 \\ 29.17 \end{bmatrix} mm \qquad r_C = \begin{bmatrix} 27.62 \\ 23.71 \\ 15.89 \\ 7.20 \\ 23.94 \\ 18.83 \\ 12.41 \\ 25.99 \\ 32.70 \end{bmatrix} mm$$

Critical bolt radius: $r_{max} := \max(r_C) = 32.7\ mm$ — The critical bolt furthest away from the centre is "B9"

Transverse force on bolt: $F_{qM.max} := \dfrac{M_Z \cdot r_{max}}{\sum r_C^{\ 2}} = 902.6\ N$ — [Pt.2 - Eq.12] $\qquad F_{Qmax} := F_{qM.max}$

Wanted safety factor: $S_{G.req} := 1.2$

Minimum req. clamp load: $F_{KQ} := \dfrac{S_{G.req} \cdot F_{Qmax}}{\mu_{Tmin}} = 5.42\ kN$

ans. $F_{KQ} = 5.42\ kN$
==========

S2 - Nominal Bolt Diameter

Bolt data parameters - For ISO 4762 M8x20-A4 (class 70)

Note: Use minimum coefficients of friction.

Nominal diameter:	$d := 8\ mm$	Friction coefficient in the threads:	$\mu_{Gmin} := 0.2$
Pitch:	$P := 1.25\ mm$	Friction in head bearing area:	$\mu_{Kmin} := 0.2$
Effective bolt head diameter:	$d_W := 12.33\ mm$	Tensile strength of bolt:	$R_m := 700\ MPa$
Diameter of clearence hole:	$d_h := 9\ mm$	Yield strength of the bolt:	$R_{p0.2min} := 450\ MPa$

Calculated parameters

Pitch diameter: $d_2 := d - \frac{3\sqrt{3}}{8} P = 7.188\ mm$

$H = \frac{\sqrt{3}}{2} \cdot P$

Minor diameter of the bolt: $d_3 := d - P\left(\frac{17\sqrt{3}}{24}\right) = 6.466\ mm$

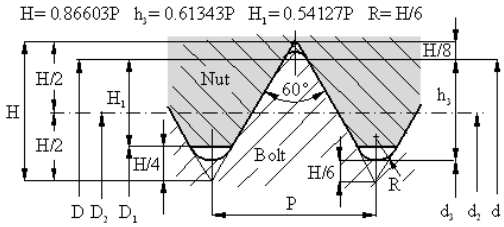

S3 - Tightening Factor

Torque wrench: $\alpha_A := 1.6$

S4 - Max Assembly Pretension

Calculation quanteties

Stress diameter: $d_S := 0.5\ (d_2 + d_3) = 6.83\ mm$

Stress area: $A_S := \frac{\pi}{4}\ (d_S)^2 = 36.6\ mm^2$

Parameters

Bolt capacity utililization factor: $\nu := 0.9$

Calculations

Allowed assembly stress: $\sigma_{Mzul} := \nu\ R_{p0.2min} = 405\ MPa$

Maximum permitted assembly preload:

$$F_{Mzul} := A_S \frac{\nu\ R_{p0.2min}}{\sqrt{1 + 3\left(\frac{3}{2}\frac{d_2}{d_S}\left(\frac{P}{\pi\ d_2} + 1.155\ \mu_{Gmin}\right)\right)^2}}$$

ans. $F_{Mzul} = 11.67\ kN$
==========

S5 - Min Assembly Pretension

Minimum assembly preload: $F_{Mzul.min} := \frac{F_{Mzul}}{\alpha_A}$

ans. $F_{Mzul.min} = 7.3\ kN$
==========
This value is higher than the minimum required clamping force identified in S1.

S6 - Simplify and Prepare CAD-geometry

S7 - Prepare and Run FE-analysis

Parameters

Coefficient of Friction in the clamping interface: $\mu_{Tmin} = 0.2$

Coefficient of friction in the head bearing area: $\mu_{Kmin} = 0.2$

S8 - Results and Analysis

Max assembly preload

Max Acheived preload: $F_{Vmax} := 11.70\ kN$

Max bolt load: $F_{Smax} := 11.75\ kN$

Max bolt bending moment: $M_{Sbo} := 1.8\ N\ m$

Min assembly preload

Min Acheived preload: $F_{Vmin} := 7.29\ kN$

Average clamping force in the interface pr. bolt: $F_{KR.min} := \frac{65.76}{n_S}\ kN = 7.31\ kN$

Max Work moment on BJ: $M_{Z.max} := 131\ N\ m$

S9 - Work Stress

Note! bending stress is included

Parameters

Residual torque factor: $k_t := 0.5$

Calculation quanteties

Bending modulus: $W_S := \frac{\pi}{32} d_S^3 = 31.24\ mm^3$

Thread moment: $M_G := F_{Mzul} \cdot \frac{d_2}{2} \cdot \left(\frac{P}{\pi\ d_2} + 1.155\ \mu_{Gmin} \right) = 12\ N\ m$

Polar moment of inertia: $W_p := \frac{\pi}{16} \cdot d_S^3 = 62.48\ mm^3$

Calculations

Axial stress: $\sigma_{zb.max} := \frac{F_{Smax}}{A_S} + \frac{M_{Sbo}}{W_S} = 378.58\ MPa$

Torsional stress: $\tau_{max} := \frac{M_G}{W_p} = 192.25\ MPa$

Working stress: $\sigma_{red.B} := \sqrt{\sigma_{zb.max}^2 + 3\ (k_t \cdot \tau_{max})^2} = 413.6\ MPa$

Bending stress

$\sigma_{Sbo} := \frac{M_{Sbo}}{W_S} = 57.61\ MPa$

Bending stress contribution to work stress

$\Delta\sigma_{Sbo.p} := \frac{\sigma_{Sbo}}{\sigma_{red.B}} = 13.93\%$

Assessment

Criteria: $\sigma_{red.B} = 413.57\ MPa$ < $R_{p0.2min} = 450\ MPa$

Safety factor: $S_F := \frac{R_{p0.2min}}{\sigma_{red.B}} = 1.09$

==========

S10 - Clamping Requirements

Analytic slipping safetyfactor

Max actual transverse shear-load on bolt: $F_{qM.max} := \frac{M_{Z.max} \cdot r_{max}}{\sum r_C^2} = 961.3\ N$

Required clamp load to transmit transverse loads: $F_{KQerf} := \frac{F_{qM.max}}{\mu_{Tmin}} = 4.81\ kN$

Slipping safety-factor for minimum preload: $S_{G.gl} := \frac{F_{Vmin} \cdot \mu_{Tmin}}{F_{qM.max}} = 1.52$ $S_G := \frac{F_{KR.min}}{F_{KQerf}} = 1.52$ $S_G \geq 1.2$

Slipping safety-factor for maximum preload: $S_{G.gl} := \frac{F_{Vmax} \cdot \mu_{Tmin}}{F_{qM.max}} = 2.43$

Analytic shear safetyfactor

Shear capacity of bolt: $\tau_B := 0.72 \cdot R_m = 504\ MPa$ [VDI 2230 Pt. 1 - Table 7]

Safety factor for shearing of bolt: $S_A := \frac{\tau_B \cdot A_S}{F_{qM.max}} = 19.2$ $S_A \geq 1.1$

S11 - Tightening Torque

Average head friction diameter: $D_{Km} := \frac{d_W + d_h}{2} = 10.67\ mm$

Tightening Torque: $M_A := F_{Mzul} \cdot \left(0.16\ P + 0.58\ d_2\ \mu_{Gmin} + \frac{D_{Km}}{2}\ \mu_{Kmin} \right) = 24.5\ N\ m$

Minimum breaking torque for M8-70 is 32 Nm (ISO 3506)

==========

S12 - Approve or Iterate

========
APPROVED
========

Additional Calculations

Additional bolt load: $F_{SA} := F_{Smax} - F_{Vmax} = 0.05\ kN$

Embedding

Embedding for surface roughness < 10μm: $f_Z := (3+3+2)\ \mu m = 8\ \mu m$ $\quad F_Z = \dfrac{f_Z}{\delta_S + \delta_P}$

For comparison, during preloading, the bolt were adjusted: $\Delta l_M := 3.1 \cdot 10^{-2}\ mm$ $\quad \Delta F_M := 11.7\ kN$ $\quad \delta_J := \dfrac{\Delta l_M}{\Delta F_M} = (2.65 \cdot 10^{-3})\ \dfrac{mm}{kN}$

Analytic calculation of resiliensies:

Parameters: $E_S := 200\ GPa$ $\quad E_P := E_S$ $\quad l_{Gew} := 4\ mm$ $\quad l_K := l_{Gew}$

Calculation quanteties: $A_N := \dfrac{\pi}{4} d^2$ $\quad A_{d3} := \dfrac{\pi}{4} d_3^{\ 2}$ $\quad I_N := \dfrac{\pi}{64} d^4$ $\quad I_{d3} := \dfrac{\pi}{64} d_3^{\ 4}$

Axial resilience of the bolt are calculated:

$l_G := 0.5 \cdot d$ $\quad l_M := 0.33\ d$ $\quad l_{SK} := d\ 0.4 = 3.2\ mm$

$\delta_G := \dfrac{l_G}{E_S \cdot A_{d3}} = (6.1 \cdot 10^{-7})\ \dfrac{mm}{N}$ $\quad \delta_M := \dfrac{l_M}{E_P \cdot A_N} = (2.6 \cdot 10^{-7})\ \dfrac{mm}{N}$

$\delta_{GM} := \delta_G + \delta_M = (8.7 \cdot 10^{-7})\ \dfrac{mm}{N}$

Unengaged loaded part of the thread

$\delta_{Gew} := \dfrac{l_{Gew}}{E_S \cdot A_{d3}} = (6.09 \cdot 10^{-4})\ \dfrac{mm}{kN}$

$\delta_{SK} := \dfrac{l_{SK}}{E_S \cdot A_N} = (3.18 \cdot 10^{-7})\ \dfrac{mm}{N}$

$\delta_S := \delta_{SK} + \delta_{Gew} + \delta_{GM} = (1.8 \cdot 10^{-3})\ \dfrac{mm}{kN}$

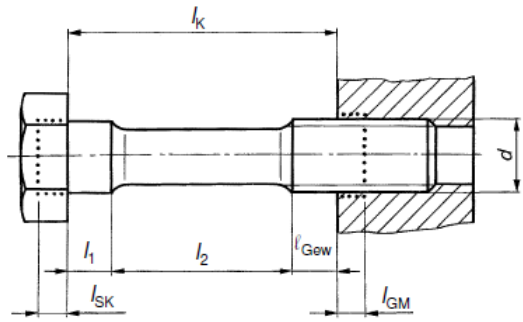

A worst case will be using the resilience of only the bolt: $F_{Z.1} := \dfrac{f_Z}{\delta_S} = 4.45\ kN$

Using the resilience of the joint derived from FEA: $F_{Z.2} := \dfrac{f_Z}{\delta_J} = 3.02\ kN$

Thus, the minimum residual clamp force would be: $F_{KR.min.Z} := F_{Vmin} - \begin{bmatrix} F_{Z.1} \\ F_{Z.2} \end{bmatrix} = \begin{bmatrix} 2.84 \\ 4.27 \end{bmatrix} kN$

Resulting in unsatisfactoring safety-factor against slipping: $S_{G.Z} := \dfrac{F_{KR.min.Z}}{F_{KQerf}} = \begin{bmatrix} 0.59 \\ 0.89 \end{bmatrix}$

Scenario with higher thread friction

Control of resulting preload if thread friction are higher: $\mu_{Gmin} = 0.2$ => $\mu_{Gmin.1} := 0.30$

$\mu_{Kmin} = 0.2$ => $\mu_{Kmin.1} := 0.30$

The resulting assembly preload: $F_{M.max} := \dfrac{M_A}{\left(0.16\ P + 0.58\ d_2\ \mu_{Gmin.1} + \dfrac{D_{Km}}{2}\ \mu_{Kmin.1}\right)} = 8.04\ kN$

$F_{M.min} := \dfrac{F_{M.max}}{\alpha_A} = 5.02\ kN$

ans. $S_{G.gl} := \dfrac{F_{M.min} \cdot \mu_{Tmin}}{F_{qM.max}} = 1.04$ Thus, according to this analytic calculation, the resulting preload if the friction is 0.3 would still be okay.

==========

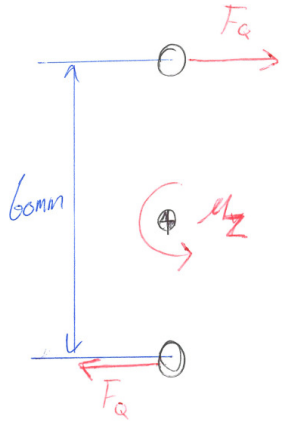

Calculation for additional BJ

Moment in the Joint: $M_{Z.2} := 100\ N\ m$

Critical bolt radius: $r_2 := 30\ mm$

Transverse force on bolt: $F_{qM2.max} := \dfrac{M_{Z.2} \cdot r_2}{\left(30^2 + 30^2\right)\ mm^2} = 1.67\ kN$ [Pt.2 - Eq.12]

$F_{Q2max} := F_{qM2.max}$

Alternative simple calculation: $F_{qM2.max} := \dfrac{M_{Z.2}}{2 \cdot r_2} = 1.67\ kN$

Required Slip Resistance: $F_{KQ2erf} := \dfrac{F_{Q2max}}{\mu_{Tmin}} = 8.33\ kN$

Wanted safety factor: $S_{G.req} := 1.2$

Minimum req. clamp load: $F_{KQ2} := S_{G.req} \cdot F_{KQ2erf} = 10\ kN$

ans. $F_{KQ2} = 10\ kN$

==========

Thread Strength and Required Length of Engagement

Note that there is two factors that will lead to better load distribution on the threads than in a normal case:
1) Titanium is more resilient than Steel
2) The outgassing hole in the bolt

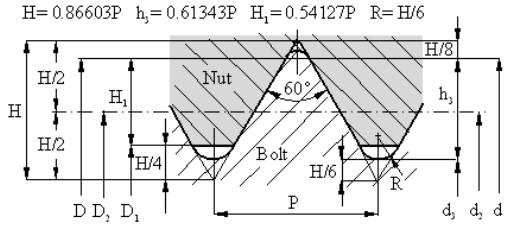

Parameters	***Bolt***	***Clamped parts***
Tensile strength:	$R_{mS} := 700\ MPa$	$R_{mM} := 530\ MPa$
Shear strength:	$\tau_{BS.min} := 0.72 \cdot R_{mS} = 504\ MPa$	$\tau_{BM.min} := 410\ MPa$
Dimensions with tolerance: [ISO 965-2 - 6H/6g]	$d_{min} := 7.760\ mm$	
	$D_{2.max} := 7.348\ mm$	$d_1 := d - \dfrac{5\sqrt{3}}{8} P = 6.647\ mm$
		$D_1 := d_1$ $D_2 := d_2$
Effective thread length:	$l_{eff} := 20\ mm - l_K = 16\ mm$	

Determination of Critical Thread

Thread strength ratio: $R_S = \dfrac{A_{SGM} \cdot \tau_{BM}}{A_{SGS} \cdot \tau_{BS}}$

Criteria:

$R_S > 1$ bolt thread is critical

$R_S < 1$ internal thread is critical

A_{SG} is the thread shear area of for the bolt / tapped threads

τ_B is the shear strength

$$R_S := \frac{d \cdot \left(\frac{P}{2} + (d - D_2) \cdot \tan(30\ deg)\right)}{d \cdot \left(\frac{P}{2} + (d_2 - D_1) \cdot \tan(30\ deg)\right)} \cdot \frac{\tau_{BM.min}}{\tau_{BS.min}} = 0.95$$

```
Thread_Critical(R_S) := | if R_S > 1
                        |   | return "bolt thread"
                        | if R_S < 1
                        |   | return "Internal thread"
```

Ans.

$Thread_Critical(R_S) =$ "Internal thread"

==========

Stripping Force of Internal Threads

The calculation of strength in the threads is solely based on the shear stress on the nut materials caused by the tensile force in the bolt thread and that the influence of superimposed bending stresses in the thread turns can be ignored.

The correction factors C1 and C3 take into account among other things the reduction in the shear area resulting from flexure.

Parameter C1:

"s" is the equivalent diameter of the material surrounding the internal thread.

$s := 20\ mm$ $\qquad \frac{s}{d} = 2.5$

$$C_1 := \begin{cases} \text{if } 1.4 \le \frac{s}{d} < 1.9 \\ \quad C_1 \leftarrow 3.8 \cdot \frac{s}{d} - \left(\frac{s}{d}\right)^2 - 2.61 \\ \text{if } \frac{s}{d} > 1.9 \\ \quad C_1 \leftarrow 1 \\ \text{if } \frac{s}{d} < 1.4 \\ \quad \text{return "not valid"} \end{cases}$$

$C_1 = 1$

=======

Parameter C3:

$R_S = 0.949$

$$C_3 := \begin{cases} \text{if } R_S \le 0.43 \\ \quad C_3 \leftarrow 1 \\ \text{if } 0.43 < R_S < 1 \\ \quad C_3 \leftarrow 0.728 + 1.769\ R_S - 2.896\ R_S^2 + 1.296\ R_S^3 \\ \text{if } R_S \ge 1 \\ \quad C_3 \leftarrow 0.897 \end{cases}$$

$C_3 = 0.906$

=======

Shear area for nut/internal thread: $A_{SGM} := \overrightarrow{\pi \cdot d_{min} \cdot \left(\frac{l_{eff}}{P}\right) \cdot \left(\frac{P}{2} + (d_{min} - D_{2.max}) \cdot \tan(30\ deg)\right)} = 269.3\ mm^2$

Stripping force of internal thread: $F_{mGM} := C_1\ C_3\ \tau_{BM.min} \cdot A_{SGM} = 100.05\ kN$

Reference stripping force, with no correction: $F_{mGM.ref} := \tau_{BM.min} \cdot A_{SGM} = 110.4\ kN$

Breaking stress of free loaded bolt thread: $F_{mS} := R_{mS} \cdot A_S = 25.6\ kN$

Criteria **(R11/1)**: $F_{mS} = 25.6\ kN$ < $F_{mGM} = 100\ kN$

$Status_R11.1 = \text{"Ok"}$

==========

$$Status_R11.1 := \begin{cases} \text{if } F_{mS} < F_{mGM} \\ \quad \text{return "Ok"} \\ \text{"Not Ok"} \end{cases}$$

Load case specific data:

Utilisation of thread capacity: $\nu_{mGM} := \frac{F_{Smax}}{F_{mGM}} = 11.7\%$

Thread stripping force safety factor: $S_{mGM} := \frac{F_{mGM}}{F_{Smax}} = 8.51$

Required effective length of tapped threads:

$$m_{ges.min} := \frac{R_{mS} \cdot A_S \cdot P}{C_1 \cdot C_3 \cdot \tau_{BM.min} \cdot \left(\frac{P}{2} + (d_{min} - D_{2.max}) \cdot \tan(30\ deg)\right) \cdot \pi \cdot d_{min}} + 2\ P = 6.6\ mm$$

Note: The "2P" is a margine for non-effective thread length, like chamfer.

Criteria: **ans.** $m_{ges.min} = 6.6\ mm$ < $l_{eff} = 16\ mm$

$Status_thread_length = \text{"Ok"}$

==========

$$Status_thread_length := \begin{cases} \text{if } m_{ges.min} < l_{eff} \\ \quad \text{return "Ok"} \\ \text{"Not Ok"} \end{cases}$$

Summary of Key Results

Calculation step	Results		
S1 - Workload	$F_{Qmax}=902.6\ N$ $F_{KQ}=5.4\ kN$		
S2 - Nominal Bolt Diameter	$d=8\ mm$	$P=1.25\ mm$	$R_{p0.2min}=450\ MPa$
S3 - Tightening Factor	$\alpha_A=1.6$		
S4 - Max Assembly Pretension	$\nu:=0.9$ $F_{Mzul}=11.7\ kN$	$\mu_{Gmin}=0.2$ $\sigma_{Mzul}=405\ MPa$	$\mu_{Kmin}=0.2$
S5 - Min Assembly Pretension	$F_{Mzul.min}=7.3\ kN$		
S6 - Simplify and Prepare CAD-geometry	$d_3=6.47\ mm$		
S7 - Prepare and Run FE-analysis	$\mu_{Tmin}=0.2$	$\mu_{Kmin}=0.2$	
S8 - Extracted Results	$F_{Vmax}=11.7\ kN$ $F_{Vmin}=7.29\ kN$	$F_{Smax}=11.75\ kN$ $F_{KR.min}=7.31\ kN$	$M_{Sbo}=1.8\ N\ m$ $M_{Z.max}=131\ N\ m$
S9 - Work Stress	$\sigma_{red.B}=413.6\ MPa$ <	$R_{p0.2min}=450\ MPa$	$S_F=1.09$
S10 - Clamping requirements	$S_G=1.5$	$S_A=19.2$	
S11 - Tightening Torque	$M_A=24.5\ N\ m$		
S12 - Approve or Iterate	======== **APPROVED** ========		

Additional Calculations

Additional bolt load:	$F_{SA}:=F_{Smax}-F_{Vmax}=0.05\ kN$	
Minimum clamp load with embedding:	$F_{KR.min.Z}=\begin{bmatrix}2.84\\4.27\end{bmatrix}\ kN$	$S_{G.Z}=\begin{bmatrix}0.59\\0.89\end{bmatrix}$
Result of +50% friction:	$S_{G.gl}=1.04$	
Minimum length of thread engagement:	$m_{ges.min}=6.6\ mm$	
Utilisation of thread capacity:	$\nu_{mGM}=11.74\%$	

APPENDIX E

VDI 2230 AND FEA SEMINAR PRESENTATION

ENGINEERING SEMINAR

Application of FE-analysis in Design and Verification of Bolted Joints According to VDI 2230

December 2017

Jørgen Apeland EN / MME / EDM

Norwegian University of Science and Technology

CERN | EN ENGINEERING DEPARTMENT

Jørgen Apeland

- Mechanical Engineering at NTNU

NTNU Norwegian University of Science and Technology

- Technical student at CERN
  - EN – MME – EDM
- Supervisors:
  - Luca Dassa, CERN
  - Torgeir Welo, NTNU

Introduction

Share what I have learned, and discuss relevant topics of bolted joints and FEA.

⇒Determine bolt from workload, define preload, and verify bolt stress / clamping

⇒Importance of joint design, and how different factors influence joint performance

Scope:

The participant should feel confident with use of VDI 2230 and FEA in design and verification of BJs. Thus:

- Know central terms and principles in VDI 2230
- Know how FEA and VDI 2230 can be combined
- Get introduced to further VDI 2230 calculations and verifications
- Know how to improve the joint design and performance
- Know where to look for more information

3

Motivation

- Safe and reliable BJ design!
  - Initial state: Proposed design
  - Task: Verify acc. to joint requirements
    - Clamping, bolt stress, preload, tightening torque
    - Suggest improvements of joint design

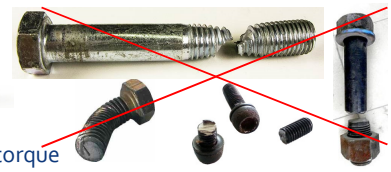

- Critical and not accessible BJs
  => justify time on analysis

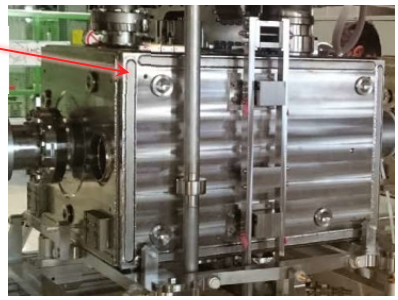

- Benefits of VDI 2230 and FEA:

Time

Quality

4

Agenda

1. **Basic Concepts of Bolted Joints and VDI 2230**
2. Combining FEA and VDI 2230
3. Further Calculations and Verifications
4. Improvements of Bolted Joint Design
5. Support Material and References
6. Summary

VDI 2230

- Structured approach to design and verification of BJs
- 13 R-steps of the analytic procedure
- Mathcad available for analytic calculations
  - Challenging to combine with FEA
  - Not all calculations needed
- References to VDI 2230 in presentation:

  [Pt. X-Y] - X= 1 or 2, Y= Table / Figure / Page
- Nomenclature [Pt.1 - Ch.2]

Part 1

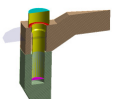

Part 2

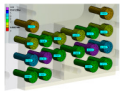

Inputs:		
R0	nominal diameter, limiting measurement	d, G
R1	tightening factor	α_A
R2	minimum clamp load	F_{Kerf}
Distortion triangle:		
R3	dividing the working load/ load factor	F_{SA}, F_{PA}, Φ
R4	preload changes	F_Z, $\Delta F'_{Vth}$
R5	minimum assembly preload	$F_{M\,min}$
R6	maximum assembly preload	$F_{M\,max}$
Stress cases and strength verifications:		
R7	assembly stress	$\sigma_{red,M}$, F_{Mzul}
R8	working stress	$\sigma_{red,B}$, S_F
R9	alternating stress	σ_a, σ_{ab}, S_D
R10	surface pressure	p_{max}, S_p
R11	minimum length of engagement	$m_{eff\,min}$
R12	slipping, shearing	S_G, $\tau_{Q\,max}$
R13	tightening torque	M_A

Material Data

- Proof stress - $R_{p0.2\min}$

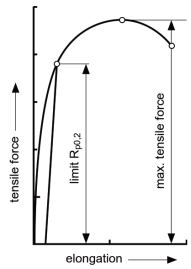

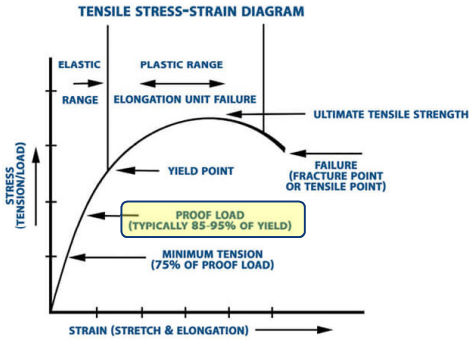

- Table in VDI 2230: [Pt.1-Table A9]
  - Materials: Structural steel, Stainless steel, Aluminum, Titanium
  - Properties: E-modulus, 0.2% proof stress, shearing strength, limiting surf. pressure
- VDI 2230: Mostly valid for Steel – but contain references for other materials

Types of Bolts

Hexagon head

Hexagon socket head

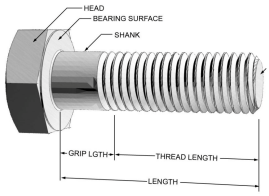

Full thread bolt

Shank bolt

Shoulder bolt

Necked-down bolts

Some factors that influence choice:
- ❑ Shear load
- ❑ Bending moment
- ❑ Static load, non critical joint
- ❑ Critical joint, as tension element to provide preload

Types of Joints

- **Non critical Joints**
  - **Function:** Fixing components, covers, thermalisation points, sensors, …
  - **Characteristics:** No workload, static conditions
  - **Criteria:** Should not loosen, not overtighten the bolt <= **Max** tightening torque?
  - **Preload range: 30-75%** of proof stress
- Template for Tightening Torque (Check calculation support)

Input: Friction factors and Proof Stress

Tightening Torques M3-M12 Bolts

Basic parameters

Friction in threads: **0.3**

Friction in head bearing: **0.15**

0.2% proof stress: **450** MPa

Tightening Torques & Corresponding Assembly Preloads - Standard Bolts

		Utilization of Bolt Capacity									
	Stress section	100%		90%		75%		50%		30%	
Bolt	mm^2	Nm	kN	Nm	kN	Nm	kN	Nm	kN	Nm	kN
M3	5.0	1.3	1.5	1.2	1.4	1.0	1.1	0.7	0.8	0.4	0.5
M4	8.8	2.9	2.6	2.6	2.4	2.2	2.0	1.5	1.3	0.9	0.8
M5	14.2	5.9	4.3	5.3	3.9	4.4	3.2	2.9	2.1	1.8	1.3
M6	20.1	10.1	6.0	9.1	5.4	7.6	4.5	5.0	3.0	3.0	1.8
M8	36.6	24.6	11.1	22.1	10.0	18.4	8.3	12.3	5.5	7.4	3.3
M10	58.0	48.8	17.6	43.9	15.9	36.6	13.2	24.4	8.8	14.6	5.3
M12	84.3	84.7	25.7	76.2	23.1	63.5	19.3	42.4	12.9	25.4	7.7

Types of Joints

Single-bolted joints				Multi-bolted joints				Bolted joints
concentric or eccentric		in a plane	axial symmetry			symmetrical	asymmetrical	bolt axes
cylinder or prismatic body	beam	beam	circular plate	flange with sealing gasket	flange with plane bearing face	rectangular multi-bolted joint	multi-bolted joint	joint geometry
①	②	③	④	⑤	⑥	⑦	⑧	
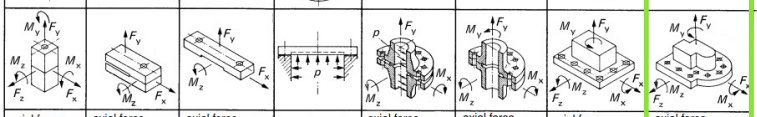								relevant loads
axial force F_A transverse force F_Q working moment M_B	axial force F_A transverse force F_Q moment in the plane of the beam M_Z	axial force F_A transverse force F_Q moment in the plane of the beam M_Z	internal ressure p	axial force F_A (pipe force) working moment M_B internal pressure p	axial force F_A torsional moment M_T working moment M_B	axial force F_A transverse force F_Q torsional moment M_T working moment M_B	axial force F_A transverse force F_Q torsional moment M_T working moment M_B	forces and moments
VDI 2230		limited treatment by VDI 2230		DIN EN 1591 AD 2000 Note B7	limited treatment by VDI 2230			calculation procedure
bending beam theory with additional conditions			plate theory		limited treatment using simplified models			
finite element method (FEM)								

Types of Joints

Bolts ONLY clamp one element to another, and should not experience bending / shear.
Friction and the clamping force are what hold the joint together.

Through Bolted Joint (TBJ)

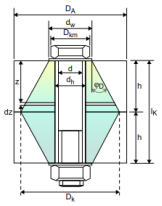

Tapped Thread Joint (TTJ)

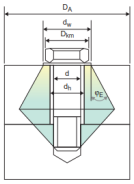

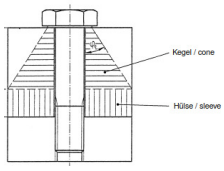

TBJs:
- Larger clamping length
- Better distribution of clamping pressure

Axial or Transverse loaded joints

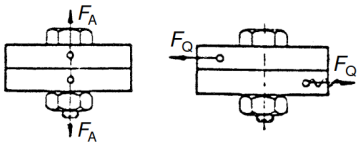

Axial load: F_A

Transverse load: $F_Q < F_V \cdot \mu_{Tmin}$ (Preload)

$$\Rightarrow F_{V.req} > \frac{F_Q}{\mu_{Tmin}}$$

Basic Joint Diagram

- Stiffness $k\ [N/mm] = \frac{E \cdot A}{l}$ $\quad F = k \cdot f$
- Resilience $\delta\ [mm/N] = k^{-1} = \frac{l}{E \cdot A}$ $\quad F = \frac{f}{\delta}$
- Load factor: $\Phi = n \cdot \frac{\delta_P}{\delta_P + \delta_S}$ $\quad \Phi \approx 0.05$

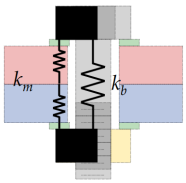

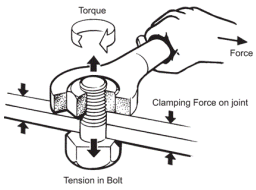

Workload
Bolt load
Preload
Clamping force
Bolt elongation
Parts compression

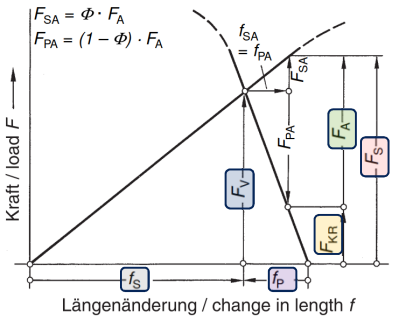

Joint Diagram for Max/Min Preload

Verification concept with Max / Min preload, with maximum workload applied:

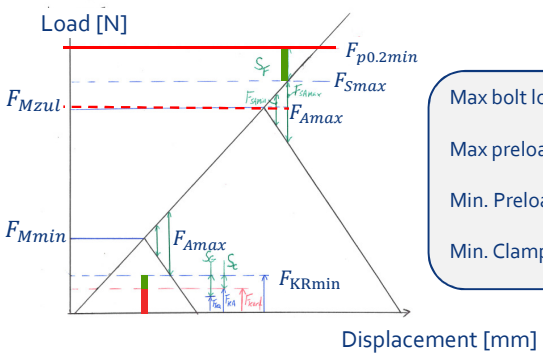

Max bolt load:	$F_{Smax} = F_{Mzul} + \Phi \cdot F_A$
Max preload:	F_{Mzul}
Min. Preload:	$F_{Mmin} = \frac{F_{Mzul}}{\alpha_A} - Preload\ losses$
Min. Clamp load:	$F_{KRmin} = F_{Mmin} - (1 - \Phi)F_A$

Joint Opening and Prying

Force / moment equilibrium

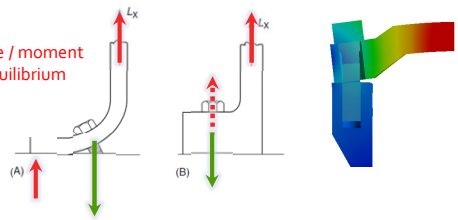

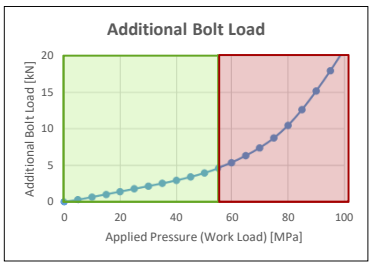

- Increased axial bolt load and bolt bending

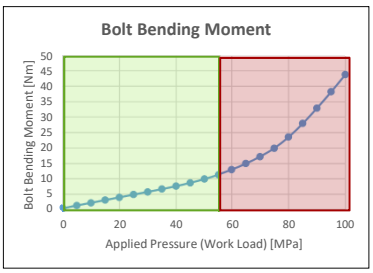

- Relevant:
  - Soft geometries (by design or material)
  - Eccentric loads

30 MPa:

60 MPa:

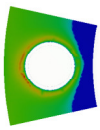

Joint Opening and Prying

When will a joint open?

Deformation cone is relieved at point of opening

=> load goes into bolt in-stead

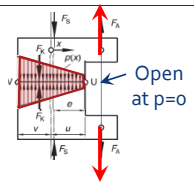

Analytic - Limit Criteria G [Pt.1 – Ro]

Interface width <

TBJ: $G = h_{min} + d_W$

TTJ: $G' \approx (1{,}5...2) \cdot d_W$

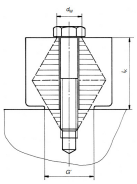

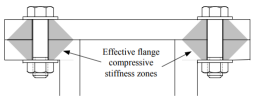

FEA

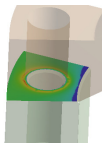

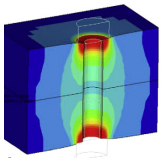

Compare with / without workload, with active preload

When sufficient bolts are used in a joint such that the **strain cones overlap**, the joint behaves as if it were a **continuous piece of material** and there was no joint at all.

15

Agenda

1. Basic Concepts of Bolted Joints and VDI 2230
2. **Combining FEA and VDI 2230**
3. Further Calculations and Verifications
4. Improvements of Bolted Joint Design
5. Support Material and References
6. Summary

16

Overall FEA-procedure

- Simplified workflow for FEA – VDI 2230
  => More advanced steps can be added
- Iterate if not approved
- Now:
  - Go through the steps
  - Explain relevant concepts

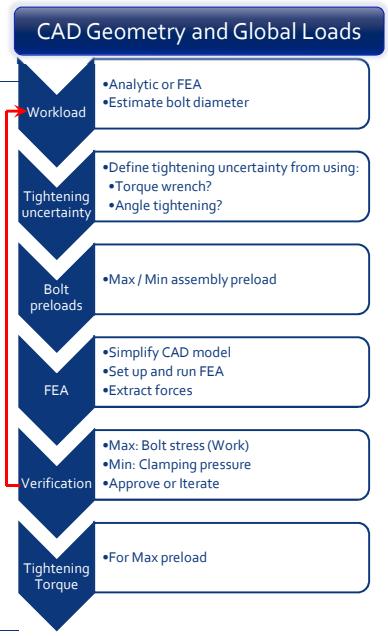

Identify Workload [Pt.2 – Ch. 6]

Goal: Estimate **bolt diameter** from maximum **bolt workload**

Initial status:

(1) Unknown bolt size	**(2) Bolt size is known**
=> Estimate bolt size	Can skip this step, and use selected bolt.

Note 1: If bolt size is known => estimation can be practical as a first indicator

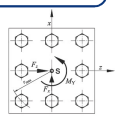

Analytic Calculation [Pt.2 – Ch. 6]

- **Rigid Body Mechanics:** Assume uniform distribution, proportional to radius, no prying
- **Elastomechanics:** Replacing constraints with supports and springs

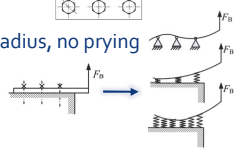

FEA [Pt.2 – Ch. 7.2.1]

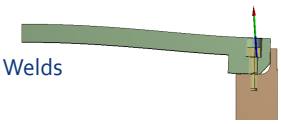

- Class I – Bonded interface or Spot Welds
- Class II – Beam

Advantage: Prying loads is included in bolt workload

Note 2: If multiple loads => most unfortunate combination

Note 3: No preload in sim. affect compliance and friction grip
=> might affect load distribution

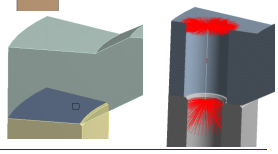

Estimate Bolt Diameter [Pt.1 – Ro]

VDI 2230 bolt estimation table: Rough-scaling of the actual workload based on defined criteria

Example

Dynamically and eccentric loaded by 8500N. Torque wrench to be used.

[Pt.1 – Table A7]

Table A7. Estimating the diameter range of bolts

1	2	3	4
Load in N	Nominal diameter in mm		
	Strength grade		
	12.9	10.9	8.8
250			
400			
630			
1 000	3	3	3
1 600	3	3	3
2 500	3	3	4
4 000	4	4	5
6 300	4	5	6
10 000	5	6	8
16 000	6	8	10
25 000	8	10	12
40 000	10	12	14
63 000	12	14	16
100 000	16	18	20
160 000	20	22	24
250 000	24	27	30
400 000	30	33	36
630 000	36	39	

1 2 3

A In Column 1, select the next highest load to the loading acting on the bolted joint. If during combined loading (longitudinal and transverse loads) $F_{A\,max} < F_{Q\,max} / \mu_{T\,min}$, then only $F_{Q\,max}$ is to be used.

B The required minimum preload $F_{M\,min}$ is obtained by increasing this number by the following number of steps:

B1 If the joint is to be designed with $F_{Q\,max}$:

four steps for static or dynamic transverse load

B2 If the joint is to be designed with $F_{A\,max}$:

two steps for dynamic and eccentrically applied axial load

or

one step for dynamically and concentrically or statically and eccentrically applied axial load

or

no steps for statically and concentrically applied axial load

C The required maximum preload $F_{M\,max}$ obtained by increasing this load $F_{M\,min}$ by:

two steps for tightening the bolt with a simple tightening spindle which has been set by the retightening torque

or

one step for tightening using a torque wrench or precision spindle, adjusted by means of dynamic torque measurement or elongation measurement of the bolt, or by a pneumatic impulse driver

or

no steps for tightening by angle monitoring in the plastic range or by computer-controlled yield-point monitoring

D Next to the number found, Column 2 to Column 4 give the required bolt dimensions in mm for the selected strength grade of the bolt.

*Steel grades

Estimate Bolt Diameter – non-steel bolts

Why other bolts?

- Match thermal contraction of plates => reduce preload loss
- Improved corrosion properties
- Lower load factor => lower additional bolt load / moment

Method of matched proof load:

Proof load: $F_{p0.2} = R_{p0.2} \cdot A_S$

Matched loads: $F_{p0.2.Bolt_1} = F_{p0.2.Bolt_2}$

Diameter Bolt 2: $d_2 = \sqrt{\frac{R_{p0.2.Bolt_1}}{R_{p0.2.Bolt_2}} \cdot (d_1)^2}$

Tightening Uncertainty [Pt.1 – R1]

Factors affecting uncertainty: Friction, accuracy in measurement / reading, resilience of joint

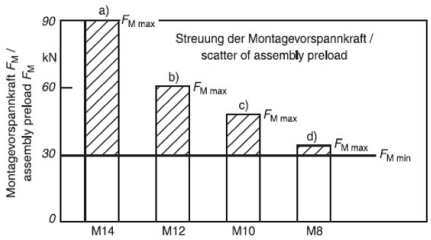

a) Impact wrench
b) Bolt installation spindle
c) Torque wrench or precision bolt installation spindle
d) Yield-controlled bolt installation spindle

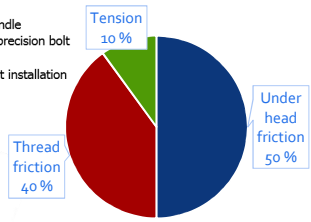

[Pt.1 – Table A8]

α_A	Method
1.0	Yield controlled tightening
1.1 – 1.2	Elongation control or ultrasound monitoring
1.2 – 1.4	Rotation angle controlled tightening Hydraulic frictionless tightening
1.4 – 2.5	Torque controlled tightening
2.5 - 4	Impact wrench, impulse driver, by hand

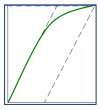

Preloads [Pt.1 – R7]

Utilization factor: ν $\quad \sigma_{red.Mzul} = \nu \cdot R_{p0.2\min}$

Define amount of proof stress to be allowed during assembly.

VDI 2230 suggest ν=0.9 (90%) (which is 75-85% of yield)

Static load, not critical: ν= 0.3 (30%) to ν=0.75 (75%)

Benefits of high utilization: no loosening, prying, accept more losses

Note: With high utilization, low safety factor – but more safe due to

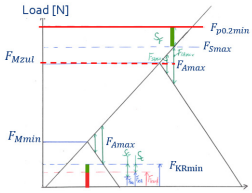

Max assembly preload

Stress at assembly

$$F_{Mzul} = A_0 \frac{\nu \cdot R_{p0.2\min}}{\sqrt{1 + 3\left[\frac{3}{2}\frac{d_2}{d_0}\left(\frac{P}{\pi \cdot d_2} + 1{,}155\mu_{G\min}\right)\right]}}$$

(Pt.1 – Eq. R7/2)

=> max torsion from tightening and max preload

Min assembly preload

Lowest probable preload

$$F_{Mzul.min} = \frac{F_{Mzul}}{\alpha_A} - Preload\ losses$$

=> Due to losses and uncertainties

FEA

Simplify CAD model => Set up & run FEA => Extract forces

Simulation Classes:

- Stress cross section: d_S =14.14 mm
- Thread minor diameter: d_3 =13.55 mm
- Analytic resilience: d_δ =11.47 mm

Class II

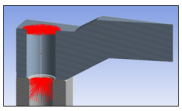

Class III

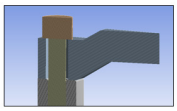

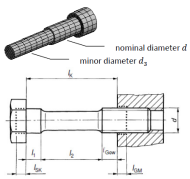

$$A_{\sigma z} = \frac{l_k}{E_S \cdot \delta_S} \quad I_{\sigma z} = \frac{l_k}{E_S \cdot \beta_S}$$

Non linearities:

Linear	Non-linear
Material	Frictional contact Large deformations

Extract results from simulation with **Max** / **Min** preload

MAX: Maximum bolt load - F_{Smax}

(bolt bending moment - M_{Sbo})

MIN: Clamping pressure / Prying

→ Verifications

Verifications

Work stress [Pt.1 – R8]

- Max bolt stress with workload
- Residual tightening torque ($k_t = 0.5$)
- Bending stress included here, not in VDI 2230

$$\sigma_{red.B} = \sqrt{\left(\frac{F_{Smax}}{A_S} + \frac{M_{Sb}}{W_S}\right)^2_{max} + 3(k_t \cdot \tau_{max})^2} \qquad \text{(R8/4)}$$

Axial — Bending — Residual torsion from tightening

$$\sigma_{red.B} < R_{p0.2min}$$

Clamping pressure and Slipping [Pt.1 – R2 / R12]

- Extract clamping force in interface => uniform pressure
- Check if **slipping** is present: ANSYS status or Analytic calc.
- Assess **pressure distribution** in interface, and check **joint opening**
  - Note: Effect of mesh refinement and tapped threads on pressure

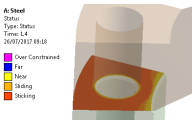

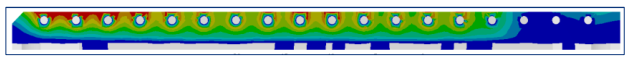

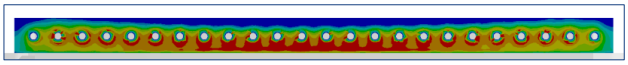

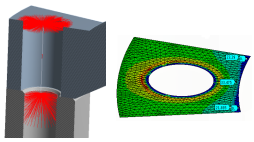

Verifications

Joint opening

Methods:

- Clamping pressure
- Displacement of joint edges (Deformation cone - G)

If opening: Indication of possible prying

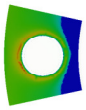

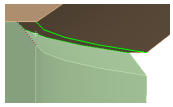

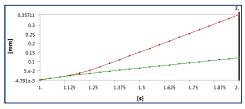

Prying

Important to know if present:

- Higher risk with uncertainty in workload
- Risk of bolt failure from fatigue <= bending

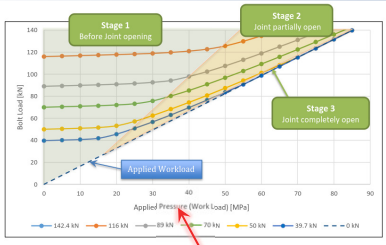

Actions:

- Joint design <= stiffer material / geometry
- Account for it <= sufficient safety factor with bending stress
- Increase preload <= reduce uncertainties / losses, higher strength

To make graph:
Sub-steps needed
Max workload x 1.2

Calculation of Tightening Torque [Pt.1 – R13]

Tightening torque to achieve max preload F_{Mzul}:

$$M_A = F_{M.zul}\left(\underbrace{0.16P + 0.58 \cdot d_2 \cdot \mu_{G.\min}}_{\text{thread}} + \underbrace{\frac{D_{K.\min}}{2}\mu_{K.\min}}_{\text{bolt head bearing}}\right) \qquad \text{(R13/1)}$$

Coefficients of friction

- Typical values available in: [Pt.1 – Table A5]
- Calculated tightening torques for ν=0.9 in [Pt.1 – table A1-A4]
- CERN MME lab measurements on EDMS

Risk of wrong coefficients of friction:

Higher than in calc. => Lower preload Lower than in calc.=> Higher preload

- Washer effect on friction
- Traditional strategy: Lubrication => low friction => lower risk - Not at CERN

Overall FEA-procedure

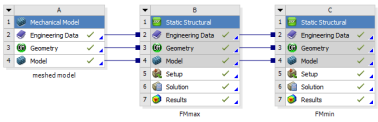

Sim#	Description
(Sim 0)	Scope: Identify workload Preload: No Workload: Maximum workload
Sim 1 Max	Scope: Check maximum bolt load Preload: Max preload Workload: Maximum workload
Sim 2 Min	Scope: Check clamping conditions Preload: Minimum preload Workload: Maximum workload x 1.2 Details: Sub-steps needed to plot load curves

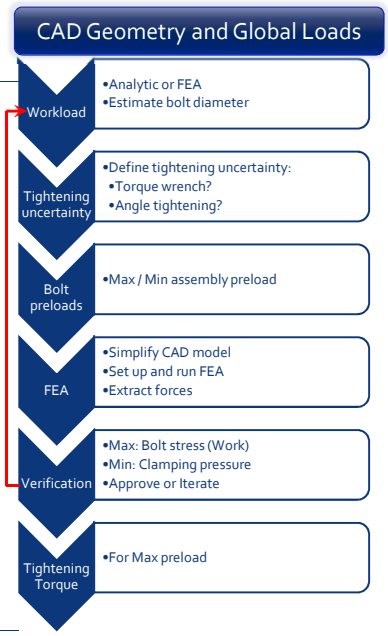

Validity in FEA aided analysis

- Material
  - Material properties: E-modulus, Strength Temperature?
  - Friction factors (numerical representation)
  - Material non-linearities
- BCs
  - Contact representation
- Workload
  - Certainty of workload – all included?
  - System displacements / loads?
- Mesh
  - Clamping pressure distribution
  - Deformation cone and Resilience representation

<u>Testing and Verification</u>

- Physical testing => analyze bolts
  - Visual inspection of plastic deformations
  - Measure elongation (yield)
  - Loosening torque
- Analytic calculations

=> Control FEA results with calculations

CADFEM ANSYS Bolt Toolkit

- Plugin for Bolt Assessment in ANSYS available at CERN:
  - ANSYS Interface
  - Database with bolt data
  - VDI 2230 equations for safety factors and stress

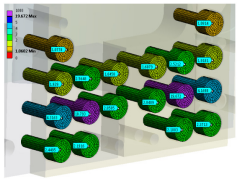

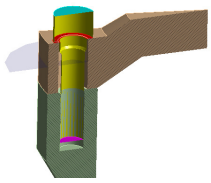

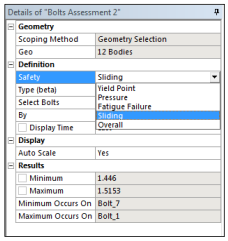

My findings:

- In some cases for MBJs, can be practical. Require experience and training.
- More safe to use "basic approach" with calculation support.

Agenda

1. Basic Concepts of Bolted Joints and VDI 2230
2. Combining FEA and VDI 2230
3. **Further Calculations and Verifications**
4. Improvements of Bolted Joint Design
5. Support Material and References
6. Summary

Preload Losses [Pt.1 – R4 / Ch. 5.4.2]

Analytic resilience must be known: [Pt.1 – R3]. FEA also possible.

Embedding / Relaxation

- Local plastic deformations during assembly / loading. Flattening of bearing and thread area
- Depend on surface roughness, number of interfaces, and material
- Guide values in [Pt.1-Table 5]
- NASA: 5% of max preload F_{Mzul}
- Too high bearing pressure => creep [R10]

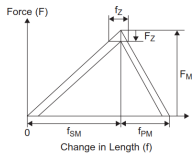

$$F_Z = \frac{f_Z}{\delta_S + \delta_P} \quad \text{(R4/1)}$$

Differential thermal expansion

Will give **relief** or **increase** in bolt load:

Plate contract more than **bolt** => Reduced load

Bolt contract more than **plate** => Increased load

Should only be considered in:

Max bolt load <= if bolt load increase

Minimum clamping <= if bolt load decrease

$$\Delta F'_{\mathrm{Vth}} = \frac{l_{\mathrm{K}} \cdot (\alpha_{\mathrm{S}} \cdot \Delta T_{\mathrm{S}} - \alpha_{\mathrm{P}} \cdot \Delta T_{\mathrm{P}})}{\delta_{\mathrm{S}} \frac{E_{\mathrm{SRT}}}{E_{\mathrm{ST}}} + \delta_{\mathrm{P}} \frac{E_{\mathrm{PRT}}}{E_{\mathrm{PT}}}} \quad \text{(R4/2)}$$

To avoid this: Similar thermal expansion

31

Fatigue [Pt.1 – R9 / Ch. 5.5.3]

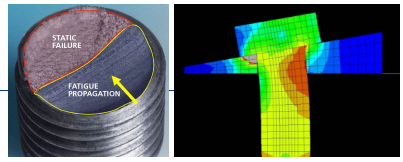

Poor design of joint and low preload

=> Fatigue failure with small loads

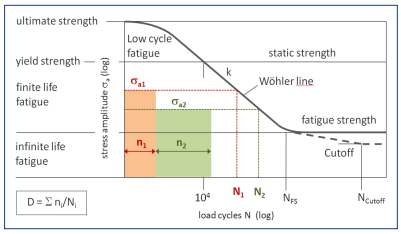

Influencing Factors:

- Notches in bolt (Stress x4-x10)
- Stiff bolt or "Soft" joint design
  => High bending moment
- Rolled / Cut threads
- Heat treatment before / after
- Bolt loosening => loose preload => prying

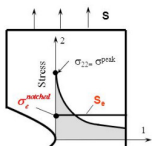

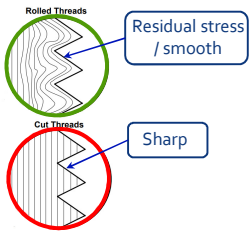

Example:

For M6: $\sigma_{ASV} = 60\ MPa$ 8.8: $\frac{\sigma_{ASV}}{R_{p0.2min}} = 9.4\%$

NB! Remember notch factor

Stress amplitude

$$\sigma_{\mathrm{ab}} = \frac{\sigma_{\mathrm{SAbo}} - \sigma_{\mathrm{SAbu}}}{2}$$

32

Tapped Thread Length [Pt. 1 – R11 / Ch. 5.5.5]

- Rule of thumb: 1.5 x d
- Table available
- Calculate with VDI 2230
  - Match capacity: Thread shear = Axial bolt
  - Assume uniform distribution

Material of components		Length of engagement l_e[3] according to property class of screw			
		3.6 / 4.6	4.8...6.8	8.8	10.9
Steel with R_m N/mm²	≤ 400	0.8 · d	1.2 · d	–	–
	400...600	0.8 · d	1.2 · d	1.2 · d	–
	> 600...800	0.8 · d	1.2 · d	1.2 · d	1.2 · d
	> 800	0.8 · d	1.2 · d	1.0 · d	1.0 · d
Cast iron		1.3 · d	1.5 · d	1.5 · d	–
Copper alloys		1.3 · d	1.3 · d	–	–
Light metals[2]	Cast Al alloys	1.6 · d	2.2 · d	–	–[3]
	Pure aluminium	1.6 · d	–	–	–[3]
	Al alloy, hardened	0.8 · d	1.2 · d	1.6 · d	–[3]
	not hardened	1.2 · d	1.6 · d	–	–[3]
Soft metals, plastics		2.5 · d	–	–	–

[1] For dynamic loads the specified value of l_e must be increased by approx. 20%.
[2] Fine pitch threads require approx 25% greater lengths of engagement.
[3] For higher strength screws, the shear strength of the internal thread material as calculated in VDI 2230 must be taken into account.

Source: Roloff / Matek

Stripping force of internal thread:

$$F_{mGM} = \tau_{BM.min} \cdot \pi \cdot d_{min} \cdot \left(\frac{l_{eff}}{P}\right) \cdot \left(\frac{P}{2} + (d_{min} - D_{2.max}) \cdot tan(30\ deg)\right)$$

- Load distribution

  Bolt and tapped thread material

  +: Hole in bolt or thin thread wall

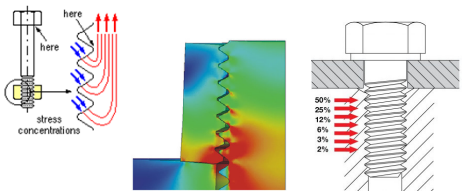

Slipping / Shearing [Pt.1-R12 / Ch. 5.5.6)

- ANSYS plots

"Status" analysis

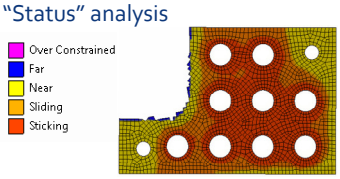

Slipping distance

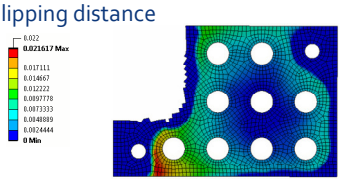

- Analytic calculation

Extracted loads from FEA: Clamping force / transverse force / moment

Safety against **slipping**:

$$S_G = \frac{F_{KR\min}}{\left(\frac{F_{Q\max}}{\mu_{T\min}}\right)} > 1.2/1.8 \qquad \text{(R12/4)}$$

Max transverse load

Required clamp force

Safety against **shear**:

$$S_A = \frac{\tau_B \cdot A_\tau}{F_{Q\max}} \geq 1.1 \qquad \text{(R12/7)}$$

Max transverse load

Agenda

1. Basic concepts of Bolted Joints and VDI 2230
2. Combining FEA and VDI 2230
3. Further Calculations and Verifications
4. **Improvements of Bolted Joint Design**
5. Support Material and References
6. Summary

Improvements of Bolted Joint Design

Lower Load Factor

How:

- Increased clamping length
- Reduced shank bolt
- Softer bolt / stiffer clamped plates material
- TBJ instead of TTJs, because of cone volume
- Countersink clamped plates

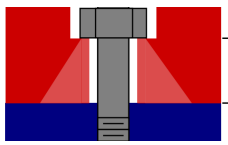

$$\frac{\delta_P}{\delta_P + \delta_S} = \Phi \quad \Rightarrow \quad \Phi \cdot F_A = F_{SA}$$

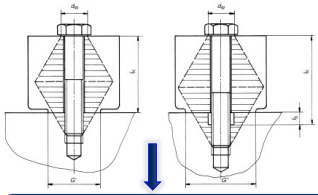

- Better pressure distribution
- Increased clamping length

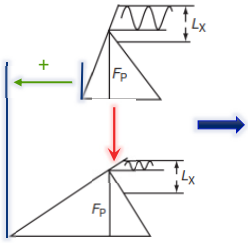

- Lower amplitude
  => Fatigue
- Larger deformation
  => Preload losses
  => Bolt loosening

Improvements of Bolted Joint Design

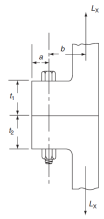

Avoid Joint Opening

- **Stiff design** by geometry / materials
- **Reduce eccentricity** in load application (b)
- **High preload** by bolt strength and more precise tightening

Minimise Preload Losses

- **Reduce load factor** by recommendations of previous slide
  => Higher deformation capacity

Thermal: Match thermal expansion factor for bolt / plates

Embedding: Low surface roughness, and low number of interfaces

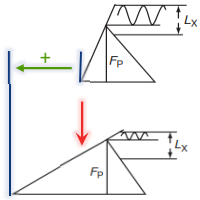

Avoid Loosening

- Minimise preload losses
- High preload
- Retaining elements

VDI 2230 suggested clamping length: $\frac{l_K}{d} \geq (3...5)$

Agenda

1. Basic Concepts of Bolted Joints and VDI 2230
2. Combining FEA and VDI 2230
3. Further Calculations and Verifications
4. Improvements of Bolted Joint Design
5. **Support Material and References**
6. Summary

Support Material and References

- VDI 2230 on CDS — With many useful tables to guide and support design and verification
- *Systematic calculation of highly stressed bolted joints; Joints with one cylindrical bolt*, VDI2230 Part 1, 2014.
- *Systematic calculation of highly stressed bolted joints; Multi bolted joints*, VDI2230 Part 2, 2014.

- ISO Standards
- *Fasteners - Clearance holes for bolts and screws*, ISO 273, 1979.
- *Hexagon socket head cap screws*, ISO 4762, 2004.
- *Hexagon head bolts - product grades A and B*, ISO 4014, 1999.

- *My reports:*

EDMS 1760853	*Project thesis:* Assessment of Bolted Joints According to VDI 2230 using FE-analysis
EDMS 1770646	*Research notes:* Studies into Application of FEA in Assessment of Bolted Joints
EDMS 1866760	*MSc Thesis:* Application of FE-analysis in Design and Verification of Bolted Joints at CERN

- *Other*
- *Calculation support and examples of FEA and VDI 2230*
- *KAMAX Bolt Compendium*
- J. H. Bickford, *Introduction to the Design and Behaviour of Bolted Joints, Fourth Edition*, 2007.

Summary

1. Basic Concepts of Bolted Joints and VDI 2230
   - About VDI 2230, types of bolts and joints, joint diagram, and prying
2. Combining FEA and VDI 2230
   - FEA Procedure: Workload, Estimate bolt dia., Tightening uncertainty, Preloads, FEA, Verifications, Tightening torque, Validity, and CADFEM
3. Further Calculations and Verifications
   - Preload losses, Fatigue, Tapped thread length, Slipping and Shearing
4. Improvements of Bolted Joint Design

Take-aways

- Combining VDI 2230 and FEA **increase quality** of assessment, and **save time**
- Many ways to influence joint performance – attention to detail
  - Material E-modulus and strength, bolt type and design, Joint geometry, tightening method, …
- Best practice:
  - Low load factor (much more resilient bolt than clamped plates)
  - High preload
- **Testing** should be performed to verify theoretical assessment

Questions / Comments ? Experiences ?

Let's discuss…

Feedback: Unclear? More about / less about…

CERN | EN ENGINEERING DEPARTMENT

Thank you for your time!

APPENDIX F

REVISED CALCULATIONS FOR HE-VESSEL JOINTS

Calculations for FE-analysis of He-vessel Joints

Analysis performed by: Jørgen Apeland | **Date of Analysis:** Oktober 2017

Calculation case: DQW Crab Cavity He-vessel Bolted Joints | **According to procedure:** VDI 2230 - Basic FEA Workflow

Color codes: **Input parameters** **Calculation quantities** **Results** **Functions** **Criteria check**

S1 - Workload

Coefficient of friction in the clamping interface: $\mu_{Tmin} := 0.3$

Below, an analytic approach is made to identify the workloads as a first estimate to identify the required preload.

1 - Slipping for "Upper Cover"

Number of bolts: $i_1 := 2 \cdot 27 + 2 \cdot 24 = 102$

Assumed axial workload from pressure: $F_{A.1} := 350\ N$

Assumed load-factor: $\Phi_1 := 0.1$

The axial workload from pressure will give a relief in the residual clamping load in the interface.

Resulting relief in clamping force: $F_{PA.1} := (1 - \Phi_1)\ F_{A.1} = 315\ N$

Transverse load from pressure: $F_{Q.p} := 37.6\ kN$

Transverse load from weight: $F_{Q.m} := g\ (200\ kg - 25.2\ kg) = 1.71\ kN$

Total transverse load on bolts: $F_{Q.tot} := F_{Q.p} + F_{Q.m} = 39.31\ kN$

Transverse load on one bolt: $F_{q.max} := \frac{F_{Q.tot}}{i_1} = 385.4\ N$

Assuming uniform distribution of loads, and no axial workloads on the bolts.

Required safety factor against slipping: $S_{G.req} := 1.2$

Minimum clamp-load to avoid slipping: $F_{KQ} := \frac{S_{G.req} \cdot F_{q.max}}{\mu_{Tmin}} = 1.54\ kN$

Required clamping load: $F_{Kerf} := F_{KQ} + F_{PA.1} = 1.86\ kN$

2 - Axial workload on "Beam side" plate

Number of bolts: $i_2 := 2 \cdot 27 + 2 \cdot 18 = 90$

Axial load from pressure: $F_{p.2} := 31.3\ kN$

Axial workload pr. bolt: $F_{A.2} := \frac{F_{p.2}}{i_2} = 347.8\ N$

Assuming uniform distribution of loads.

3 - Axial and slipping for "Downstream / upstream" plates

Number of bolts: $i_3 := 2 \cdot 24 + 2 \cdot 18 = 84$

Axial load from pressure: $F_{p.3} := 22.7\ kN$

Axial workload pr. bolt: $F_{A.3} := \frac{F_{p.3}}{i_3} = 270.2\ N$

Assuming uniform distribution of loads.

Since this bolt load is lower than the two previous cases, this bolt loading is not critical.

Maximum analytic workload on the bolt

Maximum transverse load: $F_{Q.max} := F_{q.max} = 385.4\ N$

Minimum clamp-load to avoid slipping: $F_{KQ} = 1.54\ kN$

Maximum axial load: $F_{A.max} := F_{A.2} = 347.8\ N$

==========

S2 - Nominal Bolt Diameter

Bolt data parameters

Nominal diameter:	$d := 6\ mm$	Friction coefficient in the threads:	$\mu_{Gmin} := 0.3$
Pitch:	$P := 1\ mm$	Friction in head bearing area:	$\mu_{Kmin} := 0.3$
Effective bolt head diameter:	$d_W := 8.74\ mm$	Yield strength of the bolt:	$R_{p0.2min} := 820\ MPa$
Diameter of clearence hole:	$d_{h.max} := 6.9\ mm$	Thread length:	$l := 20\ mm$
Diameter of outgassing hole:	$d_g := 1.75\ mm$		

Note!
Apply minimum coefficients of friction.

Calculated parameters

Pitch diameter: $d_2 := d - \frac{3\sqrt{3}}{8} P = 5.35\ mm$

$H = \frac{\sqrt{3}}{2} \cdot P$

Minor diameter of the bolt: $d_3 := d - P\left(\frac{17\sqrt{3}}{24}\right) = 4.773\ mm$

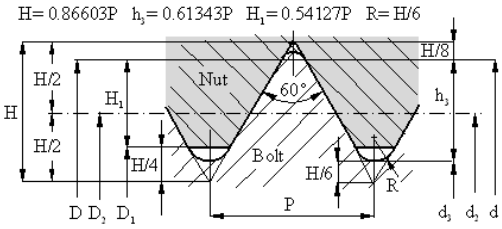

S3 - Tightening Factor

Torque wrench: $\alpha_A := 1.6$

S4 - Max Assembly Pretension

Calculation quanteties

Stress diameter: $d_S := 0.5\ (d_2 + d_3) = 5.06\ mm$

Stress area: $A_S := \frac{\pi}{4} (d_S)^2 = 20.1\ mm^2$

Reduced stress area: $A_{S.g} := \frac{\pi}{4} (d_S^2 - d_g^2) = 17.7\ mm^2$

Parameters

Bolt capacity utililization factor: $\nu := 0.9$

Calculations

Allowed assembly stress: $\sigma_{Mzul} := \nu\ R_{p0.2min} = 738\ MPa$

Maximum permitted assembly preload:

$$F_{Mzul} := A_{S.g} \frac{\nu\ R_{p0.2min}}{\sqrt{1 + 3\left(\frac{3}{2}\frac{d_2}{d_S}\left(\frac{P}{\pi\ d_2} + 1.155\ \mu_{Gmin}\right)\right)^2}}$$

ans. $F_{Mzul} = 8.73\ kN$
==========

S5 - Min Assembly Pretension

Minimum assembly preload: $F_{Mmin} := \frac{F_{Mzul}}{\alpha_A}$

ans. $F_{Mmin} = 5.46\ kN$
==========

S6 - Simplify and Prepare CAD-geometry

S7 - Prepare and Run FE-analysis

Parameters

Coefficient of Friction in the clamping interface: $\mu_{Tmin} = 0.3$

Coefficient of friction in the head bearing area: $\mu_{Kmin} = 0.3$

Calculation of theoretical beam parameters:

Minor diameter area: $A_{d3.g} := \frac{\pi}{4}\left(d_3^{\,2} - d_g^{\,2}\right) = 15.49\ mm^2$

Minor second area areal moment of inertia: $I_{d3.g} := \frac{\pi}{64}\left(d_3^{\,4} - d_g^{\,4}\right) = 25.02\ mm^4$

Torsional stiffness: $J := \frac{\pi}{32}\left(d_3^{\,4} - d_g^{\,4}\right) = 50.04\ mm^4$

S8 - Results and Analysis

Must be updated with values from the revised simulations

Max assembly preload

Max bolt bending moment: $M_{Sbo} := 3430\ N\ mm$

Acheived preload: $F_{Vmax} := 4.5\ kN$

Workload: $F_A := 500\ N$

Max bolt load: $F_{Smax} := 4650\ N$

Min assembly preload

Acheived preload: $F_{Vmin} := 4.5\ kN$

S9 - Work Stress

Note: In this calculated work-stress, bending stress is included. That is not the case for the standard VDI 2230 equation.

Parameters

Residual torque factor: $k_t := 0.5$

Calculation quanteties

Bending modulus: $W_{S.g} := \frac{\pi}{32}\left(\frac{d_S^{\,4} - d_g^{\,4}}{d_S}\right) = 12.55\ mm^3$

Notice that the outgassing hole has been included, so it is a hollow cylinder that is considered.

Thread moment: $M_G := F_{Mzul} \cdot \frac{d_2}{2} \cdot \left(\frac{P}{\pi\ d_2} + 1.155\ \mu_{Gmin}\right) = 9.5\ N\ m$

Polar moment of inertia: $W_{p.g} := \frac{\pi}{16} \cdot \left(\frac{d_S^{\,4} - d_g^{\,4}}{d_S}\right) = 25.1\ mm^3$

Calculations

Normal stress: $\sigma_{zb.max} := \frac{F_{Smax}}{A_{S.g}} + \frac{M_{Sbo}}{W_{S.g}} = 535.7\ MPa$

Torsional stress: $\tau_{max} := \frac{M_G}{W_{p.g}} = 377.77\ MPa$

Working stress: $\sigma_{red.B} := \sqrt{\sigma_{zb.max}^{\,2} + 3\left(k_t \cdot \tau_{max}\right)^2} = 627.7\ MPa$

Bending stress

$\sigma_{Sbo} := \frac{M_{Sbo}}{W_{S.g}} = 273.3\ MPa$

Bending stress contribution to work stress:

$\Delta\sigma_{Sbo.p} := \frac{\sigma_{Sbo}}{\sigma_{red.B}} = 43.5\%$

Assessment

Criteria: $\sigma_{red.B} = 627.73\ MPa \quad < \quad R_{p0.2min} = 820\ MPa$

$Work_Stress := \left\| \begin{array}{l} \text{if } \sigma_{red.B} < R_{p0.2min} \\ \quad \text{return "Ok"} \\ \text{"Not OK"} \end{array} \right.$

$Work_Stress = \text{"Ok"}$

Safety factor: $S_F := \frac{R_{p0.2min}}{\sigma_{red.B}} = 1.31$

==========

S10 - Clamping Requirements

S11 - Tightening Torque

Average head friction diameter: $D_{Km} := \frac{d_W + d_{h.max}}{2} = 7.82\ mm$

Tightening Torque: $M_A := F_{Mzul} \cdot \left(0.16\ P + 0.58\ d_2\ \mu_{Gmin} + \frac{D_{Km}}{2}\ \mu_{Kmin}\right) = 19.8\ N\ m$

==========

S12 - Approve or Iterate

==========
APPROVED
==========

Additional Calculations According to VDI 2230

R0 - Checking limiting size G

Parameters

Width of the interface: $\begin{bmatrix} c_{T.AC} \\ c_{T.B} \end{bmatrix} := \begin{bmatrix} 25 \\ 18 \end{bmatrix} mm$

Eccentric distance e: $\begin{bmatrix} e_{AC} \\ e_B \end{bmatrix} := \begin{bmatrix} 13 \\ 5 \end{bmatrix} mm$

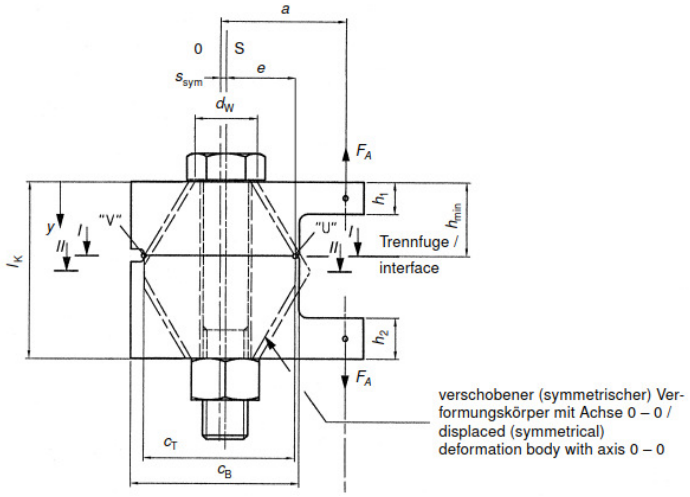

Criteria

This criteria is defined for TTJs in Steel. Exceeding the limiting dimensions entails a relatively large calculation error.

For eccentrically clamped joints, approxemately constant interface pressure can be expected on the bending tension side of the basic solid if the outer contour in the region of the interface is not separated from the bolt azis S-S by a greater distance than G/2:

$$e \leq \frac{G}{2}$$

Compliance with this requirement takes priority over the basic requirement $c_T < G$.

For TTJs:

$$\begin{bmatrix} G'_{min} \\ G' \end{bmatrix} := d_W \begin{bmatrix} 1.5 \\ 2 \end{bmatrix} = \begin{bmatrix} 13.1 \\ 17.5 \end{bmatrix} mm$$

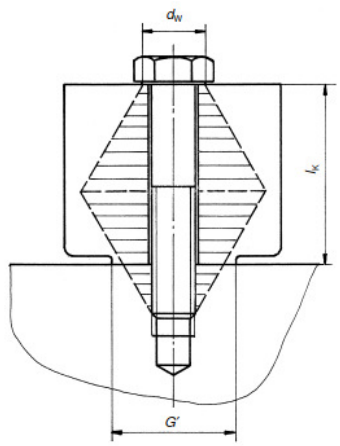

Assuming an approximate constant pressure, although at a lower level than above, the following criteria can be used:

$$G'_{max} := 3\ d_W = 26.2\ mm$$

Control

$e_B = 5\ mm$ < $0.5\ G'_{min} = 6.6\ mm$

$e_{AC} = 13\ mm$ < $0.5\ G'_{max} = 13.1\ mm$

Conclusion

Joint A and C only comply with the requirement based on G'_{max}.
Joint B comply with all the requirements.

It should however be noted that Joint B has an edge in the interface. The components are also made of Titanium, and it is unclear how the deformation cone is affected by a more resilient material.

R3 - Analytic Resilience and Load Factors

Parameters

Elastic modulus of bolt (S) and clamped parts (P): $E_S := 110\ GPa$ $E_P := E_S$ Titanium Gr. 5 and Gr. 2

Clamping length: $l_K := 11\ mm$

Calculation quantities

Bolt quantities: $l_1 := 3\ P$ $l_{Gew} := l_K - l_1 = 8\ mm$ $l_{SK} := d\ 0.4$ $l_G := d\ 0.5$ $l_M := d\ 0.33$

Bolt areas, considering outgassing hole: $A_{d3.g} := \frac{\pi}{4}\left(d_3{}^2 - d_g{}^2\right) = 15.49\ mm^2$ $A_{N.g} := \frac{\pi}{4}\left(d^2 - d_g{}^2\right) = 25.87\ mm^2$

Areal moment of Intertia: $I_{N.g} := \frac{\pi}{64}\left(d^4 - d_g{}^4\right)$

Axial Resilience of the Bolt

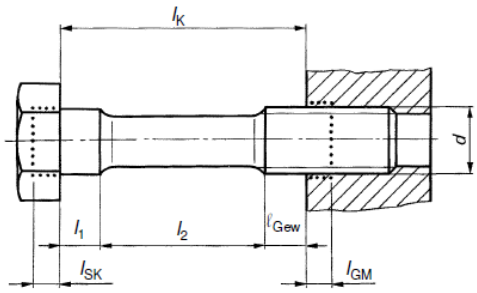

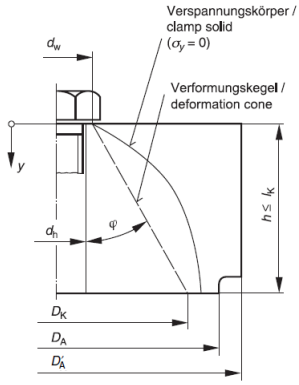

Head: $\delta_{SK} := \dfrac{l_{SK}}{E_S \cdot A_{N.g}}$

Shank: $\delta_1 := \dfrac{l_1}{E_S \cdot A_{N.g}}$

Threaded region: $\delta_{Gew} := \dfrac{l_{Gew}}{E_S \cdot A_{d3.g}}$

Bolt threads: $\delta_G := \dfrac{l_G}{E_S \cdot A_{d3.g}}$

Nut threads: $\delta_M := \dfrac{l_M}{E_P \cdot A_{N.g}}$

Nut: $\delta_{GM} := \delta_G + \delta_M$

Sum: $\delta_S := \delta_{SK} + \delta_1 + \delta_{Gew} + \delta_{GM}$

Ans.
The axial resilience of the M6 bolt is: $\delta_S = (9.05 \cdot 10^{-3}) \dfrac{mm}{kN}$
==========

For comparison, a body with uniform diameter equal to the thread minfor diameter would have the following resilience:

$$\delta_{S.d3} := \frac{l_K}{E_S \cdot A_{d3.g}} = 0.006 \frac{mm}{kN} \qquad \Delta\delta_p := \frac{\delta_S - \delta_{S.d3}}{\delta_{S.d3}} = 40.2\%$$

Thus, the analytic resilience is $\Delta\delta_p = 40.2\%$ more resilient than a uniform cylinder of same length. If using a beam with the exact diameters, the resilience will be similar to that of the uniform cross-section.

If more resilient, the bolt will absorb a smaller share of the applied workload in the preloaded bolt.

Bending Resilience of the Bolt

Head: $\beta_{SK} := \dfrac{l_{SK}}{E_S \cdot I_{N.g}} = (3.45 \cdot 10^{-7}) \dfrac{1}{N\ mm}$

Shank: $\beta_1 := \dfrac{l_1}{E_S \cdot I_{N.g}} = (4.32 \cdot 10^{-7}) \dfrac{1}{N\ mm}$

Threaded region: $\beta_{Gew} := \dfrac{l_{Gew}}{E_S \cdot I_{d3.g}} = (2.91 \cdot 10^{-6}) \dfrac{1}{N\ mm}$

Bolt threads: $\beta_G := \dfrac{l_G}{E_S \cdot I_{d3.g}} = (1.09 \cdot 10^{-6}) \dfrac{1}{N\ mm}$

Nut threads: $\beta_M := \dfrac{l_M}{E_P \cdot I_{N.g}} = (2.85 \cdot 10^{-7}) \dfrac{1}{N\ mm}$

Nut: $\beta_{GM} := \beta_G + \beta_M = (1.38 \cdot 10^{-6}) \dfrac{1}{N\ mm}$

Sum: $\beta_S := \beta_{SK} + \beta_1 + \beta_{GM} + \beta_{Gew} = (5.06 \cdot 10^{-6}) \dfrac{1}{N\ mm}$

Ans.
The bending resilience of the M6 bolt is: $\beta_S = (5.06 \cdot 10^{-6}) \dfrac{1}{N\ mm}$
==========

Resilience of the clamped parts

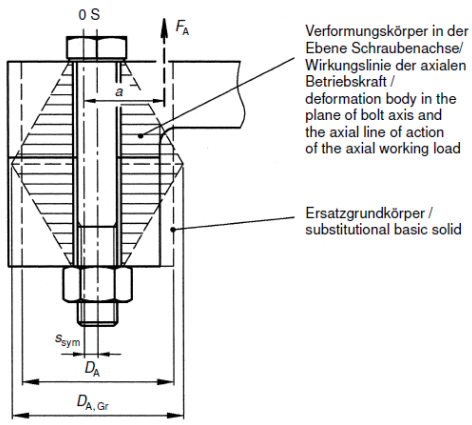

Assuming the deformation model consist of two deformation cones, and that the interface is wide enough so that no deformation sleve is present. Ref. page 47 VDI 2230 Pt. 1, For TBJs, estimations can be performed of the plate resilience with $\varphi := 0.6$, with a maximum error of 5%.

for TTJ: $w := 2$, $\varphi = 34.38\ deg$

Limiting diameter: $D_{A.Gr} := d_W + w \cdot l_K \cdot \tan(\varphi) = 23.8\ mm$

Substitutional outside diameter of the basic solid at the interface: $\begin{bmatrix} D_{A.AC} \\ D_{A.B} \end{bmatrix} := \begin{bmatrix} c_{T.AC} \\ c_{T.B} \end{bmatrix} = \begin{bmatrix} 25 \\ 18 \end{bmatrix} mm$

Joint A and C: $D_{A.AC} = 25\ mm$ > $D_{A.Gr} = 23.79\ mm$ For Joint A and C, the deformatoin cone consist of one substitutional deformation cone.

Joint B: $D_{A.B} = 18\ mm$ < For Joint B, a partial sleeve will be present.

==========

For deformation body with deformation cone only

$$\delta_{P.Z}(d_h) := \frac{2 \ln\left(\frac{(d_W + d_h)\cdot(d_W + w\ l_K \tan(\varphi) - d_h)}{(d_W - d_h)\cdot(d_W + w\ l_K \tan(\varphi) + d_h)}\right)}{w \cdot E_P \cdot d_h \cdot \pi \cdot \tan(\varphi)}$$

$$\delta_{P.AC} := \delta_{P.Z}(d_{h.max}) = (9.46 \cdot 10^{-4})\ \frac{mm}{kN}$$

For deformation body with deformation cone and sleeve

$$\delta_P(d_h, D_A) := \frac{\frac{2}{w\ d_h \tan(\varphi)} \ln\left(\frac{(d_W + d_h)\cdot(D_A - d_h)}{(d_W - d_h)\cdot(D_A + d_h)}\right) + \frac{4}{D_A^{\ 2} - d_h^{\ 2}}\left(l_K - \frac{(D_A - d_W)}{w \tan(\varphi)}\right)}{E_P\ \pi}$$

$$\delta_{P.B} := \delta_P(d_{h.max}, D_{A.B}) = (9.94 \cdot 10^{-4})\ \frac{mm}{kN}$$

Relative comparison: $\Delta\delta_P := \frac{\delta_{P.B} - \delta_{P.AC}}{\delta_{P.AC}} = 5.08\%$

Average resilience of the clamped parts: $\delta_P := 0.5\ (\delta_{P.AC} + \delta_{P.B}) = (9.7 \cdot 10^{-4})\ \frac{mm}{kN}$

==========

Considering eccentric clamping, the resiliense of the clamped parts are:

Eccentricity from centre of clamping interface: $\frac{c_{T.AC}}{2} - e_{AC} = -0.5\ mm$

$\frac{c_{T.B}}{2} - e_B = 4\ mm$

$\begin{bmatrix} s_{sym.AC} \\ s_{sym.B} \end{bmatrix} := \begin{bmatrix} -0.5 \\ 4 \end{bmatrix} mm$

$D_A := \begin{bmatrix} D_{A.AC} \\ D_{A.B} \end{bmatrix}$ $s_{sym} := \begin{bmatrix} s_{sym.AC} \\ s_{sym.B} \end{bmatrix}$

Areal moment of inertia of deformation body: $I_{V.Bers} := \overrightarrow{0.147 \cdot \frac{(D_A - d_W)\cdot d_W^{\ 3} \cdot D_A^{\ 3}}{D_A^{\ 3} - d_W^{\ 3}}} = \begin{bmatrix} 1667.0 \\ 1026.3 \end{bmatrix} mm^4$

Substitutional cone: $I_{VE.Bers} := \overrightarrow{I_{V.Bers} + s_{sym_1}^{\ 2} \cdot \frac{\pi}{4} D_A^{\ 2}} = \begin{bmatrix} 1789.7 \\ 1089.9 \end{bmatrix} mm^4$

Only cone present: $I_{Bers} := I_{VE.Bers}$

Resilience for eccentric loading & clamping $\delta'_P := \delta_P + \frac{s_{sym_1}^{\ 2} \cdot l_K}{E_P \cdot I_{Bers}} = \begin{bmatrix} 9.84 \cdot 10^{-4} \\ 9.93 \cdot 10^{-4} \end{bmatrix} \frac{mm}{kN}$

Average clamped parts resilience: $\delta'_P := 0.5\ \sum \delta'_P = (9.88 \cdot 10^{-4})\ \frac{mm}{kN}$

Ans.

The resilience of the clamped parts are: $\delta'_P = (9.88 \cdot 10^{-4})\ \frac{mm}{kN}$

==========

Supplementing resilience for TTJs, related to the effect of tapped threads on the resilience: $\delta_{PZu} := (w - 1)\ \delta_M = (6.96 \cdot 10^{-4})\ \frac{mm}{kN}$

Load factor

Table 3. Basic types of loading and clamping and associated load factors

	loading	concentric ($a = 0$)		eccentric ($a \neq 0$)	
	clamping	concentric	eccentric	concentric	eccentric
loading by F_A	load introduction under head ($n = 1$)	Φ_K	Φ^*_K	Φ_{eK}	Φ^*_{eK}
	load introduction in plate ($n < 1$)	Φ_n	Φ^*_n	Φ_{en}	Φ^*_{en}
loading by M_B		Φ_m [a)]	Φ^*_m	– [b)]	– [b)]

[a)] without importance for F_{SA}
[b)] External bending (working) moments don't have an eccentrical effect.

Concentric load factor: $\Phi_K := \frac{\delta_P + \delta_{PZu}}{\delta_S + \delta_P} = 0.166$

Load factor for eccentric clamping: $\Phi'_K := \frac{\delta'_P + \delta_{PZu}}{\delta_S + \delta'_P} = 0.168$

==========

Note that for these load factors, the load introduction factor is assumed to be 1. Thus, that the load is introduced under the bolt-head.

Calculation of Beam Properties for FEA

Based on the analytic properties of the bolt, equivalent values to use when defining the beam properties can be calculated from (Eq. 79), VDI 2230 Pt.2.

Beam input values:

For comparison:

Beam length: $l_{K.FE} := 10\ mm$ $\quad l_K = 11\ mm$

Equivalent area: $A_{ers} := \frac{l_{K.FE}}{E_S \cdot \delta_S} = 10.05\ mm^2$ $\quad A_{d3.g} = 15.49\ mm^2$ $\quad \frac{A_{ers}}{A_{d3.g}} = 64.9\%$

Equivalent aream moment of intertia: $I_{ers} := \frac{l_{K.FE}}{E_S \cdot \beta_S} = 17.97\ mm^4$ $\quad I_{d3.g} = 25.02\ mm^4$ $\quad \frac{I_{ers}}{I_{d3.g}} = 71.8\%$

$J_{ers} := 2\ I_{ers} = 35.94\ mm^4$

R4 - Preload Changes

Embedding Note: Does in principle only apply to Steel.

Assuming surface roughness height Rz < 10 μm.

According to "Table 5": $f_Z := (3 + 2.5 + 1.5)\ \mu m = 7\ \mu m$

Resulting preload loss from embedding: $F_Z := \frac{f_Z}{\delta_S + \delta'_P} = 697\ N$

NASA Estimate: $5\% \cdot F_{Mzul} = 436.53\ N$

==========

Table 5. Guide values for amounts of embedding of bolts, nuts and compact clamped parts made of steel, without coatings

Average roughness height *Rz* according to ISO 4287 [a)]	Loading	Guide values for amounts of embedding in µm		
		in the thread	per head or nut bearing area	per inner interface
< 10 µm	tension/compression shear	3 3	2,5 3	1,5 2
10 µm up to < 40 µm	tension/compression shear	3 3	3 4,5	2 2,5
40 µm up to < 160 µm	tension/compression shear	3 3	4 6,5	3 3,5

[a)] mean value from the maximum surface roughness *Rt* of at least two sampling lengths; with five sampling lengths *Rz* corresponds with a good approximation to the "old" *Rz* of DIN 4768

Thermal Contraction Effects

The thermal integrals from 293K to 4K is used to determine the thermal deformations:

	Titanium Gr.2	***Titanium Gr.5***	
Therma integrals:	$A_{T_Ti2} := 0.00151$	$A_{T_Ti5} := 0.00173$	Source: EDMS 1530740

Change in length of bolt and clamped parts: $\Delta l_S := l_K \cdot -A_{T_Ti5} = -0.019\ mm$ $\quad \Delta l_P := l_K \cdot -A_{T_Ti2} = -0.017\ mm$

The thermal deformation is: $\Delta f_{Vth} := \Delta l_S - \Delta l_P = -0.002\ mm$

Preload loss due to thermal contraction: $\Delta F'_{Vth} := \frac{\Delta f_{Vth}}{\delta_S + \delta_P} = -242\ N$

$Status_\Delta F'_{Vth} := \begin{cases} \text{if } \Delta F'_{Vth} \le 0 \\ \quad \text{return "Preload Increase"} \\ \text{"Preload loss"} \end{cases}$

$Status_\Delta F'_{Vth} =$ "Preload Increase"

Note that as the bolt will contract more than the plate. This will give an increase in preload. This could be considered in the calculation of Work Stress. In terms of minimum preload, the most conservative is to ignore this effect.

Sum of losses

The sum of the preload losses are: $F_{loss} := \Delta F'_{Vth} + F_Z = 456\ N$

Resulting minimum preload: $F_{Mmin.Z} := F_{Mmin} - F_Z = 4.76\ kN$

R9 - Alternating Stress - Fatigue

Additional bolt load: $F_{SA} := F_{Smax} - F_{Vmax}$

The additional stress in the bolt that will vary with the workload is: $\sigma_{zb.max} := \frac{F_{SA}}{A_{S.g}} + \frac{M_{Sbo}}{W_{S.g}} = 281.8\ MPa$ $\begin{bmatrix} \sigma_{SAbo} \\ \sigma_{SAbu} \end{bmatrix} := \begin{bmatrix} \sigma_{zb.max} \\ 0\ MPa \end{bmatrix}$

The resulting stress amplitude is: $\sigma_{ab} := \frac{\sigma_{SAbo} - \sigma_{SAbu}}{2} = 140.9\ MPa$

Permissable continous alternating stress for bolts rolled before heat treatment: $\sigma_{ASV} := 0.85 \left(\frac{150}{d\ mm^{-1}} + 45 \right) MPa = 59.5\ MPa$ $r_{ASV} := \frac{\sigma_{ASV}}{R_{p0.2min}} = 7.3\%$

The fatigue limit makes up $r_{ASV} = 7.3\%$ of the bolt proof stress.

Criteria: $\sigma_{ab} = 140.88\ MPa$ < $\sigma_{ASV} = 59.5\ MPa$

$Status_R9 = \text{"Not Ok"}$

$Status_R9 := \begin{cases} \text{if } \sigma_{ab} < \sigma_{ASV} \\ \quad \text{return "Ok"} \\ \text{"Not Ok"} \end{cases}$

The safetyfactor against fatigue is: $S_D := \frac{\sigma_{ASV}}{\sigma_{ab}} = 0.42$ $S_{D.req} := 1.2$

R10 - Surface Pressure Under the Bolt Head

Limiting surface pressure: $p_G := 1340\ MPa$

Head bearing area: $A_{p.min} := \frac{\pi}{4} \left(d_W{}^2 - d_{h.max}{}^2 \right) = 22.6\ mm^2$

Pressure in assembly state: $p_{Mmax} := \frac{F_{Mzul}}{A_{p.min}} = 386.3\ MPa$

Pressure in working state: $p_{Bmax} := \frac{F_{Smax}}{A_{p.min}} = 205.7\ MPa$ $p_{Mmax} := \max(p_{Bmax}, p_{Mmax}) = 386.3\ MPa$

Safety factor: $S_p := \frac{p_G}{p_{Mmax}} = 3.47$

R11- Thread Strength and Required Length of Engagement

Note that there is two factors that will lead to better load distribution on the threads than in a normal case:
1) Titanium is more resilient than Steel
2) The outgassing hole in the bolt

Parameters	***Bolt***	***Clamped parts***
Tensile strength:	$R_{mS} := R_{p0.2min} = 820\ MPa$	$R_{p0.2_Ti2} := 275\ MPa$ $R_{mM} := R_{p0.2_Ti2}$
Shear strength:	$\tau_{BS.min} := 600\ MPa$	$\tau_{BM.min} := 0.6 \cdot 345\ MPa = 207\ MPa$
Dimensions with tolerance: [ISO 965-2 - 6H/6g]	$d_{min} := 5.794\ mm$	$d_1 := d - \frac{5\sqrt{3}}{8} P = 4.917\ mm$
	$D_{2.max} := 5.50\ mm$	$D_1 := d_1$ $D_2 := d_2$
Effective thread length:	$l_{eff} := (l - l_K) = 9\ mm$	

H= 0.86603P h_3= 0.61343P H_1= 0.54127P R= H/6

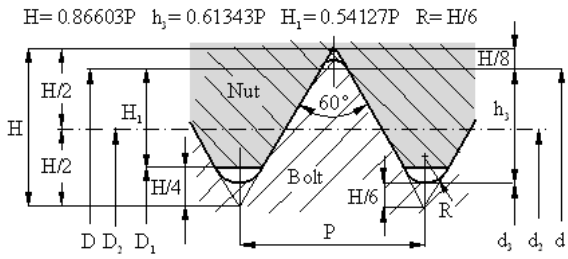

Determination of Critical Thread

Thread strength ratio: $R_S = \dfrac{A_{SGM} \cdot \tau_{BM}}{A_{SGS} \cdot \tau_{BS}}$

A_{SG} is the thread shear area of for the bolt / tapped threads
τ_B is the shear strength

Criteria:

$R_S > 1$ bolt thread is critical

$R_S < 1$ internal thread is critical

$$Thread_Critical(R_S) := \begin{array}{l} \text{if } R_S > 1 \\ \quad \text{return "bolt thread"} \\ \text{if } R_S < 1 \\ \quad \text{return "Internal thread"} \end{array}$$

$$R_S := \frac{d \cdot \left(\frac{P}{2} + (d - D_2) \cdot \tan(30\ deg)\right)}{d \cdot \left(\frac{P}{2} + (d_2 - D_1) \cdot \tan(30\ deg)\right)} \cdot \frac{\tau_{BM.min}}{\tau_{BS.min}} = 0.403$$

Ans.

$Thread_Critical(R_S) =$ "Internal thread"

==========

Stripping Force of Internal Threads

The calculation of strength in the threads is solely based on the shear stress on the nut materials caused by the tensile force in the bolt thread and that the influence of superimposed bending stresses in the thread turns can be ignored.

The correction factors C1 and C3 take into account among other things the reduction in the shear area resulting from flexure.

Parameter C1:

"s" is the equivalent diameter of the material surrounding the internal thread.

$s := 10\ mm$ $\qquad \dfrac{s}{d} = 1.67$

$$C_1 := \begin{array}{l} \text{if } 1.4 \le \frac{s}{d} < 1.9 \\ \quad C_1 \leftarrow 3.8 \cdot \frac{s}{d} - \left(\frac{s}{d}\right)^2 - 2.61 \\ \text{if } \frac{s}{d} > 1.9 \\ \quad C_1 \leftarrow 1 \\ \text{if } \frac{s}{d} < 1.4 \\ \quad \text{return "not valid"} \end{array}$$

$C_1 = 0.95$

=======

Parameter C3:

$R_S = 0.403$

$$C_3 := \begin{array}{l} \text{if } R_S \le 0.43 \\ \quad C_3 \leftarrow 1 \\ \text{if } 0.43 < R_S < 1 \\ \quad C_3 \leftarrow 0.728 + 1.769\ R_S - 2.896\ R_S^2 + 1.296\ R_S^3 \\ \text{if } R_S \ge 1 \\ \quad C_3 \leftarrow 0.897 \end{array}$$

$C_3 = 1$

=====

Shear area for nut/internal thread: $A_{SGM} := \overrightarrow{\pi \cdot d_{min} \cdot \left(\frac{l_{eff}}{P}\right) \cdot \left(\frac{P}{2} + (d_{min} - D_{2.max}) \cdot \tan(30\ deg)\right)} = 109.7\ mm^2$

Stripping force of internal thread: $F_{mGM} := C_1\ C_3\ \tau_{BM.min} \cdot A_{SGM} = 21.48\ kN$

Reference stripping force, with no correction: $F_{mGM.ref} := \tau_{BM.min} \cdot A_{SGM} = 22.71\ kN$

Breaking stress of free loaded bolt thread: $F_{mS} := R_{mS} \cdot A_{S.g} = 14.5\ kN$

Criteria **(R11/1)**: $F_{mS} = 14.5\ kN$ < $F_{mGM} = 21.5\ kN$

$$Status_R11.1 := \begin{array}{l} \text{if } F_{mS} < F_{mGM} \\ \quad \text{return "Ok"} \\ \text{"Not Ok"} \end{array}$$

$Status_R11.1 =$ "Ok"

==========

Load case specific data:

Utilisation of thread capacity: $\nu_{mGM} := \dfrac{F_{Smax}}{F_{mGM}} = 21.7\%$

Thread stripping force safety factor: $S_{mGM} := \dfrac{F_{mGM}}{F_{Smax}} = 4.62$

Required effective length of tapped threads:

$$m_{ges.min} := \frac{R_{mS} \cdot A_{S.g} \cdot P}{C_1 \cdot C_3 \cdot \tau_{BM.min} \cdot \left(\frac{P}{2} + (d_{min} - D_{2.max}) \cdot \tan(30\ deg)\right) \cdot \pi \cdot d_{min}} + 2\ P = 8.09\ mm$$

Note: The "2P" is a margine for non-effective thread length, like chamfer.

Criteria: **ans.** $m_{ges.min}=8.1\ mm$ < $l_{eff}=9\ mm$

$Status_thread_length:=$ if $m_{ges.min}<l_{eff}$ return "Ok" "Not Ok"

$Status_thread_length=$ "Ok"

==========

Considering non-uniform load distribution in the thread, the following assessment can be performed:

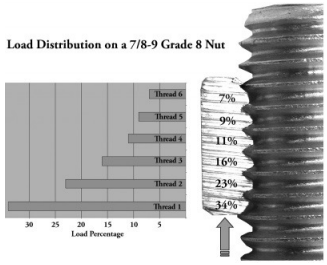

Numer of internal threads: $n:=\frac{l_{eff}}{P}=9$

Stripping force pr. thread: $F_{mGM_n}:=\frac{F_{mGM}}{n}=2.4\ kN$

Say the $n_t:=2$ first threads should be able to hold $\lambda_P:=50\%$ of the load:

$Non_uniform_status:=$ if $n_t\ F_{mGM_n}>F_{Mzul}\ \lambda_P$ return "Ok" "Not Ok"

$n_t\ F_{mGM_n}=4.77\ kN$ > $F_{Smax}\ \lambda_P=2.33\ kN$

$Non_uniform_status=$ "Ok"

==========

The $n_t=2$ first thread(s) can hold $\frac{n_t\ F_{mGM_n}}{F_{Smax}}=102.6\%$ of the load.

R12 - Safety Margin Against Slipping

Negative preload loss, thus increase in preload from thermal contraction should not be included: $\Delta F'_{Vth.f}:=$ if $\Delta F'_{Vth}<0$ $=0\ kN$ 0 kN

Analytic minimum residual clamping force: $F_{KR.min}:=\frac{F_{Mzul}}{\alpha_A}-(1-\Phi'_K)\ F_{A.max}-F_Z-\Delta F'_{Vth.f}=4.47\ kN$ **(R12/1)**

Required clamp load to transfer the maximum transverse load: $F_{KQerf}:=\frac{F_{Q.max}}{\mu_{Tmin}}=1.3\ kN$ **(R12/2)**

Criteria: $F_{KQerf}>F_{KR.min}$ **(R12/3)**

Safety factor: $S_G:=\frac{F_{KR.min}}{F_{KQerf}}=3.5$ > $S_{G.req}:=1.2$ $Status_R12_4:=$ if $S_G>S_{G.req}$ "Ok" **(R12/4)**

$Status_R12_4=$ "Ok"

==========

Safety against sharing of the bolt: $S_A:=\frac{\tau_{BS.min}\cdot A_{d3.g}}{F_{Q.max}}=24.1$ > $S_{A.req}:=1.1$ $Status_R12_7:=$ if $S_A>S_{A.req}$ "Ok" **(R12/7)**

$Status_R12_7=$ "Ok"

==========

Summary of Key Results

Calculation step	Results		
S1 - Workload	Maximum transverse load:	$F_{Q.max}=385.4\ N$	
	Minimum clamp-load to avoid slipping:	$F_{KQ}=1.54\ kN$	
	Maximum axial load:	$F_{A.max}=347.8\ N$	
S2 - Nominal Bolt Diameter	$d=6\ mm$	$P=1\ mm$	
S3 - Tightening Factor	$\alpha_A=1.6$		
S4 - Max Assembly Pretension	$\mu_{Gmin}=0.3$		
	$\nu=0.9$		
	$F_{Mzul}=8.7\ kN$	$\sigma_{Mzul}=738\ MPa$	
S5 - Min Assembly Pretension	$F_{Mmin}=5.5\ kN$		
S6 - Simplify and Prepare CAD-geometry			
S7 - Prepare and Run FE-analysis	$\mu_{Tmin}=0.3$	$\mu_{Kmin}=0.3$	
S8 - Extracted Results	$F_{Vmax}=4.5\ kN$	$F_{Smax}=4.65\ kN$	$M_{Sbo}=3.43\ N\ m$
	$F_{Vmin}=4.5\ kN$	$F_A=0.5\ kN$	
S9 - Work Stress	$\sigma_{red.B}=627.7\ MPa$ <	$R_{p0.2min}=820\ MPa$	$S_F=1.31$ $Work_Stress=$ "Ok"
	==========		
S10 - Clamping requirements			
S11 - Tightening Torque	$M_A=20\ N\ m$		
S12 - Approve or Iterate	========== APPROVED ==========		

Additional Calculations

FE-based quanteties

Additional bolt load: $F_{SA} = 150\ N$

Load factor: $\Phi_{FE} := \frac{F_{SA}}{F_A} = 0.3$

R0 - Checking limiting size G

$e_B = 5\ mm$ < $0.5\ G'_{min} = 6.6\ mm$

$e_{AC} = 13\ mm$ < $0.5\ G'_{max} = 13.1\ mm$

R3 -Analytic Resilience and Load Factors

Axial resilience: $\delta_S = \left(9.05 \cdot 10^{-3}\right) \frac{mm}{kN}$

Bending resilience: $\beta_S = \left(5.06 \cdot 10^{-6}\right) \frac{1}{N\ mm}$

Resilience of clamped parts: $\delta'_P = \left(9.88 \cdot 10^{-4}\right) \frac{mm}{kN}$

Load factor: $\Phi'_K = 0.168$

Calculation of Beam Properties for FEA

Beam length: $l_{K.FE} = 10\ mm$

Equivalent area: $A_{ers} = 10.05\ mm^2$

Equivalent areal moment of intertia: $I_{ers} = 17.97\ mm^4$

R4 - Preload Changes

Loss from embedding: $F_Z = 697.3\ N$

Loss from thermal contraction: $\Delta F'_{Vth} = -241.5\ N$

R10 - Surface Pressure Under the Bolt Head

Safety factor: $S_p = 3.47$

R11 - Thread Strength and Required Length of Engagement

$Thread_Critical\left(R_S\right) = \text{“Internal thread”}$

$Status_R11.1 = \text{“Ok”}$

Utilisation of thread capacity: $\nu_{mGM} = 21.7\%$

Thread stripping safety factor: $S_{mGM} = 4.6$

Required thread length $m_{ges.min} = 8.09\ mm$ < Effective thread length $l_{eff} = 9\ mm$

$Status_thread_length = \text{“Ok”}$

$Non_uniform_status = \text{“Ok”}$

R12 - Safety Against Slipping

$S_G = 3.5$ $Status_R12_4 = \text{“Ok”}$

$S_A = 24.1$ $Status_R12_7 = \text{“Ok”}$